Decision-making Under Uncertainty for the Operation of Integrated Energy Systems

Blanco, Ignacio

Publication date:
2019

Document Version
Publisher's PDF, also known as Version of record

Decision-making Under Uncertainty for the Operation of Integrated Energy Systems

Ignacio Blanco

Kongens Lyngby 2018

Technical University of Denmark
Department of Applied Mathematics and Computer Science
Richard Petersens Plads, building 324,
2800 Kongens Lyngby, Denmark
Phone +45 4525 3031
compute@compute.dtu.dk
www.compute.dtu.dk

Summary (English)

This thesis deals with the development and application of solution approaches in the form of optimization problems for energy operators and companies that operate under uncertain conditions in an integrated energy system setting.

The integration of renewable and partly unpredictable energy sources has increased the need for flexibility in the power systems. One of the possibilities to provide this flexibility is by integrating different energy systems such as heat and power. The motivation of this thesis is to provide solutions that facilitate the operation of integrated energy systems under uncertain conditions.

Nowadays, heat and power systems are coupled by the participation of district heating companies in electricity markets, which is subject to many uncertainties such as volatility in electricity prices and renewable heat and power production. In this thesis, we propose decision support solutions for district heating producers to optimize their production and create bids for the day-ahead and balancing electricity markets. The proposed methods protect the operator against the different potential realizations of uncertainty.

Another solution approach proposed in this thesis is motivated by the replacement of conventional fuel sources with more sustainable fuels such as biomass. The delivery of this type of sustainable fuels is often settled in long-term contracts before the actual demand is known. In this thesis, we explore new ways of reducing the impact of uncertainty in supply planning and evaluate new contract designs for large combined heat and power producers using decision-making under uncertainty.

Concerning the operation of the power system under uncertain power production, we use the unit commitment problem to explore new ways of handling uncertainty and exploiting the operational modes of large combined heat and power plants to integrate higher shares of wind power production. The proposed methods deal with a large amount of uncertain data that may result in computationally hard optimization problems. Therefore, we develop new solution approaches that are capable of handling large-scale optimization problems with a significant amount of uncertain data providing suitable solutions for the decision-maker while drastically reducing the solution time of the problem.

All the solution approaches presented in this thesis are used for extensive analyses of the realistic systems used as case studies. These analyses evaluate e.g., how uncertainty affects the obtained solution in terms of operating costs and how the studied systems can react to the uncertainty.

Resumé (Danish)

Denne afhandling udvikler og implementerer metoder til at løse optimeringsproblemer for energiaktører som opererer under usikre betingelser i et integreret energiforsyningssystem.

Integrering af vedvarende og delvist uforudsigelige energikilder har øget efterspørgslen på fleksibilitet i energisystemer. En af mulighederne for at skabe denne fleksibilitet er ved at integrere forskellige energisystemer som varme og elektricitet. Motivationen for denne afhandling er at udvikle løsninger der gør det muligt at styre integrerede energisystemer under usikre forhold.

I dag er varme og elektricitet forbundne gennem fjernvarme selskaber og elmarkeder hvilke giver usikkerheder i form af udsving på elpriser og produktion af vedvarende varme og elektricitet. I denne afhandling foreslår vi beslutningsværktøjer til fjernvarmeselskaber til at optimere deres produktion og til at byde ind i day-ahead og balance elmarkederne. De foreslåede metoder beskytter desuden operatører mod forskellige potentielle realiseringer af usikkerhed.

En anden løsning som denne afhandling foreslår, er motiveret af udskiftningen af konventionelle energikilder med vedvarende energikilder såsom biomasse. Levering af denne type af vedvarende energi skal oftest aftales lang tid i forvejen, før efterspørgslen er kendt. I denne afhandling kigger vi på metoder til at reducere betydningen af usikkerhed i planlægningen af udbud og evaluerer nye kontraktstrukturer for store kombinerede varme- og elproducenter ved brug af beslutningstagen under usikkerhed.

Til styring af elnetværk med hensyn til usikkerhed i elproduktionen, bruger vi

”unit commitment problem” til at udforske nye måder at håndtere usikkerhed og til at udnytte de store kombinerede varme- og elselskabers forskellige operationelle tilstande til at integrere mere vindenergi. Disse foreslåede metoder bruger store mængder af data med indbygget usikkerhed hvilken kan resultere i beregningsmæssigt svære problemer. Derfor har vi udviklet nye løsningsmetoder som kan håndtere store optimeringsproblemer med store mængder af usikkert data. Disse metoder giver rimelige løsninger til beslutningstagere samtidig med at de drastisk reducerer beregningstiden.

Alle metoder som er præsenteret i denne afhandling er blevet omfattende analyseret med realistiske systemer som case-studier. Disse analyser evaluerer hvordan usikkerhed influerer den fundne løsning i forhold til operationelle udgifter og hvordan det undersøgte system kan reagere på denne usikkerhed.

Preface

This thesis was conducted at the Department of Applied Mathematics and Computer Science at the Technical University of Denmark (DTU Compute) in partial fulfillment of the requirements for acquiring a Ph.D. degree. This thesis is founded by Innovation Fund Denmark through the Centre for IT-Intelligent Energy Systems in cities (CITIES Project - no. 1035-00027B).

The thesis addresses the development of operational models based on optimization under uncertainty to support the decision-making process of companies and operators in an integrated energy system environment.

This thesis consists of a summary report and five scientific papers listing the work carried out during the period between November 2015 and October 2018.

Kgs. Lyngby, 31-October-2018

Ignacio Blanco

Acknowledgements

Firstly, I would like to thank my supervisor Professor Henrik Madsen for his guidance and for always helping me steer my thesis in the right direction. I would like to express my sincerest gratitude to Juan M. Morales for admitting me as a PhD student after having supervised my Master's thesis, and given me this opportunity, constant support and feedback during my PhD studies. You have been a tremendous mentor for me. Thank you for your patience, motivation and extensive knowledge. A third person who has played a crucial role for me to complete this thesis and who I would like to direct a special thanks to is Daniela Guericke. I would like to thank you for the hours you selflessly have put on my thesis during discussions, brainstormings, proof-readings and collaboration. You have been an immense support for me ever since you started at DTU.

I would also like to thank Anders N. Andersen for the brilliant ideas, projects and advises you have shared with me during these years. I have learned a lot from our collaboration which has been a very important contribution to the outcome of this PhD thesis. My sincerest thanks also goes to Professor Jong-Bae Park and Doctor Hyoung-yong Song for the fruitful collaboration and the amazing welcoming I received from you in Korea. I hope that our collaboration continues in the future. It goes without saying that I always will be grateful to all my friends in the Power Systems lab at Konkuk University for making me feel as one of the team since the very first day.

I also want to dedicate a thanks to all my colleagues in the section of Dynamical Systems at DTU, the old ones and the new ones, for the good times we have had and we hopefully will continue to have in the future. To Hanne and Janne for

always being so helpful and treating all of us so good. I would also like to thank the people in the CITIES project for all the knowledge and good moments that we have shared.

To my friends in Denmark (Tattini, Dani, Wojtek, Dudu, Sebastian, Tommaso, Panos, Julito and all who I do not name) you have all been a very important part of my life and you have made me feel at home during all these years.

I cannot thank my mother, father and brother enough for their support. I know you are very proud. I would like to dedicate a special thanks to my father, who has been reminding me about the thesis deadline every day since day one. Last but not least, thanks to Christina for your love, for your unconditional support in good and bad times.

List of Publications

Scientific Publications in This Thesis

A I. Blanco and J. M. Morales "An Efficient Robust Solution to the Two-Stage Stochastic Unit Commitment Problem". In: *IEEE Transactions on Power Systems*, Volume 32, Pages 4477 - 4488, March 2017.

B I. Blanco, H. Y. Song, D. Guericke, J. M. Morales, J. B. Park and H. Madsen "Integration of different CHP steam extraction modes in the stochastic unit commitment problem". Under review in: *IEEE Transactions on Sustainable Energy*, 2018.

C I. Blanco, A. N. Andersen, D. Guericke and H. Madsen "A novel bidding method for combined heat and power units in district heating system". Under review in: *Energy Systems*, 2018.

D I. Blanco, D. Guericke, A. N. Andersen and H. Madsen, "Operational planning and bidding for district heating systems with uncertain renewable energy production". In: Energies, 11(12), 3310.

E I. Blanco, D. Guericke, J. M. Morales and H. Madsen, "A two-phase stochastic programming approach to biomass supply planning for combined heat and power plants". Under review in: *OR Spectrum*, 2018.

Dissemination of Research at Conferences

Some of the works carried out during the PhD study have been presented at the following conferences.

F I. Blanco and J. M. Morales "An Efficient Robust Solution to the Two-Stage Stochastic Unit Commitment Problem". In: *Optimization challenges in the evolution of energy networks to smart grids* , Coimbra, Portugal, October 2016.

G I. Blanco and J. M. Morales "An Efficient Robust Solution to the Two-Stage Stochastic Unit Commitment Problem". In: *INFORMS Annual Meeting 2017*, Nashville, United States, November 2016.

H I. Blanco, D. Guericke , J. M. Morales and H. Madsen "A two-phase stochastic programming approach to biomass supply planning for combined heat and power plants". In: *IFORS 2017, 21st Conference of the International Federation of Operation and Research Societies*, Quebec City, Canada, July 2017.

I I. Blanco, D. Guericke , J. M. Morales and H. Madsen "A two-phase stochastic programming approach to biomass supply planning for combined heat and power plants". In: *ECSO 2017, European Conference on Stochastic Programming*, Rome, Italy, September 2017.

J I. Blanco, H. Y. Song, D. Guericke, J. M. Morales, J. B. Park and H. Madsen "Integration of different CHP steam extraction modes in the stochastic unit commitment problem". In: *INFORMS Annual Meeting 2018*, Phoenix, Arizona, November 2018.

Contents

Part I

Summary Report

Chapter 1

Introduction

This chapter is divided into three parts. First, Section 1.1 provides an overview of the context and motivation of this thesis. Second, Section 1.2 presents the objectives of this thesis and how these have been approached. Finally, Section 1.3 summarizes the structure of the thesis.

1.1 Context and Motivation

For more than two decades, sustainability and reduction of greenhouse gas emissions is on the agenda of industrialized countries. To this end, several political measures have been applied throughout this time. One of these measures is the reduction of CO_2 emissions in the energy sector. This reduction has been achieved by replacing fossil fuels with renewable energy sources (RES). In 2010 the European Union (EU) elaborated a plan to reduce the green-house gas emissions by 20%, increase the share of renewable energies by at least 20% and increase energy savings by 20%. Furthermore, the goals for 2030 are a 40% cut in greenhouse gas emissions compared to 1990 levels, a 27% share of renewable energy consumption and a minimum of 27% energy savings compared with the business-as-usual scenario [1]. Nowadays, the share of RES in final energy use varies widely between EU countries. Despite it has increased up to 17%, further efforts are needed until 2020, especially, to integrate RES in the current

power system [2]. More specifically, in Denmark (one of the countries leading the low-carbon transition), the planned government actions are much more ambitious. Denmark expects to cover 50% of the energy consumption by the use of renewables in 2030 and be totally free of fossil fuel by 2050 [3].

1.1.1 Towards a fossil-free energy sector

The vast integration of RES into the power system leads to a technical issue. Most of the RES are dependent on partly unpredictable weather conditions and consequently they can not provide an immediate response to the power system requirements, which means they are non-flexible units. Due to the fact that electricity can not be stored in large quantities and the production and consumption must match at every moment, the integration of RES in the power system produces imbalances. These imbalances translate into volatility in prices, planning inaccuracy, breakdowns in the power system and many other challenges that the transmission system operator (TSO) and the agents involved in the power system must deal with.

To solve these challenges, different solutions to provide flexibility and fast response in power systems have been explored [4]. All these solutions belong to the concept of *smart grids* and are briefly described as follows. First, *cross-border electricity interconnections* ensure security of supply and fast response to allocate excess of RES production. The goal is to strongly connect electricity regions and expand the transmission capacity between them to ensure the security of supply, reduce the risk of blackouts and decrease the need for new power plants. Second, *demand response* mechanisms intend to consider consumers as active flexibility providers that give a fast response to the fluctuating RES power. Third, *energy systems integration* that consists of combining several energy carriers and infrastructures to maximize the value of every energy unit. This concept is explained in more detail in Section 1.1.2. In this thesis, we focus on the integration of two energy systems (heat and power), and therefore the concept of integrated energy systems is crucial to understand the work done in this project.

1.1.2 Energy Systems Integration

Energy Systems Integration (ESI) is an approach that analyzes the multiple ways of exploiting the synergies between different energy systems and investigates how they can operate together. ESI combines the co-optimization of energy carriers such as electricity, fuels or dammed water with infrastructures such

as transportation, sewer systems, district heating or the natural gas network to maximize the efficiency of each system and reduce losses [5]. In addition, a larger integration of RES can be achieved through ESI allowing real-time coordination between agents involved in the energy system to balance the power fluctuations. To perform this coordination, direct and fast communication between the agents involved is needed. Since all energy systems operate individually and in different scales, this communication requires an efficient processing of data to perform real-time control of the entire system so they can respond to the signals sent by other agents. A detailed description of how integrated energy systems work, the current situation in Europe as well as research contributions is given in Section 2.1, Chapter 2.

1.2 Thesis Objectives & Contributions

Many studies, such as [6] and [7], agree that even though industrialized countries have a well-developed energy system infrastructure, their operation is not always well coordinated and this coordination becomes critical for the integration of a high share of RES. Due to the current design of the energy systems (e.g., heating, cooling, power or natural gas), their optimal coupling in an ESI context can be achieved through the operation of these systems by means of an integrated market [8]. Consequently, this thesis focuses on developing models to optimize the operation and trading strategy of energy companies that own a portfolio of different multi-commodity generation units that support the integration of energy systems on a city scale. We analyze potential business cases for these companies and consider the uncertainty involved in the process. We focus on the coupling of the power and heating sectors since some previous studies such as [9] and [10] have acknowledged the value of combined heat and power units, electric boilers and heat pumps to integrate RES by the participation of these heating and power producers in the electricity market.

The above mentioned models rely on the use of mathematical programming methods that optimize the operation of the units while considering the uncertainty that arises from the integration of RES in energy systems. Thus, we exploit the field of decision-making under uncertainty and more specifically stochastic programming [11]. The use of stochastic programming will result in planning tools that help the decision-maker to deal with the integrated management of energy systems considering the impact of uncertainty. Decision-making under uncertainty often translates into large-scale optimization problems with large amount of data and variables to be solved. In addition, when the commitment status of the units is included, binary variables are needed to model these problems creating large mixed integer programs that require lengthy computa-

tional times to be solved. Therefore, this thesis also focuses on implementing techniques that can decompose the problem in order to achieve suitable results. These techniques are based on combining decomposition and parallelization techniques [12] for large-scale programs that are capable of reducing the solution time while providing suitable solutions for the decision-maker. The use of these techniques allows integrating a larger amount of binary variables and uncertain data into our decision-making process.

During this thesis, the objectives presented above have been addressed in several works.

First of all, the design and evaluation of new bidding strategies for district heating (DH) producers have been tackled in Paper C and Paper D. More specifically, in Paper C, we introduced a bidding strategy for DH producers that hedges against volatility in electricity prices by defining the bidding price as a function of the replaced heat production using combined heat and power plants instead of heat boilers. In Paper D, we propose a sequential bidding strategy for DH producers with uncertain RES heat and power production. The model deals with uncertainty by creating price dependent bids and offer the flexibility provided by the portfolio of units to the system operator in the balancing market. Another business case concerning fuel contracting for DH producers is tackled in Paper E. In this work, we design a solution approach that hedges against the uncertainty involved in the biomass contracting process for large-scale heat and power plants.

The decomposition of large-scale optimization problems has been tackled in Paper A and Paper B. These papers propose strategies to deal with a large amount of RES production in power systems. These strategies consist of a parallelization and decomposition scheme that speeds up the solution of unit commitment problems that integrates non-dispatchable RES sources. In the case of Paper B, we also integrate a detailed description of the operation of large-scale CHP plants. The formulation of these techniques can be adapted to other stochastic programming problems that include a large number of binary variables in all the stages of the decision-making process. The nature of the proposed techniques allows the method to select the scenarios that best characterize the uncertainty and reduce the loss of generality in the decomposition process. Furthermore, in Paper E we propose a two-phase solution approach that divides the decision-making process into one planning problem and one operational problem. This structure resembles the decision-making process in practice, making the problem computationally tractable and provides suitable solutions that allow the decision-maker to exploit the proposed design of the contracts.

To conclude this section, please note that since one of the goals of this thesis is to provide companies with tools for the optimal operation in integrated energy

systems, most of the papers presented have been carried out in collaboration with companies. Many of the ideas, highlights and projects of this dissertation come from the need of companies to elaborate new tools for their decision-making processes. On top of that, most of the case studies have been elaborated using real data provided by these companies.

1.3 Thesis Structure

The thesis is structured as follows. Part I consists of a report summarizing the contribution of this thesis. This report subdivides into several chapters. Chapter 2 introduces the concept of integrated energy systems and the status of this integration in the EU and Denmark. The chapter mainly focuses on the integration of power and heating systems and shows how the agents involved in DH systems participate in the electricity markets. Chapter 3 describes the methodologies used in this thesis: Mixed-integer linear programming, stochastic optimization, forecasting, and decomposition techniques. Chapter 4 analyzes the value of integrating uncertainty in decision-making problems and summarizes the main results obtained in the thesis. Chapter 5 closes Part I providing conclusions and perspectives.

Part II gathers the publications that contribute to this thesis.

Paper A is a journal article published in *IEEE Transaction on Power Systems*. It consists of an innovative formulation of the two-stage stochastic unit commitment problem that proposes a decomposition and parallelization scheme yielding robust commitment plans that drastically reduce the solution time.

Paper B is a collaboration with Konkuk University and the Korea District Heating Corporation and is under review at *IEEE Transactions on Sustainable Energy*. This paper describes a system that integrates the operation of conventional thermal units with large combined heat and power plants under high shares of wind power penetration. The problem is solved using an improved formulation of the method proposed in Paper A

Paper C is a collaboration with EMD International and is under review at: *Energy Systems*. This publication presents a novel bidding strategy for district heating producers in the day-ahead market.

Paper D is a collaboration with Hvide Sande Fjernvarme and EMD International. The paper has been published in *Energies* and presents a sequential bidding strategy for district heating producers with high integration of RES heat and power production within their system.

Paper E is a collaboration with Ørsted and is under review at: *OR Spectrum*. This paper presents a biomass contracting strategy that optimizes the fuel supply planning for large power and heat production units and includes mechanisms to deal with the planning uncertainties.

Chapter 2

Context & Background

In this chapter, Section 2.1 gives an overview of integrated energy systems on a cities scale. The uncertainty affecting the operation of these systems is mentioned in Section 2.2. Special focus is given to the joint operation of power and district heating systems described in Section 2.3. The technologies and the different types of combined heat and power plants that have been modelled in this thesis are presented in Section 2.4 and Section 2.5, respectively. Finally, the operation of a district heating system in electricity markets is described in Section 2.6.

2.1 Integrated Energy Systems

Energy systems have evolved from being small and local services into large and continental systems that deliver services throughout vast areas (e.g., power grids, gas networks, large district heating systems, etc.). Today, the extensive integration of non-dispatchable RES implies that a successful operation does not rely on the power system alone, but on the entire energy system and its full integration. As each energy system is very complex to operate individually, it is required to facilitate the aggregation and synchronization of the agents connected to the energy systems. In order to do so, mathematical and statistical

methods such as Big Data, forecasting, control and optimization are applied [13]. When developing mathematical models to optimize integrated energy systems, it is important that properties and dynamics of individual components of the system are analyzed and understood. These models simulate the operation of the agents in the system providing optimal signals to the rest of the system components. For example, in Paper D we show that a signal from the electricity market registering a low electricity price, will immediately result in a bid to buy a certain volume of power and produce heat using the electric boiler. However, in order to proceed with the operation, we first need to know if the amount of generated heat will not saturate the storage. Thus, for each decision we make, the operator has to analyze whether the decision is optimal compared to all other possible choices and feasible in the operation of the system.

There already exist energy system optimization models that seek the optimal way of configuring today's energy system to fulfill the long-term policy requirements. Two examples are Balmorel [14] and TIMES-DTU [15]. The Balmorel model focuses on the electricity and district heating sectors, providing a system dispatch as well as power price profiles. TIMES-DTU analyzes all power and district heating sectors in the Nordic countries as well as power trade profiles in other European countries. It renders power and heat demands for all industry sectors and their possible future demand scenarios. Both models have a medium-term or long-term planning horizon and do therefore not account for the dynamics of the system and the uncertainty related to RES in a short-term planning horizon. Consequently, there is a need for sophisticated tools that cover the short-term dynamics of the electricity market and RES [16]. Based on this need, methods used to describe the real-time flexibility of the consumers have been developed (e.g. [17, 18, 19, 20]). These methods are able to use data of the end-users in real-time and send signals to the system operator to activate or deactivate units, giving flexibility to the system and flattening the electricity price curve-profile. To optimally aggregate these agents that operate in different temporal and geographical scales, there are concepts such as the Smart-EnergyOS [21], which uses signals from the market to provide direct and indirect control to the end users. Furthermore, the uncertainties that affect the operation of the integrated energy system must be taken into account to provide reliable solutions to the decision-maker. Therefore, stochastic programming and robust optimization have been successfully applied as planning tools for integrating RES [22].

Figure 2.1 shows a general overview of how the different resources (RES, hydro, fossil fuels and biomass), generation and transmission systems (power, district heating and gas network) and services or end-users (residential, industrial and transport) relate to each other on a cities scale. Henceforth, we differentiate between two different agent coordination schemes for integrating the energy systems. First, the integration between the various energy production and trans-

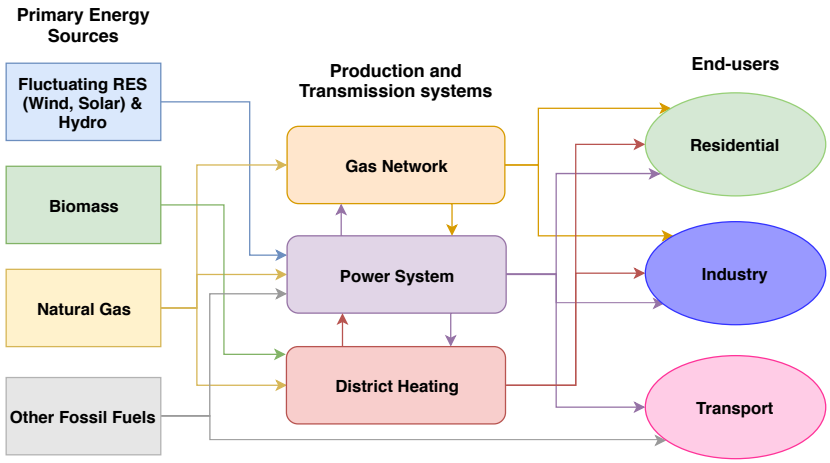

Figure 2.1: Generalized overview of the interaction between different energy resources, production and transmission systems and end-users in a cities scale.

mission systems and secondly the integration between systems and end-users.

Systems Integration:

In 2017, the electricity produced in the EU originated from around 15% RES, 10% hydro, 25% nuclear and 48% from conventional thermal plants [23]. In 2017 natural gas produced 23% of the total electricity generation in the EU and 70% of the space heating and hot water in both residential and industrial sectors [24]. The capacity of storing gas inside the gas network in the EU is approximately 79 billion m^3, which corresponds to 85000 GWh. The coordination between the power systems and the gas network is mainly achieved by the joint operation of power and gas markets [25]. The amount of gas stored in the pipelines defines the fuel spot price which directly affects the cost of electricity production modifying the electricity market spot price [26].

The interaction between the power systems and the district heating (DH) systems is incentivized by the price signals sent from the electricity market. For example, when the electricity prices are high, a DH producer will submit an offer to produce power using their combined heat and power (CHP) plants. On the contrary, if the electricity prices are low, the DH producer will activate the electric boilers or heat pumps instead. The amount of heat produced by the CHP plants and electric boilers/heat pumps, is usually higher than the actual

heat demand and is therefore stored for later use. In this way, DH systems can be used as an energy buffer to store excess production of RES and they can also, based on the requirements of the system, provide extra power production when needed [27]. In Paper B, we show how the operation of a steam-extraction CHP unit can introduce flexibility to the power system by the integration of more RES and by reducing its total production cost. In Paper C and Paper D, we show that the DH plants should plan the heat production and bids to respond the electricity market prices and maximize their profits. Moreover, for large district heating networks, both electricity market clearing and district heating production can be solved simultaneously [28].

Systems & End-users Integration:

The coordination between the different systems and services is done through demand response processes. In this case, the consumption can be adjusted by the service side, see Figure 2.1, to the actual needs of the system. For example, it has been studied how the industrial refrigeration sector, more specifically refrigeration in supermarkets, can provide flexibility to the power system by adapting the cooling needs according to price signals from the electricity market [29]. In the residential sector, heat pumps can provide flexibility to the power system by the use of model predictive control (MPC) to adjust the heat production to the price signals received from the market [19, 30]. In water treatment plants the vast amount of electricity needed to pump and air the water to eliminate impurities, makes these units a potential candidate to provide effective demand response in the system [20]. Finally, the transport sector, more specifically the batteries of electric vehicles, can be used as an energy buffer to store excess power production from RES during night hours and feed in electricity to the grid when energy consumption peaks occur. This concept is called *vehicle-to-grid* [31].

2.2 Uncertainty Affecting in the Operation of Integrated Energy Systems

Uncertainty is always present in a decision-making process. In energy systems, we can categorize this uncertainty depending on its source (market, weather, policies, behaviour or technologies) and time framework considered in the decision-making process (long-term, mid-term or short-term). The relevant uncertainties should be considered accordingly in our decision-making process. For example, if we as decision-makers are planning to expand the capacity of our power sys-

tem, we could consider uncertainty regarding taxation policies affecting the cost of the technologies. On the other hand, if we as decision-makers are planning the operation of one power production unit over a time-span of one day (the following day), maybe taxation policies is not the uncertainty that we should look at as it will not fluctuate over that time period. However, the electricity prices profile would be an uncertainty to consider.

In this thesis, we mainly focus on the uncertainty that affects the operation of the units over a short-term period. This short-term uncertainty does mostly occur by the system's fluctuation of RES. The high integration of RES makes the energy production partly unpredictable until the time of actual delivery. As a consequence, these uncertainties must be taken into consideration when planning the operation of the system. Another aspect to take into consideration is that big volumes of imbalances in RES production can directly affect the electricity prices. The number of uncertainties to consider is limited due to computational aspects, therefore other type of uncertainties such as the heat and power demand in the short-term have been neglected. The reason is that these uncertainties are easier to predict as they do not depend on RES volatility.

Although we mainly focus on short-term uncertainty in this thesis, we do however also tackle the issue of integrating mid-term uncertainties that affect the planning of the energy systems over a longer time-span. The modeling of mid-term uncertainties can be found on Paper E where we consider the fuel demand of an energy production system as uncertain for a time interval of one year.

2.3 Coupling of District Heating and Power Systems

District heating is a heat production system in which buildings in a district, a town, a city or a region are connected to a centralized heat production plant. They are connected through pipes that carry hot water at different temperatures for space heating and other water heating purposes. This approach of distributing heat avoids on-site electric or gas boilers and allows any available source to produce heat, which increases the efficiency of the system and therefore also reduces CO_2 emissions [32]. Among the EU countries, Latvia has the highest share of households connected to DH (65%), followed by Denmark (63%). Sweden, Finland, Poland, Estonia and Lithuania have a share more than 50%. Despite the goal of the EU to achieve the electrification of the heating sector, it is shown how DH systems will play a crucial role in the development of smart energy systems by fulfilling the same reduction in fuel consumption and CO_2 levels while reducing the total cost for heating and cooling demand by 15% [33].

To accomplish the full integration of DH systems in a fossil-free energy system, there are challenges that need to be addressed. For instance, heat and cooling technologies will have to improve further. Other challenges that need to be addressed are the supply of low-temperature for DH and integration of waste heat from the industrial sector. If these challenges are met, DH systems will be an integrated part of a smart energy system with 100% of renewable energy production, the so-called 4th Generation District Heating [34].

Historically, DH networks have been single and isolated systems. Nevertheless, in the case of Denmark (where the wind power integration is so high that in 2017, 44% of the electricity consumption was covered by wind power and more than 60% of the consumers received heat from the DH), the DH system is playing a significant role in the integration of the fluctuating renewable energy production. This is achieved by providing energy balancing services to the power grid [35] and reducing wind power curtailment [36]. The integration of the DH systems is obtained by operating the different units as a portfolio in order to adapt to the current situation of the energy system. This integration increases efficiency and reduces imbalances by providing flexibility. Figure 2.2 describes this flexibility. In periods with a high generation of RES, the heat production shifts to heat-only units or units that transform power to heat and lower the imbalance in the power grid while fulfilling the heat demand. During periods with less power production from RES, CHP plants can provide extra power generation. In Paper B we simulate a realistic case of the Danish transmission grid in which we include large CHP units in order to provide flexibility in the system. We show that by using real-time coordination between large CHP units and RES production, we can reduce the system cost by decreasing the wind spillage and maintaining the load and heat production at the actual demand level. In addition, we show in Paper D how DH systems can respond to the fluctuating RES production in the power system providing flexibility by their participation in the balancing market.

2.4 Description and Components of District Heating Systems

Due to operational means, DH systems can be divided into three subsystems. First, the DH plant includes the heat production units (CHP, heat pumps, boilers etc.) as well as the heat tank storage systems. Second, the DH network that consists of the pipes and pumps that carry the heat to the consumers. Third, the DH users that can be the direct end-users or a secondary distribution network, depending on the size of the network. In this thesis, we focus on DH plants and their optimal operation as a portfolio of units. In Denmark, there

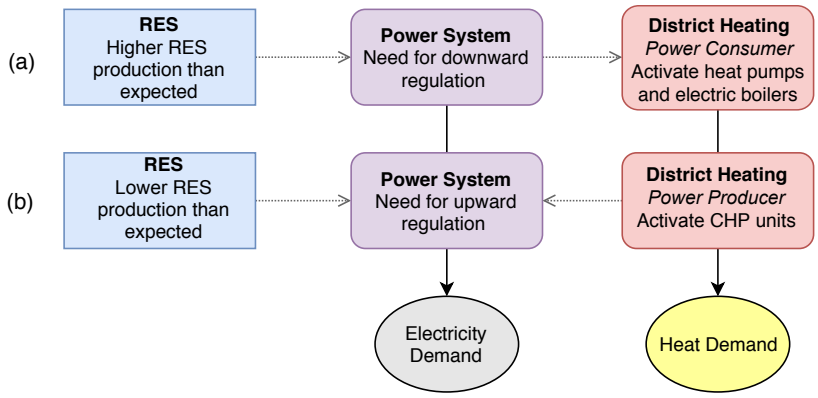

Figure 2.2: Representation of the synergy between district heating and the power system. In the first case (a), where the RES production is high, the district heating provides flexibility to the power system behaving as a load. In case (b) the RES production is low and the district heating acts as a producer.

are six large and around 400 medium-small DH systems. From the total heat production, we distinguish two areas of usage. The first usage area is space heating where the heat is directly transmitted from the distribution network or a heat exchanger at a higher temperature. The second usage area is domestic hot water where drinking water is heated in a heat exchanger, by using heat from the distribution network. Of the total heat production for space heating and domestic hot water produced by DH systems in Denmark, large DH systems produce around 55% [27]. These systems are usually located in areas with a significant population density where large CHP units produce most of the heat and where the network is comprised of various distribution networks joined by a transmission grid. This can be seen for example in the DH system of greater Copenhagen [37] and the city of Aarhus [38]. Medium or small size DH systems generate the remaining 45% of the total heat production. These systems usually consist of a single distribution network, one base load unit (small-scale CHP unit), peak load units (reserve boilers) and a heat tank storage.

During the last years, the electricity prices have dropped to historically low levels due to the integration of RES into the system resulting in the heat production from CHP units to significantly decrease in favor of heat only units [27]. In order to take advantage of the low electricity prices, the installed capacity of heat pumps and electric boilers has increased over the last years [39]. In addition to this, district heating producers are now integrating clean and renewable heating sources such as solar thermal, biomass and waste heat. Figure 2.3 illustrates a representative small-medium scale district heating plant in Denmark.

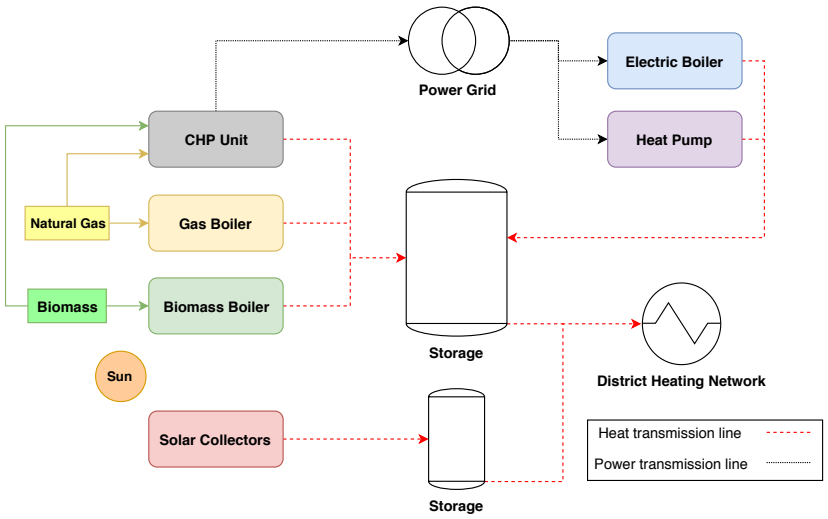

Figure 2.3: Representation of a conventional small-medium sized DH plant.

A more detailed description of the different heat production units as well as the tank storage are described in the reminder of this section. Most of the data, technology characteristics and costs are obtained from [27, 40, 41]. We encourage the reader to consult these sources for a more detailed description of the systems and its components. For the sake of clarity, we exclude CHP technology in this section as it is introduced in Section 2.5, where it is explained in more detail.

2.4.1 Gas boilers

Gas boilers run in most cases on natural gas (they can use other fuel sources such as biogas or diesel, although the use of these two fuel types can cause rapid deterioration due to the sulfur content). The capacity of gas boilers usually varies between 1 and 20 MW-thermal. The combustion of the fuel takes place in a fire tube that is in direct contact with the water. Starting gas boilers on a cold shut down status takes a maximum of 30 minutes until they work at full capacity. In addition, gas boilers are highly efficient and therefore very reliable during the peak production times. Since they do not generate power, they are not affected by the volatility of electricity prices. Nevertheless, the high taxes and the non-direct interaction with the electricity market make these units less competitive.

2.4.2 Biomass boilers

Biomass boilers for DH systems run, in most cases, with wood-pellets or straw. The way biomass boilers work is similar to gas boilers. The capacity of available commercial heat-only biomass boilers usually varies between 0.5 and 25 MW-thermal. Compared to conventional fossil fuels, biomass boilers can save a significant amount of CO_2 emissions and fuel costs [42]. Since they are considered as clean energy [43], their lower taxation, reliability and efficiency makes them a very competitive heat production unit regarding costs and, therefore, utilized as base load units.

2.4.3 Electric boilers

Electric boilers have a simple design and are divided into two categories, those using electrical resistance and those using electrodes. The first type operates with a capacity between 1 and 2 MW-thermal while the latter has more capacity than the first but a maximum limit of 25MW-thermal [44]. The only feeding source is electricity and its conversion rate from electrical energy to heat energy is around 100 %. Electric boilers are very fast units, capable of starting up and shutting down in a few seconds (from 0% to 100% of their nominal capacity in 30 seconds). This flexibility and fast response capability makes electric boilers a significant player when it comes to providing regulation in the electricity market. In other words, since they can absorb a substantial amount of power from the grid in such a short time, they can provide high flexibility in the form of down-regulation for frequency control reserves. In few cases, some DH producers buy electricity from the day-ahead market to turn on the electric boilers. However, the general rule in Denmark is to use electric boilers as peak load production units, activating them when the system operator needs balancing regulation.

2.4.4 Heat pumps

Heat pumps base their working principle on the Carnot cycle [45]. They can produce both heat and cold by reversing their flow. Heat pumps are divided into two technologies; compression and absorption. The former uses an electric source to compress the refrigerant and increase the temperature. The latter uses a high-temperature source to raise the temperature of the refrigerant and produce its evaporation using less energy than in compression. The coefficient of performance (COP), describes the ratio between heat output and electricity input. The COP value typically varies between 3 and 5, which makes heat

pumps a very efficient technology when transforming power into heat or cooling. The capacity of compression heat pumps in district heating systems is usually between 3 and 5 MW-thermal and for absorption heat pumps it can go up to 12 MW-thermal. For both technologies, the output temperature can reach up to 90 °C. From a market perspective, large-scale heat pumps in district heating systems are not designed for a fast start/stop, therefore they are constrained from participating in providing regulation. The solution to this issue is to install real-time controllers in the heat pumps to adapt their production to the market signals more than only by considering the start/stop status. However, this can result in an increase of the investment and operation cost of the heat pumps.

2.4.5 Solar collectors

There exist many technologies for solar collectors but the most common one used for DH systems is the flat solar collector where the water circulates inside inner tubes on a dark color absorber plate. The heated water is usually stored in a spare tank. Due to its reduction in installation and production costs, the integration of large solar fields in DH systems has grown significantly in Europe [46]. In Denmark there exists more than 35 solar DH systems and over the last ten years, the installation of large solar thermal units (more than 1000 m^2) has evolved from less than 0.1 km^2 to more than 0.75 km^2. It is expected that in Denmark, by 2025, solar DH will cover about 20% of the total DH consumption on an annual basis [27]. During the sunny days in the spring and summer seasons, these units can cover the entire demand of the DH network and store the excess of production. However, since they rely on weather conditions, a sophisticated integration with the rest of the heat production units is required and operators must consider the uncertainty of these units for the optimal planning production. An alternative is to increase the size of the storage for the solar thermal field but this raises the investment cost and complicates the operation of the system.

2.4.6 Heat tank storage

For DH systems we distinguish between seasonal storage, that consists of underground facilities usually made of concrete with a capacity up to 120000 m^3, and short-term storage that are tanks made of steel designed to store approximately 12 hours of full load heat production at the heating plant (between 800 and 2000 m^3 for small/medium size DH systems). In Denmark there is a total capacity of 65 GWh of heat storage installed [47]. Storage plays a critical role in DH systems, it allows the heat production units to optimize their heat produc-

tion towards maximizing profits in the electricity market without comprising the heat supply. When the excess heat production is higher than the actual demand, the heat is stored, and vice versa, the operator can make use of the storage when the heat production is lower than the demand.

2.5 Combined Heat and Power Plants

Co-generation units, also called combined heat and power plants, produce both heat and power simultaneously by using the excess heat generated in the electricity production process in order to feed a heating network. In comparison to conventional power production units and on-site heating boilers, the use of co-generation results in energy savings of approximately 40%. Around 15% of today's total electricity production in the EU originates from CHP units. With new political initiatives and policies in the EU, some studies have calculated that this percentage will increase to 20% by 2030 [48]. In Denmark, 70% of the DH generation and more than 60% of the Danish electricity generation originates from CHP units. From this point, we will distinguish between large and centralized CHP units that provide 85% [49] of the installed centralized capacity and local CHP units, which have been replacing the electricity production of these centralized units from 0 to 20% during the last two decades [50]. Large CHP units are usually located in centralized DH areas, consisting of a steam turbine, which is heated by coal, natural gas or biomass and uses the excess heat from the turbine to feed the DH network. Small CHP units usually consist of engines fed by natural gas.

Over the last years, due to the integration of wind power and the reduction of the electricity prices, the use of centralized and local CHP plants is decreasing in favor of other heat production technologies such as solar collectors, electric boilers and heat pumps [44]. Consequently, new political initiatives such as favorable taxation schemes for co-generation producers, new planning tools to provide real-time control of the units or new bidding strategies for optimal market participation and fuel supply planning are required to make CHP units more competitive.

The remainder of this section describes the most common types of co-generation units and their underlying principles. Additionally, we provide an overview of the types of fuels that are used to feed these co-generation units.

2.5.1 CHP Technologies

CHP technologies can be divided into two categories, the topping cycle and the bottoming cycle. In the topping cycle, the fuel is first used to produce electricity and heat is afterwards recovered for later use. In the bottoming cycle, the fuel is applied first to generate thermal energy at a high temperature for industrial purposes and then transform the excess heat into power. In this section, we focus on the topping cycle technologies. The technical information presented below is obtained from [51, 52, 53] where we encourage the reader to look for a more detailed description.

2.5.1.1 Steam Turbine Co-generation System

Steam turbines base their working principles on the Rankine cycle. The fuel burns in the boiler to produce high-temperature steam which expands to produce power. Generally, the two most utilized types of boilers are back-pressure and extraction condensing units. For the back-pressure type, there exists only one steam extraction point from the turbine, and there is therefore a linear relation between heat and power production which depends exclusively on the fuel injection. The extraction condensing technology allows more than one steam extraction point, hence, power production can be maintained stable while changing the output of heat (pressure and temperature). Figure 2.4 depicts the layout of both the back-pressure and extraction condensing units. Figure 2.4a shows the feasible region for heat and power production and Figure 2.4b represents the schematic diagrams for both technologies. In the case of a back pressure unit, the entire steam from the turbine flows directly to one heat exchanger (this process is represented in Figure 2.4 using the dashed green line). In the case of extraction condensing unit, we can extract steam at a certain pressure and temperature, and send it to the heat exchanger. The remaining steam flows to the condenser (this process is depicted in Figure 2.4 using the dotted violet line).

2.5.1.2 Internal Combustion Engine Co-generation System

This technology is based on the Otto thermodynamic cycle and it consists of an engine, a generator, a heat recovery unit, an exhaust system, automatic controls and an acoustic enclosure. These systems are fast responsive and therefore ideal for intermittent operation. They are very efficient in producing power and, since they are small units, heat recovery is also quite efficient and therefore, they are mainly used in small-medium size DH systems. In both Paper C and Paper D

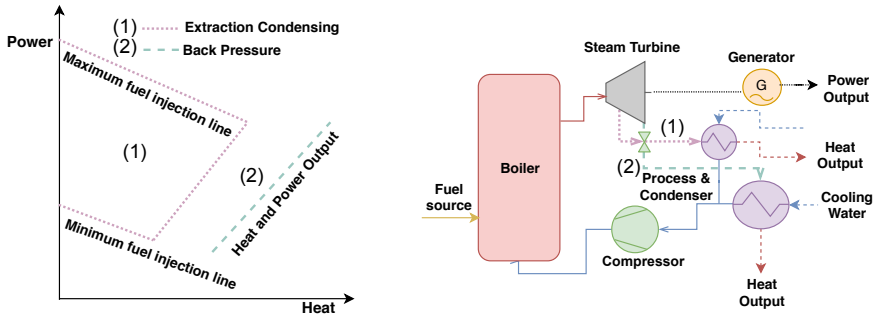

(a) Heat and power production region for back pressure and extraction condensing modes

(b) Configuration of steam-turbine cogeneration system

Figure 2.4: Schematic diagrams for steam-turbine cogeneration system and their heat-power extraction regions.

the CHP technology used by the DH systems consists of natural gas engines. The heat and power production ratio is linear and they usually operate at their maximum capacity to achieve the maximum efficiency point. Historically, they have used diesel as a fuel source but nowadays most of them are natural gas engines.

2.5.1.3 Gas Turbine Co-generation Systems

The deployment of gas turbines co-generation units has increased over the last years. These systems use the Brayton cycle, where the exhaust gas from the combustion is released at a high temperature and recovered for various purposes. They are fast, clean and very efficient when they work in combination with other technologies.

2.5.1.4 Combined Cycle Gas Turbine (CCGT) Co-generation System

CCGTs are usually large scale units that produce more than 100 MW of electricity. They combine both the Brayton and the Rankine cycle in the form of a gas turbine embedded in a heat recovery unit, that serves as a boiler, to produce steam to feed a large steam turbine. The exhaust gases, that are produced during the combustion in the gas turbine, are used to heat the steam, increase its

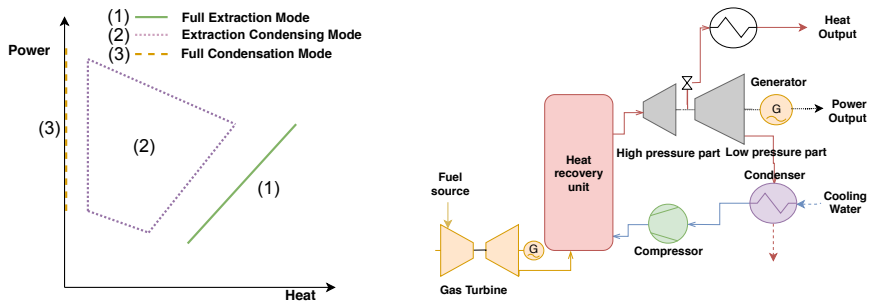

(a) Heat and power production region for bypass steam turbine

(b) Configuration of large CCGT cogeneration system

Figure 2.5: Schematic diagrams for combined cycle gas turbine (CCGT) cogeneration system and their heat-power extraction regions.

temperature and send it to the steam turbine. In the turbine there are different bodies and parts depending on the input pressure of the steam (high pressure part and low pressure part). Between these bodies, a fraction of the steam flow is extracted in order to feed the district heating network, leading to different power and heat production regions. In Paper B we formulate these steam extraction configurations and their optimal real-time operation, in order to efficiently integrate this technology in a power system with high penetration of wind power. The goal is to reduce the total system cost and the wind power spillage. Figure 2.5 provides a description of the operation and heat-power production region of this technology.

2.5.2 Fuels

In a future energy system, the use of conventional fossil fuels (oil, gas, and coal) will decrease in favor of renewable fuel sources such as biomass, biogas and hydrogen. Co-generation and more specifically, CHP units will play a significant role in this transformation. Nowadays, the CHP fuel mix in the EU is approximately 45% of natural gas followed by 20% of coal and 18% of renewable fuel sources [54]. The remaining part consists of non-combustion heat sources such as geothermal and solar thermal. The EU goal for the year 2050 is that around two-thirds of the total co-generation must origin from RES, using 44% of bio-based fuel and 18% of non-combustion sources. The remainder will origin from natural gas [55]. In Denmark, the situation is however slightly different as there is an equal mix of natural gas, coal and biomass used to produce heat and power [56], and this is expected to change in favor of bio-fuels and RES. The

Danish goal for bio-fuels and RES production is to reach 50% of the total mix by year 2030 and 100% by year 2050 [57]. Regarding biomass, many small and large CHP units fueled by this source have been installed in Denmark and many large CHP are converting from conventional fossil fuels to biomass (e.g. Avedøre power plant). This development will sooner or later result in a need for a structured biomass market, similar to the markets that already exist for natural gas, oil and coal. The way the biomass market functions today, is that prices are hedged between suppliers and consumers by agreeing biomass contracts where the prices are settled according to the calorific value of the product. These contracts are determined up to years in advance. In Paper E we propose a new methodology for large CHP units to select biomass (wood pellets) contracts, by taking uncertainty involved in the process into account and providing flexibility in the contracts in order to avoid surplus or deficit of stocks, which results in a reduction of cost for the CHP producer.

2.6 District Heating Systems and Electricity Markets

The addition of new heat production technologies (solar thermal, heat pumps and electric boilers) to the existing CHP units and fuel boilers, has increased the operational complexity of DH systems. To maximize the profits from the electricity market and therefore also minimize the heat production costs, the DH operator must operate these different units as one portfolio, taking advantage of the flexibility provided by the various units to always fulfill the heat demand and benefit from the electricity market trade. Furthermore, the extensive integration of wind power has led to consider the simultaneous operation of wind farms and CHP units [9] or the simultaneous operation of the components in DH units including RES as a virtual power plant (VPP) [58]. In Paper D we define a bidding strategy for a real DH system in Denmark that integrates wind turbines with CHP units and various heat production units into one system. Large DH systems (e.g., Greater Copenhagen) organize a heat dispatch before the electricity market takes place. In this heat dispatch, they present heat production offers for a number of supply points. The system operator analyzes if the given output plan is feasible and accepts or rejects it accordingly. This heat dispatch is only used in some very large DH systems and is therefore a very specific and local issue. Since the focus of this thesis lies on small-medium size DH units, we disregard any market operation regarding the heat supply and focus on satisfying the given heat demand. For a more detailed description on how a heat dispatch is organized, we refer the reader to [28] and [39].

To fully understand how DH producer operate in the electricity market, the next

section gives a basic overview of how liberalized electricity markets operate in the EU. Later on, we show how the operational planning for DH units is carried out.

2.6.1 Market structures and optimal market participation of DH producers

In order to present the market structure, we will focus on the NordPool market [59]. NordPool is comprised of 13 markets and trades in more than 12 European countries. Denmark is divided into two different bidding areas, called DK1 (West Denmark) and DK2 (East Denmark). *Energinet* is the transmission system operator (TSO) in Denmark. They operate the Danish power grid and they must guarantee the supply of power on a national level. The trade of electricity takes place in the following markets.

Day-ahead market:

Also known as the *Elspot market*. The producers and consumers present their offers for purchase or sales of electricity respectively before 12:00 CET for the hours on the following day, starting 12 hours later at 00:00 CET. Around 40 minutes after 12:00 CET, the bidding price for each hour of the next day is revealed and participants know at which hour they are committed to produce or consume, or on the contrary, not called to participate. The market is cleared in a merit order based on cost and participants can present several types of bids. First, "single hour orders" specify the purchase-sale volume and price at each hour. They can be price-dependent bids up to 62 price steps. Second, "block orders" consist of a specified volume for at least three consecutive time periods. These blocks can be added on top of other blocks, but just one of these can be activated, called "exclusive group offer". Finally, there are "flexibids", where participants decide on a maximum energy volume that they are willing to sell and a price limit for this. Thereafter the market operator determines the volume and price within the limit previously provided by the participant.

Reserve capacity market:

In Denmark it is the TSO who organizes the reserve capacity market. This market ensures that enough backup generation is available in case of a deviation in the production or demand side. Deviations can be caused by equipment

failures, unexpected fluctuation in RES production or unexpected changes in the consumption pattern. In this market, producers get paid by offering their availability to increase or decrease their power output according to the system requirements. This market is also cleared in a merit order based on costs. Furthermore, we distinguish between three types of reserves. First, the *primary reserve* ensures that the frequency of the system is at 50 Hz. These reserves are activated between 15 and 30 seconds after a deviation and can last up to 15 minutes. The primary reserve usually uses the inertia of the active generators to correct these imbalances. The *secondary reserve* activates the availability previously dispatched and must be deployed in a maximum of 15 minutes to complement the primary reserve and correct the imbalances in the system. Finally, the *tertiary or manual reserves* have the function of relieving the secondary reserve, and it is the TSO who decides which unit must participate (that are usually very fast and flexible generators such as small CHP units).

Intra-day markets:

Intra-day markets, also known as *Elbas*, are continuous markets that take place one hour before the energy is delivered. The trade takes place individually between two parties and despite most of the power is traded in the day-ahead market, sellers and buyers are able to trade volumes much closer to real time, bringing the market back in balance. The purpose of this market is also to make RES more competitive by reducing the uncertainty involved in the bidding process due to being closer to the hour of delivery.

Balancing Market:

This market is cleared 45 minutes before the energy is delivered, hence, it is also known as the "real-time market". This market allows producers and consumers to modify their program, adapt it to the system requirements and be compensated for those actions. This market is divided into, the regulating power market, where the TSO make use of the availability of the units to adapt to their system imbalances, and the balancing power market where the TSO sells or buys power according to the quantified imbalances [60].

For a more detailed explanation of the EU liberalized electricity markets, or more specifically the NordPool electricity market, we encourage the reader to see [61] and [62], presenting an extensive description of the market apart from conducting a comprehensive study of integrating renewable and demand-response into the electricity market.

In both Paper C and Paper D, we present bidding strategies for optimal participation of DH systems that operate a portfolio of different heat and power production units. The day-ahead bids play an essential role in the operation of the units and due to the uncertainty in electricity prices and RES production, they are very challenging to optimize. However, these are not the only bids that DH producers can make. Figure 2.6 describes the bidding process of a district heating producer. This process starts one day before the energy is delivered, by submitting their offers (one per hour) to buy or sell electricity from/to the day-ahead market. They present a volume of power and the price that the DH operator is willing to sell or purchase such volume. On top of this offer, they can add an availability offer for the reserve market. Most of the DH producers add this offer in case the offer presented to the day-ahead market gets rejected. This means that in case the day-ahead market offer is accepted, they usually don't offer availability. Furthermore, 45 minutes before the energy is delivered they can present offers for upward or downward regulation. These offers are named activation bids and are paid as the balancing marginal price. In NordPool, this price is higher than the day-ahead clearing price for upward regulation and lower if downward regulation is needed. In Denmark, in addition to these activation bids, there exists a special regulation [60]. This special regulation is a paid-as-bid agreement of the TSO with the balance responsible parties. Special regulation is usually activated due to bottlenecks in the power transmission grid. One example of special regulation is when the Danish system provides downward regulation in the case that excess production of wind power in North Germany congests the transmission lines. The German TSO pays this service as paid-as-bid. Danish producers do not know which kind of downward regulation service they are providing (activation or special regulation) until they get paid for the service. Moreover, medium and small DH system do not trade directly in the market, but they submit their offers to a trader that aggregates all bids of their portfolio of producers and consumers and optimize their bids to the market. These traders can also act as the balance responsible party and respond to the market fluctuations by managing all their assets.

2.6.2 Optimal production planning for DH units

Several techniques such as mixed integer linear programming, Lagrangian relaxation, fuzzy linear programming or heuristics have been proposed to efficiently operate the portfolio of heat production units that form a DH system [63]. Particularly, mixed integer linear programming prevails over the other techniques due to the smooth implementation of these programs with available commercial solvers. In addition, there exist commercial planning tools for DH systems such as *energyPRO* [64] which are also widely applied by researchers. To provide the operational planning of the studied energy systems, in this thesis we use mixed

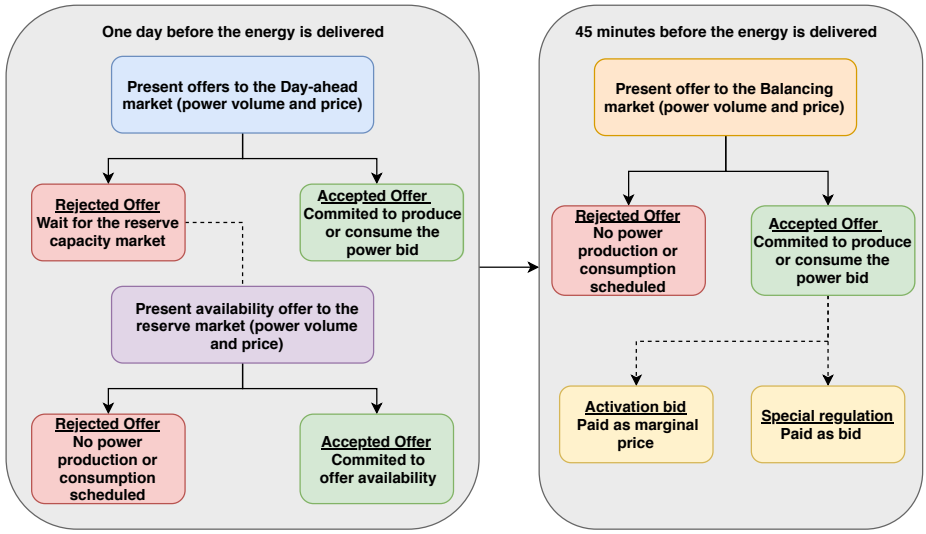

Figure 2.6: Usual electricity market bidding process of a district heating producer.

integer linear programming which is later described in Section 3.1.

2.6.3 Uncertainty affecting the operation of DH plants

Uncertainties in the operation of DH plants can appear in multiple ways. For example, to plan a new heat production technology to install in the DH unit, the variation of the fuel price (e.g., natural gas, oil or biomass) in the long-term is a critical factor to consider. However, the fuel price is not an important issue in order to plan the operation of the plant on a daily basis, because fuel prices do not fluctuate significantly from one day to another since fuel contracts are usually signed long time in advance. On the other hand, uncertainties such as volatility in electricity prices and solar radiation do not directly affect the design of the system but rather its daily operation. Therefore, it becomes critical for the DH producer to identify the uncertainties and how to deal with them. For instance, the volatility in electricity prices (especially in the regions with high penetration of wind power) arises from the volatility of RES production [65]. An efficient way for DH producers to hedge against the volatility of electricity prices and forecast errors is to participate in both day-ahead and balancing markets [66] and design optimal bidding tools that make this market participation more effective. For example, in Paper C, we develop an optimal bidding method for DH producers that help to protect the bids against price volatility. In the case

of a more extensive system such as power grids, the TSO must directly integrate the expected wind power production in the planning process. A similar situation for the DH producer is the solar thermal production. The DH operator must consider the uncertain solar power output when operating the system. As it was mentioned in Section 2.4.5, the growing installed capacity of solar thermal in DH systems throughout Europe, makes the optimal market participation and system operation to rely on knowing the solar production in advance. In Paper D, we quantify how the uncertain thermal solar output, volatility in electricity prices and wind power production affects the operation in a real DH system that includes a solar collector field as well as a wind farm.

Chapter 3

Methodologies

This chapter gives an overview of the methodology based on mathematical optimization theory. This methodology is the basis for the solution approaches presented throughout the thesis to provide decision support tools for the optimal operation of the analyzed energy systems.

Section 3.1 introduces the basic notation for mixed-integer linear programming problems. Section 3.2 describes the methodologies used for the decision-making process under uncertainty as well as forecasting and scenario generation methods used in this thesis as well as the methodologies employed to evaluate the uncertainty in the solutions. Finally, Section 3.3 describes different methodologies to solve and simplify large-scale optimization programs.

3.1 Mixed Integer Linear Programming

Mixed integer linear programming has been widely applied to solve problems in engineering and science [67, 68] and also for optimization problems in energy systems [69, 22]. A mixed integer linear program is a linear programming problem in which some of the variables are defined as integer variables [70]. Suppose

we have the following linear program.

$$\underset{x_j}{\text{Min.}} \quad \sum_{j=1}^{n} c_j x_j \tag{3.1}$$

$$\text{s.t} \quad \sum_{j=1}^{n} A_{i,j} x_j \geq b_i \qquad \forall i = 1, 2, ..., m \tag{3.2}$$

$$x_j \geq 0 \qquad \forall j = 1, 2, ..., n \tag{3.3}$$

where A is an m by n matrix, c is an n-dimensional row, b an m-dimensional column, and x is an n-dimensional column that is formed by variables. If we define some of the variables as integer values, we have a mixed integer linear program with the following standard form.

$$\underset{x_j, y_k}{\text{Min.}} \quad \sum_{j=1}^{n} c_j x_j + \sum_{k=1}^{p} h_k y_k \tag{3.4}$$

$$\text{s.t} \quad \sum_{j=1}^{n} A_{i,j} x_j + \sum_{k=1}^{p} G_{i,k} y_k \geq b_i \qquad \forall i = 1, 2, ..., m \tag{3.5}$$

$$x_j \geq 0 \qquad \forall j = 1, 2, ..., n \tag{3.6}$$

$$y_k \in \mathbb{N}^+ \qquad \forall k = 1, 2, ..., p \tag{3.7}$$

where G is an m by p matrix, h is a p-dimensional row, and y is a p-dimensional column of integer variables. In this specific case, vector y has a positive domain of natural numbers. In the models presented in this thesis, the only type of integer variables are binary variables with the feasible set $\{0, 1\}$.

3.2 Decision-making Under Uncertainty

The decision-making process in energy systems is subject to uncertainty. From politicians deciding on the long-term energy policy of a country to managers deciding the short-term scheduling of a power plant, uncertainty is always present. Decision-making under uncertainty helps to handle the uncertainty by its integration in the decision-making process. Many of the decision-making processes can be represented as optimization problems, where the decisions to be taken are described as a set of decision variables [22]. To model and characterize the uncertainty there exist several methods [71], however in this thesis we focus on stochastic programming which is one of the most used methodologies for integrating uncertainty into the decision-making problem.

3.2.1 Stochastic Programming

A stochastic program [11] is a mathematical program where some of the parameters of the model are uncertain. In this thesis, it is assumed that the uncertain parameters take values in a discrete probability space. Each of these values, represent one possible realization of the uncertainty. The set of the possible realizations are called *scenarios*. Stochastic programming consists of making a decision now for an uncertain future where the impact of this uncertain future is represented as an expectation of possible outcomes for the given decision. In this work, we focus on two-stage stochastic programming, where the decision-making process can be divided into two phases. For more than two phases, we have to formulate a multi-stage stochastic programming, however, these models are out of scope for this thesis. A typical linear two-stage stochastic program is defined as follows.

$$\underset{x,y_\omega}{\text{Min.}} \quad c^\top x + \sum_{\omega\in\Omega} \pi_\omega q_\omega^\top y_\omega \tag{3.8}$$

$$\text{s.t} \quad Ax \geq b \tag{3.9}$$

$$W_\omega y_\omega \geq h_\omega - T_\omega x \qquad \forall\omega = 1, 2, ..., \Omega \tag{3.10}$$

$$x, y_\omega \in \mathbb{R}^+ \qquad \forall\omega = 1, 2, ..., \Omega \tag{3.11}$$

where A and b are known parameters and h_ω, T_ω and W_ω are uncertain parameters. The decision variable vector x is known as *here-and-now* or *first-stage* decisions, which is taken before the uncertainty is revealed. Once the uncertainty reveals, the *wait-and-see* or *second-stage* decisions y_ω adapt to the realization of the uncertainty. This model uses a discrete number of possible realizations of the uncertainty, described using the scenario index ω. The second-stage decisions are depending on the scenario realization and therefore, they are called recourse. The total cost of the optimization problem is defined by the cost of the decisions $c^\top x$ and the expected cost of the recourse variables $\sum_{\omega\in\Omega} \pi_\omega q_\omega^\top y_\omega$, where π_ω represents the probability of occurrence of scenario ω.

Stochastic programming has been used in most of the papers within this thesis. In Paper A, we build a two-stage stochastic unit commitment problem using wind power production as uncertain input. Paper B uses stochastic programming with uncertain wind power production to integrate the operation of cogeneration units in the power system. The operation of the cogeneration units are considered as recourse function that they adapt to the uncertain wind power production. In Paper D stochastic programming is used to formulate the optimal bidding strategy for a complex district heating system that includes RES production. In this case the uncertainty comes from the electricity prices and the uncertain wind power and solar heat production. Finally, Paper E uses stochastic programming to integrate uncertain fuel prices, electricity prices and

heat demands for both short-term and mid-term planning problems.

3.2.2 Adjustable Robust Optimization

Robust optimization [72] is an optimization technique where the uncertain parameters are described using continuous uncertainty sets. In order to include the possible outcomes of the uncertainty, these uncertainty sets can be formed in several ways (as authors in [73] describe). In contrast to stochastic programming, the "classical" robust optimization approach provides a solution that is feasible for all possible realization of the described uncertainty and optimal for the worst-case realization of the uncertainty set. Within robust optimization we can find problems without recourse, where once the decision is taken, we can not adapt future decisions to the real outcome of the uncertainty. We can also find problems with recourse function, where the recourse takes the form of a continuous variable [74].

In this thesis we use an *adjustable robust optimization* approach which is formulated similar to a two-stage stochastic problem. The robustness is modelled optimizing the problem for the worst-case realization of the uncertainty, where the uncertainty is described as a finite set of scenarios. This type of robust optimization is described by authors in [22]. A typical adaptable robust optimization problem is defined as follows:

$$\underset{x}{\text{Min.}} \; c^\top x + \underset{q,h,T,W}{\text{Max.}} \; \underset{y}{\text{Min.}} \; q^\top y \tag{3.12}$$

$$\text{s.t} \; Ax \geq b \tag{3.13}$$

$$Wy \geq h - Tx \tag{3.14}$$

$$x, y \in \mathbb{R}^+ \tag{3.15}$$

$$\big(q, h, T, W\big) \in \mathbb{U} \tag{3.16}$$

In our case, the uncertainty set $\mathbb{U}$ is replaced by a finite number of scenarios ω. Therefore, the adaptable robust optimization problem (3.12)-(3.16), can be rewritten as:

$$\underset{x}{\text{Min.}} \; c^\top x + \underset{\omega \in \Omega}{\text{Max.}} \; \underset{y_\omega}{\text{Min.}} \; q_\omega^\top y_\omega \tag{3.17}$$

$$\text{s.t} \; Ax \geq b \tag{3.18}$$

$$W_\omega y_\omega \geq h_\omega - T_\omega x \qquad \forall \omega = 1, 2, ..., \Omega \tag{3.19}$$

$$x, y_\omega \in \mathbb{R}^+ \qquad \forall \omega = 1, 2, ..., \Omega \tag{3.20}$$

Using the column-and-constraint generation method proposed in [75], we can

reformulate the optimization problem (3.17)-(3.20) as:

$$\underset{x,y_\omega,\beta}{\text{Min.}} \quad c^\top x + \beta \tag{3.21}$$

$$\text{s.t} \quad \beta \geq q_\omega^\top y_\omega \qquad \forall \omega = 1, 2, ..., \Omega \tag{3.22}$$

$$Ax \geq b \tag{3.23}$$

$$W_\omega y_\omega \geq h_\omega - T_\omega x \qquad \forall \omega = 1, 2, ..., \Omega \tag{3.24}$$

$$x, y_\omega \in \mathbb{R}^+ \qquad \forall \omega = 1, 2, ..., \Omega \tag{3.25}$$

where, β is an auxiliary variable bounded from below by the set of linear constraints (3.22) and resembles the worst-case cost of the recourse function. We refer to the optimization problem (3.21)-(3.25) as the *scenario-based formulation of a two-stage robust problem*. We use this formulation of the adaptable robust optimization problem in Paper A and Paper B. For both cases we adapt the *conservativeness* of the robust solution using more than one auxiliary variable to formulate several worst-case recourse costs and calculate the expected value of these worst-cases scenarios in the objective function. We call the latter model the *hybrid stochastic-robust* problem and it is used in both Paper A and Paper B.

3.2.3 Evaluating the Solution of Stochastic Programming and Robust Optimization

Once it is decided to apply stochastic programming or robust optimization to solve a problem, the solution obtained must be evaluated. The objective is to analyze how much do we earn from using stochastic programming compared to other solutions (e.g., improve our forecasting, use a deterministic approach or solve our problem using heuristic methods). In this context, authors have proposed different ways to account for the value of integrating uncertainty in the decision-making process [11, 22]. In this section, we refer to three of them, the *expected value of perfect information* (EVPI), the *value of the stochastic solution* (VSS) and the *out-of-sample test*. For more information regarding the EVPI and VSS, we refer the reader to [22] where the authors provide a detail explanation of how these values are calculated.

Expected Value of Perfect Information (EVPI)

The EVPI provides an economic measure of how much the decision-maker should be willing to pay in return for having perfect information. This measure is calculated as the difference between the solution obtained from solving the stochastic

programming problem and the expected value when solving each scenario individually.

Value of Stochastic Solution (VSS)

The VSS is the gain that the decision-maker obtains from solving the problem using stochastic programming compared to the deterministic approach. The process to obtain this value is to solve a deterministic problem using the expected value of the scenarios as the uncertain parameter. Once this problem is solved, we fix the obtained first-stage decisions vector in the two-stage stochastic problem. The difference between the solution obtained from this latter problem and the solution of the stochastic one is the VSS.

The VSS can be also obtained with respect to the robust solution. In this case, the first-stage decisions obtained from the robust optimization problem are fixed into the stochastic one. The other way around is to use the vector of first-stage decisions obtained solving the stochastic programming problem and fix them in the adaptable robust optimization problem. This solution indicates how the value of the stochastic solution behaves when the expected worst-case realization of the uncertainties realizes. We call the analysis of these values *in-sample test*.

In-sample tests are carried out in Paper A and Paper B to evaluate the performance of the solutions obtained using stochastic programming and robust optimization. The logical outcome of this test is that the stochastic solution behaves better in terms of cost when the expected realization of the uncertainty occurs. On the other hand, the solution obtained solving the robust problem, behaves better than stochastic one when the worst-case realization of the uncertainty realizes. Using this in-sample test, we show how the hybrid method proposed in both Paper A and Paper B yields intermediate solution in terms of conservativeness. It means that this *hybrid* solution behaves better than the *stochastic* when the worst-case realization of the uncertainty realizes and better than the *robust* solution when the expected outcome of the uncertainty occurs. In this sense, in-sample test provide good estimates to control the conservativeness of the obtained solution.

Out-of-sample Test

In the previous section, we explained that the in-sample test evaluates the obtained solution using samples of the uncertainty that were considered when solving the optimization problem. An out-of-sample test evaluates the solution

using samples of the uncertainty that were not considered when addressing the optimization problem. In this way, the outcome provided by the out-of-sample test is more realistic in terms of performance than the outcome provided by the in-sample analysis. The most accurate data to perform an out-of-sample test are the real future observations of the uncertainty. In case no observations of the uncertainty are available, an alternative method to provide an out-of-sample is generating new samples of the uncertainty that were not used to solve the optimization problems. In all papers proposed in this thesis with the exception of Paper A, we test our results in an out-of-sample test. To be more specific, in Paper C, Paper D and Paper E we use real data provided by industrial partners and also available public data to validate our decision-making process. In Paper B we generate new values of the uncertainty that were not previously used in the optimization problem in order to evaluate our decisions.

3.2.4 Forecasting and Scenario Generation

In this section, we describe the forecasting and scenario generation techniques used throughout this thesis. We first describe the forecasting and scenario generation methods used to obtain electricity prices and heat loads prognosis. The forecasting and scenario generation for wind power production is explained afterwards. Finally, we provide the reader with some background about the clustering techniques that have been used in this thesis.

Forecasting Electricity Prices and Heat Loads

Time series models have been used to predict electricity prices in Paper C, Paper D and Paper E as well as predicting heat demand in Paper E. Data in electricity prices and heat loads have an internal structure (correlation, trend and seasonal variation) that time series models can detect and predict. To include this dependent structure, we use a class of models called *Autoregresive Integrated Moving Average* (ARIMA) models [76]. Nevertheless, not only the information contained in the time series is necessary to predict prices or loads. Some other external signals (e.g. weather conditions) that influence the present and past of the data should be taken into consideration as seasonal and exogenous variables [77]. In the following equation, we describe an ARIMA model that includes seasonality and external regressors describing the exogenous variables. This type of model is called SARIMAX (*Seasonal Autoregressive Integrated Moving Average models with exogenous factor*) and it has been successfully applied to predict day-ahead electricity prices and loads (see for instance [78],[79],[80] and [81]).

A SARIMAX model is defined as follows:

$$\phi_p(B)\Phi_P(B^s)\nabla^d\nabla_s^D y_t = \beta_k x_{k,t}^\top + \theta_q(B)\Theta_Q(B^s)\varepsilon_t$$

where y_t is the forecast variable, in this case the electricity price or heat load for time t, ε_t is the forecast error term (white noise), $\phi_p(B)$ is the autorregresive (AR) polynomial of pth-order, $\theta_q(B)$ is the moving average (MA) polynomial of qth-order, $\Phi_P(B^s)$ stands for the Pth-order seasonal AR term, $\Theta_Q(B^s)$ stands for the Qth-order seasonal MA term, ∇^d and ∇_s^D are the differentiating operator and the seasonal differentiating operator respectively, $x_{k,t}$ is the vector containing the k-th exogenous inputs integrated in the model for time t and finally β_k is the coefficient value for each k-exogenous input. The estimation and adjustment of ARIMA models are based on the Box-Jenkins methodology, which comprises a series of steps described in [82]. Furthermore, it is worth to mention that for electricity prices and load prediction, if the variance increases over time, we should make a logarithmic transformation of the data. If mean and variance are not constant in time (non-stationary process) we should differentiate the data to remove the trend and obtain a stationary mean.

The scenario generation process for time series models used in this thesis is based on the method used in [83], where they propose a scenario-generation technique applicable to time series models using a Monte Carlo simulation. The process consists of sampling the error term assuming that it follows a normal distribution to create a set of scenarios for the stochastic process.

Forecasting Wind Power Production

In this thesis, we use well known and straight-forward scenarios generation techniques and forecasting methods for wind power production that can be easily replicated for other authors. In Paper A and Paper B, for a given set of wind power point forecast at different sites, we follow the steps done in [83] and [84] considering the time dependency of different locations to create scenarios where the stochastic process is cross-correlated over time and locations. This is an important consideration to avoid bottlenecks and imbalances for the TSO when operating the power system.

In Paper D we use historical data for wind speed and wind power production to generate the wind power curve that is divided into different intervals where polynomial regressions are fitted. The procedure is the same as the one presented by the authors in [85].

Clustering Techniques for Scenario Reduction

To better describe the possible outcomes of the uncertainty, it is essential to create a large number of scenarios. However, this large number of scenarios can make the problem computationally intractable and therefore, it is important to find a balance between the input number of scenarios and its computational limitations. In addition, when we use scenario generation techniques, we obtain these scenarios by sampling the same error distribution, generating equiprobable scenarios. Clustering techniques help us to obtain scenarios which describe the properties of the entire sample appropriately. For a general overview of different clustering techniques, we encourage the readers to see [86], where most of the clustering techniques used in the thesis are described. More references can be found within the papers presented in this thesis.

Clustering techniques can be divided into two groups, *hierarchical* and *non-hierarchical*. Hierarchical clustering methods create different clusters of very similar scenarios nested to other large clusters of less related scenarios. Hierarchical methods are usually *agglomerative*, which means that the clusters are created in a bottom-up manner. Non-hierarchical clustering methods group the scenarios by partitioning the entire data set, rendering non-overlapping groups or clusters that have no hierarchical relation between them. One of the most well-known non-hierarchical clustering methods is the *k-means* algorithm [87], which selects k initial clusters, and assigns each data point to its closest center, where the center is the mean value of the points within the cluster. This process is repeated until the distance between centers and data points remains the same. In Paper B and Paper D we used *partition around medoids* (PAM) [88], a non-hierarchical clustering similar to *k-means*. Instead of minimizing the distance of the data points around representative means, it uses actual data points or *medoids* to define the centroids of the clusters. In Paper A, we make a comparison of how different clustering techniques perform in the solution of a two-stage stochastic problem. In this work, we built several clusters and use the scenarios within each cluster to provide a robust solution that minimizes the expected cost of the system.

3.3 Solution Techniques for Large-scale Programs

The modeling of some specific systems requires dealing with a vast number of variables and constraints that make the model too large to be tractable for some conventional solvers, especially when integer variables are added. MILP problems are solved using the branch-and-bound algorithm [89] where the solution

time can grow exponentially with the number of added variables. Consequently, there exist methods to speed up the solution process and help the decision-maker to obtain appropriate results. In the following, we present methods that reduce the computational burden of these problems, decreasing the solution time and solve them to optimality or to a solution that is good enough for our decision-making process.

3.3.1 Decomposition Techniques

Decomposition techniques are a general approach used to solve optimization problems. These techniques consist of breaking up one optimization problem into smaller ones and solving them separately, reconstructing the entire optimization problem in an iterative process. These techniques are able to solve the problem to optimality.

To apply decomposition techniques, we need to identify if the model has a structure that is amenable for decomposition. This structure can be recognized when two specific cases arise. The first case is when the model has complicating constraints and the second one when the model has complicating variables. The typical structure of a linear programming problem with complicating constraints is presented in equations (3.26)-(3.31), where if constraint (3.30) is relaxed or not enforced, problem (3.26)-(3.31) can be divide into three different optimization problems, i.e. one per decision variable x, y and z.

$$\underset{x,y,z}{\text{Min.}} \quad c_1^\top x + c_2^\top y + c_3^\top z \tag{3.26}$$

$$\text{s.t} \quad A_1 x \geq b \tag{3.27}$$

$$E_1 y \geq d \tag{3.28}$$

$$F_1 z \geq g \tag{3.29}$$

$$A_2 x + E_2 y + F_2 z \geq h \tag{3.30}$$

$$x, y, z \in \mathbb{R}^+ \tag{3.31}$$

On the other hand, the structure presented in the optimization problem (3.32)-(3.35) is a problem with complicating constraints.

$$\underset{x,y,z}{\text{Min.}} \quad c_1^\top x + c_2^\top y + c_3^\top z \tag{3.32}$$

$$\text{s.t} \quad A_1 x + F_1 z \geq b \tag{3.33}$$

$$E_1 y + F_2 z \geq d \tag{3.34}$$

$$x, y, z \in \mathbb{R}^+ \tag{3.35}$$

where if variable z gets a fixed value $\widehat{z}$, the problem can be decomposed into two different problems, one for decision variable x and the second one for decision

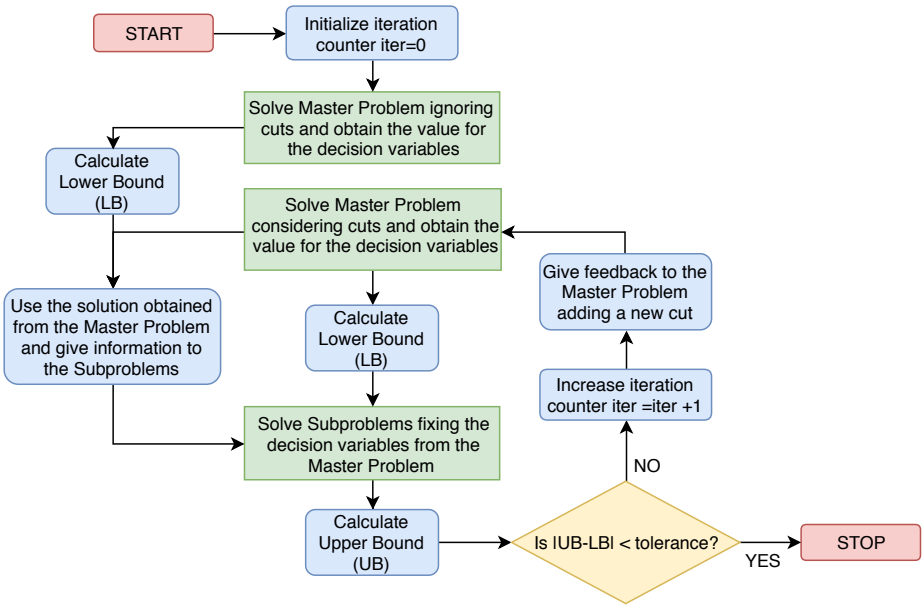

Figure 3.1: Diagram describing a typical decomposition process for two-stage stochastic programming problems.

variable y. The authors in [12] present several techniques to tackle this type of problems. However, they present Benders [90] and Dantzig-Wolfe [91] decomposition algorithms as the suitable techniques to solve problems with complicating variables and complicating constraints respectively.

From now on, we focus on decomposition techniques for problems with complicating variables. The way these type of decomposition techniques divide and solve the optimization problem is by creating one single master problem and one or more subproblems. These subproblems can be solved in sequence or in parallel. The solutions obtained from solving the subproblems are used to bound the master problem. At the same time, the subproblems are solved fixing the decision variables that come from the master problem. This method is repeated in an iterative process until the lower bound (usually the solution of the master problem) and the upper bound (form by the decision variable given by the master problem and a combination of the solutions given by the subproblems) reach a certain tolerance gap. When this happens we can say that we have reached the optimal solution for the optimization problem. Figure 3.1 depicts graphically a general approximation of how a decomposition technique for problems with complicating variables works.

Generally, decomposition techniques use the dual information of the subproblems to form cuts in the master problem. One cut or several cuts per iteration are added. These cuts are essentially a dual reconstruction of the objective function that iteratively bounded the problem until the solution space gets closer to the original one. In order to achieve accurate values in our cuts, strong duality must hold, therefore, all variables in the subproblems must be continuous.

Decomposition for Two-stage Stochastic Programming

In stochastic programming, the number of scenarios added to our problem is critical towards having a realistic representation of the uncertainty. However, a large number of scenarios can significantly increase the computational burden of our problem. In addition, as it was mentioned in Section 3.2.1, the decision variables in a two-stage stochastic programming problem can be divided into two groups (first-stage and second-stage variables). Since they are present at both stages, first-stage decisions are considered as complicating variables. Therefore, two-stage stochastic programs are very good candidates for applying decomposition techniques. First, because it can be useful to reduce the computational burden when a significant number of scenarios are included, and second because they present a structure that is very amenable for decomposition. In the following, we present the usual formulation of a dual decomposed two-stage stochastic programming problem with complicating variables assuming that the subproblems are always feasible. The stochastic optimization problem (3.8)-(3.11) presented in Section 3.2.1, is divided into a master problem (3.36)-(3.38) and Ω subproblems (3.39)-(3.41).

Master Problem:

$$\underset{x^i}{\text{Min.}} \quad c^\top x^i + \sum_{\omega \in \Omega} \pi_\omega \theta_\omega(x^i) \tag{3.36}$$

$$\text{s.t} \quad Ax^i \geq b \tag{3.37}$$

$$x^i \in \mathbb{R}^+ \tag{3.38}$$

All the decision variables have the superscript i which stands for the actual iteration number. As Figure 3.1 describes, these values are updated every iteration. In the Master problem, the first-stage decision vector x^i is the decision variable.

In the subproblems, the second-stage decision vector y^i_ω is the vector of decision variables and $\widehat{x}$ is given as an input from the master problem. In the master problem (3.36)-(3.38) we add the auxiliary function $\theta_\omega(x^i)$ that represents the cost of the second-stage decisions.

Subproblem for scenario ω :

$$\underset{y^i_\omega}{\text{Min.}} \quad q^\top_\omega y^i_\omega \tag{3.39}$$

$$\text{s.t} \quad W_\omega y^i_\omega \geq h_\omega - T_\omega \widehat{x} \quad : \gamma_\omega \tag{3.40}$$

$$y^i_\omega \in \mathbb{R}^+ \tag{3.41}$$

Once the subproblems are formulated, we need to define the auxiliary variable $\theta_\omega(x^i)$ as a function of the first-stage decision vector, therefore we use the dual formulation of the subproblems (3.39)-(3.41) given as follows.

Dual subproblem for scenario ω :

$$\underset{\gamma^i_\omega}{\text{Max.}} \quad (h_\omega - T_\omega \widehat{x} \ )^\top \gamma^i_\omega \tag{3.42}$$

$$\text{s.t} \quad W^\top_\omega \gamma^i_\omega \leq q_\omega \tag{3.43}$$

$$\gamma^i_\omega \in \mathbb{R}^+ \tag{3.44}$$

The function $\theta_\omega(x^i)$ in (3.36) can be replaced using the cut formulated in equation (3.47), where in this case x^i is a decision variable and the dual value γ^i_ω is given as a parameter $\widehat{\gamma}_\omega$. Notice that if strong duality holds, objective function (3.39) equals (3.42) and therefore, auxiliary variable θ^i_ω gets the cost value for the second-stage decisions at each scenario ω. The master problem with cuts is given by (3.45)-(3.48).

Master Problem:

$$\underset{x^i, \theta^i_\omega}{\text{Min.}} \quad c^\top x^i + \sum_{\omega \in \Omega} \pi_\omega \theta^i_\omega \tag{3.45}$$

$$\text{s.t} \quad Ax^i \geq b \tag{3.46}$$

$$\theta^i_\omega \geq (h_\omega - T_\omega x^i \ )^\top \widehat{\gamma}_\omega \qquad \forall \omega = 1, 2, ..., \Omega \tag{3.47}$$

$$x^i \in \mathbb{R}^+ \tag{3.48}$$

To calculate how the solution converges to optimal, we use the Upper Bound (UB), and the Lower Bound (LB) given by:

$$\text{LB} = c^\top x^{i*} + \sum_{\omega \in \Omega} \pi_\omega \theta^{i*}_\omega$$

$$\text{UB} = c^\top x^{i*} + \sum_{\omega \in \Omega} \pi_\omega (h_\omega - T_\omega \widehat{x} \ )^\top \gamma^{i*}_\omega$$

Most of the decomposition techniques used for two-stage stochastic programming problems follow a similar approach as the one presented above. Three

of the most used methods in literature to decompose two-stage stochastic programming problems are the L-Shaped method [92], Benders decomposition and Dual Dynamic Programming [93]. These methods also take care of the feasibility in the subproblems by formulating feasibility cuts. However, as it was said before, if integer variables exit at both levels (first and second stage) we can not ensure an optimal solution in our optimization problem due to the strong duality property.

3.3.2 Approximation methods for Two-stage Stochastic Programming

Like decomposition techniques, heuristics are applied when the size of the optimization problem does not allow conventional algorithms to solve these problems to optimality. The use of heuristics does not guarantee to find the optimal solution and consequently, their goal is to ensure suitable results in reasonable computation time according to the decision-maker's point of view.

For two-stage stochastic programs, several authors suggest decomposition techniques as heuristics. However, we count decomposition techniques as methods that can ensure optimality following the previously presented means in Section 3.3.1. Contrarily, we consider heuristics or approximation methods as those techniques that do not follow a regular decomposition scheme structure and in addition, they can not ensure optimality. To provide an example, one of the most well-known heuristic methods to solve two-stage stochastic programming is the Progressive Hedging algorithm [94], where the extensive form of the optimization problem is divided and solved individually per scenario. The variable decision vector is iteratively updated until we reach a solution that is good enough for the decision-maker.

In this thesis, new approaches that mix decomposition techniques and heuristics have been applied. The motivation was to explore new ways of defining decomposition techniques based on primal cuts that could exploit the properties of the scenarios. In addition, due to the introduction of integer variables in both the first and the second stage, the use of primal cuts is an advantage since no strong duality property must hold. Therefore, in Paper A we propose two variants of the same decomposition technique that are based on primal cuts to ensure a robust solution by selecting scenarios that provide the worst-case dispatch cost. These two decomposition techniques resemble the structure presented in Figure 3.1. They are able to solve the model by providing similar results compared to using the extensive form of the problem saving a significant amount of solution time. In Paper B, we make use of heuristics to improve the decomposition technique proposed in Paper A achieving significant results in terms of solution

time and robustness of the decision-making process.

Finally, in Paper E, we propose a planning problem that due to its dimension and characteristics, an extensive formulation of the problem is totally intractable. Therefore, we use an approximate solution approach based on two phases. The first phase solves a planning problem for a mid-term horizon (one year). The scheduled plan obtained from solving the first phase is later used to solve a short-term operational planning problem. This proposed approach allows integrating the various levels of details in the optimization problem including integer variables that make the extensive form of the problem intractable. Our method obtains solutions that are accurate enough for the proposed decision-making process.

Chapter 4

Basic Models & Key Findings

In this chapter, we briefly describe some highlights of the research presented in Part II of this thesis. This section is divided into two parts. In section 4.1, we introduce the stochastic unit commitment problem providing a simplified example in Section 4.1.1 that will help the reader to understand some of the findings achieved in Paper A and Paper B. These findings are later presented in Sections 4.1.2 and 4.1.3, respectively. In Section 4.2, we tackle the operation of a DH system where we show a demo case in Section 4.2.1 to provide a better comprehension of the findings presented afterwards in Sections 4.2.2, 4.2.3 and 4.2.4 for Paper C, Paper D and Paper E, respectively.

4.1 Two-Stage Stochastic Unit Commitment Problem

The integration of energy systems requires a proper scheduling of the available energy generation and consumption units. These units consist of various agents and technologies in which certain technical and operational conditions must be satisfied to optimally plan the scheduling. The family of mathematical models that formulate the necessary constraints and provides solutions that minimize the costs, is named Unit Commitment (UC) problems. When uncertainty is

involved in the operation of the system, i.e., RES production or uncertain demand, the UC problem can be adapted to describe this uncertainty. There exists a vast literature describing this problem, proposing solution methods as well as different techniques to deal with uncertainty (e,g., see [95] and [96] and references therein).

One of these methods consists of using stochastic programming to define the uncertainty via scenarios. These scenarios are aggregated into the unit commitment problem to describe the possible outcomes of the uncertainty. The formulation of this problem is called Stochastic Unit Commitment (SUC) (first introduced in [97]). The advantages of using the SUC to integrate uncertain power production have been widely studied and discussed in the literature (see for instance the references provided in Paper A and Paper B). Therefore, in this thesis, we use the SUC in many variants to formulate our problems and study the effect of the uncertainty in the integration of the proposed energy systems. The formulation of a two-stage SUC under uncertain RES production in its general form writes as the stochastic programming problem previously presented in the model (3.8)-(3.11), where the vector of first-stage decisions x is formed by the commitment decisions (turn on and off the units). The second-stage decision vector y_ω, comprises the actions that can be adopted in the system to hedge against the realization of the uncertainty (e.g., upward and downward production, load shedding or turn on fast generators). In this problem, the uncertainty is modeled through a finite set of scenarios that represent the possible outcomes of the RES production.

4.1.1 Simplified example of the Two-stage Stochastic Unit Commitment (SUC) Problem

In this section, we present a simplified version of a two-stage SUC resembling the model in Paper A and Paper B but excluding several technical details. The idea is to provide the reader with a simplified overview of how the decision given by the unit commitment is highly affected when uncertainty is considered. In this context, we provide both in-sample and out-of-sample tests to evaluate our decision-making process and to introduce those concepts for a better survey of the findings presented in this chapter. For this specific example, we use a power system that consists of six nodes, three loads, three conventional and one stochastic generators. Figure 4.1 provides the technical data for the lines as well as the location of the loads and generators and the % consumption of each load compared to the total load profile (shown in Figure 4.2b). Table 4.1 provides the remaining technical data used in this test case and Table 4.2 the nomenclature. In addition, we use three wind power production scenarios depicted in Figure 4.2a with a probability of occurrence of $\pi_{\omega 1} = 0.45$, $\pi_{\omega 2} = 0.25$ and $\pi_{\omega 3} = 0.30$.

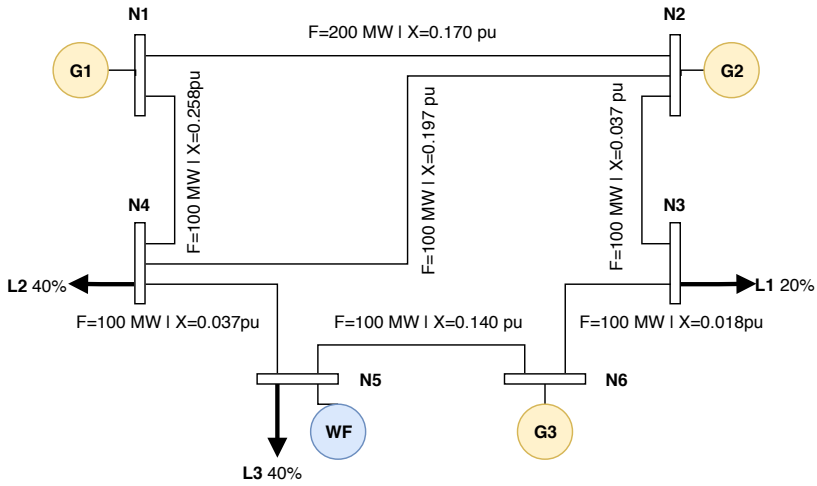

Figure 4.1: Illustration of the 6-Bus system used in our case study where the reactance and maximum capacity of the lines as well as the % of consumption per load is depicted.

Table 4.1: Technical characteristics and power production costs of the units

Unit	C_g^F [\$/h]	C_g^V [\$/MWh]	C_g^{SU} [\$]	C_g^{SD} [\$]	$\overline{P}_g$ [MW]	$\underline{P}_g$ [MW]
g1	177	13.5	100	50	220	100
g2	130	40	200	100	100	10
g3	137	17.7	0	0	40	10

The cost for involuntary load curtailment (C^L) amounts to 500\$ per MWh.

The simplified two-stage SUC presented in this section formulate as follows. The objective function (4.1) minimizes the expected total system cost, where $\mathcal{H}$ is the vector that contains the first-stage decisions indicating the commitment plant of the units and $\mathcal{W}$ is the vector containing the second-stage decisions which defines the real-time operation of the units (see Table 4.2).

$$\underset{\mathcal{H},\mathcal{W}}{\text{minimize}} \quad \sum_{t\in T}\sum_{g\in G}\left(C_g^F u_{g,t} + C_g^{SU} y_{g,t} + C_g^{SD} z_{g,t}\right) \tag{4.1}$$

$$+ \sum_{\omega\in\Omega} \pi_\omega \left[\sum_{t\in T}\sum_{g\in G} C_g^V P_{g,t,\omega} + \sum_{t\in T}\sum_{l\in L} C^L L_{l,t,\omega}^{SH}\right]$$

Table 4.2: Notation

	Sets
T	Set of time periods t
N	Set of nodes n
G	Set of conventional generation units g
F	Set of stochastic power production units f
L	Set of loads l
Ω	Set of scenarios ω
F_n	Set of stochastic power production units located at node n
L_n	Set of loads connected at node n
G_n	Set of conventional generation units located at node n
M_n	Set of nodes $m \in N$ that are connected to node n by a transmission line
	Parameters
C_g^F, C_g^V	Fixed/variable production cost of conventional generation unit g
C_g^{SU}, C_g^{SD}	Start-up/Shut-down cost of conventional generation unit g
$L_{l,t}$	Demand for load l at time t
$X_{n,m}$	Reactance of line $n-m$
$\overline{F}_{n,m}$	Maximum flow capacity of line $n-m$
$\overline{P}_g, \underline{P}_g$	Maximum/minimum power production of conventional generation unit g
C^L	Cost of involuntary load curtailment
$W_{f,t,\omega}$	Power production from stochastic generation unit f at time t in scenario ω
π_ω	Probability of scenario ω
	First-stage variables ($\mathcal{H}$)
$u_{g,t}$	Binary variable equal to 1 if unit g is online at time t and 0, otherwise
$y_{g,t}$	Binary variable equal to 1 if unit g is starting up at time t and 0, otherwise
$z_{g,t}$	Binary variable equal to 1 if unit g is shutting down at time t and 0, otherwise
	Second-stage variables ($\mathcal{W}$)
$P_{g,t,\omega}$	Power produced by conventional generation unit g at time t in scenario ω
$L_{l,t,\omega}^{SH}$	Power curtailment from load l at time t in scenario ω
$W_{f,t,\omega}^{SP}$	Power curtailment from stochastic power production unit f at time t in scenario ω
$\delta_{n,t,\omega}$	Voltage angle at node n, time t in scenario ω
β	Auxiliary variable for the worst-case dispatch cost

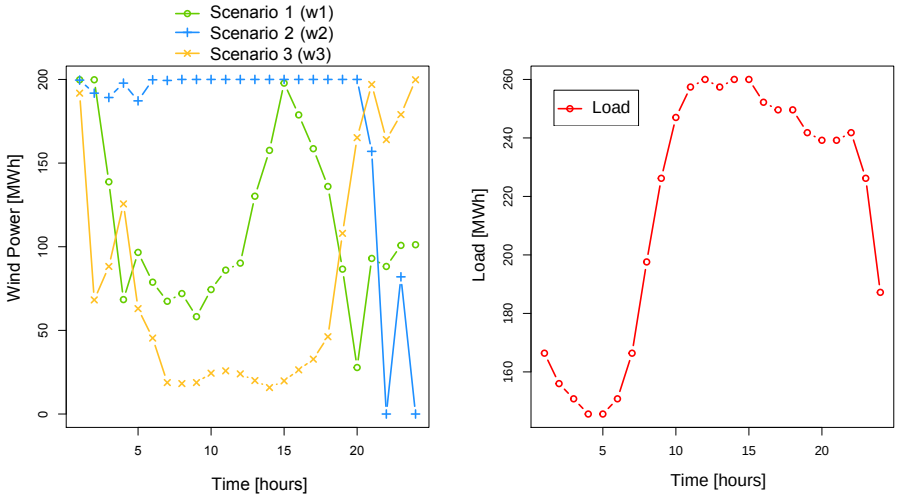

(a) Scenarios for wind power production [MWh]

(b) Total System Load Profile [MWh]

Figure 4.2: Wind power production scenarios and total load profile for 24 hours used to run our case study.

Constraints (4.2)-(4.3) define the commitment status of the units.

$$y_{g,t} - z_{g,t} = u_{g,t} - u_{g,t-1} \qquad (\forall g, \forall t) \qquad (4.2)$$

$$y_{g,t} + z_{g,t} \leq 1 \qquad (\forall g, \forall t) \qquad (4.3)$$

The power balance in the system is given by Equation (4.4).

$$\sum_{g \in G_n} P_{g,t,\omega} - \sum_{l \in L_n} L_{l,t} + \sum_{l \in L_n} L^{SH}_{l,t,\omega} + \sum_{f \in F_n} W_{f,t,\omega} - \sum_{f \in F_n} W^{SP}_{f,t,\omega} = \sum_{m \in M_n} \frac{(\delta_{n,t,\omega} - \delta_{m,t,\omega})}{X_{n,m}} \qquad (\forall n, \forall t, \forall \omega \in \Omega) \qquad (4.4)$$

The maximum and minimum amount of power production is bounded by constraint (4.5).

$$\underline{P}_g u_{g,t} \leq P_{g,t,\omega} \leq \overline{P}_g u_{g,t} \qquad (\forall g, \forall t, \forall \omega \in \Omega) \qquad (4.5)$$

Constraints (4.6) limits the power that flows between the lines.

$$-\overline{F}_{n,m} \leq \frac{(\delta_{n,t,\omega} - \delta_{m,t,\omega})}{X_{n,m}} \leq \overline{F}_{n,m} \qquad (\forall n, m \in M_n, \forall t, \forall \omega \in \Omega) \qquad (4.6)$$

The maximum load shedding and wind spillage are limited by constraints (4.7) and (4.8).

$$L^{SH}_{l,t,\omega} \leq L_{l,t} \qquad (\forall l, \forall t, \forall \omega \in \Omega) \tag{4.7}$$

$$W^{SP}_{f,t,\omega} \leq W_{f,t,\omega} \qquad (\forall f, \forall t, \forall \omega \in \Omega) \tag{4.8}$$

Finally, constraints (4.9)-(4.10), define the domain for the decision variables.

$$P_{g,t,\omega}, L^{SH}_{l,t,\omega}, W^{SP}_{f,t,\omega} \geq 0 \qquad (\forall g, \forall l, \forall f, \forall t, \forall \omega \in \Omega) \tag{4.9}$$

$$u_{g,t}, y_{g,t}, z_{g,t} \in \{0, 1\} \qquad (\forall g, \forall t) \tag{4.10}$$

In addition to a SUC, we can also formulate the UC as an *adaptable robust optimization* problem given by (4.11)-(4.13).

$$\underset{\mathcal{H},\mathcal{W},\beta}{\text{minimize}} \quad \sum_{t\in T}\sum_{g\in G}\left(C^F_g u_{g,t} + C^{SU}_g y_{g,t} + C^{SD}_g z_{g,t}\right) + \beta \tag{4.11}$$

$$\text{s.t.} \quad \beta \geq \sum_{t\in T}\sum_{g\in G} C^V_g P_{g,t,\omega} + \sum_{t\in T}\sum_{l\in L} C^L L^{SH}_{l,t,\omega}, \quad \forall \omega \in \Omega \tag{4.12}$$

$$(4.2) - (4.10) \tag{4.13}$$

where β is the auxiliary variable that represents the worst-case dispatch cost. We solve the stochastic problem (4.1)-(4.10) and the robust adaptable problem (4.11)-(4.13) using the three wind power production scenarios depicted in Figure 4.2a. In addition, we solve a deterministic unit commitment problem where we only include the expected value of the wind power production and no scenarios. This value is calculated as $\widehat{W}_{f,t} = \sum_{\omega\in\Omega} \pi_\omega W_{f,t,\omega}$. The first-stage decisions (commitment plan) obtained for the three different problems as well as the commitment and total system costs are shown in Figure 4.3.

In this case, we are not interested in evaluating the total system cost of the three different cases, but how the provided commitment decisions perform once the uncertainty realizes and what the value of incorporating uncertainty in our decision-making process is. Thus, we perform both an in-sample and out-of-sample test to evaluate the solutions obtained decisions.

In-sample Test

As it was explained in Section 3.2.3, we first calculate the EVPI and the VSS. In this case, the EVPI gets a value of 6594$. It means that the decision-maker is willing to pay 13.7% of the total system cost to obtain perfect information of

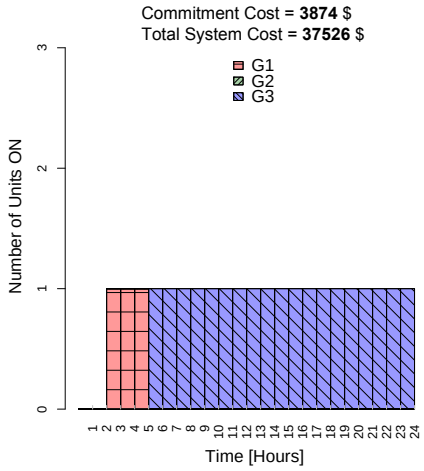

(a) Commitment solution and system costs for the *deterministic* problem

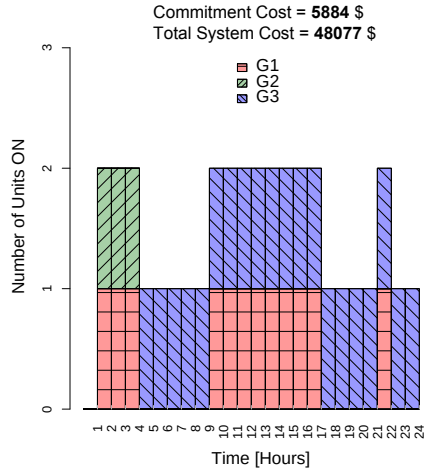

(b) Commitment solution and system costs for the *stochastic* problem

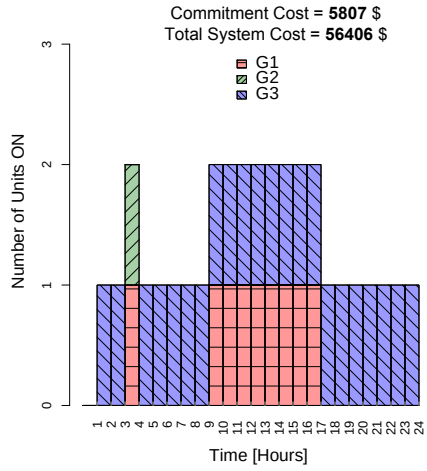

(c) Commitment solution and system costs for the *adaptable robust* problem

Figure 4.3: First-stage or commitment solution obtained by solving the SUC using the *deterministic*, *stochastic* and *adaptable robust* approach.

Table 4.3: In-sample test for the analyzed system

Model	Expected System Cost [$]	Worst-case System Cost [$]
Stochastic Commitment	48077	58968
Robust Commitment	51736	56406

the wind power production. The VSS obtains a value of 50120$ which translates on 133% of the total system cost for the deterministic approach. This means that the value of using stochastic programming is very high. The reason is that the commitment solution provided by the deterministic problem (see Figure 4.3a) is optimal just in case the expected value of the scenarios realizes. In case the realization of the uncertainty deviates from its prediction, we face load curtailments that are highly penalized. To evaluate the value of using stochastic programming or adaptable robust optimization, we show in Table 4.3 an in-sample test. The solution of the stochastic problem is evaluated when the wort-case realization of the uncertainty (i.e., the scenario that yields the highest balancing cost) realizes. In addition, we can observe how the commitment solution provided by the robust optimization problem behaves when the expected outcome of the uncertainties occurs. Moreover, the results from Table 4.3 show how the stochastic commitment is more risk-neutral in the sense that if a worst-case realization of the uncertainty realizes, the obtained solution yields higher total system operating cost than the robust commitment. On the other hand, it shows how the robust commitment provides a more risk-averse and conservative solution. In this case, the robust solution protects us against odd realizations of the uncertainty but in case the system cost performed as expected, the solution deteriorates.

Out-of-sample Test

In order to perform an out-of-sample test, we evaluate the solution of the deterministic, stochastic and robust commitments for 300 different realizations of the wind power production based on real daily observations. Figure 4.4 shows the distribution of the system cost for the observations obtained from the three different commitment solutions. We can see the worst distribution in terms of cost for the solutions obtained using the deterministic commitment compared to the stochastic and robust. The difference between the distributions obtained by the robust and stochastic unit commitment may not look as significant as the difference to the deterministic. However, if we look in more detail, and calculate the mean values for the first half quantile (from 0% to 50% of the observations), the value of the stochastic and robust commitment is 53711$ and

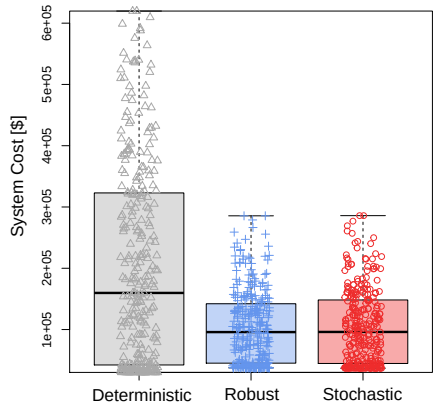

Figure 4.4: Boxplot of the observations obtained for the deterministic, robust and stochastic commitment solving the UC problem for 300 different realizations of wind power production.

54305$ respectively and if we take the mean values for the second half quantile (from 50% to 100% of the observations), the values for the stochastic and robust are 154474$ and 153751$ respectively. Thus, the out-of-sample test confirms the results obtained in the in-sample test (Table 4.3) in the sense that the robust commitment solution provides a more risk-averse commitment, that protects better in those cases when the operating costs are higher. In case the uncertainty reveals providing lower operating costs, the stochastic commitment gives better results than the robust due to the risk-neutral nature of this decision. Finally, if we compare the solutions obtained using the deterministic commitment with the stochastic and robust, the out-of-sample test confirms the result obtained in the VSS showing the high value of integrating uncertainty in the decision-making process.

4.1.2 Managing the uncertainty in large-scale programs using the SUC

As it is mentioned in Section 3.3 the use of a large amount of data to define the uncertainty may lead to intractable optimization problems. Therefore, in Paper A we propose a novel approach that decomposes the optimization problem and simplifies the set of scenarios used to represent the uncertainty. The pro-

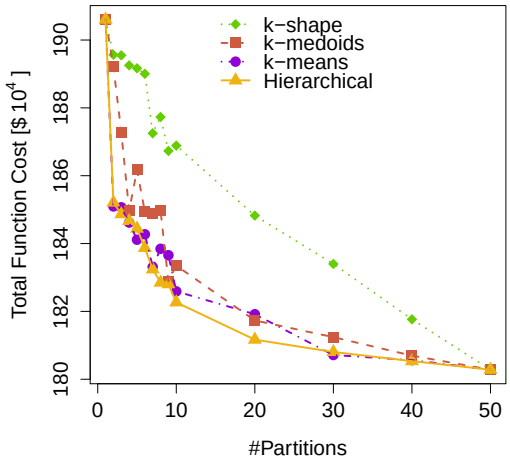

Figure 4.5: Figure A.1 presented Paper A shows the total system cost of the *Hybrid* UC for different clustering techniques and number of partitions.

posed solution divides the set of uncertainty using clustering techniques. Once the clusters (or partitions of the uncertainty set) are created, we solve a SUC problem, where the worst-case dispatch cost of each cluster is represented using an auxiliary variable. The expected operating cost of the system is calculated using the expected value of these worst-case dispatch costs. We named this model *Hybrid* UC problem. Figure 4.5 shows the operating costs of the *Hybrid* UC using a different number of partitions and clustering techniques. The figure shows how the Hybrid UC provides solutions that intermediate in terms of cost compared to the SUC and the *adaptable robust* UC. Indeed, if we only use one partition for the entire set of uncertainties, the model is the same as the *adaptable robust* UC. On the contrary, if the value of the partitions equals the number of scenarios, the *Hybrid* UC is indeed the SUC. The structure of the Hybrid UC is very amenable for decomposition and parallelization, and therefore we exploit it accordingly. In the same Paper A, we propose two parallelization and decomposition schemes based on primal cuts that drastically reduce the solution time. In addition, using an in-sample test, we evaluate the solution obtained by these two decompositions and parallelization techniques. Table 4.4 displays some of the results presented in Table A.2 from Paper A.

In Table 4.4, we can see how the Variant 1 and the Variant 2 of the Scenario Partition and Decomposition Algorithm (SPDA1 and SPDA2), that are both

Table 4.4: Solution time and in-sample test performed in Table A.2 obtained from Paper A where EC and WC are respectively the Expected and Worst-case system costs for all the given commitments or first-stage decisions.

		1 P (Robust)	3 P	5 P	8 P	10 P	50 P (Stochastic)
Time [min]	**raw HUC**	1322.7	687.6	767.4	721.6	788.1	140.2
	SPDA1	28.6	32.7	64.8	102.8	107.7	
	SPDA2		51.1	33.6	81.5	80.1	
WC [$\$10^4$]	**raw HUC**	190.6035	190.6821	190.6360	190.8254	190.7072	191.8024
	SPDA1		190.6345	190.6426	190.6831	190.7932	
	SPDA2		190.7367	190.6573	190.6494	190.6978	
EC [$\$10^4$]	**raw HUC**	180.4169	180.4438	180.4131	180.3176	180.3397	180.2738
	SPDA1		180.4005	180.3980	180.3250	180.3448	
	SPDA2		180.4123	180.3832	180.3297	180.3562	

described in detail in Algorithm 1 and 2 in Paper A respectively, reduce the solution time compared to the extensive formulation of the SUC. Moreover, the two decomposition approaches provide robust solutions that perform relatively well in terms of expected and worst-case system operating cost. The reason is that the algorithm selects those scenarios that better represent the worst possible outcome of the recourse function by reconstructing the optimization problem using only the chosen scenarios throughout the iterative process.

To assess the value of the *Hybrid* UC and its proposed decomposition-and-parallelization schemes, we go a step further in Paper B. Here, we present a model that integrates binary variables at both first-stage and second-stage decision vectors, drastically increasing the computational burden of the problem. Consequently, a decomposition technique such as SPDA1 that uses primal cuts is a good candidate to simplify the solution of the problem. In order to improve the solution in the SPDA1 algorithm, presented in Paper A Algorithm 1, we make use of heuristics to determine the optimal number of partitions for the specific problem. The entire process is described in Algorithm 3 in Section B.6 in Paper B. The obtained first-stage decisions vector for the extensive form of the SUC, *adaptable robust* UC and *Hybrid* UC using the improved version of the SPDA1 is analyzed using an out-of-sample test shown in Figure 4.6, which is a reconstruction of the results presented in Table B.5 (Paper B). For the sake of visibility, the highest 15% of the values have been removed. The solution time obtained is presented on the x-axis in brackets. In the same Figure, we can see how the commitment solution provided by the *Hybrid* UC problem using the improved SPDA1 behaves relatively well in terms of costs compared to the stochastic and robust commitments, achieving lower solution times. The details

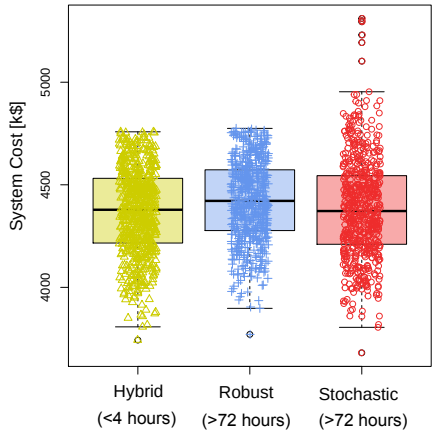

Figure 4.6: Boxplots for the lowest 85% observations from the values presented Table B.5 in Paper B. We display the values for the *Hybrid*, *Stochastic* and *Robust* commitment decisions. In brackets, we can find the solution time for each specific model.

of this process and its solution are presented in Paper B.

We can conclude this section saying that the use of the SUC problem has been successfully applied in this thesis to create new methods in the form of algorithms to deal with uncertainty in large-scale programs. These methods are capable of simplify the uncertainty set while maintaining the value of the stochasticity in the optimization problems.

4.1.3 Assessing the value of cogeneration units in power systems with high penetration of RES using the SUC

The study proposed in Paper B uses the SUC to integrate the operational modes of large-scale CHP units into the power system. These operational modes consist of different steam extraction configuration in the steam turbine of these large cogeneration units. The goal is to evaluate the effect of a real-time operation of these modes to hedge against the uncertain wind power production and provide more flexibility in the power system. To propose a realistic evaluation, we integrate the operation of the CHP units in the SUC using a realistic represen-

Table 4.5: Simplified version of Table B.3 in Paper B that performs an in-sample test comparing the results obtained by solving the stochastic and robust models for the expected (EXP) and worst-case (WC) cost of the recourse function using the operation modes of the CHP units as first-stage (1st) or second-stage (2nd) decisions. The table also shows the amount of hours that the units have been operating using different modes.

	EXP [10^3\$]	WC [10^3\$]	Time [h]	Gap [%]
Stochastic (2nd)	**4229.830**	5719.115	72	1.957
Stochastic (1st)	4230.465	6901.632	72	1.021
Robust (2nd)	4294.168	5687.532	72	1.463
Robust (1st)	4305.223	**5671.541**	40.89	0.999
EXP	m_0 [h]	m_1 [h]	m_2 [h]	m_3 [h]
Stochastic (2nd)	40	55.22	0.56	0.22
Stochastic (1st)	45	51	0	0
Robust (2nd)	45	46.82	4.12	0.06
Robust (1st)	47	44	4	1
WC	m_0 [h]	m_1 [h]	m_2 [h]	m_3 [h]
Stochastic (2nd)	40	42.9	11.36	1.74
Stochastic (1st)	45	51	0	0
Robust (2nd)	45	40.40	9.62	0.98
Robust (1st)	47	44	4	1

tation of the Danish transmission grid. In Table 4.5 (obtained from Table B.3 in Paper B), we display the results of an in-sample test. The obtained results show how using a real-time operation of the modes can provide more flexibility to the units helping the system to adapt to the RES imbalances and reduce the total system operating costs.

4.2 Operation of DH Systems

As it was mentioned in Section 2.3, the integration of the DH and power systems is achieved through the participation of the DH units in the power market. In this section we propose a small case to illustrate the operation of a conventional DH unit responding to different prices incentives from the market. Moreover, we summarize some of the findings in this thesis regarding bidding strategies under uncertainty for DH systems as well as fuel contracting mechanisms that consider uncertain future demand within the contracting process.

Table 4.6: Notation

Sets	
$\mathcal{H}$	Generation units $h \in \{\text{CHP, GB, EB}\}$
$\mathcal{H}^{\text{CHP}}$	Combined heat and power units {CHP}
$\mathcal{H}^{\text{EB}}$	Power-to-heat units {EB}
$\mathcal{H}^{\text{GB}}$	Heat-only production units {GB}
$\mathcal{T}$	Set of time periods t
Parameters	
$\overline{Q}_h/\underline{Q}_h$	Maximum/minimum heat generation for unit h [MW-heat]
$\overline{P}_h/\underline{P}_h$	Maximum/minimum power production or consumption for unit h [MW-el]
$\overline{S}/\underline{S}$	Maximum/minimum heat storage in tank [MWh-heat]
C^h	Heat production cost for unit h [DKK/MWh-heat]
φ^h	Power-to-heat ratio for unit h [MWh-heat/MWh-el]
L^{Heat}	Heat demand [MWh-heat]
λ_t	Electricity prices at time t [DKK/MWh-el]
S^0	Initial heat storage [MWh-heat]
Variables	
$q_{h,t}$	Heat production from unit h at time t
$p_{h,t}$	Power production from unit h at time t
$u_{h,t}$	Binary variable equal to 1 if unit h is on at time t, and 0 otherwise

4.2.1 Simplified example of the optimal operation of a DH system

To show how to model the optimal planning of a DH system using mixed integer linear programming, we use the case depicted in Figure 4.7, which consists of a small DH plant that integrates one heat only unit (gas boiler), one CHP unit, one electric boiler, and one heat tank storage.

The operational costs and the technical characteristics of the units can be found in Table 4.7. Figure 4.8 depicts the electricity price forecast and heat demand for 24 hours, where we have two different scenarios of electricity prices, using a high and a low price profile. The notation used in this example is shown in Table 4.6.

We use a mixed integer linear program to solve the optimal planning for this system. Note that this is a deterministic model and the two electricity prices scenarios presented in Figure 4.8a are solved separately. Objective function

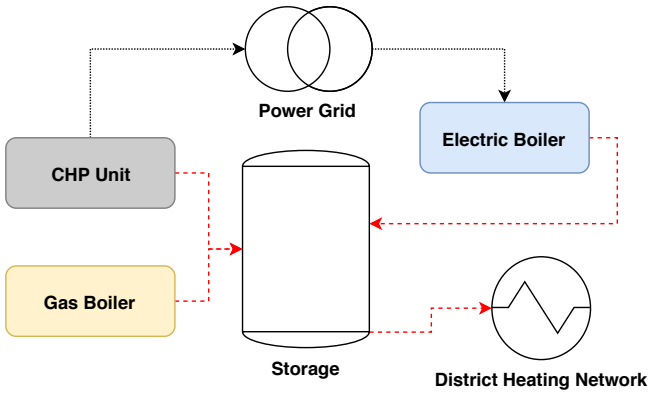

Figure 4.7: Configuration of DH system use as case example

Table 4.7: Technical characteristics and heat production costs of the units

Unit	C	$\overline{Q}$	$\overline{P}$	φ	$\overline{S}$
CHP Unit (CHP)	600	3	2.5	1.20	-
Gas Boiler (GB)	350	10	-	-	-
Electric Boiler (EB)	250	3	3	1	-
Storage (ST)	-	-	-	-	30

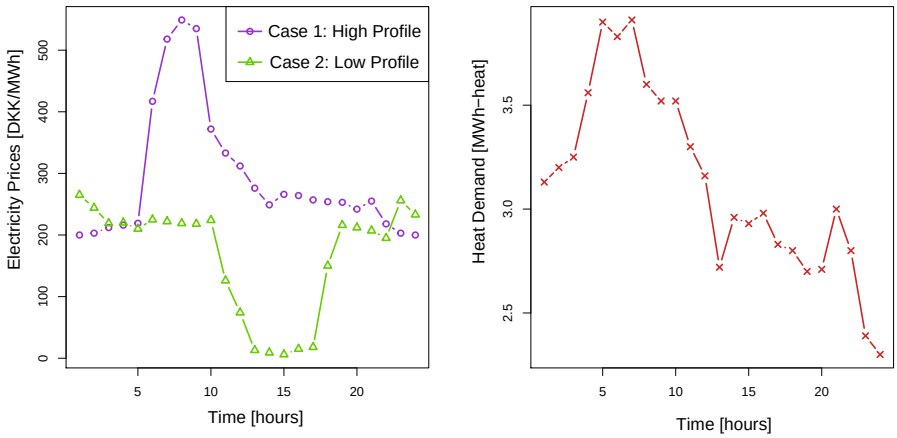

(a) Electricity prices profiles (high and low) [DKK/MWh-el]

(b) Heat consumption profile [MWh-heat]

Figure 4.8: Electricity price (high and low) and heat demand profiles for a time period of 24 hours

(4.14) minimizes the total heat production costs for the entire day. The function includes the electricity prices (λ_t) at each time period that must be discounted to the heat production cost of the CHP unit and summed up to the cost of producing heat in the electric boiler.

$$\text{Min.} \sum_{t\in\mathcal{T}}\Big[\sum_{h\in\mathcal{H}^{\text{CHP}}}\big(C^h-\lambda_t\varphi^h\big)q_{h,t}+\sum_{h\in\mathcal{H}^{\text{EB}}}\big(C^h+\lambda_t\varphi^h\big)q_{h,t}+\sum_{h\in\mathcal{H}^{\text{GB}}}C^h q_{h,t}\Big] \tag{4.14}$$

Constraint (4.15) limits the heat production to the capacity of the unit.

$$q_{h,t}\le\overline{Q}_h \qquad (\forall h\in\mathcal{H},\forall t\in\mathcal{T}) \tag{4.15}$$

The ratio between power and heat production is described in the set of equations (4.16), where we assume linearity between the generated heat and power. The power production of the CHP units is limited by constraint (4.17). For this specific case, we assume that if the CHP unit is activated it must produce at its peak in order to achieve the maximum efficiency. Therefore, $\underline{P}_h=\overline{P}_h$ for $h\in\mathcal{H}^{\text{CHP}}$. We also assume that the production of the electric boiler can range from 0 to its maximum, thus $\underline{P}_h=0$ for $h\in\mathcal{H}^{\text{EB}}$.

$$q_{h,t}=\varphi^h p_{h,t} \qquad (\forall h\in\mathcal{H}^{\text{CHP}}\cup\mathcal{H}^{\text{EB}},\forall t\in\mathcal{T}) \tag{4.16}$$

$$\underline{P}_h u_{h,t}\le p_{h,t}\le\overline{P}_h u_{h,t} \qquad (\forall h\in\mathcal{H}^{\text{CHP}}\cup\mathcal{H}^{\text{EB}},\forall t\in\mathcal{T}) \tag{4.17}$$

The following constraints and equations model the heat storage of the system. Equations (4.18) determine the heat storage level for all time periods $t\in\mathcal{T}$. In case $t=1$, s_{t-1} is replaced by parameter S^0 that represents the heat tank storage level at the beginning of the time horizon. In this example we assume a value of 10 MWh-heat. Constraint (4.19) limits the storage level to its maximum capacity and equality (4.20) avoids emptying the storage at the end of the time horizon. For security reasons, producers limit the minimum heat storage ($\underline{S}$) to a certain level. However, in this case, we decide to define $\underline{S}=0$.

$$s_t=s_{t-1}+\sum_{h\in\mathcal{H}}q_{h,t}-L_t^{\text{Heat}} \qquad (\forall t\in\mathcal{T}) \tag{4.18}$$

$$\underline{S}\le s_t\le\overline{S} \qquad (\forall t\in\mathcal{T}) \tag{4.19}$$

$$s_{|\mathcal{T}|}=S^0 \tag{4.20}$$

The solution displayed in Figure 4.9 shows how the system reacts for two different price signals. When the electricity prices are high, the system uses the CHP unit to satisfy the heat demand while selling the power generated maximizing its profit, as Figures 4.9a and 4.9c show. On the contrary, Figures 4.9b and 4.9d show how the low electricity prices influence the producer to obtain power from the grid and turn on the electric boiler.

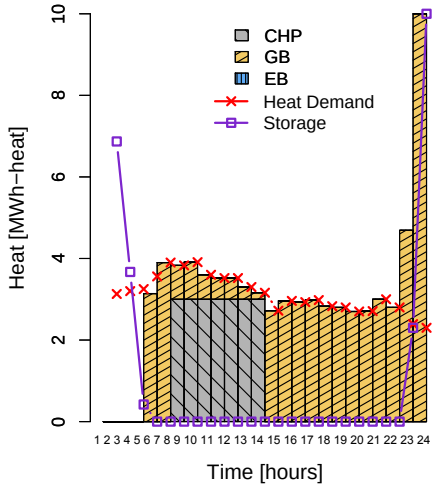

(a) Optimal heat production for the high electricity profile

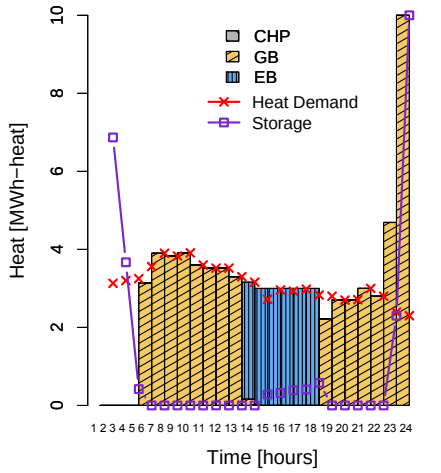

(b) Optimal heat production for the low electricity profile

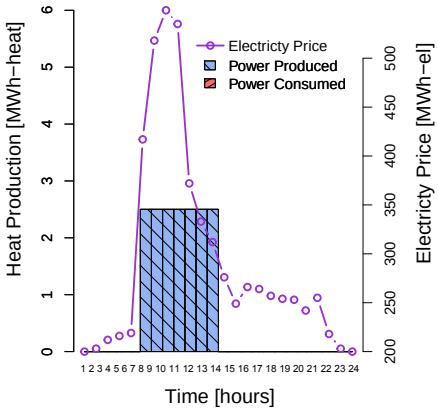

(c) Optimal power production and consumption for the high electricity profile

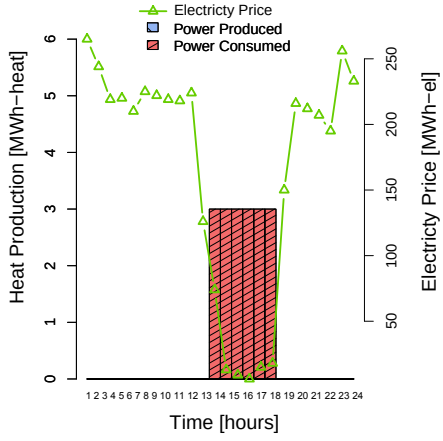

(d) Optimal power production and consumption for the low electricity profile

Figure 4.9: Optimal operation for the planning problem (4.14)-(4.20) using two different profiles of electricity price and same heat demand.

Larger DH systems require more sophisticated optimization problems than the one presented in the example. In addition, the optimal operation of these systems in the various electricity markets requires analyzing how the participation in these markets affects the heat production plan of the system, forcing the producer to update the heat production plan every time they submit a new offer. Consequently, as in power systems planning problems, the use of mixed integer linear programs to optimize the heat production of DH plants can be advantageous for the DH system operator. Specially, nowadays, due to the integration of solar thermal collectors and the high volatility in electricity prices, the uncertainty involved in the operation of the system suppose a significant challenge for its optimal operation.

4.2.2 Managing electricity price uncertain trading in the day-ahead market for DH systems

In the daily operation of a DH system, the operators must submit offers to the day-ahead market one day before the delivery of energy takes place. These operators rely on electricity price forecasts to submit their offers. The volume of power and the corresponding price is usually determined by the difference of producing heat with the CHP unit and the cost of producing the same amount of heat with the base load unit. This type of bidding, which is quite extended among DH producers, places the bids only when it is profitable according to the given electricity price forecast, leaving the remaining hours of the day with no offers. Consequently, in case the real electricity prices deviate from the forecast values, the submitted bids can be very inaccurate. Therefore, in Paper C we develop a bidding method for the day-ahead market based on replacing conventional heat production by CHP units. The power produced by the CHP units is traded in the day-ahead market at the marginal costs.

Figure 4.10 (obtained from Figure C.6a in Paper C) consist of an *out-of-sample* test using 144 real data of day-ahead electricity prices for different months and regions in the NordPool market. The figure provides the total system cost for these 144 months in terms of distance to the solution obtained having perfect information in day-ahead electricity prices. The results displayed in this figure show how our bidding method (HURB) provides very accurate bids that hedge against the uncertain electricity prices obtaining profits that are very close to perfect information. In addition, our method outperforms other bidding methods obtained from the literature applied in our case study. These methods compete in the same market framework like the one we have in NordPool and besides they have been developed for price takers, they are not designed for DH producers specifically but mostly for thermal generators. These results point out the need for new bidding techniques that account the flexibility of the DH

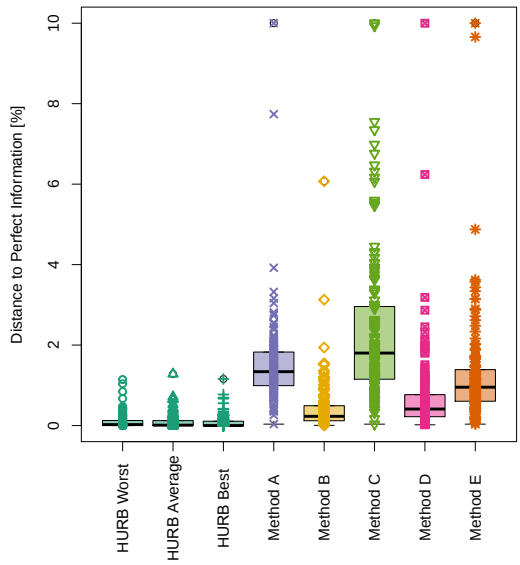

Figure 4.10: Figure C.6a presented in Paper C compares the value of using different bidding methods for the day-ahead market.

units towards improving their integration in the power system by an optimal participation in the electricity market.

4.2.3 Managing electricity price and RES production uncertain by trading in sequential markets

To study how a DH system that includes RES production is affected by the uncertainty in its daily operation, we use a bidding strategy based on stochastic programming in Paper D. This bidding strategy (proposed by the authors in [98]) can optimally exploit the flexibility of DH systems to create price dependent bids for the day-ahead and balancing markets while incorporating RES uncertain production in the planning process.

The obtained results in Paper D show that the use of stochastic programming to create price dependent bids helps to reduce the total system costs compared to the classical approach where the operator places their bids according to the electricity price forecast. Moreover, the participation of the DH system in the balancing market translates in more profits by adapting the production of the

units to the market requirements. Thus, in Paper D, we present four different cases of how a DH system with RES production can provide upward and downward regulation in the balancing market using the flexibility of the units. The way the system provides upward regulation is by selling the excess wind power production that was not sold in the day-ahead market and by turning-on the CHP units when the upward regulation price is high enough to make this operation profitable. In order to provide downward regulation, the system can activate the power-to-heat units (electric boiler in the case presented in Paper D) and consume power at the downward regulating price. Another mechanism to provide downward regulation is to use the wind power sold at the day-ahead market and in case of wind power shortage; we can buy this lack of wind power at the downward regulating price.

4.2.4 Managing uncertainties in the biomass supply contracting process

As mentioned in Section 2.5.2, the use of biomass for heating and electricity production purposes is being incentivized by favorable taxation schemes. Therefore, CHP units and biomass boilers can benefit from this situation by replacing conventional fossil fuels by biomass. Many types of biomass can be used to produce heat and power, however the most efficient one is wood chips. The use of large quantities of wood chips involves a constant supply that heat and power producers must plan in advance to ensure enough production to cover the heat demand. The wood chips and biomass, in general, have seasonal peak demands where the price increases according to this demand. Moreover, the wood chips cannot be stored for long periods of time because the moisture content decreases and, thus, the efficiency of the fuel. Consequently, DH producers must be very accurate with the amount of biomass they must contract. This situation motivated us to design contracting mechanisms, using stochastic programming, that allow to hedge against the uncertainty of fuel demand involved in the contracting process. For a CHP producer, the demand of biomass is determined by the heat load (e.g. in some CHP plants, the fuel demand for a cold winter is 50% higher than the heat demand for a mild winter) and by the electricity prices which determine when the CHP unit will be activated.

This work is presented in detail in Paper E, where the application of stochastic programming allows the use of options in the contracts that provide flexibility in the supplied amounts, helping to incorporate the unforeseen uncertainty in the fuel supply process. Figure 4.11 is taken from Paper E and shows how the stochastic model makes use of the options (represented with black vertical lines) while the deterministic approach neglects the use of these options. Figure 4.12, that is a reconstruction of Table E.9 presented in Paper E, shows the values

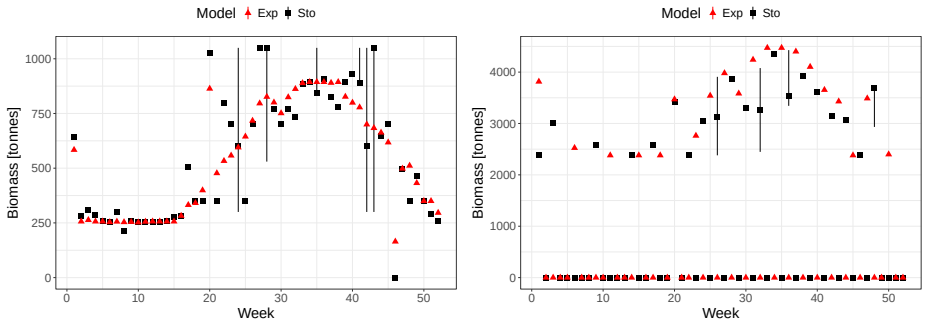

(a) Municipality A **(b)** Municipality B

Figure 4.11: Figure E.3 compares the stochastic and deterministic biomass contracts for the case study presented in Paper E.

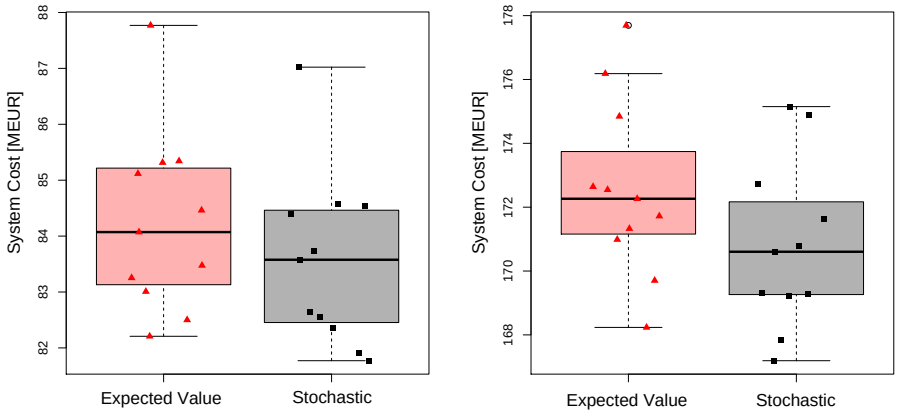

(a) Municipality A **(b)** Municipality B

Figure 4.12: Total system cost for an out-of-sample test comparing the Stochastic and Expected Value contract selection. This figure is obtained from the data displayed in Table E.9, Paper E.

obtained from an out-of-sample test. The out-of-sample test evaluates the solution for the contracts obtained using the stochastic and deterministic problems for 22 different realizations of the uncertainty obtained from real observations (11 per municipality). The figure shows how applying stochastic programming reduces the total system cost by making use of the options and adjusting the contract amounts to the real realization of the uncertainty.

Chapter 5

Conclusions & Future Research

In this thesis, we propose several solution approaches for planning problems for the operation of integrated energy systems while dealing with a large amount of uncertain data. On the one hand, we focus on decision-making problems of companies that provide both heat and power commodities to design bidding and operation strategies that consider the uncertainty involved in the process. On the other hand, we also deal with the perspective of the system operator that has to operate energy systems with a vast amount of uncertain RES production.

5.1 Contributions

Paper A and Paper B consider the point of view of a system operator, where the focus is on large power systems that integrate a high share of RES. In Paper A, we propose a new formulation of the stochastic unit commitment problem under uncertainty that allows us to find commitment plans that behave well in terms of the expected and the worst-case system operating cost. The new formulation uses clustering techniques to divide the entire set of scenarios into partitions. From each partition, we select the scenarios that result in the worst-case system operating cost. The total system cost is obtained by calculating the

expectation of these scenarios. Therefore, we can control how conservative our solution is by specifying the number of partitions. On top of that, we develop a decomposition scheme that enables an easy parallelization of the process to solve the proposed unit-commitment efficiently. The obtained results highlight how the proposed solution improves the optimality of the solution found while reducing the computational time.

This method is extended and improved in Paper B where a unit commitment problem that includes several large-scale CHP units, conventional thermal generators and a large amount of wind power production is proposed. In this problem, we model in particular the operational modes of the CHP units and integrate them in the two-stage stochastic unit commitment problem. Results show how a real-time operation of these modes can help to integrate more wind power production reducing the total system costs. In addition, we show how the proposed improved technique from Paper A reduces the computational time and provide robust unit-commitment solutions that perform well for unexpected outcomes of the uncertainty. Consequently, based on Paper A and Paper B, for computationally very challenging problems due to binary variables at both the first and second stages as well as significant amounts of uncertain data, our decomposition-and-parallelization approach presents a suitable method to reduce the solution time of the problem. Moreover, this solution provides robust unit commitments that behave well in terms of the expected and worst-case system operating cost.

Regarding optimal coupling of DH units and power systems, we propose operational planning and bidding strategies for companies owning a portfolio of CHP and power-to-heat units in Paper C and Paper D. We create the bids for these operators under the price-taker assumption. In Paper C, we only consider the day-ahead market to design a new bidding strategy that bases the power production offers on replacing heat production from heat-only units by CHP generation in an iterative process. We simulate results for an entire year of operation on a daily basis using real data from the market and applying different lengths of receding horizon. To evaluate our results, we compare our method in an out-of-sample test with several bidding strategies proposed in the literature for price-takers. The obtained results show how our method results in the lowest cost and has a higher percentage of won bids, yielding solutions that are very close to the ones provided assuming perfect information in future electricity prices.

In Paper D, we go a step forward by integrating RES in the bidding process and using sequential bidding strategies to correct the uncertainty produced by these RES. In this problem, we use stochastic programming to create price dependent bids for the day-ahead market. Once this market is cleared, we also submit offers to the balancing market at each hour of the following day considering the

actual operation of the DH system. In addition, we evaluate how the different uncertainties affect the bidding process in our system. The results point out that the main driver that affects the costs of the system is the uncertain electricity price followed by uncertainty in power production, while uncertainty in solar heating production does not affect the cost of the system due to heat storage. In this paper, we also assess how special agreements between the system operator and the DH producer can significantly reduce the total system cost. This agreement consists of using the power produced by the wind power generators owned by the DH company to activate the electric boiler applying a different taxation scheme to this type of electricity consumption. Furthermore, we evaluate the use of the flexibility provided by DH systems to offer balancing regulating power. The results show the economic benefits of trading in this type of markets.

Finally, this thesis presents a trading strategy for biomass-fueled large CHP units in Paper E. In this work, we propose a new design for contracts that include options. These options consist of paying the supplier for the availability of biomass in case the amount previously agreed in the contracts is altered. This strategy allows the producer and supplier to hedge against the uncertainty involved in the contracting selection process. This selection of contracts is performed a long time before the fuel is delivered, and therefore, the quantities agreed in those contracts may change from the actual need at the moment of producing the energy. To solve this problem, we make use of stochastic programming to integrate the uncertainties that affect the required fuel amount. In addition, due to the large size of the problem and the number of binary variables involved, we divide the approach into two phases. First, the biomass contract selection problem and, second, the operational planning. This structure resembles the planning process in practice. To assess our results, we perform an out-of-sample test using real data that evaluates one year of system operation. The obtained results show that stochastic programming is required for the system to purchase options and that the use of these options translates into lower costs.

To conclude this section of contributions, we can state that the use of decision-making under uncertainty tools can improve the operational process of companies that intend to deliver different energy commodities such as heat and power in an integrated energy system environment. We show how considering the uncertainties in the planning process can significantly reduce the system operating cost.

5.2 Future Research

The models proposed in this thesis can be the basis for further research.

Concerning the hybrid decomposition-and-parallelization approach proposed in Paper A and improved in Paper B, we see several ways to continue the research and consolidate this technique as a good alternative for two-stage stochastic problems with binary variables at both stages and uncertain data. First, future research should focus on proving that the optimality is not lost when solving the decomposed and parallelized version of the *Hybrid* problem compared to its extensive form. Second, this methodology requires a thorough comparison with other solutions obtained using different risk aversion methodologies. Finally, it would be of great interest to extend the application of this technique for all kind of two-stage stochastic problems under a significant amount of uncertain data using more sophisticated sets of uncertainty obtained by using probabilistic forecasting instead of point forecast.

Towards the improvement of bidding strategies for district heating producers in a competitive electricity markets setup, we envision several extensions of our work. Regarding the novel bidding strategy proposed in Paper C, the use of this method can be extended to systems that integrate a portfolio of renewable heat and power production units. In addition, other bidding strategies that account for the technical restrictions of the generating units must be taken into account; like for example block bids. About the sequential bidding strategy proposed in Paper D, this work can be applied for trading companies that manage a wide portfolio of units. This problem would need two major considerations that should be addressed properly for future research. First, if this portfolio of heat and power production units is big enough to affect the electricity price, we can not consider the situation of price-taker anymore but need a price-maker perspective. Consequently, we must consider problems using equilibrium constraints (bi-level programming problems) to integrate the electricity price into our optimization process. Second, the size of these problems may lead to lengthy computational times, and new decomposition-parallelization techniques that fit with the problem formulation must be explored. Needless to say that not only heating and power units must be taken into consideration in this bidding process, but also the integration of other energy systems including the optimal operation of water treatment plants or electric vehicles.

The supply planning strategy proposed in Paper E opens up several paths for future research to study the possible business opportunities for the biomass suppliers. This business opportunity is given by providing optimal prices for the options in contracts based on the expected demand of future fuel and possible reallocation of fuel supplies. In this case, again bi-level programming can be used

to define the prices of these options according to the expected future needs of the heat and power plants. Concerning the heat and power producer perspective, a broader portfolio of fuels should be considered in the optimization problem. This portfolio should minimize the total system cost considering a sustainable mix of fuels. Furthermore, future research should compare the two-phase approach with other decomposition techniques for two-stage stochastic programs from literature in more detail.

In general, future research should focus on integrating even more energy systems by bringing together more technologies and energy vectors into unified large-scale optimization problems. These optimization problems must co-optimize the entire production and consumption of these units minimizing the total system cost and integrating a larger share of RES.

Bibliography

[1] European Commission. *2030 Energy Strategy*. https://ec.europa.eu/energy/en/topics/energy-strategy-and-energy-union/2030-energy-strategy. (Accessed on 07/27/2018).

[2] European Environment Agency. *Renewable energy in Europe 2017 — Recent growth and knock-on effects*. file:///C:/Users/igbl/Downloads/Renewable%20energy%20in%20Europe%202017.pdf. (Accessed on 07/27/2018).

[3] International Energy Agency. *Energy Policies of IEA Countries - Denmark 2017 Review*. http://www.iea.org/publications/freepublications/publication/EnergyPoliciesofIEACountriesDenmark2017Review.pdf. (Accessed on 07/27/2018).

[4] H. Lund et al. "Smart energy and smart energy systems". In: *Energy* 137 (2017), pp. 556–565.

[5] M. F. Ruth and B. Kroposki. "Energy systems integration: an evolving energy paradigm". In: *The Electricity Journal* 27.6 (2014), pp. 36–47.

[6] P. A. Østergaard. "Reviewing optimisation criteria for energy systems analyses of renewable energy integration". In: *Energy* 34.9 (2009), pp. 1236–1245.

[7] S. Weitemeyer et al. "Integration of Renewable Energy Sources in future power systems: The role of storage". In: *Renewable Energy* 75 (2015), pp. 14–20.

[8] M. O'Malley et al. "Energy systems integration: defining and describing the value proposition". In: *Contract* 303 (2016), pp. 275–3000.

[9] A. Hellmers et al. "Operational strategies for a portfolio of wind farms and CHP plants in a two-price balancing market". In: *IEEE Trans. Power Syst* 31.3 (2016), pp. 2182–2191.

[10] P. Meibom et al. "Value of electric heat boilers and heat pumps for wind power integration". In: *Wind Energy: An International Journal for Progress and Applications in Wind Power Conversion Technology* 10.4 (2007), pp. 321–337.

[11] J. R. Birge and F. Louveaux. *Introduction to stochastic programming*. Springer Science & Business Media, 2011.

[12] A. J. Conejo et al. *Decomposition techniques in mathematical programming: engineering and science applications*. Springer Science & Business Media, 2006.

[13] B. Kroposki et al. *Energy Systems Integration: A Convergence of Ideas [Online]. NREL*. 2012.

[14] H. Ravn et al. *Balmorel*. http://www.balmorel.com/images/downloads/balmorel-a-model-for-analyses-of-the-electricity-and-chp-markets-in-the-baltic-sea-region.pdf. (Accessed on 08/07/2018).

[15] Loulou et al. *Documentation for the TIMES Model*. https://iea-etsap.org/docs/Documentation_for_the_TIMES_Model-Part-I_July-2016.pdf. (Accessed on 08/07/2018).

[16] H. Madsen et al. "Integrated energy systems; aggregation, forecasting, and control". In: *DTU International Energy Report 2015*. Technical University of Denmark (DTU), 2015, pp. 34–40.

[17] R. G. Junker et al. "Characterizing the energy flexibility of buildings and districts". In: *Applied Energy* 225 (2018), pp. 175–182.

[18] H. A. Nielsen and H. Madsen. "Modelling the heat consumption in district heating systems using a grey-box approach". In: *Energy and Buildings* 38.1 (2006), pp. 63–71.

[19] R. Halvgaard et al. "Economic model predictive control for building climate control in a smart grid". In: *Innovative Smart Grid Technologies (ISGT), 2012 IEEE PES*. IEEE. 2012, pp. 1–6.

[20] R. Halvgaard et al. "Waste Water Treatment Plants and the Smart Grid". In: *DTU Sustain Conference 2014*. Technical University of Denmark (DTU). 2014.

[21] H. Madsen et al. "Control of electricity loads in future electric energy systems". In: *Handbook of Clean Energy Systems* (2015), pp. 1–26.

[22] J. M. Morales et al. *Integrating renewables in electricity markets: operational problems*. Vol. 205. Springer Science & Business Media, 2013.

[23] Eurostat. *Electricity statistics 2017*. https://ec.europa.eu/eurostat/statistics-explained/index.php?title=File:Electricity_statistics_2017_(in_GWh)-T1.png. (Accessed on 10/26/2018).

[24] European Commission. *Natural gas demand in Europe in 2017 and short term expectations*. https://www.oxfordenergy.org/wpcms/wp-content/uploads/2018/04/Natural-gas-demand-in-Europe-in-2017-and-short-term-expectations-Insight-35.pdf. (Accessed on 08/07/2018).

[25] J. D. Sharples. "The importance of gas storage facilities in the European gas and power markets". In: *International Journal of Environmental Studies* 73.3 (2016), pp. 369–378.

[26] C. Ordoudis et al. "Exploiting flexibility in coupled electricity and natural gas markets: A price-based approach". In: *PowerTech, 2017 IEEE Manchester*. IEEE. 2017, pp. 1–6.

[27] Danish Energy Agency. *Regulation and planning of district heating in Denmark*. https://ens.dk/sites/ens.dk/files/contents/material/file/regulation_and_planning_of_district_heating_in_denmark.pdf. (Accessed on 08/09/2018).

[28] L. Mitridati and P. Pinson. "Optimal coupling of heat and electricity systems: A stochastic hierarchical approach". In: *Probabilistic Methods Applied to Power Systems (PMAPS), 2016 International Conference on*. IEEE. 2016, pp. 1–6.

[29] N. O'Connell et al. "Regulating power from supermarket refrigeration". In: *Innovative Smart Grid Technologies Conference Europe (ISGT-Europe), 2014 IEEE PES*. IEEE. 2014, pp. 1–6.

[30] M. Zugno et al. "A bilevel model for electricity retailers' participation in a demand response market environment". In: *Energy Economics* 36 (2013), pp. 182–197.

[31] J. Tomić and W. Kempton. "Using fleets of electric-drive vehicles for grid support". In: *Journal of power sources* 168.2 (2007), pp. 459–468.

[32] H. Lund and P. A. Østergaard. "Electric grid and heat planning scenarios with centralised and distributed sources of conventional, CHP and wind generation". In: *Energy* 25.4 (2000), pp. 299–312.

[33] D. Connolly et al. "Heat Roadmap Europe: Combining district heating with heat savings to decarbonise the EU energy system". In: *Energy Policy* 65 (2014), pp. 475–489.

[34] H. Lund et al. "4th Generation District Heating (4GDH): Integrating smart thermal grids into future sustainable energy systems". In: *Energy* 68 (2014), pp. 1–11.

[35] *Flexibility in the Power System - Danish and European experiences*. https://ens.dk/sites/ens.dk/files/Globalcooperation/flexibility_in_the_power_system_v23-lri.pdf. (Accessed on 08/11/2018). 2015.

[36] J. Li et al. "Optimal operation of the integrated electrical and heating systems to accommodate the intermittent renewable sources". In: *Appl. Energy* 167 (2016), pp. 244–254.

[37] State of Green. *District Heating in the Copenhagen Region*. https://stateofgreen.com/en/partners/ramboll/solutions/district-heating-in-the-copenhagen-region/. (Accessed on 08/09/2018).

[38] State of Green. *District heating in the City of Aarhus*. https://stateofgreen.com/en/partners/city-of-aarhus/solutions/district-heating-in-the-city-of-aarhus/. (Accessed on 08/09/2018).

[39] M. G. Nielsen et al. "Economic valuation of heat pumps and electric boilers in the Danish energy system". In: *Applied Energy* 167 (2016), pp. 189–200.

[40] Danish Energy Agency. *Technology Data for Energy Plants for Electricity and District heating generation*. https://ens.dk/sites/ens.dk/files/Analyser/technology_data_catalogue_for_energy_plants_el_and_dh_-_aug_2016_update_juli2018.pdf. (Accessed on 08/10/2018).

[41] *Projekt Teknologikatalog – kort introduktion*. https://ens.dk/sites/ens.dk/files/Analyser/technologydata_for_energy_plants_-_may_2012_ver_juli2018.pdf. (Accessed on 08/11/2018).

[42] L. Gustavsson et al. "Reducing CO2 emissions by substituting biomass for fossil fuels". In: *Energy* 20.11 (1995), pp. 1097–1113.

[43] B. V. Mathiesen, H. Lund, and D. Connolly. "Limiting biomass consumption for heating in 100% renewable energy systems". In: *Energy* 48.1 (2012), pp. 160–168.

[44] E. R. Soysal et al. "Electric Boilers in District Heating Systems: A Comparative Study of the Scandinavian market conditions". In: *Swedish Association for Energy Economics Conference 2016*. 2016.

[45] K. E. Herold, R. Radermacher, and S. A. Klein. *Absorption chillers and heat pumps*. CRC press, 2016.

[46] C. Winterscheid, J.-O. Dalenbäck, and S. Holler. "Integration of solar thermal systems in existing district heating systems". In: *Energy* 137 (2017), pp. 579–585.

[47] Danish Energy Agency. *District heating – Danish and Chinese experience*. https://ens.dk/sites/ens.dk/files/energistyrelsen/Nyheder/district_heating_danish-chinese_experiences.pdf. (Accessed on 08/11/2018).

[48] Cogeneration Observatory and Dissemination Europe. *European Cogeneration Roadmap*. http://www.code2-project.eu/wp-content/uploads/CODE-2-European-Cogeneration-Roadmap.pdf. (Accessed on 08/11/2018).

[49] Danish Energy Agency. *Energy Statistics 2016*. https://ens.dk/sites/ens.dk/files/Statistik/energy_statistics_2016.pdf. (Accessed on 08/11/2018).

[50] P. A. Østergaard. "Regulation strategies of cogeneration of heat and power (CHP) plants and electricity transit in Denmark". In: *Energy* 35.5 (2010), pp. 2194–2202.

[51] Bureau of Energy Efficiency. *Cogeneration*. https://beeindia.gov.in/sites/default/files/2Ch7.pdf. (Accessed on 08/14/2018).

[52] Cooper Development Assosiaction. *Power Quality and Utilisation Guide Distributed Generation and Renewables - Cogeneration*. http://copperalliance.org.uk/uploads/2018/03/835-cogeneration.pdf. (Accessed on 08/14/2018).

[53] D. Flin. *Cogeneration: a user's guide*. Vol. 11. IET, 2010.

[54] COGEN Europe. *Cogeneration as Part of a Sustainable Energy Future*. http://turkoted.org/uploads/dokumanlar/Key%20Note%20Speaker%20Hans%20Korteweg-Cogeneration%20as%20Part%20of%20a%20Sustainable%20Energy%20Future.pdf. (Accessed on 10/26/2018).

[55] COGEN Europe. *Europe Report Cogeneration 2050*. http://www.cogeneurope.eu/medialibrary/2011/08/16/9a4fbfd5/30062011-COGEN-Europe-report-Cogeneration-2050.pdf. (Accessed on 08/14/2018).

[56] Energinet. *Environmental Report 2017 - Environmental report for Danish electricity and CHP for 2016 status year*. file:///C:/Users/igbl/Downloads/Miljrapport%202017_EN%20(1).pdf. (Accessed on 08/14/2018).

[57] Cogeneration Observatory and Dissemination Europe. *Final Cogeneration Roadmap Member State: Denmark*. http://www.code2-project.eu/wp-content/uploads/Code-2-D5-1-Final-non-pilor-Roadmap-Denmark_f2.pdf. (Accessed on 08/14/2018). 2014.

[58] J. Z. Riveros et al. "Bidding strategies for virtual power plants considering CHPs and intermittent renewables". In: *Energy Conversion and Management* 103 (2015), pp. 408–418.

[59] *Nord Pool*. https://www.nordpoolgroup.com/. (Accessed on 08/15/2018).

[60] D. Energinet. "Regulation C2—The Balancing Market and Balance Settlement". In: *Doc no* (2008).

[61] M. Zugno. "Optimization Under Uncertainty for Management of Renewables in Electricity Markets". PhD thesis. Technical University of Denmark (DTU), 2013.

[62] J. S. Gallego and H. Madsen. "Inverse Optimization and Forecasting Techniques Applied to Decision-making in Electricity Markets". PhD thesis. Technical University of Denmark (DTU), 2017.

[63] M. Pirouti et al. "Optimal operation of biomass combined heat and power in a spot market". In: *PowerTech, 2011 IEEE Trondheim*. IEEE. 2011, pp. 1–7.

[64] *EMD International A/S energyPRO - Simulate, analyze and optimize operations of energy plants*. https://www.emd.dk/energypro/. (Accessed on 08/16/2018).

[65] J. C. Ketterer. "The impact of wind power generation on the electricity price in Germany". In: *Energy Economics* 44 (2014), pp. 270–280.

[66] P. Sorknæs, H. Lund, and A. N. Andersen. "Future power market and sustainable energy solutions–The treatment of uncertainties in the daily operation of combined heat and power plants". In: *Applied Energy* 144 (2015), pp. 129–138.

[67] E. Castillo et al. *Building and solving mathematical programming models in engineering and science*. Vol. 62. John Wiley & Sons, 2011.

[68] J. K. Karlof. *Integer programming: theory and practice*. CRC Press, 2005.

[69] F. Javed and N. Arshad. "On the use of linear programming in optimizing energy costs". In: *International Workshop on Self-Organizing Systems*. Springer. 2008, pp. 305–310.

[70] L. A. Wolsey. "Mixed integer programming". In: *Wiley Encyclopedia of Computer Science and Engineering* (2007), pp. 1–10.

[71] A. Soroudi and T. Amraee. "Decision making under uncertainty in energy systems: State of the art". In: *Renewable and Sustainable Energy Reviews* 28 (2013), pp. 376–384.

[72] A. Ben-Tal, L. El Ghaoui, and A. Nemirovski. *Robust optimization*. Vol. 28. Princeton University Press, 2009.

[73] D. Bertsimas and D. B. Brown. "Constructing uncertainty sets for robust linear optimization". In: *Operations research* 57.6 (2009), pp. 1483–1495.

[74] D. Bertsimas, D. B. Brown, and C. Caramanis. "Theory and applications of robust optimization". In: *SIAM review* 53.3 (2011), pp. 464–501.

[75] B. Zeng and L. Zhao. "Solving two-stage robust optimization problems using a column-and-constraint generation method". In: *Operations Research Letters* 41.5 (2013), pp. 457–461.

[76] H. Madsen. *Time series analysis*. CRC Press, 2007.

[77] R. Weron. *Modeling and Forecasting Electricity Loads and Prices: A Statistical Approach*. Hugo Steinhaus Center, Wroclaw University of Technology, 2006.

[78] Z. Zhao et al. "Improving short-term electricity price forecasting using day-ahead LMP with ARIMA models". In: *Power & Energy Society General Meeting, 2017 IEEE*. IEEE. 2017, pp. 1–5.

[79] S. Voronin, J. Partanen, and T. Kauranne. "A hybrid electricity price forecasting model for the Nordic electricity spot market". In: *International Transactions on Electrical Energy Systems* 24.5 (2014), pp. 736–760.

[80] M. Xie et al. "A seasonal ARIMA model with exogenous variables for elspot electricity prices in Sweden". In: *European Energy Market (EEM), 2013 10th International Conference on the*. IEEE. 2013, pp. 1–4.

[81] M. Tripathi, K. Upadhyay, and S. Singh. "Short-term load forecasting using generalized regression and probabilistic neural networks in the electricity market". In: *The Electricity Journal* 21.9 (2008), pp. 24–34.

[82] G. E. Box et al. *Time series analysis: forecasting and control*. John Wiley & Sons, 2015.

[83] A. J. Conejo, M. Carrión, J. M. Morales, et al. *Decision making under uncertainty in electricity markets*. Vol. 1. Springer, 2010.

[84] P. Pinson et al. "Wind energy: Forecasting challenges for its operational management". In: *Statistical Science* 28.4 (2013), pp. 564–585.

[85] P. Pinson et al. "Local linear regression with adaptive orthogonal fitting for the wind power application". In: *Statistics and Computing* 18.1 (2008), pp. 59–71.

[86] T. Hastie, R. Tibshirani, and J. Friedman. "Unsupervised learning". In: *The elements of statistical learning*. Springer, 2009, pp. 485–585.

[87] J. Blömer et al. "Theoretical analysis of the k-means algorithm–A survey". In: *Algorithm Engineering*. Springer, 2016, pp. 81–116.

[88] L. Kaufman and P. J. Rousseeuw. *Finding groups in data: an introduction to cluster analysis*. Vol. 344. John Wiley & Sons, 2009.

[89] J. Clausen. "Branch and bound algorithms-principles and examples". In: *Department of Computer Science, University of Copenhagen* (1999), pp. 1–30.

[90] J. F. Benders. "Partitioning procedures for solving mixed-variables programming problems". In: *Numerische mathematik* 4.1 (1962), pp. 238–252.

[91] G. B. Dantzig and P. Wolfe. "Decomposition principle for linear programs". In: *Operations research* 8.1 (1960), pp. 101–111.

[92] R. M. Van Slyke and R. Wets. “L-shaped linear programs with applications to optimal control and stochastic programming”. In: *SIAM Journal on Applied Mathematics* 17.4 (1969), pp. 638–663.

[93] T. Rotting and A. Gjelsvik. “Stochastic dual dynamic programming for seasonal scheduling in the Norwegian power system”. In: *IEEE Transactions on Power Systems* 7.1 (1992), pp. 273–279.

[94] R. T. Rockafellar and R. J.-B. Wets. “Scenarios and policy aggregation in optimization under uncertainty”. In: *Mathematics of operations research* 16.1 (1991), pp. 119–147.

[95] W. van Ackooij et al. “Large-scale unit commitment under uncertainty: an updated literature survey”. In: *Annals of Operations Research* (2018), pp. 1–75.

[96] Q. P. Zheng, J. Wang, and A. L. Liu. “Stochastic Optimization for Unit Commitment—A Review”. In: *IEEE Transactions on Power Systems* 30.4 (2015), pp. 1913–1924. ISSN: 0885-8950. DOI: 10.1109/TPWRS.2014.2355204.

[97] T. Shiina and J. R. Birge. “Stochastic unit commitment problem”. In: *International Transactions in Operational Research* 11.1 (2004), pp. 19–32.

[98] H. Pandžić et al. “Offering model for a virtual power plant based on stochastic programming”. In: *Appl. Energy* 105 (2013), pp. 282–292.

Part II

Publications

Paper A

An Efficient Robust Solution to the Two-Stage Stochastic Unit Commitment Problem

Authors:
Ignacio Blanco and Juan M. Morales

Published in:
IEEE Transactions on Power Systems 32, no. 6 (2017): 4477-4488.

An Efficient Robust Solution to the Two-Stage Stochastic Unit Commitment Problem

Ignacio Blanco[1], Juan M. Morales[2]

Abstract

This paper provides a reformulation of the scenario-based two-stage unit commitment problem under uncertainty that allows finding unit-commitment plans that perform reasonably well both in expectation and for the worst case. The proposed reformulation is based on partitioning the sample space of the uncertain factors by clustering the scenarios that approximate their probability distributions. The degree of conservatism of the resulting unit-commitment plan (that is, how close it is to the one provided by a purely robust or stochastic unit-commitment formulation) is controlled by the number of partitions into which the said sample space is split. To efficiently solve the proposed reformulation of the unit-commitment problem under uncertainty, we develop two alternative parallelization and decomposition schemes that rely on a column-and-constraint generation procedure. Finally, we analyze the quality of the solutions provided by this reformulation for a case study based on the IEEE 14-node power system and test the effectiveness of the proposed parallelization and decomposition solution approaches on the larger IEEE 3-Area RTS-96 power system.

Nomenclature

The notation used throughout the paper is stated below for quick reference. Other symbols are defined as required.

[1]Department of Applied Mathematics and Computer Science, Technical University of Denmark, DK-2800 Kgs. Lyngby, Denmark

[2]Department of Applied Mathematics, University of Malaga, SP-29071, Málaga, Spain

Indexes and Sets

T	Set of time periods t.
N	Set of nodes n.
G	Set of conventional generation units g.
F	Set of stochastic power production units f.
L	Set of loads l.
Ω	Set of scenarios ω, ranging from 1 to λ.
P	Set of partitions p, ranging from 1 to k.
Ω_p	Set of scenarios ω in partition p.
F_n	Set of stochastic power production units located at node n.
L_n	Set of loads connected at node n.
G_n	Set of conventional generation units located at node n.
M_n	Set of nodes $m \in N$ that are connected to node n by a transmission line.
Ω'_p	Reduced set of scenarios ω in partition p.

Parameters

C_g^F, C_g^V	Fixed/variable production cost of conventional generation unit g.
C_g^{SU}, C_g^{SD}	Start-up/Shut-down cost of conventional generation unit g.
$L_{l,t}$	Demand for load l at time t.
RU_g, RD_g	Ramp-up/Ramp-down rate for conventional generation unit g.
UT_g, DT_g	Minimum-up/Minimum-down time for unit g
L_g^{UP}, L_g^{DW}	Number of time periods conventional generation unit g must be online/offline counting from $t = 1$.
IS_g	Initial status of unit g, equal to 1 if online at $t = 0$ and 0, otherwise.
ON_g, OFF_g	Number of time periods unit g has been online/offline prior to $t = 1$.
$X_{n,m}$	Reactance of line $n - m$.
$F_{n,m}^{max}$	Maximum flow capacity of line $n - m$.
P_g^{max}, P_g^{min}	Maximum/minimum power production of conventional generation unit g
P_g^{SU}, P_g^{SD}	Maximum starting-up/shutting-down power production of conventional generation unit g.
P_g^{IS}	Power output of conventional unit g at $t = 0$.
C^L	Cost of involuntary load curtailment.
$W_{f,t,\omega}$	Power production from stochastic generation unit f at time t in scenario ω.
π_ω	Probability of scenario ω.

ρ_p	Weight associated with partition p.

First-stage variables

$u_{g,t}$	Binary variable equal to 1 if unit g is online at time t and 0, otherwise.
$y_{g,t}/z_{g,t}$	Binary variable equal to 1 if unit g is starting up/shutting down at time t and 0, otherwise.

Second-stage variables

$P_{g,t,\omega}$	Power produced by conventional generation unit g in scenario ω at time t.
$L^{SH}_{l,t,\omega}$	Power curtailment from load l in scenario ω at time t.
$W^{SP}_{f,t,\omega}$	Power curtailment from stochastic power production unit f in scenario ω at time t.
$\delta_{n,t,\omega}$	Voltage angle at node n, time t and scenario ω.
α	Auxiliary variable used in the scenario-based robust unit commitment formulation
θ_p	Auxiliary variable used in the hybrid unit commitment formulation

A.1 Introduction

The increasing reliance on partly unpredictable renewable power supply has prompted the revision of the procedures used for power system operations. This is the case, for example, of the tool used by system operators to decide the commitment of power plants, that is, to solve the so-called *unit commitment problem* (UC). Two-stage stochastic programming [A1] and robust optimization [A2] have become the most popular and explored techniques of optimization under uncertainty to improve unit-commitment decisions in terms of both cost-efficiency and system reliability.

The formulation and solution of the unit commitment problem using either stochastic programming or robust optimization—the result of which is typically referred to as *stochastic* and *robust unit commitment*, respectively— has been subject of numerous studies by the scientific community; see, for instance, [A3, A4, A5, A6, A7, A8, A9, A10, A11], among many others and variants.

Essentially, the stochastic unit commitment problem (SUC) makes use of a probabilistic model for the uncertain input factors such as demand, equipment failures and partly-predictable renewable power production to minimize a certain quantile of the induced system cost distribution or its expectation. Most often than not, this probabilistic model is approximated by a set of scenarios that describe plausible realizations of such random factors. In order for the stochastic solution to be reliable, the amount of scenarios that need to be considered must be large, which may render an intractable optimization problem, or carefully generated, which motivates the topic of *scenario reduction techniques* [A12, A13, A14]. Furthermore, the probabilistic model from which these scenarios may be drawn may carry, in itself, some level of uncertainty as well.

In contrast, the robust unit commitment problem (RUC) seeks a commitment plan that allows the system to withstand the worst-case realization of the uncertain factors at a minimum cost. While this approach saves the decision-maker from having to probabilistically characterize these factors, it may yield too conservative solutions as the worst-case scenario rarely occurs.

In recent years, several methods have been proposed to make decisions under uncertainty that perform *relatively well* under the premises of *both* the stochastic and the robust approaches, that is, in expectation and for the worst case. Illustrative examples of these methods can be found in [A15, A16, A17, A18], where hybrid stochastic-robust solution strategies are developed for optimal air-quality and municipal solid-waste management, electricity trading for power microgrids and energy contracting for a portfolio of renewable power generation technologies, respectively. What makes all these solution strategies *hybrid* is that some of the uncertain parameters are assumed to follow certain probability distributions, while others are solely known to belong to some uncertainty sets.

Within the context of the unit commitment problem, we highlight the work in [A19] and [A20]. More specifically, the authors in [A19] propose a mathematical formulation that delivers the unit-commitment plan that minimizes a user-controlled weighted sum of the expected and the worst-case costs. The solution approach introduced in [A20], even if presented as a method to tackle the stochastic unit commitment problem, seeks to determine a unit-commitment plan that is robust against an *ambiguous* probability distribution of renewable energy generation, an ambiguity that is the result of the always limited availability of data and that is modeled in practice as a vector of imperfectly known probabilities. Thus, as the amount of historical data increases, the ambiguity of such a probability distribution diminishes and so does the need for robustness and the degree of conservatism of the stochastic unit-commitment solution. This approach can also be regarded as a form of *distributionally robust optimization* [A21].

Our work shares with [A19] and [A20] the aim of finding a solution to the stochastic unit commitment problem that is robust in some sense, but our motivation and the methodology we propose to this end are essentially different. We assume that the probability distributions of the uncertain parameters—in our case, the wind power production—are known, but that, as it normally occurs in practice, computational tractability only allows us to solve the stochastic unit commitment problem for a scenario-based approximation of such distributions. In principle, we shall consider a large number of scenarios for this approximation to be accurate enough. In any case, we group these scenarios using a clustering technique—for instance, the *k-means clustering algorithm* [A22], which has been reported to feature good performance in similar contexts [A23, A24]—. Each of the so-obtained clusters is referred to as a *partition*. We then formulate and solve a two-stage unit-commitment problem that minimizes the expected value of the system operating costs, where the expectation is taken over the collection of worst-case scenarios within each partition. The probability assigned to each of these worst-case scenarios is equal to the probability of the partition it belongs to, which is, in turn, computed by summing up the probabilities of the scenarios that form part of the partition in question.

For convenience, we employ the term *hybrid unit commitment problem* and the acronym HUC to refer to the proposed reformulation of the UC problem. This reformulation brings two major advantages, namely:

1. It allows finding solutions to the two-stage unit commitment problem with a decreasing degree of conservatism by increasing the number of partitions. In fact, if only one partition is considered, the HUC delivers the (scenario-based) robust unit-commitment solution (where by "scenario-based", we mean the solution given by the robust formulation of the two-stage unit-commitment problem in the particular case that the uncertainty is modeled as a finite set of atoms, outcomes or scenarios). In contrast, if the number of partitions is made to coincide with the number of scenarios, the HUC solution boils down to the stochastic unit-commitment plan. Furthermore, as we show later, the computational time required to find the HUC solution increases with the number of partitions considered, with the solution algorithm being very fast for a small number of them. This provides a practical way to adjust the level of conservatism of the unit-commitment solution depending on time availability.

2. It is amenable to decomposition and paralellization in various ways and levels and, hence, it can be efficiently solved. Indeed, based on the column-and-constraint generation procedure described in [A11], we provide and compare two alternative decomposition schemes to solve the HUC problem. These two schemes basically differ in whether the worst-case scenarios within each partition are identified independently for each partition or not.

The remainder of this paper is organized as follows. Section A.2 begins by providing mathematical formulations for the scenario-based two-stage stochastic and robust unit commitment problems, in that order, and finishes with the formulation of the proposed hybrid unit commitment problem. Furthermore, in this section we explain how we use a clustering method to construct the partitions in the HUC model and how these can be employed to control the degree of conservatism of the resulting unit-commitment plan. Section A.3 introduces the proposed parallelization and decomposition strategies to solve the HUC problem. Section A.4 analyzes and discusses results from two case studies based on standard IEEE power systems. Finally, in Section A.5 the main conclusions of our work are summarized, including possible avenues for future research.

A.2 Mathematical Formulation

In the two-stage unit commitment problem under uncertainty, decision variables are divided into two groups. The first group constitutes the commitment plan itself and consists of the 0/1 variables $u_{g,t}$, $y_{g,t}$, $z_{g,t}$, which determine the on/off status, the start-up, and the shutdown of generating unit g in time period t, respectively. These decisions are to be made, in general, one day in advance of the actual delivery of electricity and, in any case, before the realization of the uncertain factors. In this paper, we consider for simplicity that the system uncertainty stems only from the wind power production, which is modeled as a finite set Ω of scenarios $W_{f,t,\omega}$ with $\omega \in \Omega$.

The second-stage decision variables, namely, $P_{g,t,\omega}$, $L^{SH}_{l,t,\omega}$, $W^{SP}_{f,t,\omega}$ and $\delta_{n,t,\omega}$ determine the economic dispatch of the conventional generating units, the amount of load that is involuntarily shed, the amount of wind power production that is curtailed, and the voltage angles at the network nodes, respectively. These variables adapt to the specific realization of the uncertainty and as such, are augmented with the scenario index ω.
We start by providing the mathematical formulation of the two-stage *stochastic* unit commitment problem. In all cases, we consider that the marginal production cost of the wind generation is zero.

A.2.1 Two-Stage Stochastic Unit Commitment (SUC)

The two-stage stochastic unit commitment problem can be formulated as follows:

$$\underset{\mathcal{H},\mathcal{W}}{\text{minimize}} \quad \sum_{t\in T}\sum_{g\in G}\left(C_g^F u_{g,t} + C_g^{SU} y_{g,t} + C_g^{SD} z_{g,t}\right) \tag{A.1}$$
$$+ \sum_{\omega\in\Omega} \pi_\omega \left[\sum_{t\in T}\sum_{g\in G} C_g^V P_{g,t,\omega} + \sum_{t\in T}\sum_{l\in L} C^L L_{l,t,\omega}^{SH}\right]$$

$$\text{s.t.} \quad y_{g,t} - z_{g,t} = u_{g,t} - u_{g,t-1} \tag{A.2}$$
$$(\forall g, \forall t \in \{2,...,T\})$$

$$y_{g,t} - z_{g,t} = u_{g,t} - IS_g \tag{A.3}$$
$$(\forall g, \forall t \in \{1\})$$

$$y_{g,t} + z_{g,t} \leq 1 \tag{A.4}$$
$$(\forall g, \forall t \in \{1,...,T\})$$

$$u_{g,t} = IS_g \tag{A.5}$$
$$(L_g^{UP} + L_g^{DW} > 0, \forall g, \forall t \leq L_g^{UP} + L_g^{DW})$$

$$\sum_{\tau=t-UT_g+1}^{t} y_{g,\tau} \leq u_{g,t} \tag{A.6}$$
$$(\forall g, \forall t > L_g^{UP} + L_g^{DW})$$

$$\sum_{\tau=t-DT_g+1}^{t} z_{g,\tau} \leq 1 - u_{g,t} \tag{A.7}$$
$$(\forall g, \forall t > L_g^{UP} + L_g^{DW})$$

$$\sum_{g\in G_n} P_{g,t,\omega} - \sum_{l\in L_n} L_{l,t} + \sum_{l\in L_n} L_{l,t,\omega}^{SH} + \sum_{f\in F_n} W_{f,t,\omega} \tag{A.8}$$
$$- \sum_{f\in F_n} W_{f,t,\omega}^{SP} = \sum_{m\in M_n} \frac{(\delta_{n,t,\omega} - \delta_{m,t,\omega})}{X_{n,m}}$$
$$(\forall n, \forall t, \forall \omega \in \Omega)$$

$$P_{g,t,\omega} \leq P_g^{max} u_{g,t} \tag{A.9}$$
$$(\forall g, \forall t, \forall \omega \in \Omega)$$

$$P_{g,t,\omega} \geq P_g^{min} u_{g,t} \quad (\forall g, \forall t, \forall \omega \in \Omega) \tag{A.10}$$

$$P_{g,t,\omega} \leq (P_g^{IS} + RU_g) u_{g,t} \quad (\forall g, \forall t \in \{1\}, \forall \omega \in \Omega) \tag{A.11}$$

$$P_{g,t,\omega} \geq (P_g^{IS} - RD_g) u_{g,t} \quad (\forall g, \forall t \in \{1\}, \forall \omega \in \Omega) \tag{A.12}$$

$$P_{g,t,\omega} - P_{g,t-1,\omega} \leq (2 - u_{g,t-1} - u_{g,t}) P_g^{SU} + (1 + u_{g,t-1} - u_{g,t}) RU_g \quad (\forall g, \forall t \in \{2, ..., T\}, \forall \omega \in \Omega) \tag{A.13}$$

$$P_{g,t-1,\omega} - P_{g,t,\omega} \leq (2 - u_{g,t-1} - u_{g,t}) P_g^{SD} + (1 - u_{g,t-1} + u_{g,t}) RD_g \quad (\forall g, \forall t \in \{2, ..., T\}, \forall \omega \in \Omega) \tag{A.14}$$

$$L_{l,t,\omega}^{SH} \leq L_{l,t} \quad (\forall l, \forall t, \forall \omega \in \Omega) \tag{A.15}$$

$$W_{f,t,\omega}^{SP} \leq W_{f,t,\omega} \quad (\forall f, \forall t, \forall \omega \in \Omega) \tag{A.16}$$

$$-F_{n,m}^{max} \leq \frac{(\delta_{n,t,\omega} - \delta_{m,t,\omega})}{X_{n,m}} \leq F_{n,m}^{max} \quad (\forall n, m \in M_n, \forall t, \forall \omega \in \Omega) \tag{A.17}$$

$$P_{g,t,\omega}, L_{l,t,\omega}^{SH}, W_{f,t,\omega}^{SP} \geq 0 \quad (\forall g, \forall l, \forall f, \forall t, \forall \omega \in \Omega) \tag{A.18}$$

$$u_{g,t}, y_{g,t}, z_{g,t} \in \{0, 1\} \quad (\forall g, \forall t) \tag{A.19}$$

where $\mathcal{H} = \{u_{g,t}, y_{g,t}, z_{g,t}\}$ and $\mathcal{W} = \left\{P_{g,t,\omega}, L_{l,t,\omega}^{SH}, W_{f,t,\omega}^{SP}, \delta_{n,t,\omega} : \omega \in \Omega\right\}$ are the sets of here-and-now and wait-and-see decisions, respectively. Furthermore, following [A25], the initial state conditions are given by

$$IS_g = \begin{cases} 1 & \text{if } ON_g > 0 \\ 0 & \text{if } ON_g = 0 \end{cases}$$

$$L_g^{UP} = \min\{T, (UP_g - ON_g)IS_g\}$$
$$L_g^{DW} = \min\{T, (DT_g - OFF_g)(1 - IS_g)\}$$

Problem (A.1)–(A.19) takes the form of a standard two-stage unit commitment formulation, which is similar, to a large extent, to those provided in the numerous works on the topic, see, for instance, [A6, A26] and references therein. The objective is to minimize the expected system operating cost (A.1), which is made up of the no-load, start-up, shutdown, and variable production costs of the conventional generating units, and the cost of involuntarily load curtailment, in that order. Equations (A.2)–(A.4) model the changes in the on/off-commitment status of the power plants as these are started up or shutdown throughout the scheduling horizon, while (A.5)–(A.7) impose their minimum up- and down-time requirements. Equalities (A.8) constitute the set of nodal power balance equations according to a DC power flow model. The maximum and minimum power outputs of the generating units are enforced by (A.9) and (A.10), respectively, and their ramping limits through (A.11)–(A.14), as in [A8] and [A9]. The sets of inequalities (A.15) and (A.16) limit the involuntary load curtailment and the wind power spillage to the eventual power that is consumed and the eventual wind power that is produced, respectively. The set of equations (A.17) guarantee compliance with the transmission capacity limits. Finally, constraints (A.18) and (A.19) constitute variable declarations.

A.2.2 Two-Stage Robust Unit Commitment (RUC)

The two-stage robust unit commitment problem can be written as follows:

$$\min_{\mathcal{H}} \sum_{t\in T}\sum_{g\in G}\left(C_g^F u_{g,t} + C_g^{SU} y_{g,t} + C_g^{SD} z_{g,t}\right) + \mathcal{Q}(\mathcal{H}) \tag{A.20}$$
$$\text{s.t. } (A.2) - (A.7), (A.19) \tag{A.21}$$

where

$$\mathcal{Q}(\mathcal{H}) = \max_{\omega\in\Omega} \min_{\mathcal{W}} \sum_{t\in T}\sum_{g\in G} C_g^V P_{g,t,\omega} + \sum_{t\in T}\sum_{l\in L} C^L L_{l,t,\omega}^{SH} \tag{A.22}$$
$$\text{s.t. } (A.8) - (A.18) \tag{A.23}$$

In the particular case that the uncertainty set Ω is comprised of a *finite* number of atoms, outcomes or scenarios ω, the two-stage robust unit-commitment

problem (A.20)–(A.23) can be equivalently recast as follows:

$$\underset{\mathcal{H},\mathcal{W},\alpha}{\text{minimize}} \sum_{t\in T}\sum_{g\in G}\left(C_g^F u_{g,t} + C_g^{SU} y_{g,t} + C_g^{SD} z_{g,t}\right) + \alpha \tag{A.24}$$

$$\text{s.t. } \alpha \geq \sum_{t\in T}\sum_{g\in G} C_g^V P_{g,t,\omega} + \sum_{t\in T}\sum_{l\in L} C^L L_{l,t,\omega}^{SH}, \ \forall \omega \in \Omega \tag{A.25}$$

$$(A.2) - (A.19) \tag{A.26}$$

For convenience and ease of reference, the set of equations (A.24)–(A.26) is hereafter referred to as *the scenario-based formulation of the two-stage robust unit-commitment problem*. Note that the auxiliary variable α equals the worst-case dispatch cost at the optimum. This variable is bounded from below by a finite set of linear constraints (A.25), one per scenario, that involve the second-stage decision variables $P_{g,t,\omega}$ and $L_{l,t,\omega}^{SH}$. Thus, the objective of the problem (A.24)–(A.26) is to minimize the total system operating cost for the worst-case scenario of the uncertainty.

In the following section, we introduce the proposed hybrid formulation of the two-stage unit commitment problem under uncertainty.

A.2.3 Hybrid Unit Commitment Problem (HUC)

Let us now split the set Ω into k partitions with $P = \{1, ..., k\}$ being the partition set. We then define the series of subsets $\Omega_1, \ldots, \Omega_p, \ldots, \Omega_k$, with $\Omega_i \bigcap \Omega_j = \emptyset$ for all $i \neq j$ and $\Omega_1 \bigcup \ldots \Omega_p \bigcup \ldots \Omega_k = \Omega$, such that Ω_p is linked to partition $p \in P$. Furthermore, each partition $p \in P$ is assigned a probability $\rho_p \geq 0$ such that $\sum_{p\in P} \rho_p = 1$.

The proposed hybrid two-stage unit commitment problem writes as follows:

$$\min_{\mathcal{H}} \sum_{t\in T}\sum_{g\in G}\left(C_g^F u_{g,t} + C_g^{SU} y_{g,t} + C_g^{SD} z_{g,t}\right) + \mathcal{R}(\mathcal{H}) \tag{A.27}$$

$$\text{s.t. } (A.2) - (A.7), (A.19) \tag{A.28}$$

where

$$\mathcal{R}(\mathcal{H}) = \sum_{p\in P} \rho_p \left(\max_{\omega\in\Omega_p} \min_{\mathcal{W}} \sum_{t\in T}\sum_{g\in G} C_g^V P_{g,t,\omega} + \sum_{t\in T}\sum_{l\in L} C^L L_{l,t,\omega}^{SH}\right) \tag{A.29}$$

$$\text{s.t.} \qquad (A.8) - (A.18) \tag{A.30}$$

In the particular case that the uncertainty set Ω is *finite*, that is, $\Omega = \{1, ..., \lambda\}$, where λ is the total number of possible outcomes or scenarios, problem (A.27)–(A.30) can be equivalently reformulated as follows:

$$\underset{\mathcal{H},\mathcal{W},\theta_p}{\text{minimize}} \quad \sum_{t\in T}\sum_{g\in G}\left(C_g^F u_{g,t} + C_g^{SU} y_{g,t} + C_g^{SD} z_{g,t}\right) + \\ + \sum_{p\in P} \rho_p \theta_p \tag{A.31}$$

$$\text{s.t.} \quad \theta_p \geq \sum_{t\in T}\sum_{g\in G} C_g^V P_{g,t,\omega} + \sum_{t\in T}\sum_{l\in L} C^L L_{l,t,\omega}^{SH} \tag{A.32}$$

$$(\forall p \in P,\ \forall \omega \in \Omega_p)$$

$$(A.2) - (A.19) \tag{A.33}$$

where Ω_p is comprised of all the scenarios $\omega \in \Omega$ that belong to partition $p \in P$ and where the probability ρ_p assigned to partition p is computed as the sum of the probabilities of the scenarios that form part of it, that is,

$$\rho_p = \sum_{\omega\in\Omega_p} \pi_\omega \quad \forall p \in P \tag{A.34}$$

The objective (A.31) is then to minimize the expected system operating cost over the scenarios that deliver the worst-case dispatch cost within each partition.

Indeed, the auxiliary variable θ_p, one per partition $p \in P$, equals the worst-case dispatch cost within partition p, in a similar way as the auxiliary variable α does in the robust unit commitment formulation (A.24)–(A.26) for the whole set of scenarios Ω. This way, problem (A.31)–(A.33) is expected to yield a unit-commitment plan that is "in between" the robust and the stochastic unit-commitment solutions in terms of the expected and the worst-case system operating cost. Furthermore, the closeness of the HUC solution to the stochastic and robust unit-commitment plans, and consequently its degree of conservatism, are controlled by the number k of partitions or clusters into which the scenarios are grouped. Indeed, if the number of partitions equals the number of scenarios, that is, $k = \lambda$, the HUC model (A.31)–(A.33) reduces to (A.1)–(A.19) and the stochastic solution is obtained. In contrast, if only one single partition is considered ($k = 1$), we have that $\Omega_1 = \Omega$ and therefore, problem (A.31)–(A.33) boils down to the scenario-based robust unit-commitment formulation (A.24)–(A.26). As a result, the HUC solution coincides with the robust solution in such a case.

Hence, we can increase the degree of conservatism of the HUC solution by diminishing the number of partitions, and vice versa. For $1 < k < \lambda$, however,

how efficiently and quickly the HUC solution transits from the robust to the stochastic unit-commitment plan, as k increases, depends on the performance of the clustering technique. Later on in this paper, we evaluate and compare the performance of the proposed HUC formulation when solved using a range of different clustering methods. More specifically, we consider three non-hierarchical clustering techniques, namely, the k-means, k-medoids, and k-shape algorithms, which are used to group a data set into a given number k of clusters. In brief, these algorithms assign each scenario $\omega \in \Omega$ to the partition Ω_p, $p \in P$, with the nearest mean (k-means), the closest representative scenario (k-medoids) [A27], or the most similar scenario-shape using a cross-correlation measure (k-shape) [A28]. In particular, the k-means algorithm [A22] has been reported to showcase a good performance in other related applications, e.g., for solving a probabilistic production cost model in [A23] and a transmission and generation expansion planning problem in [A24]. Furthermore, we also test an agglomerative hierarchical clustering method [A27], where the dissimilarity of two clusters is measured as the maximum of the pairwise distances of the scenarios in the clusters. This method produces a hierarchy of partitions whereby the two nearest clusters merge into a new one as one moves up the hierarchy. Therefore, the top level in the hierarchy consists of one single cluster that comprises the complete set of scenarios.

A.3 Solution Strategy: Parallelization and Decomposition

It is well known that the unit commitment problem is mixed-integer, NP-hard, and generally requires long solution times. This is especially true for realistic instances of the two-stage unit commitment problem under uncertainty. In the following we describe two alternative parallelization-and-decomposition schemes that we have designed to efficiently solve the proposed HUC formulation (A.31)–(A.33). For ease of exposition, we divide this description in two parts. In the first one, we explain how problem (A.31)–(A.33) can be decomposed per partition and scenario, while in the second part we elaborate on how the solution to the decomposed problem can be parallelized.

A.3.1 Problem Decomposition via Column-and-constraint Generation

We provide and discuss below two alternative ways to decompose the HUC problem (A.31)–(A.33), which we present as two variants of the same *Scenario*

Partition and Decomposition Algorithm (SPDA).

A.3.1.1 Scenario Partition and Decomposition Algorithm—Variant 1 (SPDA1)

Let us consider a certain partition $p \in P$ that comprises the subset of scenarios Ω_p. Note that, for determining the optimal solution to the HUC problem (A.31)–(A.33), we only need those (hopefully few) scenarios in Ω_p that deliver the worst-case dispatch cost over partition p for *any* feasible unit-commitment plan. Identifying those scenarios, however, may be computationally very costly. Instead, we describe below a procedure to find a subset $\Omega'_p \subset \Omega_p$ under which the HUC formulation provides a unit commitment solution close to the one given under the full scenario set Ω_p. Furthermore, the proposed algorithm builds the reduced sets Ω'_p, $p \in P$, in parallel for each partition p.

To build Ω'_p from Ω_p, the latter being the outcome of a certain clustering algorithm, we develop a master-subproblem decomposition scheme *per partition* based on the column-and-constraint generation procedure described in [A11]. In the sequel we will refer to this decomposition scheme as *Primal Cut Algorithm* after the solution strategy introduced in [A9] whereby the master problem is gradually enlarged with the addition of cuts expressed in terms of the primal variables.

Each master problem (one per partition) is a mixed-integer programming problem that involves both first-stage and second-stage decision variables and that has the following form at iteration i of the column-and-constraint generation algorithm:

$$\underset{\mathcal{H}^i, \mathcal{W}^i, \theta_p}{\text{minimize}} \quad \sum_{t \in T} \sum_{g \in G} \left(C_g^F u_{g,t}^i + C_g^{SU} y_{g,t}^i + C_g^{SD} z_{g,t}^i \right) + \theta_p \tag{A.35}$$

$$\text{s.t.} \qquad (A.2) - (A.7), (A.19) \tag{A.36}$$

$$\theta_p \geq \sum_{t \in T} \sum_{g \in G} C_g^V P_{g,t,\omega}^i + \sum_{t \in T} \sum_{l \in L} C^L L_{l,t,\omega}^{SH,i}, \quad \forall \omega \in \Omega_p'^i \tag{A.37}$$

$$(A.8) - (A.18), \quad \forall \omega \in \Omega_p'^i \tag{A.38}$$

where $\mathcal{H}^i = \left\{ u_{g,t}^i, y_{g,t}^i, z_{g,t}^i \right\}$ and $\mathcal{W}^i = \left\{ P_{g,t,\omega}^i, L_{l,t,\omega}^{SH,i}, W_{f,t,\omega}^{SP,i}, \delta_{n,t,\omega}^i : \omega \in \Omega_p'^i \right\}$. Note that $\Omega_p'^0 = \emptyset$. As the algorithm proceeds, $\Omega_p'^i$ is augmented with those possibly few scenarios $\omega \in \Omega_p$ that are needed to reconstruct the partition-worst-case recourse cost as a function of the first-stage decision variables $u_{g,t}^i$,

$y^i_{g,t}$, and $z^i_{g,t}$ in the form of (A.37)–(A.38).

Constraint (A.37) can be interpreted as a primal cut, as compared to those cuts that are constructed from dual information, as it is the case, for example, of a standard Benders cut.

The subproblems are linear programming problems (LP) that determine the second-stage decision variables $P^i_{g,t,\omega}$, $L^{SH,i}_{l,t,\omega}$, $W^{SP,i}_{f,t,\omega}$, and $\delta^i_{n,t,\omega}$ with $u^i_{g,t}$, $y^i_{g,t}$, and $z^i_{g,t}$ fixed at the values given by the master problem. A subproblem like (A.39)–(A.40) is solved for each scenario $\omega \in \Omega_p$.

$$\underset{\mathcal{W}^i_\omega}{\text{minimize}} \quad \sum_{t\in T}\sum_{g\in G} C^V_g P^i_{g,t,\omega} + \sum_{t\in T}\sum_{l\in L} C^L L^{SH,i}_{l,t,\omega} \tag{A.39}$$

$$\text{s.t.} \quad (A.8) - (A.18) \tag{A.40}$$

where $\mathcal{W}^i_\omega = \left\{P^i_{g,t,\omega}, L^{SH,i}_{l,t,\omega}, W^{SP,i}_{f,t,\omega}, \delta^i_{n,t,\omega}\right\}$.

The scenario ω' for which the associated subproblem (A.39)–(A.40) yields the highest dispatch cost or is infeasible is used to construct a set of primal constraints in the form of (A.37)–(A.38) that is added to the master problem by setting $\Omega^{'i+1}_p = \Omega^{'i}_p \bigcup \{\omega'\}$. It is worth noticing, however, that subproblem infeasibility is not a concern in our case due to the possibility of shedding load and spilling wind.

One instance of the primal cut algorithm is run for each partition $p \in P$ in parallel. Each of these instances works, therefore, with one master problem and a number of subproblems equal to the number of scenarios in each partition, that is, equal to $card\,(\Omega_p)$. Furthermore, each instance of the algorithm concludes by delivering the set of selected scenarios $\Omega'_p \subset \Omega_p$ for partition p. The last step of our solution strategy consists then in solving the HUC problem (A.31)–(A.33) where Ω_p is replaced with the reduced scenario set Ω'_p.

We describe below how this solution strategy proceeds step by step.

1. Choose the number k of partitions and apply a clustering method to the complete set of scenarios Ω in order to assign each scenario to a certain partition p.

2. Create one instance of the primal cut algorithm for each partition $p \in P$.

3. Initialization: Set $i = 0$ and $\Omega^{'0}_p = \emptyset$.

4. Solve the master problem (MP). Return the optimal solution found by the branch-and-cut algorithm and denote this solution by $(u^i_{g,t}, y^i_{g,t}, z^i_{g,t})$. Calculate a lower bound LB as $\sum_{t\in T}\sum_{g\in G}(C^F_g u^i_{g,t}+C^{SU}_g y^i_{g,t}+C^{SD}_g z^i_{g,t})+\theta_p$.

5. Solve the subproblems (SP) with the first-stage decision variables fixed at $(u^i_{g,t}, y^i_{g,t}, z^i_{g,t})$. Once the SP are solved, the scenario ω' associated with the subproblem that yields the highest dispatch cost is identified and included into the reduced set Ω'^{i+1}_p, i.e., $\Omega'^{i+1}_p = \Omega'^{i}_p \bigcup\{\omega'\}$. Compute an upper bound UB as $\sum_{t\in T}\sum_{g\in G}(C^F_g u^i_{g,t} + C^{SU}_g y^i_{g,t} + C^{SD}_g z^i_{g,t}) + \sum_{t\in T}\sum_{g\in G} C^V_g P^i_{g,t,\omega'} + \sum_{t\in T}\sum_{l\in L} C^L L^{SH,i}_{l,t,\omega'}$

6. Convergence check: If $\mid UB - LB \mid \leq \epsilon$, being ϵ a user-specified tolerance value, the iterative process stops. If $\mid UB - LB \mid > \epsilon$, then set $i := i + 1$ and go to step 4.

7. Once all the instances of the primal cut algorithm have converged, the HUC problem (A.31)–(A.33) is solved for all $p \in P$ and for all $\omega \in \Omega'_p$. The reduced set Ω'_p is made up of those scenarios $\omega \in \Omega_p$ that determine the worst-case dispatch cost within partition p.

A pseudocode for the proposed decomposition scheme is provided in Algorithm 1. For ease of notation, let x (x^i) denote the vector of first-stage variables (at iteration i).

Notice that SPDA1 works in a similar way to a scenario reduction technique that retains the most detrimental scenarios in terms of system operating cost. This confers robustness to the solution of the proposed HUC problem. Moreover, the last command line in SPDA, which involves solving the HUC model for the reduced scenario sets $\Omega'_p, \forall p \in P$, could be carried out as well via further decomposition (see, for instance, [A29]), although this possibility has not been explored in this paper.

A.3.1.2 Scenario Partition and Decomposition Algorithm—Variant 2 (SPDA2)

Algorithm SPDA1 is inspired from the idea that only a few scenarios in the full set Ω_p may be needed to determine the worst-case dispatch cost for partition p and for *any* feasible unit-commitment plan. Based on this, Algorithm SPDA1 generates one instance of the Primal Cut Algorithm *per partition*.

Algorithm 1 Scenario Partition and Decomposition Algorithm: Variant 1 (**SPDA1**)

Choose k and apply k-means to Ω.
for all $p \in P$ **do**
  Set $i := 0$ and $\Omega_p^{\prime 0} = \emptyset$
  repeat
    Solve Master Problem
    Return optimal solution x^i
    Compute Lower Bound LB
    Set $x := x^i$ and **solve** SP $\forall \omega \in \Omega_p$
    Compute Upper Bound UB
    Identify worst-case scenario ω'
    Set $\Omega_p^{\prime i+1} := \Omega_p^{\prime i} \bigcup \{\omega'\}$
    Set $i := i + 1$
  until $\mid UB - LB \mid \leq \epsilon$
  Set $\Omega_p' := \Omega_p^{\prime i-1}$
end for
Solve HUC replacing Ω_p with $\Omega_p', \forall p$

The reader should notice, however, that, in order to compute the minimum expected system operating cost over the scenarios that deliver the worst-case dispatch cost within each partition, one might not need to calculate the partition-worst-case dispatch cost for *any* feasible unit-commitment plan and therefore, one might not need all those scenarios that algorithm SPDA1 aims to identify, but possibly a smaller number of them. With this in mind, we construct a second variant of our Scenario Partition and Decomposition Algorithm, which we denote SPDA2.

Unlike its first variant, SPDA2 only generates one single instance of the Primal Cut Algorithm, that is, a single master-subproblem scheme. The master problem is a mixed-integer programming problem that takes the following form at iteration i of the column-and-constraint generation procedure:

$$\underset{\mathcal{H}^i, \mathcal{W}^i, \theta_p}{\text{minimize}} \quad \sum_{t \in T} \sum_{g \in G} \left(C_g^F u_{g,t}^i + C_g^{SU} y_{g,t}^i + C_g^{SD} z_{g,t}^i \right) + \\ + \sum_{p \in P} \rho_p \theta_p \tag{A.41}$$

$$\text{s.t. } (A.2) - (A.7), \ (A.19) \tag{A.42}$$

$$\theta_p \geq \sum_{t\in T}\sum_{g\in G} C_g^V P_{g,t,\omega}^i + \sum_{t\in T}\sum_{l\in L} C^L L_{l,t,\omega}^{SH,i}, \tag{A.43}$$

$$(\forall p \in P, \ \forall \omega \in \Omega_p^{'i})$$

$$(A.8) - (A.18), \quad \forall p \in P, \ \forall \omega \in \Omega_p^{'i} \tag{A.44}$$

where $\mathcal{H}^i = \left\{u_{g,t}^i, y_{g,t}^i, z_{g,t}^i\right\}$ and $\mathcal{W}^i = \left\{P_{g,t,\omega}^i, L_{l,t,\omega}^{SH,i}, W_{f,t,\omega}^{SP,i}, \delta_{n,t,\omega}^i : \omega \in \Omega_p^{'i}, \ p \in P\right\}$, with $\Omega_p^{'0} = \emptyset$ for all $p \in P$.

The subproblems are linear programming problems analogous to (A.39)–(A.40). At every iteration i of the algorithm, the master problem (A.41)–(A.44) produces a tentative unit-commitment plan $\mathcal{H}^i$ that is fed into the subproblems (A.39)–(A.40). The scenarios $\{\omega_1', \omega_2', \ldots, \omega_p', \ldots, \omega_k'\}$, one per partition, that result in the highest dispatch cost within each partition are used to generate primal cuts in the form of (A.43)–(A.44) that are inserted into the master problem by setting $\Omega_p^{'i+1} = \Omega_p^{'i} \bigcup \{\omega_p'\}$, $\forall p \in P$.

We provide next a step-by-step description of SPDA2.

1. Choose the number k of partitions and apply a clustering method to the full set of scenarios Ω in order to assign each scenario to a certain partition p.

2. Create one instance of the primal cut algorithm.

3. Initialization: Set $i = 0$ and $\Omega_p^{'0} = \emptyset, \forall p \in P$.

4. Solve the master problem (MP). Return the optimal solution found by the branch-and-cut algorithm and denote this solution by $(u_{g,t}^i, y_{g,t}^i, z_{g,t}^i)$. Calculate a lower bound LB as $\sum_{t\in T}\sum_{g\in G}(C_g^F u_{g,t}^i + C_g^{SU} y_{g,t}^i + C_g^{SD} z_{g,t}^i) + \sum_{p\in P}\rho_p\theta_p$.

5. Solve the subproblems (SP) with the first-stage decision variables fixed at $(u_{g,t}^i, y_{g,t}^i, z_{g,t}^i)$. Once the SP are solved, the scenarios $\{\omega_1', \omega_2', \ldots, \omega_p', \ldots, \omega_k'\}$ associated with the subproblems that yield the highest dispatch cost in each partition p are identified and included into the reduced sets $\Omega_p^{\prime i+1}$, $p \in P$, i.e., $\Omega_p^{\prime i+1} = \Omega_p^{\prime i} \bigcup \{\omega_p'\}, \forall p \in P$. Compute an upper bound UB as $UB = \sum_{t\in T}\sum_{g\in G}\left(C_g^F u_{g,t}^i + C_g^{SU} y_{g,t}^i + C_g^{SD} z_{g,t}^i\right) + \sum_{p\in P}\rho_p\left(\sum_{t\in T}\sum_{g\in G} C_g^V P_{g,t,\omega_p'}^i + \sum_{t\in T}\sum_{l\in L} C^L L_{l,t,\omega_p'}^{SH,i}\right)$.

6. Convergence check: If $\mid UB - LB \mid \leq \epsilon$, being ϵ a user-specified tolerance value, the iterative process stops and $(u^i_{g,t}, y^i_{g,t}, z^i_{g,t})$ is returned as the optimal solution to the HUC problem. If $\mid UB - LB \mid > \epsilon$, then set $i := i + 1$ and go to step 4.

A pseudocode of this solution strategy is provided in Algorithm 2 below.

Algorithm 2 Scenario Partition and Decomposition Algorithm: Variant 2 (**SPDA2**)

Choose k and apply k-means to Ω.
Set $i := 0$ and $\Omega'^0_p = \emptyset$ for all $p \in P$
repeat
    Solve Master Problem
    Return optimal solution x^i
    Compute Lower Bound LB
    Set $x := x^i$ and **solve** SP $\forall \omega \in \Omega$
    Compute Upper Bound UB
    Identify worst-case scenario ω'_p in each $p \in P$
    Set $\Omega'^{i+1}_p := \Omega'^i_p \bigcup \{\omega'_p\}$ for all $p \in P$
    Set $i := i + 1$
until $\mid UB - LB \mid \leq \epsilon$
Return $x := x^{i-1}$ as the solution to HUC

The two variants of the proposed Scenario Partition and Decomposition Algorithm have several key differences, namely:

1. SPDA2 guarantees convergence to the HUC solution that is optimal under the partition P of the full scenario set Ω, while SPDA1 does not. Indeed, SPDA1 is heuristic, because it does not ensure that the scenarios the algorithm selects from each partition p are enough to deliver the worst-case dispatch cost for that partition under *any* first-stage solution. Our numerical experiments show, however, that SPDA1 performs very well in the sense that it provides unit commitment solutions that are optimal for the full HUC problem (A.31)–(A.33). Furthermore, it should be noticed that SPDA1 can be used to warm-start SPDA2.

2. Let Ω'_1 and Ω'_2 be the reduced set of scenarios retained by the master problems of SPDA1 and the sole master problem of SPDA2 at the end of the algorithms, respectively. In all our simulations (see the case study in Section A.4) it holds that $card(\Omega'_2) \leq card(\Omega'_1) \leq card(\Omega) = \lambda$.

3. At every iteration, SPDA2 solves one single master problem, while SPDA1 solves k, but smaller master problems, with $k = card(P)$.

4. SPDA1 must solve the HUC problem for the reduced scenario set Ω_1' at the end of the algorithm.

Differences 2-4 above determine how these two variants compare in computational terms. In particular, it is expected that, since SPDA1 works with smaller master problems at each iteration, but must solve a possibly larger HUC problem in the end, SPDA1 will perform better than SPDA2 when the number of partitions is kept sufficiently low. This is corroborated by our numerical experiments.

A.3.2 Parallelization of the Solution Algorithm

In the case of SPDA1 both the outer "for-loop"and the solution to the ω-indexed subproblems in the pseudocode of "Algorithm 1" are amenable to parallelization. For this purpose, we make use of the DTU High Performance Computing (HPC) Facility [A30]. We create k jobs, each representing an instance of the primal cut algorithm for each of the k partitions into which we divide the scenario set Ω. These jobs are simultaneously submitted to the HPC Cluster, where they are concurrently executed, as there is no need for communication in between the workers (nodes or cores).

We submit each of the k jobs to a different node, using the same amount of resources per node. Within every node, the subproblems are solved in a multi-threaded environment using the Gather-Update-Solve-Scatter Facility in GAMS [A31]. This tool allows treating each subproblem, one per scenario in the partition under consideration, as a different parametrization of the same linear programming model, which is then generated only once by GAMS. Likewise, the solutions to all the subproblems (or portions thereof) are retrieved back to GAMS in a single transaction.

In the case of SPDA2, the solution to the ω-indexed subproblems are also solved in the same way as in SPDA1, that is, by means of the the Gather-Update-Solve-Scatter Facility in GAMS [A31].

A.4 Case Studies

In the following the unit-commitment solution provided by the proposed HUC formulation is tested on the IEEE 14-node power system [A32] and the IEEE

3-Area RTS-96 system. The latter power system is also used to evaluate and compare the performance of the SPDA algorithms in Sections A.4.3 and A.4.4.

The IEEE 14-node system comprises 14 nodes, 5 generators, 20 lines and 11 loads. We also add one wind farm to node 5, whose power production is modeled by the ten scenarios provided in Table A.4 of the Appendix.

The IEEE 3-Area RTS-96 system consists of 72 nodes, 96 generators, 107 lines, and 51 loads. Besides, we add 15 wind farms of 200-MW capacity each and location given by Table A.5 in the Appendix. Thus, the wind power capacity represents 29% of the total generating capacity installed in the power system. The technical characteristics of the generating units, the demand and the transmission lines are available online [A33]. The wind power production scenarios used for this case study come from [A34], where the spatio-temporal dependencies of wind power generation are considered. More specifically, the study in [A34] provides 100 scenarios of wind power production that were generated for 15 control areas and 43 lead times in western Denmark. However, for this work, only 50 equiprobable scenarios and 24 lead times are considered.

We set the MIP tolerance gap to 0 in all the simulations pertaining to the IEEE 14-node system, while we allow for a MIP tolerance gap of up to $3 \cdot 10^{-4}$ (0.03%) in those numerical experiments carried out on the IEEE 3-Area RTS-96 system.

A.4.1 Evaluation of the Effect of the Number of Partitions

We consider the IEEE 14-node system and compare the unit-commitment plans resulting from the proposed HUC formulation with those obtained using the method proposed in [A19], which we refer to as *Zhao model* hereafter. This method minimizes a convex combination of the expected and the worst-case costs, where the convex combination is defined by the decision-maker through a weighting factor α. This way, Zhao model allows for a Pareto-efficient control of the degree of conservatism of the resulting unit-commitment solution in terms of the expected and worst-case system operating costs. For this reason, we use Zhao model here as an ideal benchmark against which we compare the ability of our proposed HUC formulation to find unit-commitment plans with a varying degree of conservatism by changing the number of partitions. The comparison is conducted for a number of partitions in the HUC problem ranging from 1 to 10 and a number of values for the weighting factor in Zhao model varying from 0 to 1.

The outcome of this comparison is that both Zhao model and our HUC formulation deliver the same only two unit-commitment plans, which we denote

Table A.1: Results of the comparison between Zhao model and the proposed HUC formulation.

UCP	CCD [$]	# Partitions	ZWF	ETC [$]	WCTC [$]
1	62569	6 - 10	0.8 - 1	286602	311534
2	63505	1 - 5	0 - 0.8	287131	307030

by UCP1 and UCP2. We measure the quality of these two different unit-commitment solutions in terms of both the expected and the worst-case system operating cost. The results are collated in Table A.1. The columns of this table provide the unit-commitment plan (UCP), the commitment cost (CCD), the number of partitions considered in our HUC formulation, the value of the weighting factor used in Zhao model (ZWF), the expected total cost (ETC) and the worst-case total cost (WCTC), in that order. Costs are given in US dollars. Furthermore, recall that the pure stochastic and robust unit-commitment solutions are obtained for a number of partitions equal to 10 and 1 in the proposed HUC formulation, and for values of the weighting factor in Zhao model equal to 1 and 0, respectively.

For this specific test we have used the k-means clustering method to define the partitions.

We can see from Table A.1 that UCP2 is more conservative than UCP1 and that there exists a one-to-one correspondence between the unit-commitment solutions provided by Zhao model and those given by the proposed HUC formulation. Thus, the proposed HUC formulation offers an alternative way to control the degree of conservatism of the resulting unit-commitment solution by way of the number of partitions. Besides, the *efficient frontier* (made up of Pareto-efficient points) is, in general, non-linear and non-continuous. Consequently, tuning the solution conservatism through the number of partitions, which is a natural number that ranges from 1 to the number of scenarios considered, is more practical than doing it through a weighting factor α that is a real number belonging to the closed real interval $[0, 1]$.

A.4.2 Evaluation of the Impact of the Clustering Technique

Next we analyze how the proposed HUC formulation performs when different clustering techniques are used to construct the partitions. For this purpose, we

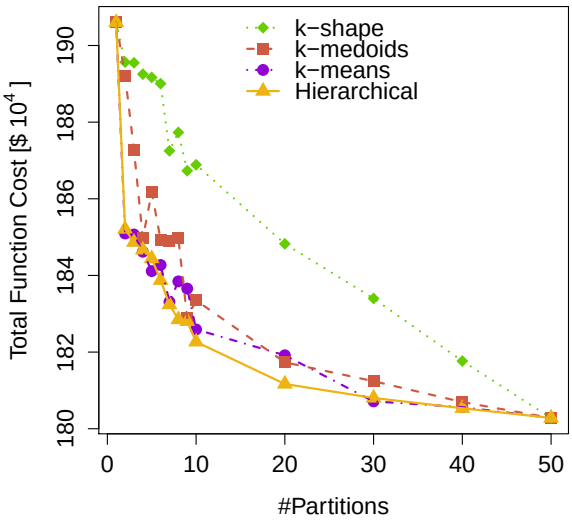

Figure A.1: HUC total cost as a function of the number of partitions and for four different clustering techniques.

conduct some numerical tests on the IEEE 3-Area RTS-96 system.

Fig. A.1 represents the objective function value (A.31) of the HUC formulation as the number of partitions increases. Each plot corresponds to a different clustering technique. As mentioned above, we consider the non-hierarchical clustering algorithms k-means, k-shape, and k-medoids, and an agglomerative hierarchical method.

In general terms, all the four clustering techniques prompt HUC solutions for which the HUC objective function value decreases as the number of partitions increases, as expected, but they do so at different speeds. In particular, the k-means and the hierarchical procedures achieve large reductions in the HUC cost with very few partitions. In practice, this means that these two clustering algorithms are able to prompt solutions from the HUC formulation that are close to the pure stochastic one with few partitions. This is clearly an advantage for two reasons at least: first, because our objective is, all in all, to approach the stochastic unit-commitment solution in a robust manner, that is, while keeping the worst-case cost under control; second, because, as we shall see later, the time required to solve the proposed HUC formulation decreases as so does the number of partitions.

In contrast, the plot corresponding to the k-shape method transits slowly from the pure robust solution to the pure stochastic one, which means that this methods requires a higher number of partitions to reduce the degree of conservatism of the UC solution.

It is interesting to note that, unlike the hierarchical clustering technique, the k-means, k-shape and k-medoids algorithms do not guarantee a monotone decrease in the HUC cost with the number of partitions. This is due to the non-hierarchical nature of these clustering methods, whereby the partitions they produce for $k-1$, k and $k+1$ clusters bear no relation, that is, they do not necessarily result from splitting or merging existing clusters.

The results that follow have been obtained using the hierarchical clustering technique, although very similar results are also obtained if the k-means algorithm is used.

A.4.3 Evaluation of the Decomposition Schemes

In this section we use the case study based on the IEEE 3-Area RTS-96 system to investigate and compare three different approaches for solving the proposed HUC formulation, namely, the two variants of the proposed Scenario Partition and Decomposition Algorithm (SPDA1 and SPDA2) and a solution strategy that merely consists in directly solving the "raw" HUC problem (without decomposition). All these alternative solution approaches are coded in GAMS using CPLEX 12.6.1 and implemented in the DTU HPC Cluster. The DTU HPC Cluster is a composite of a variety of hardware components of different technical characteristics. Therefore, we refer the reader to [A30] for further and detailed information on the cluster and its components. We solve the raw HUC (without decomposition) and the SPDA2 using one node in a multi-threading configuration that counts on 10 Intel cores, while SPDA1 is implemented in a multi-node and multi-threaded environment. In particular, partitions are solved in parallel, each in a different node of the cluster with up to 10 Intel cores per node. Lastly, the reduced HUC problem is solved using again one node employing up to 10 Intel cores. In both SPDA1 and SPDA2 the subproblems are solved using the Gather-Update-Solve-Scatter Facility in GAMS.

Table A.2 provides solutions times, achieved MIP gap (in percentage), number of scenarios retained in the final master problem, and expected and worst-case costs (in US dollars) for the three different solution strategies and for a different number of partitions. It is apparent that both SPDA1 and SPDA2 achieves remarkable time reductions without jeopardizing the solution quality at all. As expected, SPDA2 solves a last master problem with a few number of scenarios.

However, in the intermediate steps of the algorithm, SPDA1 works with smaller master problems which may make it more computationally efficient for a low number of partitions. Note also that the time savings attained by the parallelization and decomposition algorithms gradually decrease with the number of partitions.

All the results obtained so far suggest that, in a practical setup, we could tackle the stochastic unit commitment problem as follows: We solve the proposed HUC formulation using the SPDA1 algorithm, starting with one single partition (corresponding to the most risk-averse solution) and gradually increasing the number of partitions until either the decision-maker is satisfied with the performance of the last solution obtained (recall that the level of conservatism of the solution decreases with the number of partitions) or the amount of available time has been reached. Bear in mind that the k-means and the hierarchical clustering methods with few partitions prompt solutions from the HUC formulation that are close to the stochastic one and that the SPDA1 is precisely most efficient when the number of partitions is small. Note that such a procedure is not that easy to implement with the method presented in [A19], because the weighting factor α is a real number ranging from 0 to 1, both inclusive, and the relation between α and the efficient frontier can be non-linear and non-continuous. Therefore, it would be very difficult to define a step size for gradually increasing α as we can naturally do through the number of partitions.

Table A.2: Comparison of solving the HUC problem with and without decomposition.

		1 P (Robust)	**3 P**	**5 P**	**8 P**	**10 P**	**50 P (Stochastic)**
Time [min]	**raw HUC**	1322.7	687.6	767.4	721.6	788.1	140.2
	SPDA1	28.6	32.7	64.8	102.8	107.7	
	SPDA2		51.1	33.6	81.5	80.1	
GAP [%]	**raw HUC**	0.03	0.0299	0.0287	0.0297	0.0299	0.0292
	SPDA1		0.029	0.0297	0.0284	0.0206	
	SPDA2		0.03	0.0256	0.021	0.0284	
# Scen.	**raw HUC**	50	50	50	50	50	50
	SPDA1	5	10	11	17	18	
	SPDA2		8	9	12	14	
WC [$\$10^4$]	**raw HUC**	190.6035	190.6821	190.6360	190.8254	190.7072	191.8024
	SPDA1		190.6345	190.6426	190.6831	190.7932	
	SPDA2		190.7367	190.6573	190.6494	190.6978	
EC [$\$10^4$]	**raw HUC**	180.4169	180.4438	180.4131	180.3176	180.3397	180.2738
	SPDA1		180.4005	180.3980	180.3250	180.3448	
	SPDA2		180.4123	180.3832	180.3297	180.3562	

Table A.3: Results relative to the applicaction of the fast forward scenario reduction technique [A12].

# Scenarios	Time [min]	GAP [%]	EC [$\$10^4$]	WC [$\$10^4$]
5	2.8	0.0284	182.3564	212.0334
8	5.3	0.0293	181.0866	201.2821
9	7.4	0.0263	180.9487	200.6126
10	9.7	0.0294	180.9537	200.6188
11	11.1	0.0300	180.7298	197.9442
12	11.3	0.0291	180.6371	197.0820
14	11.7	0.0269	180.3185	194.0619
17	19.4	0.0287	180.2918	193.7436
18	25.6	0.0297	180.2912	193.7437

A.4.4 Comparison with a Scenario Reduction Technique.

We conclude our numerical study by comparing the unit-commitment solution given by SPDA1 or SPDA2 with that yielded by the widely-used fast forward scenario reduction technique [A12]. The results of this comparison are summarized in Table A.3 in terms of solution time (in seconds), MIP gap finally achieved (in percentage), and expected and worst-case costs (in US dollars). We use the fast forward selection algorithm to produce reduced scenario sets of varying cardinality. For the sake of a fair comparison, we make the cardinality of the reduced scenario set coincide with the number of scenarios retained (in the form of primal cuts) in the last master problem solved by SPDA1 or SPDA2 when one, two, five, eight and ten partitions are considered.

It is evident that, even though the use of a scenario reduction technique notably reduces the computational burden of the stochastic unit commitment problem, the unit-commitment solutions provided by SPDA1 and SPDA2 are significantly better in terms of the worst-case cost, while achieving expected costs close to that of the pure stochastic solution. Indeed, our solution approach yields unit-commitment plans that result in a worst-case cost that is, at least, 1.6% lower than the best worst-case cost provided by the scenario reduction technique (with 18 scenarios). Likewise, our solution approach provides unit-commitment plans that result in an expected cost that is, at most, 0.07% worse than that corresponding to the pure stochastic solution. This supports the conclusion that solving the proposed HUC formulation using either SPDA1 or SPDA2 constitutes a computationally efficient strategy to determine well-performing unit-commitment solutions in terms of the expected and worst-case costs.

A.5 Conclusion and Future Research

In this paper we propose a new formulation of the unit commitment problem under uncertainty that allows us to find unit-commitment plans that perform relatively well in terms of both the expected and the worst-case system operating cost. The new formulation relies on clustering the scenario data set into a number of partitions. The expectation of the system operating cost is then taken over those scenarios that result in the worst-case dispatch cost within each partition. The conservatism of the so-obtained unit-commitment solution (that is, how close it is to the pure scenario-based stochastic or robust unit-commitment plan) is controlled via the user-specified number of partitions. We also develop parallelization-and-decomposition schemes to efficiently solve the proposed unit-commitment formulation. Our numerical results show that our scheme is able to dramatically reduce the required running time while improving the optimality of the solution found.

We envision three avenues of future research at least. First, we would like to investigate how our methodology adapts to the case where the partitions are continuous uncertainty sets. Second, it would also be interesting to explore different possibilities to speed up the SPDA algorithms, for example, by warm-starting the solution to the proposed HUC formulation for k partitions with the solution obtained for $k-1$ partitions. Finally, we would like to extend our formulation and the associated solution approach to a multi-stage setup.

A.6 Appendix

This Appendix provides the wind power production scenarios used in the case study based on the IEEE 14-node system (Table A.4) and the location of wind farms in the 3-Area RTS-96 system (Table A.5).

Table A.4: Wind power production scenarios [MW] for the IEEE 14-node system.

	w1	w2	w3	w4	w5	w6	w7	w8	w9	w10
t1	66.45	67.06	65.39	57.12	42.9	37.8	38.64	29.12	27.96	22.35
t2	107.4	102.34	86.71	85.2	70.29	65.79	59.2	51.52	40.26	35.6
t3	113.25	103.32	100.23	90.6	74.47	66.24	63.76	51.45	47.82	37.25
t4	127.5	102.2	113.1	100.56	90.2	78.57	61.04	58.03	46.5	40.85
t5	124.2	113.68	106.08	109.2	94.6	78.48	68.32	55.3	51.84	37.95
t6	128.25	113.4	110.63	88.92	93.72	78.57	68.8	55.86	50.22	41.75
t7	152.1	147.98	127.14	116.04	101.31	91.71	78.48	73.85	60.78	52.65
t8	158.55	139.16	117.65	120.36	109.89	80.82	73.68	69.09	63.48	53.7
t9	120.15	119.14	107.77	93.24	81.4	70.65	58.64	51.24	46.2	42.5
t10	85.8	86.94	81.9	81.6	72.93	60.03	47.44	43.05	37.98	32.55
t11	148.2	141.68	133.51	128.88	105.05	89.37	82.16	67.41	52.74	52.7
t12	131.25	129.08	113.75	104.04	98.01	86.94	69.6	68.46	61.38	45.6
t13	135.45	120.12	117.65	102.36	93.61	71.28	62.4	59.5	46.98	39.55
t14	118.5	109.9	112.45	96	81.62	76.14	59.36	52.36	51.48	41.2
t15	110.25	114.52	104.39	90.84	92.51	72.18	62.4	50.96	47.46	39.9
t16	44.4	43.4	41.21	35.04	35.09	29.79	22.08	21.84	22.26	14.85
t17	5.55	6.02	5.85	4.44	4.51	3.87	3.44	2.8	2.22	2.05
t18	14.25	11.2	10.79	8.76	8.25	6.12	6.96	5.39	4.74	3.8
t19	17.1	13.72	14.69	12	10.45	8.73	7.04	8.26	6.06	4.65
t20	7.95	6.44	6.89	6.72	6.16	3.87	3.6	3.92	3.36	2.5
t21	9.6	7.84	7.41	6.84	7.7	5.67	5.44	3.92	3.78	3.05
t22	87.75	70.98	67.6	62.52	64.46	51.84	45.76	38.29	34.74	27.85
t23	119.4	104.58	114.14	98.16	88.33	70.47	66.72	61.88	49.98	45.15
t24	82.65	69.58	62.53	63.48	57.09	44.73	43.6	39.69	33.6	26.65

Table A.5: Location of wind farms in the IEEE 3-Area RTS-96 system.

Unit	Node	Unit	Node	Unit	Node	Unit	Node	Unit	Node
f_1	103	f_4	121	f_7	216	f_{10}	303	f_{13}	316
f_2	105	f_5	203	f_8	221	f_{11}	305	f_{14}	321
f_3	116	f_6	205	f_9	223	f_{12}	307	f_{15}	323

References A

[A1] J. R. Birge and F. Louveaux. *Introduction to stochastic programming*. Springer Science & Business Media, 2011.

[A2] A. Ben-Tal, L. El Ghaoui, and A. Nemirovski. *Robust optimization*. Vol. 28. Princeton University Press, 2009.

[A3] S. Takriti, J. R. Birge, and E. Long. "A stochastic model for the unit commitment problem". In: *IEEE Transactions on Power Systems* 11.3 (1996), pp. 1497–1508.

[A4] F. Bouffard, F. D. Galiana, and A. J. Conejo. "Market-clearing with stochastic security-part I: formulation". In: *IEEE T Power Syst* 20.4 (2005), pp. 1818–1826.

[A5] J. Wang, M. Shahidehpour, and Z. Li. "Security-constrained unit commitment with volatile wind power generation". In: *IEEE Transactions on Power Systems* 23.3 (2008), pp. 1319–1327.

[A6] J. M. Morales, A. J. Conejo, and J. Pérez-Ruiz. "Economic valuation of reserves in power systems with high penetration of wind power". In: *IEEE Transactions on Power Systems* 24.2 (2009), pp. 900–910.

[A7] A. Tuohy et al. "Unit commitment for systems with significant wind penetration". In: *IEEE Transactions on power systems* 24.2 (2009), pp. 592–601.

[A8] Q. Wang, Y. Guan, and J. Wang. "A chance-constrained two-stage stochastic program for unit commitment with uncertain wind power output". In: *IEEE Transactions on Power Systems* 27.1 (2012), pp. 206–215.

[A9] L. Zhao and B. Zeng. "Robust unit commitment problem with demand response and wind energy". In: *Power and Energy Society General Meeting, 2012 IEEE*. IEEE. 2012, pp. 1–8.

[A10] D. Bertsimas et al. "Adaptive robust optimization for the security constrained unit commitment problem". In: *IEEE Transactions on Power Systems* 28.1 (2013), pp. 52–63.

[A11] B. Zeng and L. Zhao. "Solving two-stage robust optimization problems using a column-and-constraint generation method". In: *Operations Research Letters* 41.5 (2013), pp. 457–461.

[A12] H. Heitsch and W. Römisch. "Scenario reduction algorithms in stochastic programming". In: *Computational optimization and applications* 24.2-3 (2003), pp. 187–206.

[A13] J. M. Morales et al. "Scenario reduction for futures market trading in electricity markets". In: *IEEE Transactions on Power Systems* 24.2 (2009), pp. 878–888.

[A14] S. Pineda and A. Conejo. “Scenario reduction for risk-averse electricity trading”. In: *IET generation, transmission & distribution* 4.6 (2010), pp. 694–705.

[A15] L. Liu et al. “A fuzzy-stochastic robust programming model for regional air quality management under uncertainty”. In: *Engineering Optimization* 35.2 (2003), pp. 177–199.

[A16] Y. Xu et al. “SRCCP: a stochastic robust chance-constrained programming model for municipal solid waste management under uncertainty”. In: *Resources, Conservation and Recycling* 53.6 (2009), pp. 352–363.

[A17] G. Liu, Y. Xu, and K. Tomsovic. “Bidding strategy for microgrid in day-ahead market based on hybrid stochastic/robust optimization”. In: *IEEE Transactions on Smart Grid* 7.1 (2016), pp. 227–237.

[A18] B. Fanzeres, A. Street, and L. A. Barroso. “Contracting strategies for renewable generators: A hybrid stochastic and robust optimization approach”. In: *IEEE Transactions on Power Systems* 30.4 (2015), pp. 1825–1837.

[A19] C. Zhao and Y. Guan. “Unified stochastic and robust unit commitment”. In: *IEEE Transactions on Power Systems* 28.3 (2013), pp. 3353–3361.

[A20] C. Zhao and Y. Guan. “Data-driven stochastic unit commitment for integrating wind generation”. In: *IEEE Transactions on Power Systems* 31.4 (2016), pp. 2587–2596.

[A21] V. Gabrel, C. Murat, and A. Thiele. “Recent advances in robust optimization: An overview”. In: *European journal of operational research* 235.3 (2014), pp. 471–483.

[A22] K. Wagstaff et al. “Constrained k-means clustering with background knowledge”. In: *ICML*. Vol. 1. 2001, pp. 577–584.

[A23] B. F. Hobbs and Y. Ji. “Stochastic programming-based bounding of expected production costs for multiarea electric power system”. In: *Operations Research* 47.6 (1999), pp. 836–848.

[A24] F. D. Munoz, B. F. Hobbs, and J.-P. Watson. “New bounding and decomposition approaches for MILP investment problems: Multi-area transmission and generation planning under policy constraints”. In: *European Journal of Operational Research* 248.3 (2016), pp. 888–898.

[A25] M. Carrión and J. M. Arroyo. “A computationally efficient mixed-integer linear formulation for the thermal unit commitment problem”. In: *IEEE Transactions on power systems* 21.3 (2006), pp. 1371–1378.

[A26] A. Papavasiliou and S. S. Oren. “Multiarea stochastic unit commitment for high wind penetration in a transmission constrained network”. In: *Operations Research* 61.3 (2013), pp. 578–592.

[A27] T. Hastie, R. Tibshirani, and J. Friedman. "Unsupervised learning". In: *The elements of statistical learning*. Springer, 2009, pp. 485–585.

[A28] J. Paparrizos and L. Gravano. "k-shape: Efficient and accurate clustering of time series". In: *Proceedings of the 2015 ACM SIGMOD International Conference on Management of Data*. ACM. 2015, pp. 1855–1870.

[A29] A. Papavasiliou, S. S. Oren, and B. Rountree. "Applying high performance computing to transmission-constrained stochastic unit commitment for renewable energy integration". In: *IEEE Transactions on Power Systems* 30.3 (2015), pp. 1109–1120.

[A30] *Central DTU HPC Cluster*. http://www.cc.dtu.dk/?page_id=342. (Accessed on 10/11/2018).

[A31] *Gather-Update-Solve-Scatter (GUSS)*. https://www.gams.com/latest/docs/S_GUSS.html. (Accessed on 10/11/2018).

[A32] *Power Systems Test Case Archive - UWEE*. http://labs.ece.uw.edu/pstca/. (Accessed on 10/11/2018).

[A33] *The REAL Lab - Renewable Energy Analysis Laboratory*. http://labs.ece.uw.edu/real/library.html. (Accessed on 10/11/2018).

[A34] P. Pinson et al. "Wind energy: Forecasting challenges for its operational management". In: *Statistical Science* 28.4 (2013), pp. 564–585.

Paper B

Integration of Different CHP Steam Extraction Modes in the Stochastic Unit Commitment Problem

Authors:
Ignacio Blanco, Hyoung-Yong Song, Daniela Guericke, Juan M. Morales, Jon-Bae Park, Henrik Madsen

Under review in:
IEEE Transactions on Sustainable Energy.

Integration of Different CHP Steam Extraction Modes in the Stochastic Unit Commitment Problem

Ignacio Blanco[1], Hyoung-Yong Song[2], Daniela Guericke[1], Juan M. Morales[3],Jong-Bae Park[4] and Henrik Madsen[1]

Abstract

This paper provides a formulation that integrates different operational modes for CHP units in the form of steam extraction configurations into the scenario-based two-stage stochastic and robust unit commitment problems under renewable power production uncertainty. The proposed formulation provides an additional flexibility to adapt to the imbalances in the power system through the interplay and real-time scheduling of the different operational modes for the CHP units. In addition, an improved solution approach based on heuristics, clustering and parallelization to speed up the model solution time is developed. Finally, the quality of the solutions is tested using a realistic test case based on the Danish transmission grid.

Nomenclature

The notation used throughout the paper is stated below for quick reference. Other symbols are defined as required.

Indexes and Sets

$\mathcal{T}$ Set of time periods t.

[1]Department of Applied Mathematics and Computer Science, Technical University of Denmark, DK-2800 Kgs. Lyngby, Denmark
[2]Korea District Heating Corporation, KR-13591 Gyeonggi-do, South Korea
[3]Department of Applied Mathematics, University of Malaga, SP-29071, Málaga, Spain
[4]Department of Electrical Engineering, Konkuk University, KR-05029 Seoul, South Korea

$\mathcal{N}$	Set of nodes n in the grid.
$\mathcal{G}$	Set of power generation units g.
$\mathcal{G}^{\mathrm{T}} \in \mathcal{G}$	Subset of conventional power generation units g.
$\mathcal{G}^{\mathrm{CHP}} \in \mathcal{G}$	Subset of combined heat and power production units g.
$\mathcal{M}$	Set of working modes m of the combined heat and power plants.
$\mathcal{M}'_m$	Set of operational modes m' that can be switched to from mode m.
$\mathcal{L}$	Set of electricity loads l.
$\mathcal{K}_n$	Set of nodes $k \in \mathcal{N}$ connected to node n by a transmission line.
$\mathcal{G}_n$	Set of power generation units g connected to node n.
$\mathcal{F}_n$	Set of stochastic power production units f connected to node n.
$\mathcal{L}_n$	Set of loads l connected to node n.
Ω	Set of scenarios ω.

Parameters

$a^{(\mathrm{CHP})}_{g,(m)}/b^{(\mathrm{CHP})}_{g,(m)}$	Fixed/Variable power production cost for power generation unit $g \in \mathcal{G}$ (CHP unit $g \in \mathcal{G}^{\mathrm{CHP}}$ using operational mode m).
$C^{\mathrm{SU}}_g/C^{\mathrm{SD}}_g$	Start-up/Shut-down cost for power generation unit g.
C^{L}	Penalty cost for load curtailment.
$U^{\mathrm{T}}_{g,(m)}/D^{\mathrm{T}}_{g,(m)}$	Number of periods conventional generation unit g (CHP unit $g \in \mathcal{G}^{\mathrm{CHP}}$ using operational mode m) must remain online/offline from the beginning of time horizon $t = 1$.
$T^{\mathrm{U}}_{g,(m)}/T^{\mathrm{D}}_{g,(m)}$	Minimum-up/Minimum-down time for power production unit g (CHP unit $g \in \mathcal{G}^{\mathrm{CHP}}$ using operational mode m).
$R^{\mathrm{U}}_g/R^{\mathrm{D}}_g$	Maximum ramp-up/ramp-down rate for power production of unit $g \in \mathcal{G}^{\mathrm{T}}$.
$R^{\mathrm{PU}}_{g,m}/R^{\mathrm{PD}}_{g,m}$	Maximum ramp-up/ramp-down rate for power production of unit $g \in \mathcal{G}^{\mathrm{CHP}}$ using operational mode m.
$R^{\mathrm{QU}}_{g,m}/R^{\mathrm{QD}}_{g,m}$	Maximum ramp-up/ramp-down rate for heat production of unit $g \in \mathcal{G}^{\mathrm{CHP}}$ using operational mode m.
$\overline{P}^{(\mathrm{CHP})}_{g,(m)}/\underline{P}^{(\mathrm{CHP})}_{g,(m)}$	Maximum/Minimum power production allowed for unit $g \in \mathcal{G}$ (CHP unit $g \in \mathcal{G}^{\mathrm{CHP}}$ using operational mode m).
$\overline{Q}_{g,m}/\underline{Q}_{g,m}$	Maximum/Minimum heat production for CHP unit $g \in \mathcal{G}^{\mathrm{CHP}}$ using operational mode m.
$\overline{S}_g/\underline{S}_g$	Maximum/Minimum capacity of the heat storage tank for CHP unit $g \in \mathcal{G}^{\mathrm{CHP}}$.
$X_{n,k}$	Reactance in line n-k.
$F_{n,k}$	Transmission capacity of line n-k.
$L_{l,t}$	Power consumed by load l at time t.

$W_{f,t}$	Power production from stochastic generator f at time t.
$Q^{\mathrm{D}}_{g,t}$	Heat demand assigned to CHP unit g at time t.
$\theta^{[\cdot]}_{g}$	Slope for the power-to-heat ratio for CHP unit $g \in \mathcal{G}^{\mathrm{CHP}}$.
$\delta^{[\cdot]}_{g}$	Intercept for the power-to-heat ratio of CHP unit $g \in \mathcal{G}^{\mathrm{CHP}}$.
$\varphi_{g,m}$	Marginal electricity loss for heat production for CHP unit $g \in \mathcal{G}^{\mathrm{CHP}}$ and operational mode $m \in \mathcal{M}$.
π_{ω}	Probability of scenario ω.

Decision variables

$x_{g,t}/y_{g,t}/z_{g,t}$	Binary variable equal to 1 if power production unit g is online/starting-up/shutting-down at time t and 0 otherwise.
$u_{g,m,t}$	Binary variable equal to 1 if unit $g \in \mathcal{G}^{\mathrm{CHP}}$ is working in mode m at time t.
$v_{g,m,m',t}$	Binary variable equal to 1 if unit $g \in \mathcal{G}^{\mathrm{CHP}}$ is changing from mode m to mode m' at time t.
$p^{(\mathrm{CHP})}_{g,(m),t}$	Power produced by unit $g \in \mathcal{G}$ (CHP unit $g \in \mathcal{G}^{\mathrm{CHP}}$ using operational mode m) at time t.
$q^{\mathrm{CHP}}_{g,m,t}$	Heat produced by CHP unit $g \in \mathcal{G}^{\mathrm{CHP}}$ working in mode m at time t.
$s_{g,t}$	Level of heat storage linked to $g \in \mathcal{G}^{\mathrm{CHP}}$ at time t.
$W^{\mathrm{spill}}_{f,t}$	Power production curtailment from stochastic generation unit f at time t.
$L^{\mathrm{shed}}_{l,t}$	Power demand curtailment from unit load l at time t.
$\phi_{n,t}$	Voltage angle at node n and time t.

B.1 Introduction

Cogeneration through combined heat and power (CHP) units is the synchronous generation of heat from electricity production. The efficiency of cogeneration can be translated to approximately 40% of savings compared to separate production of power and heat by conventional electricity production units and on-site heating boilers at households, respectively. Apart from their benefits for the environment, CHP units contribute to the decentralization of the power system and therefore, reduce losses in the electricity transmission network [B1]. During the last decades the installed cogeneration capacity has increased worldwide, and nowadays the integration of multiple energy vectors into the so-called smart energy systems, make CHP units one of the most important agents to achieve a full coordination between heat and power systems [B2]. From the

existing variety of CHP technologies (e.g. see [B3]), we focus on centralized steam bypass turbine CHP systems [B4]. These use different configurations of their components and regulate the steam extraction pressure from the turbine to the district heating network, allowing to operate the plant in different heat and power production regimes, which we call operational modes.

For a comprehensive background of how the different components of the CHP units are modeled through mixed integer linear programming (MILP), we refer to the following literature. The work presented in [B5] describes a CHP unit that integrates an extraction valve in the steam turbine, providing a realistic approach of all components in combined cycle gas turbine (CCGT) cogeneration units. The authors in [B6] present a detailed description of a biomass CHP unit that uses a bypass steam turbine connected to the district heating network. Both [B7] and [B8] present models that integrate CHP units working in different modes with renewable energy sources in district heating networks. The models define characteristic working points to describe the feasible heat and power production region of the CHP units. A more detailed study regarding the operational points of CHP units that consider different steam extraction regimes is presented in [B9]. The authors propose a model that optimizes the operation of the CHP units given different temperature supply functions that can work in two different operational modes (back pressure and extraction condensing). An optimal scheduling model for large steam-turbines CHP units is proposed in [B10]. The authors describe and model all components of the CHP units in order to create the different power and heat production regions for a bypass steam turbine. In addition, they present commitment constraints to describe the optimal operation for switching between different operational modes. Finally, [B11] defines different operational modes for a CCGT cogeneration unit that uses a bypass steam turbine. The study provides a detailed explanation of the different components as well the necessary operation needed to activate these operational modes. The presented publications consider the operation of the CHP unit alone or integrated in a district heating system. However, they do not consider the integration of CHP units in large-scale power systems. Due to the technical limitations of operating large thermal units to adapt to the renewable power fluctuations [B12], exploring the integration of the CHP units in the power grid has become a relevant subject. The flexibility provided by multiple operational modes and components as well as the inclusion of thermal storage can be used to integrate the uncertain renewable power production. In countries like Denmark, the share of renewable and partly unpredictable power generation is so high that the use of the district heating system as an energy buffer to accommodate these imbalances is wide spread. The high potential to integrate wind power fluctuations in Denmark using both centralized and decentralized CHP power plants to provide flexibility in the power system has been analyzed in [B13], where the authors conclude that in power systems with a high wind power integration more mechanisms to provide flexibility and fast response have

to be explored in order to make cogeneration a more competitive technology in terms of costs. A preliminary study done in [B14] shows that operating CHP units using different operational modes can increase the flexibility of a system with high integration of wind power. In addition, the authors in [B15] show the advantages of operating winds farms and CHP units as a portfolio and not as independent agents.

In this work we propose both a two-stage stochastic and a robust unit commitment model that accounts for the various operational modes of the CHP units. The goal is to co-optimize the configuration of the CHP units among the rest of the production units in the system in order to supply both heat and power as well as provide the flexibility needed to integrate wind power production. The different formulations of both the stochastic and robust unit commitment problem in power systems with high share of partly unpredictable energy sources, and their advantages, have been already subject in numerous studies; (i.e. [B16, B17, B18, B19, B20]). However, the introduction of the different CHP operational modes (binary variables) in the second stage, increases the computational burden of the unit commitment problem [B21]. Since a high share of wind power is included in the problem, the closer we are to the realization of the uncertainty to solve the unit commitment problem, the better it is to obtain a more accurate operation of the system. Therefore, we propose a solution approach to speed up the computational time. The proposed approach is an improved version of the decomposition and parallelization algorithm presented in [B22]. This solution is later compared to two alternative methods, namely, progressive hedging algorithm [B23] which is an efficient heuristic to solve the two-stage stochastic programming problem [B24] and a scenario reduction algorithm that uses partition around medoids (PAM) [B25]. The contributions of our paper can be summarized as follows.

1. A realistic implementation of the different CHP operational modes in the two-stage stochastic and robust unit commitment problem.
2. Analysis of the benefit in terms of costs and wind power integration of using a real-time scheduling of the CHP operational modes.
3. An enhancement of the decomposition and parallelization technique developed in [B22] by the use of heuristics.

The remainder of this paper is structured as follows. Section B.2 presents the formulations of the stochastic and robust unit commitment problem including the operational modes of the CHP units. Section B.3 presents the realistic case study used for the experiments. The results as well as the improvements carried out to speed up the model solution are shown in Section B.4. Finally, the paper is summarized in Section B.5.

B.2 Mathematical Formulation

The section is divided into four parts. First, the general two-stage stochastic unit commitment problem is formulated. Second, the different operational modes of the CHP units are integrated into the model. Third, the objective function is described. Finally, the robust optimization problem is defined. The basic formulation of the problem is similar to the one provided in [B26] and [B27].

B.2.1 General Two-stage Stochastic Unit Commitment

The basic model determines the commitment plan of the system providing information about the status of the units one day before the energy is delivered in the so-called day-ahead market. The first-stage decisions are grouped in vector $\mathcal{X}$=$\{x_{g,t}, y_{g,t}, z_{g,t}\}$. These first-stage decisions are made before the uncertainty occurs. In our problem, the uncertainty is represented by a finite set of scenarios $\omega \in \Omega$ in the form of discrete wind power production values ($W_{f,t,\omega}$). Once the uncertain wind power production realizes, we can adapt the system by means of the recourse or second-stage variables that are grouped in vector $\mathcal{Y}$=$\{u_{g,m,t,\omega}$,$v_{g,m,m',t,\omega}$, $p_{g,t,\omega}$, $L^{\text{shed}}_{l,t,\omega}$, $W^{\text{spill}}_{f,t,\omega}$, $p^{\text{CHP}}_{g,m,t,\omega}$, $q^{\text{CHP}}_{g,m,t,\omega}$, $s_{g,t,\omega}$, $\phi_{n,t,\omega}\}$. These decisions are made during the balancing stage, which is when the energy is delivered. The initial status of the variables are indexed with the superscript 0 (x^0_g, p^0_g, q^0_g, $u^0_{g,m}$) and they are independent from the scenario realization. This first part of the model (B.1a)-(B.1n) is applicable for all generators in the system. Constraints (B.1a)-(B.1e) describe the feasibility regarding the commitment decisions in the system. More specifically, equation (B.1a) determines when the unit must be switched on or turned off. Equation (B.1b) avoids to switch on and off the unit simultaneously. Constraint (B.1c) initializes the commitment value of the unit and finally constraints (B.1d) and (B.1e) ensure the minimum time that the unit must remain connected to or disconnected from the system after being switched on or shut down, respectively.

$$y_{g,t} - z_{g,t} = x_{g,t} - x_{g,t-1} \qquad (\forall g, \forall t) \qquad \text{(B.1a)}$$

$$y_{g,t} + z_{g,t} \leq 1 \qquad (\forall g, \forall t) \qquad \text{(B.1b)}$$

$$x_{g,t} = x^0_g \qquad (U^{\text{T}}_g + D^{\text{T}}_g > 0, \forall g, \forall t \leq U^{\text{T}}_g + D^{\text{T}}_g) \qquad \text{(B.1c)}$$

$$\sum_{\tau=t-T^{\text{U}}_g+1}^{t} y_{g,\tau} \leq x_{g,t} \qquad (\forall g, \forall t > U^{\text{T}}_g + D^{\text{T}}_g) \qquad \text{(B.1d)}$$

$$\sum_{\tau=t-T^{\text{D}}_g+1}^{t} z_{g,\tau} \leq 1 - x_{g,t} \qquad (\forall g, \forall t > U^{\text{T}}_g + D^{\text{T}}_g) \qquad \text{(B.1e)}$$

The maximum and minimum power production of the units is bounded by constraint (B.1f).

$$\underline{P_g} x_{g,t} \leq p_{g,t,\omega} \leq \overline{P_g} x_{g,t} \qquad (\forall g, \forall t, \forall \omega \in \Omega) \tag{B.1f}$$

Similarly to [B28] and [B19], the ramping limits of the units are ensured by constraints (B.1g) and (B.1h).

$$\begin{aligned} &p_{g,t,\omega} - p_{g,t-1,\omega} \leq (2 - x_{g,t-1} - x_{g,t})\underline{P_g} \\ &+ (1 + x_{g,t-1} - x_{g,t}) R_g^{\mathrm{U}} \qquad (\forall g, \forall t, \forall \omega \in \Omega) \end{aligned} \tag{B.1g}$$

$$\begin{aligned} &p_{g,t-1,\omega} - p_{g,t,\omega} \leq (2 - x_{g,t-1} - x_{g,t})\underline{P_g} \\ &+ (1 - x_{g,t-1} + x_{g,t}) R_g^{\mathrm{D}} \qquad (\forall g, \forall t, \forall \omega \in \Omega) \end{aligned} \tag{B.1h}$$

The set of nodal power balances according to a DC power flow model is determined by equalities (B.1i).

$$\begin{aligned} &\sum_{g \in \mathcal{G}_n} p_{g,t,\omega} - \sum_{l \in \mathcal{L}_n} \left(L_{l,t} - L_{l,t,\omega}^{\mathrm{shed}}\right) + \sum_{f \in \mathcal{F}_n} \left(W_{f,t,\omega} - W_{f,t,\omega}^{\mathrm{spill}}\right) \\ &= \sum_{k \in \mathcal{K}_n} \frac{(\phi_{n,t,\omega} - \phi_{k,t,\omega})}{X_{n,k}} \qquad (\forall n, \forall t, \forall \omega \in \Omega) \end{aligned} \tag{B.1i}$$

The maximum flow allowed between two connected nodes is restrained by constraint (B.1j).

$$\begin{aligned} &-F_{n,k} \leq \frac{(\phi_{n,t,\omega} - \phi_{k,t,\omega})}{X_{n,k}} \leq F_{n,k} \\ &(\forall n, \forall k \in \mathcal{K}_n, \forall t, \forall \omega \in \Omega) \end{aligned} \tag{B.1j}$$

The involuntary load curtailment and wind spillage are limited by equations (B.1k) and (B.1l) respectively.

$$L_{l,t,\omega}^{\mathrm{shed}} \leq L_{l,t} \qquad (\forall l, \forall t, \forall \omega \in \Omega) \tag{B.1k}$$

$$W_{f,t,\omega}^{\mathrm{spill}} \leq W_{f,t,\omega} \qquad (\forall f, \forall t, \forall \omega \in \Omega) \tag{B.1l}$$

The variable domains are given in equations (B.1m) and (B.1n).

$$x_{g,t}, y_{g,t}, z_{g,t} \in \{0, 1\} \qquad (\forall g, \forall t) \tag{B.1m}$$

$$p_{g,t,\omega}, L_{l,t,\omega}^{\mathrm{shed}}, W_{f,t,\omega}^{\mathrm{spill}} \geq 0 \qquad (\forall g, \forall l, \forall f, \forall t, \forall \omega \in \Omega) \tag{B.1n}$$

The initial conditions of the problem are determined as in [B29], where $T_g^{\mathrm{ON}}/T_g^{\mathrm{OFF}}$ are the periods of time that unit g has been online/offline before the beginning of time horizon $t = 1$.

$$x_g^0 = \begin{cases} 1 & \text{if } T_g^{\text{ON}} > 0 \\ 0 & \text{if } T_g^{\text{ON}} = 0 \end{cases}$$

$$U_g^{\text{T}} = \min\{\mathcal{T}, (T_g^{\text{U}} - T_g^{\text{ON}})x_g^0\}$$
$$D_g^{\text{T}} = \min\{\mathcal{T}, (T_g^{\text{D}} - T_g^{\text{OFF}})(1 - x_g^0)\}$$

B.2.2 Modeling of the CHP units

The extension presented in this section integrates the use of different CHP operational modes into our model. We base the modeling of operational modes on [B11] where the authors determine five different steam extraction regimes. From these regimes or modes, two are considered under abnormal or emergency situations while the other three are used in regular conditions. For this work we just consider the three latter modes that are briefly described as follows. The *Heat Mode* (m_1) is the most efficient when a large amount of heat production is needed. The entire mass of steam flows from the high pressure turbine to the district heating network. The relation between heat and power production is then linear. In the *Mixed Mode* (m_2), a fraction of the steam feeds the district heating network and the remaining steam moves to the low pressure part of the turbine. As a result we obtain a heat and power production region where the minimum heat production is limited by the opening pressure, which is determined by the size of the extraction valve. Finally, we consider the *Electricity Mode* (m_3), in which the entire steam flow serves the low-pressure turbine and nothing is fed to the district heating network. In this way, the unit achieves full condensation and the efficiency for electricity production increases. We refer to Figure B.1 where the heat and power production regions of the three different operational modes are depicted. For further details regarding the operational modes we refer to [B11].

As described in Figure B.1, equality constraints (B.2a) determine the relation between the heat and power production for the *Heat Mode* and the set of inequalities (B.2b)-(B.2d) describe the feasible region in which the *Mixed Mode* can operate.

$$p^{\text{CHP}}_{g,m_1,t,\omega} = \theta_g q^{\text{CHP}}_{g,m_1,t,\omega} + \delta_g \qquad (\forall g, \forall t, \forall \omega \in \Omega) \qquad \text{(B.2a)}$$
$$p^{\text{CHP}}_{g,m_2,t,\omega} \geq \theta^{\text{I}}_g q^{\text{CHP}}_{g,m_2,t,\omega} + \delta^{\text{I}}_g \qquad (\forall g, \forall t, \forall \omega \in \Omega) \qquad \text{(B.2b)}$$
$$p^{\text{CHP}}_{g,m_2,t,\omega} \leq \theta^{\text{II}}_g q^{\text{CHP}}_{g,m_2,t,\omega} + \delta^{\text{II}}_g \qquad (\forall g, \forall t, \forall \omega \in \Omega) \qquad \text{(B.2c)}$$
$$p^{\text{CHP}}_{g,m_2,t,\omega} \geq \theta^{\text{III}}_g q^{\text{CHP}}_{g,m_2,t,\omega} + \delta^{\text{III}}_g \qquad (\forall g, \forall t, \forall \omega \in \Omega) \qquad \text{(B.2d)}$$

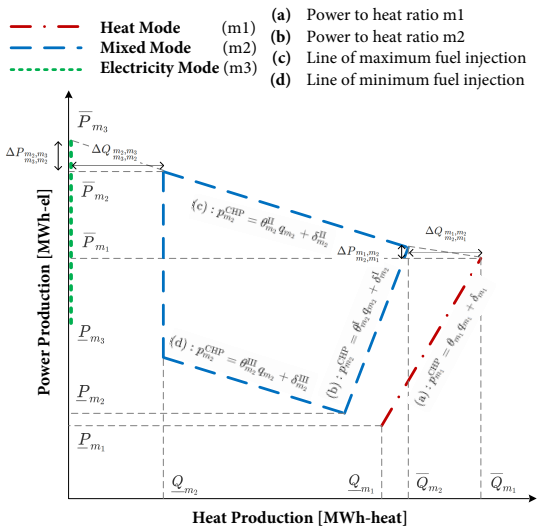

Figure B.1: Power and heat production regions for the Heat, Mixed and Electricity modes

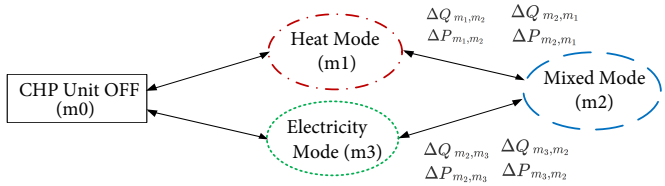

Figure B.2: Mode names and changing modes requirements

The maximum and minimum power and heat output for the CHP unit in each mode is bounded by (B.2e) and (B.2f), respectively. If the CHP unit is operating in mode m at time t, $u_{g,m,t}$ equals 1 and 0 otherwise.

$$\underline{P}^{\mathrm{CHP}}_{g,m} u_{g,m,t,\omega} \leq p^{\mathrm{CHP}}_{g,m,t,\omega} \leq \overline{P}^{\mathrm{CHP}}_{g,m} u_{g,m,t,\omega} \quad \text{(B.2e)}$$
$$(\forall g \in \mathcal{G}^{\mathrm{CHP}}, \forall m, \forall t, \forall \omega \in \Omega)$$
$$\underline{Q}_{g,m} u_{g,m,t,\omega} \leq q^{\mathrm{CHP}}_{g,m,t,\omega} \leq \overline{Q}_{g,m} u_{g,m,t,\omega} \quad \text{(B.2f)}$$
$$(\forall g \in \mathcal{G}^{\mathrm{CHP}}, \forall m, \forall t, \forall \omega \in \Omega)$$

The use and interplay between different modes is described in Figure B.2 where due to the operation of the valve, CHP units have to start and finish the operation in *Heat mode* or *Electricity mode*. Furthermore, if the low-pressure turbine is stopped (*Heat mode*), it needs a certain time until it reaches its max-

imum efficiency point which is the full condensation mode (*Electricity mode*) and therefore, changes between these two configurations require to go through the *Mixed mode*. For a more technical detailed description regarding the interplay between modes we refer the reader to [B9, B10, B11]. The power production limitations while changing modes are modeled in equations (B.2g) and (B.2h) where $\Delta P_{g,m,m'}$ is the maximum power difference allowed between modes. These equations are used additionally as ramping-up and ramping-down constraints, respectively. The power difference when starting-up and shutting-down the unit must be the minimum power production allowed in the current working mode. The same principle is applied for the heat ramping constraints (B.2i) and (B.2j) where $\Delta Q_{g,m,m'}$ is the maximum heat difference admitted between modes. Set of equations (B.2g)-(B.2j) are formulated as in [B30].

$$p^{\mathrm{CHP}}_{g,m,t,\omega} - p^{\mathrm{CHP}}_{g,m,t-1,\omega} - \sum_{m' \in \mathcal{M}'_m} p^{\mathrm{CHP}}_{g,m',t-1,\omega} \leq R^{\mathrm{PU}}_{g,m} u_{g,m,t,\omega} - \sum_{m' \in \mathcal{M}'_m} \left(R^{\mathrm{PU}}_{g,m} - \Delta P_{g,m',m}\right) v_{g,m',m,t,\omega} \quad (\forall g \in \mathcal{G}^{\mathrm{CHP}}, \forall m, \forall t, \forall \omega \in \Omega) \tag{B.2g}$$

$$p^{\mathrm{CHP}}_{g,m,t-1,\omega} - p^{\mathrm{CHP}}_{g,m,t,\omega} - \sum_{m' \in \mathcal{M}'_m} p^{\mathrm{CHP}}_{g,m',t,\omega} \leq R^{\mathrm{PD}}_{g,m} u_{g,m,t-1,\omega} - \sum_{m' \in \mathcal{M}'_m} \left(R^{\mathrm{PD}}_{g,m} - \Delta P_{g,m,m'}\right) v_{g,m,m',t,\omega} \quad (\forall g \in \mathcal{G}^{\mathrm{CHP}}, \forall m, \forall t, \forall \omega \in \Omega) \tag{B.2h}$$

$$q^{\mathrm{CHP}}_{g,m,t,\omega} - q^{\mathrm{CHP}}_{g,m,t-1,\omega} - \sum_{m' \in \mathcal{M}'_m} q^{\mathrm{CHP}}_{g,m',t-1,\omega} \leq R^{\mathrm{QU}}_{g,m} u_{g,m,t,\omega} - \sum_{m' \in \mathcal{M}'_m} \left(R^{\mathrm{QU}}_{g,m} - \Delta Q_{g,m',m}\right) v_{g,m',m,t,\omega} \quad (\forall g \in \mathcal{G}^{\mathrm{CHP}}, \forall m, \forall t, \forall \omega \in \Omega) \tag{B.2i}$$

$$q^{\mathrm{CHP}}_{g,m,t-1,\omega} - q^{\mathrm{CHP}}_{g,m,t,\omega} - \sum_{m' \in \mathcal{M}'_m} q^{\mathrm{CHP}}_{g,m',t,\omega} \leq R^{\mathrm{QD}}_{g,m} u_{g,m,t-1,\omega} - \sum_{m' \in \mathcal{M}'_m} \left(R^{\mathrm{QD}}_{g,m} - \Delta Q_{g,m,m'}\right) v_{g,m,m',t,\omega} \quad (\forall g \in \mathcal{G}^{\mathrm{CHP}}, \forall m, \forall t, \forall \omega \in \Omega) \tag{B.2j}$$

Following the work of [B31], we model the transition between modes using equation (B.2k) that coordinates the use and activation of the different working modes. In addition, the minimum time that mode m in CHP unit g must

remain activated or deactivated is defined in constraints (B.2l)-(B.2n).

$$u_{g,m,t,\omega} - u_{g,m,t-1,\omega} = \sum_{m' \in \mathcal{M}'_m} \left(v_{g,m',m,t,\omega} - v_{g,m,m',t,\omega} \right) \tag{B.2k}$$
$$(\forall g \in \mathcal{G}^{\text{CHP}}, \forall m, \forall t, \forall \omega \in \Omega)$$

$$u_{g,m,t,\omega} = u^0_{g,m} \tag{B.2l}$$
$$(U^{\text{T}}_{g,m} + D^{\text{T}}_{g,m} > 0, \forall g \in \mathcal{G}^{\text{CHP}}, \forall t \leq U^{\text{T}}_{g,m} + D^{\text{T}}_{g,m})$$

$$\sum_{\tau=t-T^{\text{U}}_{g,m}+1}^{t} \sum_{m' \in \mathcal{M}'_m} v_{g,m',m,\tau,\omega} \leq u_{g,m,t,\omega} \tag{B.2m}$$
$$(\forall g \in \mathcal{G}^{\text{CHP}}, \forall t > U^{\text{T}}_{g,m} + D^{\text{T}}_{g,m}, \forall \omega \in \Omega)$$

$$\sum_{\tau=t-T^{\text{D}}_{g,m}+1}^{t} \sum_{m' \in \mathcal{M}'_m} v_{g,m,m',\tau,\omega} \leq 1 - u_{g,m,t,\omega} \tag{B.2n}$$
$$(\forall g \in \mathcal{G}^{\text{CHP}}, \forall t > U^{\text{T}}_{g,m} + D^{\text{T}}_{g,m}, \forall \omega \in \Omega)$$

The initial conditions for the modes used by CHP units are determined as

$$u^0_{g,m} = \begin{cases} 1 & \text{if } T^{\text{ON}}_{g,m} > 0 \\ 0 & \text{if } T^{\text{ON}}_{g,m} = 0 \end{cases}$$

$$U^{\text{T}}_{g,m} = \min\{\mathcal{T}, (T^{\text{U}}_{g,m} - T^{\text{ON}}_{g,m}) u^0_{g,m}\}$$
$$D^{\text{T}}_{g,m} = \min\{\mathcal{T}, (T^{\text{D}}_{g,m} - T^{\text{OFF}}_{g,m})(1 - u^0_{g,m})\}$$

where $T^{\text{ON}}_{g,m}/T^{\text{OFF}}_{g,m}$ are the periods of time that unit $g \in \mathcal{G}^{\text{CHP}}$ has been operating in mode m before the beginning of time horizon $t = 1$. To ensure that all operational modes are mutually exclusive, we formulate (B.2o) and (B.2p), while equations (B.2q) sets the power produced in each mode to the total power production of the unit. Notice that $p_{g,t,\omega}$ in (B.2q) enters equation (B.1i).

$$u_{g,m_0,t,\omega} = 1 - x_{g,t,\omega} \qquad (\forall g \in \mathcal{G}^{\text{CHP}}, \forall t, \forall \omega \in \Omega) \tag{B.2o}$$

$$u_{g,m_1,t,\omega} + u_{g,m_2,t,\omega} + u_{g,m_3,t,\omega} = x_{g,t} \tag{B.2p}$$
$$(\forall g \in \mathcal{G}^{\text{CHP}}, \forall t, \forall \omega \in \Omega)$$

$$\sum_{m \in \mathcal{M}} p^{\text{CHP}}_{g,m,t,\omega} = p_{g,t,\omega} \qquad (\forall g \in \mathcal{G}^{\text{CHP}}, \forall t, \forall \omega \in \Omega) \tag{B.2q}$$

We model one thermal storage per unit $g \in \mathcal{G}^{\text{CHP}}$ assuming that all heat production goes to the storage and from the storage to the district heating network. Equation (B.2r) determines the storage level of each unit $g \in \mathcal{G}^{\text{CHP}}$ at each time step t as well as the heat balance in the system. In case $t = 1$ we assume

$s_{g,t-1} = s_g^0$. The maximum and minimum storage level is modeled in constraint (B.2s). Constraint (B.2t) limits the final storage level at least as the one given at the beginning.

$$s_{g,t,\omega} = s_{g,t-1,\omega} + q^{\mathrm{CHP}}_{g,t,\omega} - Q^{\mathrm{D}}_{g,t} \qquad \text{(B.2r)}$$
$$(\forall g \in \mathcal{G}^{\mathrm{CHP}}, \forall t, \forall \omega \in \Omega)$$
$$\underline{S}_g \leq s_{g,t,\omega} \leq \overline{S}_g \qquad (\forall g \in \mathcal{G}^{\mathrm{CHP}}, \forall t, \forall \omega \in \Omega) \qquad \text{(B.2s)}$$
$$s_{|\mathcal{T}|} \geq s_0 \qquad \text{(B.2t)}$$

Finally, constraints (B.2u) and (B.2v) define the variable domains.

$$u_{g,m,t,\omega}, v_{g,m,m',t,\omega} \in \{0,1\} \qquad \text{(B.2u)}$$
$$(\forall g \in \mathcal{G}^{\mathrm{CHP}}, \forall m, \forall m' \in \mathcal{M}_m^{'}, \forall t, \forall \omega \in \Omega)$$
$$p^{\mathrm{CHP}}_{g,m,t}, q_{g,m,t,\omega}, s_{g,t,\omega} \geq 0 \qquad \text{(B.2v)}$$
$$(\forall g \in \mathcal{G}^{\mathrm{CHP}}, \forall m, \forall t, \forall \omega \in \Omega)$$

B.2.3 Objective Function

The objective function (B.3) minimizes the expected system operating cost where fix and variable power production costs are divided in costs for conventional units ($g \in \mathcal{G}^{\mathrm{T}}$) and cost for CHP units ($g \in \mathcal{G}^{\mathrm{CHP}}$). A penalty costs for not supplied load is added in the form of slack variables. The marginal wind power production cost is set to zero.

$$\min_{\mathcal{X},\mathcal{Y}} \sum_{t\in\mathcal{T}} \sum_{g\in\mathcal{G}} \left(a_g x_{g,t} + C^{\mathrm{SU}}_g y_{g,t} + C^{\mathrm{SD}}_g z_{g,t}\right) \qquad \text{(B.3)}$$
$$+ \sum_{t\in\mathcal{T}} \sum_{\omega\in\Omega} \pi_\omega \Bigg(\sum_{g\in\mathcal{G}^T} b_g p_{g,t,\omega} + \sum_{g\in\mathcal{G}^{\mathrm{CHP}}} \sum_{m\in\mathcal{M}} \Big[a^{\mathrm{CHP}}_{g,m} u_{g,m,t,\omega}$$
$$+ b^{\mathrm{CHP}}_{g,m} \left(p^{\mathrm{CHP}}_{g,m,t,\omega} + \varphi_{g,m} q^{\mathrm{CHP}}_{g,m,t,\omega}\right)\Big] + \sum_{n\in\mathcal{N}} C^{\mathrm{L}} L^{\mathrm{shed}}_{n,t,\omega} \Bigg)$$

The entire model can be summarized as in (B.4a)-(B.4c).

$$\min_{\mathcal{V}} \ \text{(B.3)} \qquad \text{(B.4a)}$$
$$\text{s.t. } \text{(B.1a)} - \text{(B.1n)} \qquad \text{(B.4b)}$$
$$\text{(B.2a)} - \text{(B.2v)} \qquad \text{(B.4c)}$$

For $t = \{1\}$, the decision variables index with $t-1$ are given by $x_{g,t-1} = x^0_g$, $p_{g,t-1} = p^0_g$, $u_{g,m,t-1} = u^0_{g,m}$, $p^{\mathrm{CHP}}_{g,m,t-1} = p^0_g u^0_{g,m}$ and $q^{\mathrm{CHP}}_{g,m,t-1} = q^0_g u^0_{g,m}$.

B.2.4 Two-stage Scenario-based Robust Unit Commitment

In order to formulate a robust unit commitment problem, we adapt the two-stage stochastic unit commitment (B.4a)-(B.4c) using a column-and-constraint generation method [B32].

$$\min_{\mathcal{X},\mathcal{Y},\beta} \sum_{t\in\mathcal{T}}\sum_{g\in\mathcal{G}} \left(a_g x_{g,t} + C_g^{\mathrm{SU}} y_{g,t} + C_g^{\mathrm{SD}} z_{g,t}\right) + \beta \tag{B.5a}$$

$$\begin{aligned}\text{s.t. } \beta \geq & \sum_{t\in\mathcal{T}}\sum_{g\in\mathcal{G}^T} b_g p_{g,t,\omega} + \sum_{t\in\mathcal{T}}\sum_{n\in\mathcal{N}} C^{\mathrm{L}} L^{\mathrm{shed}}_{n,t,\omega} \\ & + \sum_{t\in\mathcal{T}}\sum_{g\in\mathcal{G}^{\mathrm{CHP}}}\sum_{m\in\mathcal{M}} a^{\mathrm{CHP}}_{g,m} u_{g,m,t,\omega} \\ & + \sum_{t\in\mathcal{T}}\sum_{g\in\mathcal{G}^{\mathrm{CHP}}}\sum_{m\in\mathcal{M}} b^{\mathrm{CHP}}_{g,m}\left(p^{\mathrm{CHP}}_{g,m,t,\omega} + \varphi_{g,m} q^{\mathrm{CHP}}_{g,m,t,\omega}\right) \\ & (\forall \omega \in \Omega)\end{aligned} \tag{B.5b}$$

$$(\text{B.1a}) - (\text{B.1n}), (\text{B.2a}) - (\text{B.2v}) \tag{B.5c}$$

where β is an auxiliary variable that is bounded from below by constraints (B.5b) and equals the worst-case dispatch cost, which replaces the expected value in the objective function.

B.3 Case Study

A simplification of the Danish transmission grid [B33] is used as case study. Only the 400 kV lines, central loads and central production units are taken into account. The study considers 13 different central units where 9 are coal power plants and the remaining 4 are CCGT cogeneration units. The total number of nodes considered is 18, where one wind farm representing the total wind generation from the nodal region is attached to each node. The heat demand is divided in four differently sized urban areas, one per CHP, all of them with a heat density of 120 TJ/km^2 per year. The wind power production scenarios are generated using the methodology described in [B34]. For the sake of simplicity, the spatio-temporal dependencies of wind power generation are considered just between the two Danish bidding areas in Nordpool named DK1 and DK2. In order to complement the original data set [B33], we use real production costs, volumes of fuel injection and more technical data for a 276 MW CCGT cogeneration unit that we extrapolated to the ones used in the Danish case study. The complementary data is given in Tables B.1 and B.2.

Table B.1: Generators Data. Units for a_g are 10^3\$. T_g^{U}, T_g^{D} are given in hours. R_g^{U} and R_g^{D} are expressed in MW/hour and finally $\overline{S}_g$ and $\underline{S}_g$ in MWh

	Type	a_g	T_g^{U}	T_g^{D}	R_g^{U}	R_g^{D}	$\overline{S}_g$	$\underline{S}_g$
g_1	Coal	5.528	6	4	220	220	-	-
g_2	Coal	5.414	6	4	220	220	-	-
g_3	Coal	5.210	6	4	220	220	-	-
g_4	Gas CHP	4.081	3	3	-	-	1687	169
g_5	Coal	7.419	6	4	220	220	-	-
g_6	Coal	3.897	6	4	200	200	-	-
g_7	Coal	1.839	6	4	220	220	-	-
g_8	Coal	2.558	6	4	220	220	-	-
g_9	Gas CHP	0.894	3	3	-	-	370	37
g_{10}	Coal	7.568	6	4	220	220	-	-
g_{11}	Gas CHP	5.715	6	4	-	-	2362	236
g_{12}	Gas CHP	1.361	3	3	-	-	563	56
g_{13}	Coal	3.110	6	4	220	220	-	-

The remaining complementary parameters are given as follows.

$$R_{g,m}^{\mathrm{PU}} = R_{g,m}^{\mathrm{PD}} = \frac{\overline{P}_{g,m}^{\mathrm{CHP}} - \underline{P}_{g,m}^{\mathrm{CHP}}}{T_{g,m}^{\mathrm{U}}} \quad (\forall g \in \mathcal{G}^{\mathrm{CHP}}, \forall m \in \mathcal{M})$$

$$R_{g,m}^{\mathrm{QU}} = R_{g,m}^{\mathrm{QD}} = \frac{\overline{Q}_{g,m}^{\mathrm{CHP}} - \underline{Q}_{g,m}^{\mathrm{CHP}}}{T_{g,m}^{\mathrm{U}}} \quad (\forall g \in \mathcal{G}^{\mathrm{CHP}}, \forall m \in \mathcal{M})$$

$$\theta_g = 1.847,\ \theta_g^{\mathrm{I}} = 1.798,\ \theta_g^{\mathrm{II}} = -0.242,\ \theta_g^{\mathrm{III}} = -0.242$$
$$(\forall g \in \mathcal{G}^{\mathrm{CHP}})$$

$$\varphi_{g,m_0} = \varphi_{g,m_1} = \varphi_{g,m_3} = 0, \varphi_{g,m_2} = -0.242$$
$$(\forall g \in \mathcal{G}^{\mathrm{CHP}})$$

The values of δ_g, δ_g^{I}, δ_g^{II}, δ_g^{III},$\Delta P_{g,m,m'}$,$\Delta Q_{g,m,m'}$ can be obtained following equations (B.2a)-(B.2d) that define the feasible region of the different operation modes at each CHP unit. Compared to [B33], all production costs have been updated to 2018, the penalty value for load shedding is set to $C^{\mathrm{L}} = 10^4$\$/MWh and the Avedøre power plant (g_{11}) has been changed in our data set from Coal to Natural Gas.

Table B.2: CHP units Data. Fix and variable costs $a_{g,m}^{\text{CHP}}$ and $b_{g,m}^{\text{CHP}}$ are given in 10^3\$ and 10^3\$/MWh respectively. $\overline{P}_{g,m}^{\text{CHP}}$, $\underline{P}_{g,m}^{\text{CHP}}$, $\overline{Q}_{g,m}^{\text{CHP}}$, $\underline{Q}_{g,m}^{\text{CHP}}$ are given in MW and finally $T_{g,m}^{\text{U}}$ and $T_{g,m}^{\text{D}}$ in hours.

	$a_{g,m}^{\text{CHP}}$	$b_{g,m}^{\text{CHP}}$	$T_{g,m}^{\text{U}}$	$T_{g,m}^{\text{D}}$
OFF (m_0)	0	0	3	3
Heat (m_1)	$26.58\overline{P}_g - a_g$	0.0724	2	1
Mixed (m_2)	$18.97\overline{P}_g - a_g$	0.0806	1	1
Elect. (m_3)	$12.68\overline{P}_g - a_g$	0.0732	4	1
	$\overline{P}_{g,m}^{\text{CHP}}$	$\underline{P}_{g,m}^{\text{CHP}}$	$\overline{Q}_{g,m}^{\text{CHP}}$	$\underline{Q}_{g,m}^{\text{CHP}}$
OFF (m_0)	0	0	0	0
Heat (m_1)	$0.817\overline{P}_g$	$0.217\overline{P}_g$	$0.778\overline{P}_g$	$0.453\overline{P}_g$
Mixed (m_2)	$0.958\overline{P}_g$	$0.311\overline{P}_g$	$0.694\overline{P}_g$	$0.174\overline{P}_g$
Elect. (m_3)	$\overline{P}_g$	$0.423\overline{P}_g$	0	0

B.4 Numerical Results

The inputs and scenario generation have been implemented in R 3.2.2, while the optimization models are built in GAMS 24.9.2 and solved using CPLEX 12.1.1. All experiments were executed on the DTU HPC Cluster using the following hardware: 2xIntel Xeon Processor X5550 and 24 GB memory RAM. The GAMS-CPLEX standard configuration was used except for the MIP tolerance gap, which was set to 1% and the number of threads limited to 4. The time out was set to 72 hours.

B.4.1 Evaluation of the operational modes as a recourse decision in the two-stage stochastic optimization problem

In the following, we evaluate real consumption and production data for one day in April 2017 where 50 scenarios for wind power production are generated to describe the uncertainty. In order to evaluate the importance of a real-time scheduling of the operational modes, we run both the two-stage stochastic and robust models (B.4a)-(B.4c) and (B.5a)-(B.5c), respectively. First, we consider the operational modes as first-stage decisions ($u_{g,m} \in \mathcal{X}$) and second, as second-stage decisions ($u_{g,m,\omega} \in \mathcal{Y}_\omega$). The first-stage or commitment decisions $\mathcal{X}$ are evaluated in Table B.3 that shows the expected (EXP) and worst-case (WC) total system cost. The same table provides the elapsed time to solve the models,

Table B.3: Comparison of the results obtained by solving the stochastic and robust models using the operation modes of the CHP units as first-stage (1st) or second-stage (2nd) decisions.

	EXP [10^3\$]	WC [10^3\$]	Time [h]	Gap [%]
Stochastic (2nd)	**4229.830**	5719.115	72	1.957
Stochastic (1st)	4230.465	6901.632	72	1.021
Robust (2nd)	4294.168	5687.532	72	1.463
Robust (1st)	4305.223	**5671.541**	40.89	0.999
EXP	m_0 [h]	m_1 [h]	m_2 [h]	m_3 [h]
Stochastic (2nd)	40	55.22	0.56	0.22
Stochastic (1st)	45	51	0	0
Robust (2nd)	45	46.82	4.12	0.06
Robust (1st)	47	44	4	1
WC	m_0 [h]	m_1 [h]	m_2 [h]	m_3 [h]
Stochastic (2nd)	40	42.9	11.36	1.74
Stochastic (1st)	45	51	0	0
Robust (2nd)	45	40.40	9.62	0.98
Robust (1st)	47	44	4	1

the MIP optimality gap reached at that time and the total number of hours that the 4 CHP units operate in each mode. In the case where we consider the operational modes as second-stage variables, we provide the average operation times in hours for all the scenarios.

Table B.3 shows that for the two-stage stochastic unit commitment (B.4a)-(B.4c) the use of a real-time control in the operational modes reduce the expected system costs by 0.015%, which is not a significant amount. However, the decrease of the worst-case cost amounts to 17.13%. This means that the system substantially profits from the flexibility provided by the different operational modes in the worst-case scenarios. The robust unit commitment problem (B.5a)-(B.5c) presents slightly different behavior than the stochastic one. More specifically, when optimizing for the worst-case realization of the total system cost, using a real-time control of the operational modes deteriorates the solution by 0.282%. This deterioration is, however, due to the fact that the use of operational modes as a first-stage decision makes the problem more tractable, reducing the solution time as well as the MIP gap. In expectation, on the contrary, a real-time control in the operational modes improves the solution by 0.256%. Taking into account that the power produced by the CHP units is between 9.5% and 10% of the total power production for all the simulations, the presented percentages can be translated into significant cost reductions for this case study. Essentially, if a large deviation of the wind power production

occurs, the CHP units must change their power production plan for the same heat demand. Therefore, a real-time control of the operational modes increases the heat and power production feasible region, facilitating the system to adapt to the uncertainty and thus reducing its operating costs.

B.4.2 Evaluation of the solution strategy

In this section we propose a methodology based on an improved version of the *scenario partition and decomposition algorithm (variant 1)* proposed in [B22]. The easy parallelization of this method as well as its ability to deal with binary variables both at the first and second stages, makes it a proper method to solve our model. The improvements exploit the rounding technique proposed in [B24] to reduce the solution time by considering partly fixed commitment decisions. In addition, more heuristics are applied in order to find a suitable number of partitions for the scenarios used in the study. The detailed description of the solution strategy is presented in Appendix B.6. This solution strategy, referred to as *improved hybrid decomposition* is compared with two other solution techniques. For the *improved hybrid decomposition*, we apply the hierarchical clustering technique [B35], which according to [B22] provides the most efficient solution in terms of speed and expected solution value. First, we compared the *improved hybrid decomposition* with a progressive hedging algorithm (PH) where the quadratic term which is entirely formed by binary variables is linearized following the method described in [B36] and referred to as *linear progressive hedging*. Secondly, the solution given by the *improved hybrid decomposition* is compared to the solution given by the stochastic model (B.4a)-(B.4c) using a reduced set of scenarios obtained by applying the partition around medoids (PAM) technique. In comparison with other clustering techniques, the result yields representative scenarios and not representative means (*k-means*), contours (*k-shape*) or group of scenarios attached to each cluster (*hierarchical*). Furthermore, in comparison to the *k-medoid* technique, PAM outperforms in terms of distances to the medoids and computational times [B25]. For the sake of a fair comparison, we assign the same values for tolerance ($\varepsilon = 20$) and thresholds ($\alpha = 0.9$ and $\beta = 0.01$) in both the *improved hybrid decomposition* and *linear progressive hedging*. The same number of scenarios finally retained by the *improved hybrid decomposition* (15 scenarios) is the number of reduced scenarios that are used for the PAM solution. All solution approaches are executed considering the operational modes of the CHP units as second-stage decisions. The results displayed in Table B.4 show that the *improved hybrid decomposition* outperforms the other techniques in terms of solution time. This is due to the parallelization process to obtain the solution for the initial fixed commitment decisions and later the total reduction of the scenario sample. In addition, the *improved hybrid decomposition* provides a commitment solution that inter-

Table B.4: Comparison of the results obtained from solving the model by using the heuristics techniques *improved hybrid decomposition* (HYB), *linear progressive hedging* (LPH) and the scenario reduction using partition around medoids (PAM).

	EXP [10^3\$]	WC [10^3\$]	Time [hours]	Gap [%]
HYB	4255.023	**5682.619**	**3.82**	0.863
LPH	4345.548	5683.238	72	1.844
PAM	**4239.787**	6926.991	51.55	0.9698

mediates between those given by the stochastic and robust unit commitment problem. Compared to the other two solution strategies, it gives the best solution for the worst-case realization of the total system cost. The best results in terms of costs for the expected total system cost are achieved by the commitment plan obtained from PAM. However, due to the reduction performed in the scenario sample, the PAM yields the highest worst-case cost. Finally and despite initializing the problem using partly fixed commitment, the large number of scenarios (50) used to solve the *linear progressive hedging* drastically increases the solution time compared to the other two methods.

B.4.3 Out-of-sample evaluation

To apprise the quality of the decisions obtained by the different models, we use an out-of-sample test by creating 1000 different wind power production scenarios using the same methodology as described in Section B.3. The parameters used to run the simulations are the same as in the previous section. Table B.5 shows the total system costs and the wind power spillage for the entire sample divided in 5 quantiles.

Table B.5 shows how the use of the operational modes as a recourse function in the stochastic and robust unit commitments reduces the total system costs for most of the quantiles. If we examine the solutions obtained, PAM provides the best solution for the 0%-25% interval but tends to deteriorate for the 75%-100% interval where the robust models give better solution than the others. For the 50%-75% interval, the commitment obtained by the stochastic (2nd) outperforms the others. On the other hand, the maximum wind spillage is given by the commitment obtained for the robust models. This is due to the fact that this later solution commits the units for a low wind power production, and in the case that the wind power production turns out to be high, a larger amount of wind power has to be spilled. For the remaining commitment solutions we can clearly see that by using the operational modes as a recourse decision,

Table B.5: Comparison of the total system cost [10^3\$] and wind spillage [MWh] for the test set

Cost [10^3\$]	0% (min.)	25%	50% (med.)	75%	100% (max.)
Stochastic (2nd)	3665	4251	**4446**	**4850**	72218
Stochastic (1st)	3642	4230	4462	5299	104187
Robust (2nd)	3754	4311	4520	5714	**61254**
Robust (1st)	3751	4306	4505	5294	64872
HYB	3734	4295	4523	4945	66850
LPH	3716	4291	4501	4948	76637
PAM	**3641**	**4226**	4451	6224	88776
Wind Spill [MWh]	0% (min.)	25%	50% (med.)	75%	100% (max.)
Stochastic (2nd)	0	0	**211**	**983**	**5563**
Stochastic (1st)	0	0	267	1076	6373
Robust (2nd)	0	166	782	1815	7711
Robust (1st)	0	185	906	1999	8203
HYB	0	132	665	1536	6683
LPH	0	0	325	1152	6181
PAM	0	0	258	1056	6199

more flexibility is provided to the system and therefore less wind power has to be spilled. From the results displayed in Table B.5 we can see that the *improved hybrid decomposition* (HYB) provides robust solutions in the sense that they do not deteriorate in terms of cost and wind spillage when an unexpected system imbalance occurs. Additionally, the method has significantly shorter computation time than the other methods.

B.5 Conclusions and future research

In this paper, we propose a new formulation for the two-stage stochastic unit commitment problem that integrates different operation modes for centralized and steam based CHP units. The modeling of the different operational modes follows a realistic case study for combined cycle gas cogeneration units that extracts the steam from a valve located between the high and low-pressure parts of the steam turbine. This model formulation that includes binary variables at both first and second stages makes the problem computationally very challenging and consequently a solution approach based on applying heuristics to an existing parallelization and decomposition scheme is proposed. To run the simulations, we use a real test case of the Danish transmission grid where we include the complementary information needed to solve our models. The obtained results show that significant system cost and wind spillage reductions

can be achieved by using a real-time operation of the modes in the CHP units. In addition, the solution approach proposed in this work drastically reduces the solution time of the model while providing a unit commitment solution that performs comparatively well in terms of expected and worst-case system operating cost. We envision two different lines of future research for this work. The first one is to integrate the formulation of the various CHP operational modes proposed in this work in a more detailed and generalized model that describes more components and modes for different types of thermal co-generation units and apply this model to a real case study. The second line of future research consists in extending the wind power production scenario generation process and analyze how the wind power fluctuations affect the dispatch of the cogeneration units and their operational modes in more detail.

B.6 Appendix

B.6.1 Introduction to the Improved Hybrid Decomposition

In this document we explain in detail how the suggested improvements for the *scenario partition and decomposition method, variant 1 (SPDA1)* proposed in [B22] are carried out. The improvements consist in applying heuristics to find a suitable number of scenario partitions or clusters for the specific problem and find a partly fixed first stage-decision to initialize the problem solution. These heuristics are based in the Progressive Hedging algorithm and rounding techniques. The Progressive Hedging algorithm was first introduced by [B23] and has been applied to solve large-scale stochastic programming problems in different applications such as forest planning [B37], resource allocation problems [B38] and unit commitments problems [B24]. The Progressive Hedging is an iterative process in which first the problem is solved for each scenario individually and the solutions obtained for the first-stage decisions are averaged for all scenarios. From these solutions a multiplier is created and afterwards, the problem is solved again for each scenario including this multiplier as a penalty in the objective function. Using a squared proximal term to calculate the distance between the first stage decision vector of each scenario and the average term of these, we can determine if the algorithm should stop. Later on, we use these values to initialize the solution of the two-stage stochastic programming problem. In our solution approach, in order to determine a suitable number of partitions, we take from Progressive Hedging the way of averaging the first-stage decision, making use of the squared proximal term to stop the algorithm. Furthermore, to initialize the solution of the problem, we use the rounding technique proposed in

[B39] where just those values close to 1 and 0 are fixed to initialize the solution. These values depend on two thresholds that we will name α and β.

B.6.2 Formulating the Hybrid Unit Commitment

In this section, the stochastic unit commitment (4a)-(4c) is reformulated to the *hybrid unit commitment* following the work done in [B22]. The finite set of scenarios Ω is divided into $|P|$ different partitions. Therefore, the entire set of scenarios Ω is divided into different subsets named Ω_p which is comprised of all the scenarios $\omega \in \Omega$ that belong to partition $p \in P$. The *hybrid unit commitment* writes as follows.

$$\min_{\mathcal{X},\mathcal{Y}_\omega\gamma_p} \sum_{t\in\mathcal{T}}\sum_{g\in\mathcal{G}} \left(a_g x_{g,t} + C_g^{\mathrm{SU}} y_{g,t} + C_g^{\mathrm{SD}} z_{g,t}\right) + \sum_{p\in P} \rho_p \gamma_p \tag{B.6a}$$

$$\text{s.t. } \gamma_p \geq \sum_{t\in\mathcal{T}}\sum_{g\in\mathcal{G}^T} b_g p_{g,t,\omega} + \sum_{t\in\mathcal{T}}\sum_{n\in\mathcal{N}} C^{\mathrm{L}} L^{\mathrm{shed}}_{n,t,\omega} \tag{B.6b}$$

$$+ \sum_{t\in\mathcal{T}}\sum_{g\in\mathcal{G}^{\mathrm{CHP}}}\sum_{m\in\mathcal{M}} a^{\mathrm{CHP}}_{g,m} u_{g,m,t,\omega}$$

$$+ \sum_{t\in\mathcal{T}}\sum_{g\in\mathcal{G}^{\mathrm{CHP}}}\sum_{m\in\mathcal{M}} b^{\mathrm{CHP}}_{g,m}\left(p^{\mathrm{CHP}}_{g,m,t,\omega} + \varphi_{g,m} q^{\mathrm{CHP}}_{g,m,t,\omega}\right)$$

$$(\forall p \in P, \forall \omega \in \Omega_p)$$

$$(\text{B.1a}) - (\text{B.1n}), (\text{B.2a}) - (\text{B.2v}) \tag{B.6c}$$

where ρ_p represents the probability attached to each partitions that is calculated as follows.

$$\rho_p = \sum_{\omega\in\Omega_p} \pi_\omega \qquad (\forall p \in P)$$

The auxiliary variable γ_p equals the worst-case system cost for partition p and therefore the second term in the objective function (B.6a) represents the expected value of the worst-case scenarios at each partition $p \in P$. To formulate the decomposition algorithm, we need to distinguish between the master problem and the subproblems. Both are formulated as in [B22]. The master problem (MP) is formed by both first-stage and second-stage decisions. It solves one per

partition $p \in P$ and for iteration i it writes as follows.

$$\min_{\mathcal{X}^i, \mathcal{Y}^i, \gamma_p} \sum_{t\in\mathcal{T}} \sum_{g\in\mathcal{G}} \left(a_g x^i_{g,t} + C^{\mathrm{SU}}_g y^i_{g,t} + C^{\mathrm{SD}}_g z^i_{g,t}\right) + \gamma_p \tag{B.7a}$$

$$\text{s.t. } \gamma_p \geq \sum_{t\in\mathcal{T}} \sum_{g\in\mathcal{G}^T} b_g p^i_{g,t,\omega} + \sum_{t\in\mathcal{T}} \sum_{n\in\mathcal{N}} C^{\mathrm{L}} L^{\mathrm{shed,i}}_{n,t,\omega} \tag{B.7b}$$

$$+ \sum_{t\in\mathcal{T}} \sum_{g\in\mathcal{G}^{\mathrm{CHP}}} \sum_{m\in\mathcal{M}} a^{\mathrm{CHP}}_{g,m} u^i_{g,m,t,\omega}$$

$$+ \sum_{t\in\mathcal{T}} \sum_{g\in\mathcal{G}^{\mathrm{CHP}}} \sum_{m\in\mathcal{M}} b^{\mathrm{CHP}}_{g,m} \left(p^{\mathrm{CHP},i}_{g,m,t,\omega} + \varphi_{g,m} q^{\mathrm{CHP},i}_{g,m,t,\omega}\right)$$

$$(\forall \omega \in \Omega^i_p)$$

$$\text{(B.1a)} - \text{(B.1n)}, \text{(B.2a)} - \text{(B.2v)} \qquad (\forall \omega \in \Omega^i_p) \tag{B.7c}$$

Where $\mathcal{X}^i$=$\{x^i_{g,t}, y^i_{g,t}, z^i_{g,t}\}$ and $\mathcal{Y}^i$=$\{u^i_{g,m,t,\omega}, v^i_{g,m,m',t,\omega}, p^i_{g,t,\omega}, L^{\mathrm{shed},i}_{l,t,\omega}, W^{\mathrm{spill},i}_{f,t,\omega}, p^{\mathrm{CHP},i}_{g,m,t,\omega}, q^{\mathrm{CHP},i}_{g,m,t,\omega}, s^i_{g,t,\omega}, \phi^i_{n,t,\omega} : \forall \omega \in \Omega^i_p\}$. One subproblem (SP) per scenario $\omega \in \Omega_p$ is solved determining the second-stage decision variables.

$$\min_{\mathcal{Y}^i_\omega} \sum_{t\in\mathcal{T}} \sum_{g\in\mathcal{G}^T} b_g p^i_{g,t,\omega} + \sum_{t\in\mathcal{T}} \sum_{n\in\mathcal{N}} C^{\mathrm{L}} L^{\mathrm{shed,i}}_{n,t,\omega} \tag{B.8a}$$

$$+ \sum_{t\in\mathcal{T}} \sum_{g\in\mathcal{G}^{\mathrm{CHP}}} \sum_{m\in\mathcal{M}} a^{\mathrm{CHP}}_{g,m} u^i_{g,m,t,\omega}$$

$$+ \sum_{t\in\mathcal{T}} \sum_{g\in\mathcal{G}^{\mathrm{CHP}}} \sum_{m\in\mathcal{M}} b^{\mathrm{CHP}}_{g,m} \left(p^{\mathrm{CHP},i}_{g,m,t,\omega} + \varphi_{g,m} q^{\mathrm{CHP},i}_{g,m,t,\omega}\right)$$

$$\text{s.t. } \text{(B.1f)} - \text{(B.1n)}, \text{(B.2a)} - \text{(B.2v)} \tag{B.8b}$$

Where $\mathcal{Y}^i_\omega$=$\{u^i_{g,m,t,\omega}, v^i_{g,m,m',t,\omega}, p^i_{g,t,\omega}, L^{\mathrm{shed},i}_{l,t,\omega}, W^{\mathrm{spill},i}_{f,t,\omega}, p^{\mathrm{CHP},i}_{g,m,t,\omega}, q^{\mathrm{CHP},i}_{g,m,t,\omega}, s^i_{g,t,\omega}, \phi^i_{n,t,\omega}\}$.

B.6.3 Solution Approach

The solution algorithm is described in the following. Note that the master problems (B.7a)-(B.7c) and subproblems (B.8a)-(B.8b) for each partition $p \in P$ are solved in parallel and that they are called instances of the SPDA1 algorithm.

1. Initialize iteration $j = 0$. Select the initial number of partitions k^j applying hierarchical clustering to the set of scenarios Ω.
2. Create k^j parallel instances of the SPDA1 algorithm.

3. Initialize iteration $i := 0$ and set $\Omega_p^i = \emptyset$.

4. Solve the master problem and return the optimal solution found for the vector of first stage decisions $\mathcal{X}_p^i$. Obtain the Lower Bound (LB) as $\sum_{t\in\mathcal{T}} \sum_{g\in\mathcal{G}} \left(a_g x_{g,t}^i + C_g^{\mathrm{SU}} y_{g,t}^i + C_g^{\mathrm{SD}} z_{g,t}^i\right) + \gamma_p$.

5. Solve the subproblems (SP) with the first-stage decision variables fixed at $\mathcal{X}_p^i$. Once all the subproblems are solved, obtain the scenario ω' that yields the highest system cost. Include this scenario in the reduce set of worst-case scenarios $(\Omega_p^{'})$ such that $\Omega_p^{'i+1} = \Omega_p^{'i} \cup \{\omega'\}$ and obtain the Upper Bound (UB) as $\sum_{t\in\mathcal{T}} \Bigg(\sum_{g\in\mathcal{G}} \left(a_g x_{g,t}^i + C_g^{\mathrm{SU}} y_{g,t}^i + C_g^{\mathrm{SD}} z_{g,t}^i\right) + \sum_{g\in\mathcal{G}^T} b_g p_{g,t,\omega}^i + \sum_{n\in\mathcal{N}} C^{\mathrm{L}} L_{n,t,\omega}^{\mathrm{shed,i}}$
$+ \sum_{g\in\mathcal{G}^{\mathrm{CHP}}} \sum_{m\in\mathcal{M}} \left[a_{g,m}^{\mathrm{CHP}} u_{g,m,t,\omega}^i + b_{g,m}^{\mathrm{CHP}} \left(p_{g,m,t,\omega}^{\mathrm{CHP},i} + \varphi_{g,m} q_{g,m,t,\omega}^{\mathrm{CHP},i}\right)\right] \Bigg)$.

6. Check convergance. If $|\mathrm{UB} - \mathrm{LB}| \leq \xi$, where ξ is the tolerance value, the iterative process i stops. If $|\mathrm{UB} - \mathrm{LB}| > \xi$ then $i := i + 1$ and go to step 4.

7. Once all partitions have converged, we obtain the first-stage decision vector for each partition $\mathcal{X}_p^j$.

8. Increase iteration number $j := j + 1$. Calculate the average value for the first-stage commitment decisions over all partitions $\overline{\mathcal{X}}^j = \sum_{p\in P} \rho_p \mathcal{X}_p^{j-1}$. Obtain squared distance $\sigma^j = ||\overline{\mathcal{X}}^j - \overline{\mathcal{X}}^{j-1}||$ (where $\overline{\mathcal{X}}^0 = 0$). If $\sigma^j \leq \varepsilon$ we stop the iteration process for j and move a step forward. If $\sigma^j > \varepsilon$, we increase the number of partitions $k^j := k^{j-1} + 1$ and go step 2.

9. Obtain the partly fixed commitment decisions using the rounding technique:

$$\overline{\mathcal{X}}^{\mathrm{round}} = \begin{cases} 1 & \text{if } \overline{\mathcal{X}}^j \geq 1 - \alpha \\ 0 & \text{if } \overline{\mathcal{X}}^j \leq \beta \\ \mathcal{X} \in \{0,1\} & \text{if } \beta < \overline{\mathcal{X}}^j < 1 - \alpha \end{cases}$$

10. Solve (B.6a)-(B.6c) for the scenarios finally retained in the set of worst-cases scenarios $\Omega_p^{'}$ using $\overline{\mathcal{X}}^{\mathrm{round}}$ as partly fixed commitment decisions.

The pseudocode for the proposed improved SPDA1 algorithm is provided in Algorithm 3.

Algorithm 3 Improved Scenario Partition and Decomposition Algorithm: Variant 1 (**Improved SPDA1**)

Set $j := 0$.
Choose initial k^0 and apply *hierarchical* clustering to Ω and obtain P^0.
repeat
  for all $p \in P^j$ **do**
    Set $i := 0$ and $\Omega_p^{'0} = \emptyset$
    repeat
      Solve Master Problem
      Return optimal solution $\mathcal{X}_p^i$
      Compute Lower Bound (LB)
      Set $\mathcal{X}_p := \mathcal{X}_p^i$ and **solve** SP $\forall \omega \in \Omega_p$
      Compute Upper Bound (UB)
      Identify worst-case scenario ω'
      Set $\Omega_p'^{i+1} := \Omega_p'^{i} \bigcup \{\omega'\}$
      Set $i := i + 1$
    until $\mid \text{UB} - \text{LB} \mid \leq \xi$
    Set $\Omega_p' := \Omega_p'^{i-1}$
  end for
  Obtain $\mathcal{X}_p^j \ \forall p \in P$
  Set $j := j + 1$.
  Compute average value $\overline{\mathcal{X}}^j$
  Obtain the quadratic distance value σ^j
  Increase number of partitions $k^j := k^{j-1} + 1$
  Apply *hierarchical* clustering to Ω and obtain P^j
until $\sigma_j \leq \varepsilon$
Calculate $\overline{\mathcal{X}}^{\text{round}}$
Solve (B.6a)-(B.6c) replacing Ω_p with $\Omega_p', \forall p$ and using $\overline{\mathcal{X}}^{\text{round}}$ as partly fixed commitment decisions.

References B

[B1] H. Lund and P. A. Østergaard. "Electric grid and heat planning scenarios with centralised and distributed sources of conventional, CHP and wind generation". In: *Energy* 25.4 (2000), pp. 299–312. ISSN: 0360-5442. DOI: https://doi.org/10.1016/S0360-5442(99)00075-4. URL: http://www.sciencedirect.com/science/article/pii/S0360544299000754.

[B2] J. Veerapen and M. Beerepoot. "Co-generation and Renewables". In: *IEA, Paris* (2011).

[B3] E. Thorin, J. Sandberg, and J. Yan. "Combined Heat and Power". In: *Handbook of Clean Energy Systems* (2015).

[B4] L. Pugi et al. "Real Time simulation of a turbine bypass controller". In: *Mechatronic and Embedded Systems and Applications (MESA), 2014 IEEE/ASME 10th International Conference on*. IEEE. 2014, pp. 1–6.

[B5] C. Kowalczyk et al. "Mathematical model of Combined Heat and Power Plant using GateCycleTM software". In: *Journal of Power Technologies* 95.3 (2015), p. 183.

[B6] K. Sartor, S. Quoilin, and P. Dewallef. "Simulation and optimization of a CHP biomass plant and district heating network". In: *Applied Energy* 130 (2014), pp. 474–483.

[B7] H. Wang et al. "Modelling and optimization of CHP based district heating system with renewable energy production and energy storage". In: *Appl. Energy* 159 (2015), pp. 401–421.

[B8] I. Dimoulkas, M. Amelin, and F. Levihn. "District heating system operation in power systems with high share of wind power". In: *Journal of Modern Power Systems and Clean Energy* 5.6 (2017), pp. 850–862.

[B9] J. P. J. Navarro et al. "The joint effect of centralised cogeneration plants and thermal storage on the efficiency and cost of the power system". In: *Energy* 149 (2018), pp. 535–549.

[B10] S. Mitra, L. Sun, and I. E. Grossmann. "Optimal scheduling of industrial combined heat and power plants under time-sensitive electricity prices". In: *Energy* 54 (2013), pp. 194–211.

[B11] M. J. Kim et al. "Optimization of CHP and thermal storage under heat demand". In: *Control and Automation (ICCA), 2016 12th IEEE International Conference on*. IEEE. 2016, pp. 277–281.

[B12] N. Troy, E. Denny, and M. O'Malley. "Base-load cycling on a system with significant wind penetration". In: *IEEE Transactions on Power Systems* 25.2 (2010), pp. 1088–1097.

[B13] J. Wang et al. "A review of Danish integrated multi-energy system flexibility options for high wind power penetration". In: *Clean Energy* 1.1 (2017), pp. 23–35.

[B14] N. Troy, D. Flynn, and M. OMalley. "Multi-mode operation of combined-cycle gas turbines with increasing wind penetration". In: *IEEE Transactions on Power Systems* 27.1 (2012), pp. 484–492.

[B15] A. Hellmers et al. "Operational strategies for a portfolio of wind farms and CHP plants in a two-price balancing market". In: *IEEE Trans. Power Syst* 31.3 (2016), pp. 2182–2191.

[B16] A. Tuohy et al. "Unit commitment for systems with significant wind penetration". In: *IEEE Transactions on power systems* 24.2 (2009), pp. 592–601.

[B17] S. Takriti, J. R. Birge, and E. Long. "A stochastic model for the unit commitment problem". In: *IEEE Transactions on Power Systems* 11.3 (1996), pp. 1497–1508.

[B18] L. Wu, M. Shahidehpour, and T. Li. "Stochastic security-constrained unit commitment". In: *IEEE Transactions on Power Systems* 22.2 (2007), pp. 800–811.

[B19] L. Zhao and B. Zeng. "Robust unit commitment problem with demand response and wind energy". In: *Power and Energy Society General Meeting, 2012 IEEE*. IEEE. 2012, pp. 1–8.

[B20] D. Bertsimas et al. "Adaptive robust optimization for the security constrained unit commitment problem". In: *IEEE Transactions on Power Systems* 28.1 (2013), pp. 52–63.

[B21] N. P. Padhy. "Unit commitment-a bibliographical survey". In: *IEEE Transactions on power systems* 19.2 (2004), pp. 1196–1205.

[B22] I. Blanco and J. M. Morales. "An efficient robust solution to the two-stage stochastic unit commitment problem". In: *IEEE Transactions on Power Systems* 32.6 (2017), pp. 4477–4488.

[B23] R. T. Rockafellar and R. J.-B. Wets. "Scenarios and policy aggregation in optimization under uncertainty". In: *Mathematics of operations research* 16.1 (1991), pp. 119–147.

[B24] C. Ordoudis et al. "Stochastic unit commitment via Progressive Hedging—extensive analysis of solution methods". In: *PowerTech, 2015 IEEE Eindhoven*. IEEE. 2015, pp. 1–6.

[B25] A. P. Reynolds et al. "Clustering rules: a comparison of partitioning and hierarchical clustering algorithms". In: *Journal of Mathematical Modelling and Algorithms* 5.4 (2006), pp. 475–504.

[B26] A. Papavasiliou and S. S. Oren. "Multiarea stochastic unit commitment for high wind penetration in a transmission constrained network". In: *Operations Research* 61.3 (2013), pp. 578–592.

[B27] J. M. Morales, A. J. Conejo, and J. Pérez-Ruiz. "Economic valuation of reserves in power systems with high penetration of wind power". In: *IEEE Transactions on Power Systems* 24.2 (2009), pp. 900–910.

[B28] Q. Wang, Y. Guan, and J. Wang. "A chance-constrained two-stage stochastic program for unit commitment with uncertain wind power output". In: *IEEE Transactions on Power Systems* 27.1 (2012), pp. 206–215.

[B29] M. Carrión and J. M. Arroyo. "A computationally efficient mixed-integer linear formulation for the thermal unit commitment problem". In: *IEEE Transactions on power systems* 21.3 (2006), pp. 1371–1378.

[B30] G. Morales-España, C. M. Correa-Posada, and A. Ramos. "Tight and compact MIP formulation of configuration-based combined-cycle units". In: *IEEE Transactions on Power Systems* 31.2 (2016), pp. 1350–1359.

[B31] C. Liu et al. "Component and mode models for the short-term scheduling of combined-cycle units". In: *IEEE Transactions on Power systems* 24.2 (2009), pp. 976–990.

[B32] B. Zeng and L. Zhao. "Solving two-stage robust optimization problems using a column-and-constraint generation method". In: *Operations Research Letters* 41.5 (2013), pp. 457–461.

[B33] V. Heinisch et al. "Effects of power-to-gas on power systems: A case study of Denmark". In: *PowerTech, 2015 IEEE Eindhoven*. IEEE. 2015, pp. 1–6.

[B34] P. Pinson et al. "Wind energy: Forecasting challenges for its operational management". In: *Statistical Science* 28.4 (2013), pp. 564–585.

[B35] T. Hastie, R. Tibshirani, and J. Friedman. *The Elements of Statistical Learning (pp. 520-529)*. 2009.

[B36] W. P. Adams, R. J. Forrester, and F. W. Glover. "Comparisons and enhancement strategies for linearizing mixed 0-1 quadratic programs". In: *Discrete Optimization* 1.2 (2004), pp. 99–120.

[B37] F. B. Veliz et al. "Stochastic optimization models in forest planning: a progressive hedging solution approach". In: *Annals of Operations Research* 232.1 (2015), pp. 259–274.

[B38] J.-P. Watson and D. L. Woodruff. "Progressive hedging innovations for a class of stochastic mixed-integer resource allocation problems". In: *Computational Management Science* 8.4 (2011), pp. 355–370.

[B39] C. Li, M. Zhang, and K. W. Hedman. "N-1 reliable unit commitment via progressive hedging". In: *Journal of Energy Engineering* 141.1 (2014), B4014004.

Paper C

A Novel Bidding Method for Combined Heat and Power Units in District Heating Systems

Authors:
Ignacio Blanco, Anders N. Andersen, Daniela Guericke and Henrik Madsen

Under review in:
Energy Systems (Springer).

A Novel Bidding Method for Combined Heat and Power Units in District Heating Systems

Ignacio Blanco[1], Anders N. Andersen[2], Daniela Guericke[1] and Henrik Madsen[1]

Abstract

We propose a bidding method for the participation of combined heat and power (CHP) units in the day-ahead electricity market. More specifically, we consider a district heating system where heat can be produced by CHP units or heat-only units, e.g., gas or wood chip boilers. We use a mixed-integer linear program to determine the optimal operation of the portfolio of production units and storages on a daily basis. Based on the optimal production of subsets of units, we can derive the bidding prices and amounts of electricity offered by the CHP units for the day-ahead market. The novelty about our approach is that the prices are derived by iteratively replacing the production of heat-only units through CHP production. This results in an algorithm with a robust bidding strategy that does not increase the system costs even if the bids are not won. We analyze our method on a small realistic test case to illustrate our method and compare it with other bidding strategies from literature, which consider CHP units individually. The analysis shows that considering a portfolio of units in a district heating system and determining bids based on replacement of heat production of other units leads to better results.

C.1 Introduction

The global target of reducing CO2-emissions from fossil fuels has required several countries, especially in the European Union, to consider efficient district heating and cooling systems as a key role in its CO2-emissions reduction strategy [C1]. Since it is assumed that fossil fuels will be mostly replaced by intermittent renewable energy sources, a higher share of district heating and cooling systems

[1]Department of Applied Mathematics and Computer Science, Technical University of Denmark, DK-2800 Kgs. Lyngby, Denmark
[2]EMD International A/S, Niels Jernesvej 10, 9220 Aalborg Ø, Denmark

can facilitate the integration of these intermittent energy sources in the energy mix [C2], contributing to balance the grid by the use of heat pumps, electric boilers, thermal storage or flexible CHP production. The efficiency of these systems has been demonstrated already in countries like Denmark and Sweden. In Denmark around 64% of the households are connected to district heating networks for space heating and domestic hot water [C3]. Nowadays, the total heat consumption in all district heating networks in Denmark is close to 130 petajoule (PJ) from which more than 65% are produced by combined heat and power (CHP) plants [C4]. The integration of renewable and intermittent energy sources (e.g. wind and photovoltaic) in liberalized electricity markets such as Nordpool [C5] lead to historical low and highly volatile electricity prices [C6, C7]. This results in a larger difficulty for CHP units to be scheduled and thus obtain profits from the electricity market [C7]. Consequently, they are being replaced by other heat production units such as heat pumps that take advantage of low electricity prices in periods where the mix of renewable energy production is high [C8, C9]. This means many district heating companies are no longer operating the system only with CHP units but in combination with other heat production units such as gas boilers, heat pumps, electric boilers or wood chip boilers. In this work, we propose a method that optimizes the power production bids of CHP units in district heating systems in the day-ahead market, making these units more competitive and scheduled in more hours. In addition, the approach provides flexibility to the power system by activating or deactivating the CHP units when required by the transmission system operator (TSO), which is reflected in the market prices.

The optimal operation of standalone CHP units has been extensively considered in literature [C10, C11, C12]. In these publications, the authors use mixed-integer linear programming to define the technical constraints of the CHP unit in combination with a thermal storage to maximize its profits in a liberalized electricity market framework.

The use of mathematical optimization to operate a portfolio of heat production units has been proposed in several publications. The most relevant publications with respect to our approach are reviewed in the following. First, the work of [C13] shows that adding a receding horizon to optimize the operation of a thermal storage yields better results in terms of costs. In [C14] the authors consider an integrated power and heat system. The goal of their approach is to coordinate the heat and power production to accommodate the intermittent generation of a wind farm in the district heating network by using a heat pump when the wind power production is high. Following the same principle of producing heat when the electricity price is low and produce power and heat with the CHP when the electricity price is high, the authors in [C15] evaluate the scheduling of different heat production units under electricity price and heat demand uncertainty with two-stage stochastic programming. Finally, the ap-

proach proposed in [C16] integrates many different heat and cooling production units and use optimization to operate them as a portfolio. The system offers capacity to the electricity market to accommodate power fluctuations by the interplay of the different units. Apart from scientific literature, there exist commercial software tools, such as *energyPRO* [C17] that schedule the production in integrated district heating systems.

The above mentioned literature considers the optimal production in district heating systems including CHP units, but neglects to determine bids that the operator should present to the electricity market. CHP units are usually more expensive to operate than other heat production units. Therefore, it has to be ensured that no economic losses due to poor bidding strategies will occur while operating the system. A typical liberalized electricity market works on a short term basis. An auction takes place on the day before the energy is delivered, the so-called day-ahead market [C18]. Further markets exist such as the reserve capacity market, intra-day market and balancing market [C18, C19, C20]. The price of electricity from one day to another is partly unknown and more unpredictable as more intermittent renewable energy technologies get into the system. Despite that methods to predict electricity prices as a function of intermittent energy sources have been proposed (e.g. [C21]), the optimal operation of CHP units cannot be determined one day in advance when the power production bids have to be submitted, since optimal scheduling is depending on electricity price forecasts.

To approach this problem, we propose a method that considers the optimal operation as well as the optimal bidding for CHP units in district heating systems. Similarly, several bidding methods for both thermal power generation and CHP units have been proposed in literature. In the following, we review those methods, which are also used for comparison in the numerical results.

First, we review bidding methods used for thermal power generation units. Although these consider the power generation unit as a standalone production unit, these methods could be used by district heating operators to determine bids for the CHP plant without taking the other units into account. One strategy is proposed by [C22]. Their bidding procedure consists of creating bounds on the uncertainty given by forecasted prices and use these bounds to generate offers. They ensure profitability in their bids by offering power volumes at two different prices, i.e., the defined lower bound and upper bound of their price forecast. Since the vast majority of possible realizations of the electricity price lie within the defined bounds, they protect their offers against uncertainty. The second method analyzed is the method presented in [C23]. This method generates different confidence intervals for electricity prices. By solving the model for each of these intervals, bidding curves can be created.

Second, we mention bidding strategies where the authors consider a single CHP unit with a thermal storage. The method proposed in [C24] determines the optimal production of the CHP unit. The bidding price is the price forecast, which is the same price used to determined the power production. In [C25] the authors construct different bidding curves for a CHP unit based on price scenarios and calculate for each offering period the power production vs. the electricity prices. These curves are submitted to the day-ahead market. The mentioned publications do not take advantage of the different heat production technologies that are connected to the district heating network. The potential of the system can be increased if these are optimized jointly as a portfolio.

Finally, in [C26] the authors propose a bidding strategy for CHP units that takes into account other heat units to define the heat production costs. Therefore, the bidding prices generated by this method are the same as those generated in ours. However, the way the volume and the bidding hours are calculated is different, because [C26] use a piece-wise linear function to activate different volumes of power at different prices according to the price forecast.

In this publication we introduce a novel bidding method for the participation of combined heat and power (CHP) units that operated in a portfolio with other heat production units in the day-ahead electricity market based on mixed-integer linear programming. The main contributions of our work are:

- Our method operates the heat production units as a portfolio and takes the costs of all units in the system into account to define the optimal bidding prices. We show that this is more beneficial for district heating providers than using state-of-the-art bidding methods for standalone CHP or thermal units.

- The bids generated by our method consider the cost of producing heat to define bids, which protects against the uncertainty of electricity prices, i.e., lost bids do not increase the operational cost.

- We develop an iterative process to generate our bids based on replacement of heat production by heat-only units that results in a higher number of offers compared to other bidding methods.

- We reimplemented the above mentioned methods for operational optimization and bidding [C22, C23, C24, C25, C26] to compare them to our bidding strategy in a case study.

- To improve the daily operation of a heat storage system, we analyze different lengths of receding horizon.

The remainder of the paper is organized as follows. In Section C.2 the operational planning problem is explained in detail. In Section C.3, we develop step by step the bidding method proposed in this work. Section C.4 presents the case study used to run our experiments. In Section C.5, an illustrative example shows how the bidding method works. Further simulations and numerical results are presented in Section C.6. Finally, we summarize our work in Section C.7.

C.2 Operational planning model

We start by introducing the mixed-integer linear program (MILP) to schedule the optimal operation of a portfolio of heat production units in a district heating system. For an overview of the nomenclature, we refer to Table C.1.

The set of considered production units is denoted by $\mathcal{U}$, which is comprised of CHP units $\mathcal{U}^{\mathrm{CHP}}$ (producing heat and power simultaneously) and heat-only units $\mathcal{U}^{\mathrm{H}}$. We consider the production over a time horizon of $\mathcal{T}$ periods, where each period is one hour due to the hourly bidding periods in the day-ahead market. Each unit $u \in \mathcal{U}$ has a maximum heat production per hour $\overline{Q}_u$ and production cost of C_u per MWh heat. The CHP units $u \in \mathcal{U}^{\mathrm{CHP}}$ have further a restriction on the minimum and maximum electricity production per hour denoted by $\underline{P}_u$ and $\overline{P}_u$, respectively. The heat-to-power ratio for the CHP units is given by φ_u. The thermal storage of the system has a minimum ($\underline{S}$) and maximum level ($\overline{S}$) and the outflow per period is limited to S^{F} (all in MWh heat). The binary parameters A_u^{DH} and A_u^{S} determine whether a heat unit u is connected to the district heating network and/or the thermal storage, respectively. The heat demand in the district heating network for each periods is given by D_t and the forecasted electricity price for each hour by λ_t.

The model determines the optimal heat production for all units $u \in \mathcal{U}$ in each period in variables $q_{u,t}$ where the production can either go directly to the district heating network ($q_{u,t}^{\mathrm{DH}}$) or to the thermal storage ($q_{u,t}^{\mathrm{S}}$). The power production of the CHP units $u \in \mathcal{U}^{\mathrm{CHP}}$ is modelled by variables $p_{u,t}$ and their status (on/off) by the binary variable $x_{u,t}$. The variables s_t and s_t^{OUT} represent the storage level and storage outflow in each period t. Note that the number of periods $\mathcal{T}$ is not limited to 24 hours, because it can be profitable to already consider the production of future days to operate the thermal storage more efficiently. The bidding method proposed in the next section is used to create hourly bids for the day-ahead market on a daily basis, thus, we shift the planning period by 24 hours after each run in a receding horizon approach.

Table C.1: Nomenclature

Sets	
$\mathcal{T}$	Set of time periods t
$\mathcal{U}$	Set of heat production units u
$\mathcal{U}^{\mathrm{CHP}} \subset \mathcal{U}$	Subset of combined heat and power production units
$\mathcal{U}^{\mathrm{H}} \subset \mathcal{U}$	Subset of heat-only production units
Parameter	
C_u	Cost for producing heat with unit $u \in \mathcal{U}$ [DKK/MWh-heat]
$\overline{Q}_u$	Max. heat production for unit $u \in \mathcal{U}$ [MWh-heat]
$\underline{Q}_{u,t}$	Min. heat production for unit $u \in \mathcal{U}, t \in \mathcal{T}$ [MWh-heat]
A_u^{DH}	Binary parameter: 1, if unit $u \in \mathcal{U}$ is connected to the district heating system, 0, otherwise
A_u^{S}	Binary parameter: 1, if unit $u \in \mathcal{U}$ is connected to the thermal storage, 0, otherwise
φ_u	Heat-to-power ratio for unit $u \in \mathcal{U}^{\mathrm{CHP}}$ [MWh-heat/MWh-el]
$\overline{P}_u$	Max. power production for unit $u \in \mathcal{U}^{\mathrm{CHP}}$ [MWh-el]
$\underline{P}_u$	Min. power production for unit $u \in \mathcal{U}^{\mathrm{CHP}}$ [MWh-el]
S^{F}	Maximum heat flow from the storage to the district heating network [MWh-heat] per period
s_0	Initial storage level [MWh-heat]
$\overline{S}$	Maximum heat storage level [MWh-heat]
$\underline{S}$	Minimum heat storage level [MWh-heat]
λ_t	Electricity price forecast for time period $t \in \mathcal{T}$ [DKK/MWh-el]
D_t	Heat demand for time period $t \in \mathcal{T}$ [MWh-heat]
Variables	
$q_{u,t} \in \mathbb{R}_0^+$	Heat production of heat unit $u \in \mathcal{U}$ in period $t \in \mathcal{T}$ [MWh-heat]
$q_{u,t}^{\mathrm{DH}} \in \mathbb{R}_0^+$	Heat production of unit $u \in \mathcal{U}$ inserted to the grid in period $t \in \mathcal{T}$ [MWh-heat]
$q_{u,t}^{\mathrm{S}} \in \mathbb{R}_0^+$	Heat production of unit $u \in \mathcal{U}$ inserted to the storage in period $t \in \mathcal{T}$ [MWh-heat]
$p_{u,t} \in \mathbb{R}_0^+$	Power production of unit $u \in \mathcal{U}^{\mathrm{CHP}}$ in period $t \in \mathcal{T}$ [MWh-el]
$s_t \in \mathbb{R}_0^+$	Thermal storage level at time period $t \in \mathcal{T}$ [MWh-heat]
$s_t^{\mathrm{OUT}} \in \mathbb{R}_0^+$	Heat flowing from the storage to the district heating in period $t \in \mathcal{T}$ [MWh-heat]
$x_{u,t} \in \{0,1\}$	Binary variable: 1, if unit $u \in \mathcal{U}^{\mathrm{CHP}}$ is on in period $t \in \mathcal{T}$ and 0, otherwise

The objective function (C.1a) minimizes the cost of producing heat by units $\mathcal{U}$, while taking the expected income from the electricity market into account.

$$\min \sum_{t\in T}\sum_{u\in\mathcal{U}^{\mathrm{CHP}}} \left(C_u\varphi_u - \lambda_t\right)p_{u,t} + \sum_{t\in T}\sum_{u\in\mathcal{U}^{\mathrm{H}}} \left(C_u q_{u,t}\right) \tag{C.1a}$$

The production and flow of heat is modeled in constraints (C.1b) to (C.1e). The heat production capacity of all units is limited by constraint (C.1b). The lower bound of the heat production is normally $\underline{Q}_{u,t} = 0$ for all units $u \in \mathcal{U}$ and time periods $t \in \mathcal{T}$, but it is a necessary restriction that we will use in some parts of our algorithm which is described in more detail in Section C.3. The produced heat is either used in the district heating system or flows to the thermal storage (C.1c). Whether the unit is connected to the district heating, the storage or both is determined by constraints (C.1d) and (C.1e).

$$\underline{Q}_{u,t} \le q_{u,t} \le \overline{Q_u} \qquad \forall t \in \mathcal{T}, \forall u \in \mathcal{U} \tag{C.1b}$$

$$q_{u,t} = q^{\mathrm{DH}}_{u,t} + q^{\mathrm{S}}_{u,t} \qquad \forall t \in \mathcal{T}, \forall u \in \mathcal{U} \tag{C.1c}$$

$$q^{\mathrm{DH}}_{u,t} \le \overline{Q_u} A^{\mathrm{DH}}_u \qquad \forall t \in \mathcal{T}, \forall u \in \mathcal{U} \tag{C.1d}$$

$$q^{\mathrm{S}}_{u,t} \le \overline{Q_u} A^{\mathrm{S}}_u \qquad \forall t \in \mathcal{T}, \forall u \in \mathcal{U} \tag{C.1e}$$

The power and heat production of a CHP unit is connected in constraints (C.1f) with the corresponding heat-to-power ratio. Constraints (C.1g) set the minimum and maximum power production of the CHP plant, if the CHP is on ($x_{u,t} = 1$) and to 0 otherwise ($x_{u,t} = 0$).

$$q_{u,t} = \varphi_u p_{u,t} \qquad \forall t \in \mathcal{T}, \forall u \in \mathcal{U}^{\mathrm{CHP}} \tag{C.1f}$$

$$\underline{P}_u x_{u,t} \le p_{u,t} \le \overline{P}_u x_{u,t} \qquad \forall t \in \mathcal{T}, \forall u \in \mathcal{U}^{\mathrm{CHP}} \tag{C.1g}$$

The heat storage is modeled through constraints (C.1h)-(C.1l). Constraints (C.1h) determine the storage level in each period while the capacity of storage is ensured by constraints (C.1i). The inflow to and outflow from the storage is limited by constraints (C.1j) and (C.1k), respectively. We ensure that the initial storage level is reached again at the end of the receding planning horizon to avoid emptying the storage every day (C.1l). In Section C.6, we further investigate how many days of receding horizon should be considered.

$$s_t = s_{t-1} + \sum_{u\in\mathcal{U}} q^{\mathrm{S}}_{u,t} - s^{\mathrm{OUT}}_t \qquad \forall t \in \mathcal{T} \tag{C.1h}$$

$$\underline{S} \le s_t \le \overline{S} \qquad \forall t \in \mathcal{T} \tag{C.1i}$$

$$\sum_{u\in\mathcal{U}} q^{\mathrm{S}}_{u,t} \le S^{\mathrm{F}} \qquad \forall t \in \mathcal{T} \tag{C.1j}$$

$$s^{\mathrm{OUT}}_t \le S^{\mathrm{F}} \qquad \forall t \in \mathcal{T} \tag{C.1k}$$

$$s_{|\mathcal{T}|} \geq s_0 \tag{C.1l}$$

Finally, the heat balance of the system is ensured by equation (C.1m), i.e., the heat output to the district heating network must match the heat demand in each period. We assume that the demand data is adjusted to take heat losses into account.

$$D_t = \sum_{u \in \mathcal{U}} q_{u,t}^{\mathrm{DH}} + s_t^{\mathrm{OUT}} \qquad \forall t \in \mathcal{T} \tag{C.1m}$$

The above stated MILP (C.1a)-(C.1m) is the basis for our bidding method described in the next section.

C.3 Bidding method

In this section we present our bidding method, named Heat Unit Replacement Bidding (HURB) method, for district heating operators. We assume that the district heating operator has enough capacity to cover the heat demand in all periods by just using heat-only units, i.e., units that are operated independently from won offers in the electricity markets. This is a reasonable assumption, because this is the case for almost all district heating systems in Europe. In particular, because not having enough capacity, such that they can operate independently from the electricity market, introduces a risk of not covering the heat demand, which is the primary goal of district heating providers.

The HURB method uses the MILP presented in Section C.2 to optimize the heat production in each time period by using the units in $\mathcal{U}$. To obtain the hourly bidding prices and power amounts offered to the day-ahead from this solution, we proceed as follows. The idea behind our bidding method is to incentivize the CHP units to place as many bids as needed to replace the heat production from heat-only units, i.e., selling power to the electricity market would lower the overall cost compared to just using heat-only units. This stems from the observation that CHP units are usually more expensive to operate than heat-only units. Thus, we would normally avoid producing with the CHP units if it is not necessary. However, if we have the chance to receive a sufficiently high price from the electricity market, such that the net costs (operational cost minus profits) of the CHP units drop below production costs of some or all of the heat-only units, it is more profitable to produce heat with the CHP units.

Based on this idea, we propose an iterative approach to determine when which heat-only unit will be replaced by CHP production. The outline is shown in Algorithm 4 and the symbols are defined in Table C.2. First, we obtain the

Table C.2: Symbols in Algorithm 4

i	Iteration counter
$\mathcal{H}$	Heat-only units in descending order of operational cost
$\mathcal{U}_i^{\mathrm{H}}$	Subset of heat-only units to be considered in iteration i
$\mathcal{O}$	Set of offers
b_u	Bidding price for unit $u \in \mathcal{U}^{\mathrm{CHP}}$
$a_{u,t}$	Bidding amount for unit $u \in \mathcal{U}^{\mathrm{CHP}}$ in period $t \in \mathcal{T}$
$k_{u,t}$	Bidding amount for unit $u \in \mathcal{U}^{\mathrm{CHP}}$ in period $t \in \mathcal{T}$ cummulated over the iterations
$(u, t, b_u, a_{u,t})$	Tuple representing an offer in set $\mathcal{O}$ valid for unit $u \in \mathcal{U}^{\mathrm{CHP}}$ in period $t \in \mathcal{T}$ with bidding price b_u and amount $a_{u,t}$

optimal heat production for all units without consideration of participation in the electricity market. This means we solve the MILP (C.1a) to (C.1m) with $\lambda_t = 0\ \forall t \in T$ and no restriction on the minimum production, i.e., $\underline{Q}_{u,t} = 0\ \forall u \in \mathcal{U}, t \in \mathcal{T}$ (see constraint (C.1b)). The optimal heat production of all heat-only units $u \in \mathcal{U}^{\mathrm{H}}$ is stored in $q^*_{u,t}$ for later use. Then we sort the heat-only units in descending order of production costs per MW heat. From this we obtain the set $\mathcal{H} = \{h_1, ..., h_n\}$ where $\mathcal{H}$ is the ordered version of set $\mathcal{U}^{\mathrm{H}}$, i.e., $h_j \in \mathcal{U}^{\mathrm{H}}$, $n = |\mathcal{U}^{\mathrm{H}}|$ and $C_{h_j} > C_{h_k} \forall j, k \in \{1, \ldots, n\}$ if $j < k$. Afterward, we iterate over the elements in set $\mathcal{H}$. In each iteration i we remove the next most expensive unit h from the set $\mathcal{U}^{\mathrm{H}}_{i-1}$ resulting in a subset $\mathcal{U}^{\mathrm{H}}_i = \mathcal{U}^{\mathrm{H}}_{i-1} \backslash \{h\}$. For the remaining heat units $u \in \mathcal{U}^{\mathrm{H}}_i$, we restrict the heat production with a lower bound $\underline{Q}_{u,t} = q^*_{u,t}$ to ensure that only production of unit h is replaced. Then we determine the optimal production for this new subset of heat-only units and all CHP units $\mathcal{U}^{\mathrm{CHP}}$ by solving the MILP (C.1a) to (C.1m) for $\mathcal{U} = \mathcal{U}^{\mathrm{H}}_i \cup \mathcal{U}^{\mathrm{CHP}}$. From the solution we can determine the periods in which the heat-only unit removed in this iteration is replaced by the CHP units. This can be derived from the power production $p^*_{u,t}$ of the CHP units in the solution. The amount offered to the market $a_{u,t}$ is the additional power production added in this iteration. If the CHP unit is not producing, i.e., $p^*_{u,t} = 0$, no offer is created.

The bidding price b_u for offering the power produced by CHP unit u is based on the production cost of the CHP unit u and the replaced heat-only unit h as shown in equation (C.2).

$$b_u = \left(C_u - C_h\right) \cdot \varphi_u \qquad \forall u \in \mathcal{U}^{\mathrm{CHP}} \tag{C.2}$$

The bidding price can be interpreted as follows. If we replace production by heat-only unit h with CHP unit u, we have to pay the production cost of the CHP unit u but we also save the production cost of heat-only unit h. To be profitable, we need to get at least the remaining amount $(C_u - C_h)$ from the market. This is our bidding price. At this price we are indifferent about whether we produce with the heat-only or with the CHP unit, because the costs for the

Algorithm 4 Heat Unit Replacement Bidding (HURB)

Set $\lambda_t = 0\ \forall t \in T$ and $\underline{Q}_{u,t} = 0\ \forall u \in U, t \in T$
Solve (C.1a)-(C.1m) and store optimal heat production $q^*_{u,t}$
Set λ_t to the electricity price forecast
$\mathcal{H} = \text{sort}(\mathcal{U}^H)$ ▷ Order heat-only units by descending C_u
$\mathcal{O} \leftarrow \emptyset$ ▷ Initialize set of offers
$k_{u,t} \leftarrow 0$ ▷ Variable storing power production
$i \leftarrow 0, \mathcal{U}^{\mathrm{H}}_i \leftarrow \mathcal{U}^{\mathrm{H}}$ ▷ Initialize iteration counter and heat-only units
for each $h \in \mathcal{H}$ **do**
  $i \leftarrow i + 1$
  $\mathcal{U}^{\mathrm{H}}_i = \mathcal{U}^{\mathrm{H}}_{i-1} \backslash \{h\}$ ▷ Remove next heat-only unit
  Set $\underline{Q}_{u,t} = q^*_{u,t} \forall u \in \mathcal{U}^{\mathrm{H}}_i$
  Solve (C.1a)-(C.1m) with $\mathcal{U} = \mathcal{U}^{\mathrm{CHP}} \cup \mathcal{U}^{\mathrm{H}}_i$ ▷ Optimize
  Get optimal solution $p^*_{u,t}$
  for each $t \in \{1, \dots 24\}$ **do**
    for each $u \in \mathcal{U}^{\mathrm{CHP}}$ **do**
      $a_{u,t} \leftarrow p^*_{u,t} - k_{u,t}$ ▷ Set amount
      if $a_{u,t} > 0$ **then** ▷ If new CHP production
        $b_u \leftarrow \left(C_u - C_h\right) \cdot \varphi_u$ ▷ Set bidding price
        $\mathcal{O} \leftarrow \mathcal{O} \cup \left(u, t, b_u, a_{u,t}\right)$ ▷ Add new offer
      end if
      $k_{u,t} \leftarrow k_{u,t} + a_{u,t}$ ▷ Cumulate power
    end for
  end for
end for
Return $\mathcal{O}$

production will be the same. By setting the bidding price in this way, we will not increase the cost even if we are not dispatched, because we have to produce the heat anyway. But if the market price is above our bidding price, we will make profits and lower our overall operational costs.

We repeat this process by iteratively removing further heat-only units from the optimization problem until only the CHP units are left. During the iterations we collect the offers for the next day (i.e., periods $t \in \{1, \dots 24\}$ although the total number of periods can be larger) in set $\mathcal{O}$. Each offer $o \in \mathcal{O}$ consist of a tuple $(u, t, b_u, a_{u,t})$ stating the CHP unit u it corresponds to, the hour t of the next day it is valid for, the bidding price b_u and amount of power $a_{u,t}$. Offers created in the process are added to this set. No previous offers are removed, because they are still valid. After the algorithm is finished, the operator can determine the bids from set $\mathcal{O}$ and present them to the market.

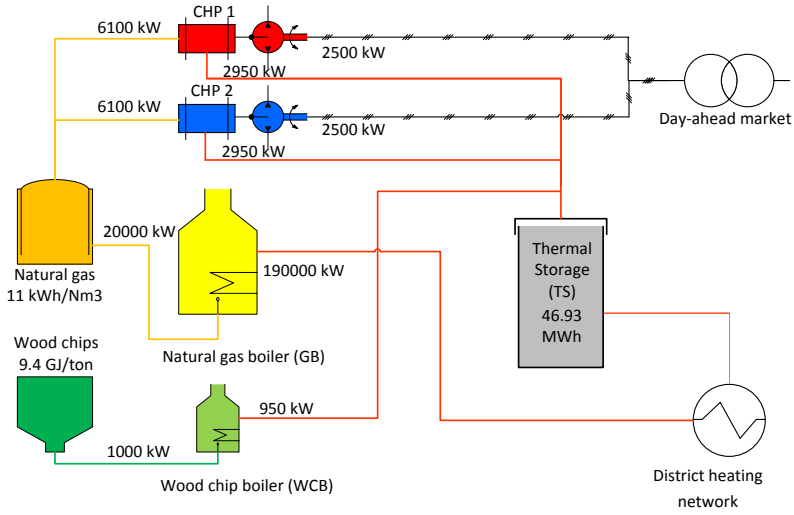

Figure C.1: Flowchart of the system

C.4 Case study

We use the following case study to demonstrate the HURB method in an illustrative example in Section C.5 and compare the numerical results to other bidding methods in Section C.6.

We consider a small district heating system as shown in Figure C.1. The system includes two CHP production units (CHP1 and CHP2) in the form of gas engines and two heat-only units, more specifically a gas boiler (GB) and wood chip boiler (WCB). Furthermore, the system includes a thermal storage (TS) that can deliver heat to the district heating network. The CHP units and the WCB are connected to the thermal storage and not directly feeding to the district heating network. The GB is not connected to the thermal storage, but directly to the district heating network instead. The parameters of the units such as production costs and technical data are given in Table C.3. The data presented is taken from the energyPRO library, which is based on actualized data from heat-only and CHP units by [C27]. The electricity prices for 2016 in the DK1 Nordpool area are taken from the Energinet datahub [C28]. The heat demand for 2016 is set to 37500 MWh-heat, comparable to 1 km^2 of an urban area with a heat density of 120 TJ/km^2. This amount represents around 2000 family households where 40% of the heat delivered is domestic hot water and grid losses, which are not weather dependent. The remaining 60% of the heat delivered is used for space heating which is dependent on the outside temperature.

Table C.3: Characteristics of the production units and the thermal storage

Unit	C_u	$\overline{Q}_u$	$\overline{P}_u$	φ_u	$\overline{S}$	$\underline{S}$	S^{F}	A_u^{DH}	A_u^{S}
CHP1	610.84	2.95	2.5	1.18	-	-	-	0	1
CHP2	610.84	2.95	2.5	1.18	-	-	-	0	1
GB	404.02	19	-	-	-	-	-	1	0
WCB	211.45	0.95	-	-	-	-	-	0	1
TS	-	-	-	-	46.93	0	46.93	-	-

We will study two different operation modes of the CHP units. First, *full load* is a restrictive mode in which if the CHP unit is on, it is forced to produced at its maximum capacity ($\underline{P}_u = \overline{P}_u = 2.5$). Many district heating providers in Denmark operate their CHP units only at full load, where it has the highest efficiency. In the other configuration, named *partial load* configuration, both CHP units can produce at partial load between $\underline{P}_u$ and $\overline{P}_u$. Note that the only change to the method that has to be made to switch between those two modes is setting parameter $\underline{P}_u$ equal to $\overline{P}_u$.

C.5 Illustrative example

This example demonstrates our bidding method HURB for the case study described in the previous section. We consider one specific day in March 2016 to illustrate the steps of Algorithm 4. We use the *full load* operation mode and an initial storage level of $s_0 = 10$ MWh-heat.

In the initialization of the algorithm, we solve the model without forcing any minimum heat production to the CHP and heat-only units and without considering the electricity price forecast. The optimal solution is depicted in Figure C.2 showing that the cheaper WCB and GB are used for production. This obtained solution ($q^*_{u,t}$) determines the heat production lower bound ($\underline{Q}_{u,t}$) for future steps in the algorithm. The algorithm continues by identifying the heat-only production units and sorting them in descending order of production costs. In our case this results in set $\mathcal{H} = \{\text{GB, WCB}\}$ because the GB has higher production cost (404.62) than the WCB (211.45).

In the first iteration $i = 1$ of the algorithm, we remove the GB from $\mathcal{U}^{\mathrm{H}}$ and solve the optimization problem (C.1a)-(C.1m) for the remaining set of units $\mathcal{U} = \{\text{WCB, CHP1, CHP2}\}$ formed by the union of the sets $\mathcal{U}^{\mathrm{CHP}} = \{\text{CHP1, CHP2}\}$ and $\mathcal{U}^{\mathrm{H}}_1 = \{\text{WCB}\}$, where the minimum production of the WCB is limited to the production from Figure C.2. The resulting optimal heat production and

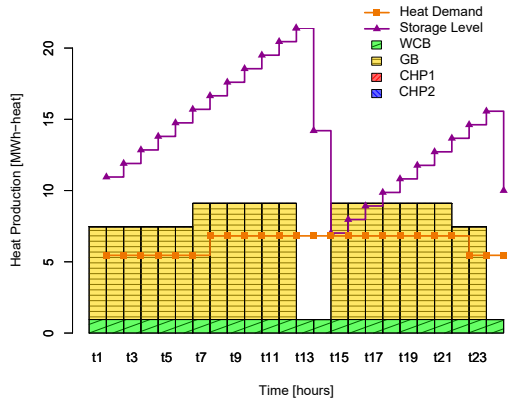

Figure C.2: Heat production with no minimum heat restriction and considering no electricity market participation.

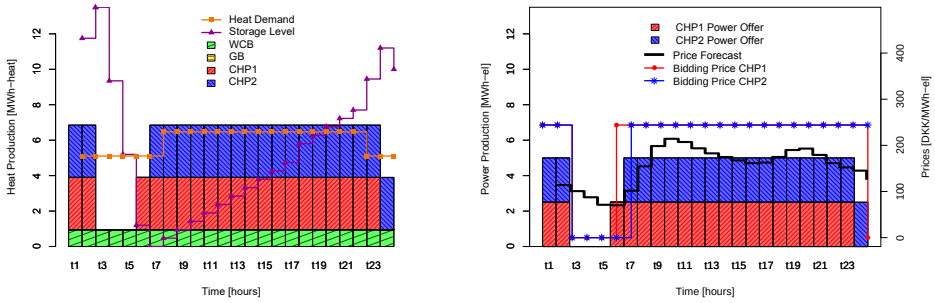

(a) Heat production and storage level of the system compared to the heat demand

(b) Power offered and bidding prices for both CHP1 and CHP2 vs. forecast electricity price

Figure C.3: Production data of the system for 24 hours when the gas boiler unit is removed (Iteration 1)

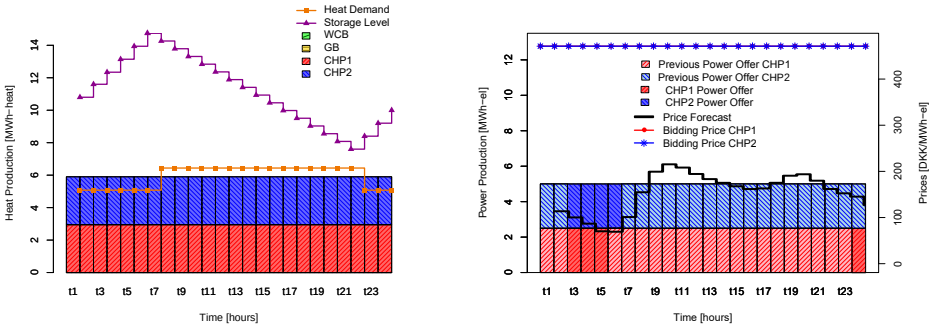

(a) Heat production and storage level of the system compared to the heat demand

(b) Power offered and bidding prices for both CHP1 and CHP2 vs. forecast electricity price

Figure C.4: Production data of the system for 24 hours when both the gas boiler unit and the wood chip boiler are removed (Iteration 2)

storage operation is shown in Figure C.3a for the given heat demand. Based on this information we determine the offers for the day-ahead market. The bidding hours and power amounts for the offers can be directly deferred from the optimal production. The optimal power production, bidding prices and price forecast for this day are depicted in Figure C.3b, where both CHP units are used in most of the hours. Except in periods 3 to 5 where both units are off, hour 6 where only CHP1 is on and hour 24 where only CHP2 is on. This means we have to determine offers for CHP1 in hours $\{1, 2, 6, \ldots, 23\}$ and for CHP2 in hours $\{1, 2, 7, \ldots, 24\}$. The power amount is always 2.5 MWh per CHP. The bidding price for the two CHP units is the same as they have the same operational cost and determined by subtracting the cost of the removed GB from the CHP operational cost and adjusted from price per MWh heat to price per MWh power. This results in the following bidding price (C.3) (see also Figure C.3b).

$$\forall u \in \mathcal{U}^{\mathrm{CHP}} \quad b_u = \left(C_u - C_{\mathrm{GB}}\right) \cdot \varphi_u = (610.84 - 404.02) \cdot 1.18 = 244.045 \tag{C.3}$$

The iteration finishes with a total number of 40 hourly offers where each offer has a power amount of 2.5 MWh and a price of 244.045 DKK.

In the second iteration $i = 2$, we remove the next most expensive heat-only unit, which is the WCB, reducing the set $\mathcal{U}_2^{\mathrm{H}}$ to an empty set. Thus, in this iteration we solve the optimization model (C.1a)-(C.1m) using just the CHP

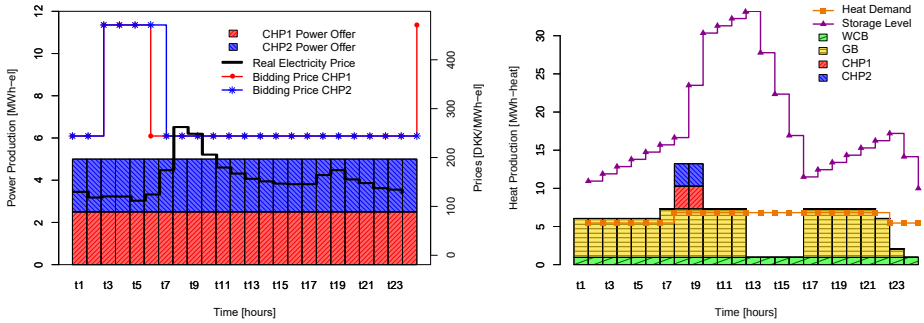

(a) Power offered and bidding prices for both CHP1 and CHP2 vs. real electricity prices

(b) Real heat production and storage level of the system compared to the heat demand

Figure C.5: Final production of the system using real data for the day studied.

units $\mathcal{U} = \mathcal{U}^{\text{CHP}}$. The resulting heat and power production is shown in Figure C.4. The hours and power amounts for the new offers are the difference between the power production in the previous iteration and this iteration. This means we add new offers for CHP1 in hours $\{3, 4, 5, 24\}$ and for CHP2 in hours $\{3, 4, 5, 6\}$. All new offers will have the amount 2.5 MWh, because the respective CHP was off before and is now producing at full load. The bidding price is calculated in equation (C.4) and this time based on the cost of the WCB.

$$\begin{aligned} \forall u \in \mathcal{U}^{\text{CHP}} \quad b_u &= \left(C_u - C_{\text{WCB}}\right) \cdot \varphi_u \\ &= (610.84 - 211.45) \cdot 1.18 = 471.279 \end{aligned} \tag{C.4}$$

Thus, the second and last iteration adds eight new offers to the set.

In total, the bidding method resulted in 48 bids. Figure C.5a shows the final offers and bidding prices presented to the market. The price depicted is now the real realization instead of the forecast used in the optimization. For the operation of the system this implies that if the real price is greater or equal than the bidding price for an specific period of time, the unit is committed to produce (in this case for hours 8 and 9). In the other periods, we are free to determine the operation of the system. Based on the optimization of model (C.1a)-(C.1m) with fixed power production in periods 8 and 9, we obtain the heat production schedule in Figure C.5b. Except in the committed hours of CHP production, we use the cheaper WCB and GB in the other periods to cover the heat demand. Furthermore, we can see from the storage level also shown in Figure C.5b that the thermal storage is used to avoid more expensive

GB production in some periods.

C.6 Numerical Results

In this section, we analyze the performance of our bidding method and compare it to the following proposed methods from literature:

- *Method A:* Bidding strategy based on the uncertainty bound given by forecasted prices [C22].
- *Method B:* Use of confidence intervals on price forecast to create bidding curves [C23].
- *Method C:* Forecasted electricity price as bidding prices [C24].
- *Method D:* Use of price scenario intervals to create bidding curves [C25].
- *Method E:* Piece-wise linear function of costs used as bidding prices [C26].

Although methods A to D are developed and designed for standalone CHP or thermal production units, they could be used also by district heating operators to determine the bids for the CHP units without taking the other units into account. We compare the HURB method to these methods to show that district heating operators have a benefit from using a method that takes the entire portfolio of units into account and should therefore use more specialized methods instead of the general applicable bidding methods. However, the HURB method would not be applicable to the general case without other heat producing units as it is considered in [C22, C23, C24, C25].

All methods base their offers on the optimal operation of the system. For a fair comparison of the bidding strategy, we use the model (C.1a)-(C.1m) to determine the optimal power production for all methods. In this way, we focus on just comparing the creation of bids and not the underlying operational planning problem. For the above mentioned methods A to E, no iterative procedure is proposed to replace heat-only units. Furthermore, the bidding prices are determined in different ways. For further information about the details of the methods we refer the reader to the mentioned references.

The following comparison of the methods is based on the totals costs by using the bidding methods for each day of the planning horizon. This daily optimization can be seen individually by just considering 24 time periods. However, we use

a receding approach and, thus, include more time periods in the operational optimization to consider the operation of the thermal storage over several days. In the end, only the offers for the first 24 hours are send to the market. For a fair comparison we ensure that the storage level at the end of the horizon is the same for all methods.

The daily usage of the bidding method also allows us to update the forecasts for electricity prices every day. For this experiment, we use time series analysis to create a SARIMA model with one day seasonality following the same approach as in [C29] including harmonic external regressors in the form of Fourier series [C30] to describe weekly seasonality (T=168 hours). The model to predict electricity prices λ_t is

$$\begin{aligned}\lambda_t = \mu + \phi_1\lambda_{t-1} + \phi_2\lambda_{t-2} + \phi_{24}\lambda_{t-24} + \theta_1\varepsilon_{t-1} + \theta_2\varepsilon_{t-2} + \theta_{24}\varepsilon_{t-24} \\ + \sum_{k=1}^{K}\left[\alpha_k \sin\left(\frac{2\pi kt}{168}\right) + \beta_k \cos\left(\frac{2\pi kt}{168}\right)\right]\end{aligned} \tag{C.5}$$

where λ_t is the estimated electricity price for period t. The coefficient μ is the intercept and λ_{t-1}, λ_{t-2}, λ_{t-24}, ε_{t-1}, ε_{t-2} and ε_{t-24} correspond to the autoregressive and moving average terms, respectively. K is a natural number chosen by minimizing the Akaike information criterion (AIC) and determines the number of Fourier terms considered. Finally, $\alpha_k, \beta_k, \phi_1, \phi_2, \phi_{24}, \theta_1, \theta_2$ and θ_{24} are the forecast parameters. More sophisticated forecasting methods based on temporal dependencies such as probabilistic forecasting can be used. We refer the reader to, e.g., [C31] where the authors create a model to predict day-ahead electricity prices based on reliable probability density forecasts.

Based on this, the evaluation process can be described as follows:

1. Choose length of receding horizon $|\mathcal{T}|$ (a multiplier of 24 to cover entire days).
2. Update forecast parameters of electricity prices for day d using the most recent observations and predict for $|\mathcal{T}|$ periods.
3. Apply bidding method (either HURB or method A-E) for $|\mathcal{T}|$ periods.
4. Evaluate the set of offers $\mathcal{O}$ for real prices of day d.
5. Get the system cost for day d.
6. Update $d = d + 1$ and go to step 2.

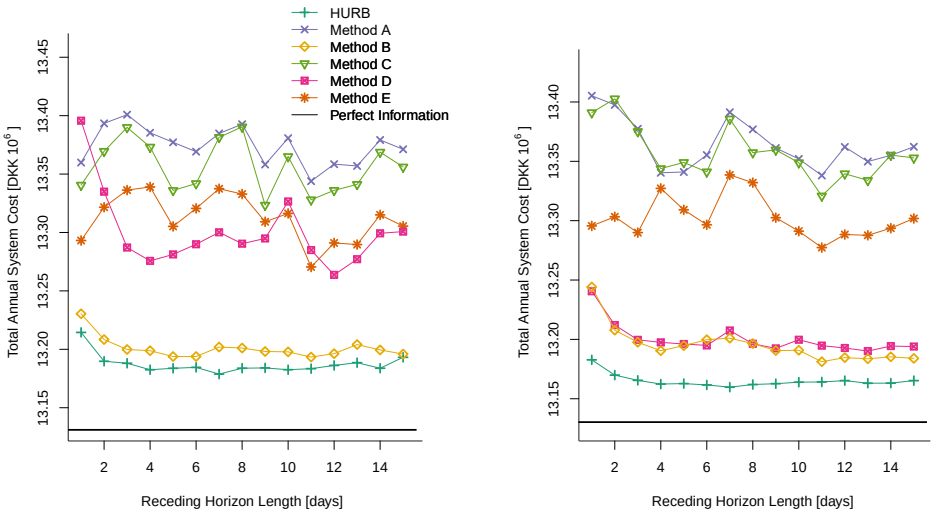

(a) *Full load configuration* **(b)** *Partial load configuration*

Figure C.6: Annual system cost per method and length of receding horizon (1 to 15 days). The black line shows the cost with perfect information (solving the entire year at once with real electricity prices).

C.6.1 Evaluation for the year 2016

We first apply the methods HURB and A to E for the year 2016. All methods are tested with different lengths of receding horizon, namely 1 to 15 days, and use the mentioned SARIMA model for forecasting the electricity prices.

Figure C.6 shows the annual system costs for all methods. Furthermore, the figure distinguishes between the two configurations *full load* (C.7a) and *partial load* (C.7b). For all lengths of receding horizon and both configurations, our method (HURB) yields the best result regarding total annual system costs, closely followed by method B. Those two methods are also very close to the total annual costs when having perfect information (black line), which are the theoretical minimal costs of the system when we solve the optimal operation for the entire year at once and have perfect information about electricity prices. Figure C.6 also shows that all methods benefit from using a receding horizon of more than one day, i.e., the solution can be improved by already considering future days for the operation of the storage.

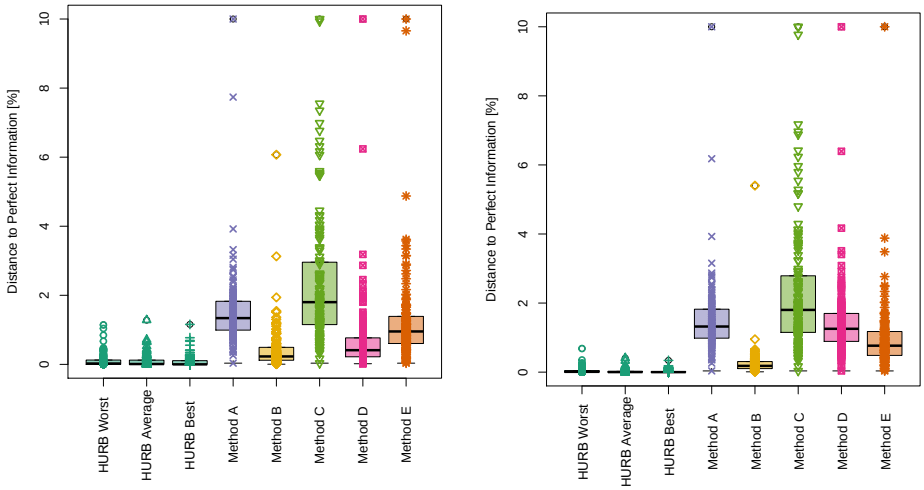

(a) *Full load configuration* **(b)** *Partial load configuration*

Figure C.7: Distance in % of montly system cost per method to the cost obtained by using perfect information. All methods are run with 1 to 15 days of receding horizon. For method A to E and HURB Best, the results show the cost for the best receding horizon. For HURB Worst, the worst receding horizon is chosen and HURB Average shows the mean difference to the perfect information solution over all lengths of receding horizon.

C.6.2 Evaluation of further electricity price sets

To get a more general result of the comparison, we evaluate a more diverse set of electricity prices, i.e., we use different samples of realization of electricity prices to evaluate how the method would perform if the electricity prices would have turned out differently. Therefore, we repeat our experiment again for the month January 2016 using the same price forecasting method as before. We use 144 samples for realizations of electricity prices obtained from different markets in the Nordpool region to evaluate the performance of the methods in the market. We use data from the regions Sweden (SE4) and Germany (DE) for the months in 2013 to 2015 and 2017. As the cost per month differ based on the prices, we compare the methods using the difference between the cost obtained by the method and the cost obtained by using perfect information regarding electricity prices (solving the entire month at once with the respective electricity prices instead of using a forecast).

Method	Full load					Partial load				
	RH	CHP 1		CHP 2		RH	CHP 1		CHP 2	
		Offers	Won	Offers	Won		Offers	Won	Offers	Won
HURB Worst	1	98.44	41.88	98.41	41.81	1	98.91	41.95	98.70	41.91
HURB Avg.	-	99.64	42.16	99.62	42.07	-	99.79	42.19	99.75	42.15
HURB Best	10	99.83	42.27	99.82	42.19	10	99.89	42.28	99.87	42.26
Method A	11	44.88	39.29	44.87	39.27	10	44.92	39.34	44.92	39.31
Method B	14	82.25	35.25	82.15	35.25	5	82.52	35.85	82.40	35.82
Method C	2	44.60	18.33	44.66	18.36	12	45.02	18.54	45.01	18.53
Method D	10	74.62	35.61	74.61	35.60	12	75.55	26.56	75.55	26.55
Method E	5	44.62	31.87	44.63	31.89	5	44.84	32.58	44.83	32.57

Table C.4: Percentage of hours with offers and won bids in the investigated month averaged over all samples (RH = receding horizon).

Figure C.7 shows the distance in % to the cost using perfect information. All methods were again evaluated using different lengths of receding horizon. For method A to E and HURB Best, the results show the cost for the best receding horizon length. For HURB Worst, the worst receding horizon is chosen and HURB Average shows the mean difference to the perfect information solution over all lengths of receding horizon. The specific number of days are also mentioned in Table C.4. Furthermore, the figure distinguishes between the two configurations *full load* (C.7a) and *partial load* (C.7b).

For both configurations HURB yields the best result, i.e., the cost are closest to perfect information cost. Even with the worst configuration of receding horizon length (HURB Worst), it leads to better results for most of the samples compared to the other methods. Our method is closely followed by method B, which outperforms the other methods A and C to E in most of the samples.

C.6.3 Discussion

To explain why our methods outperforms the others, we state the average number of hours and won bids for each method over all samples in Table C.4. The values are given in percentage of hours per month.

These values show that HURB submits more offers to the market than the other methods. On average HURB places offers in more than 98% of the hours, while the other methods have fewer bids. In particular, method A, C and E only place offers in less than 50% of the hours. HURB also wins more bids in the market compared to the others (in more than 40% of the hours). Method B [C23], which is the second best regarding cost, wins on average in less than 36% of the hours. Thus, HURB achieves a higher income from the market. Although,

method A [C22] also yields won bids close to 40% of the hours like HURB, these bids are not always profitable for the district heating operator. As method A was developed for a standalone thermal unit it does not take the other units into account to calculate the overall system costs. The bidding prices are set based on the confidence interval of the electricity price forecast, which could lie below the marginal cost of the system. Therefore, method A is not advisable for district heating operators. The same holds for method C [C24], which uses the forecast as bidding price.

Method B and D [C25] are using the forecast on electricity prices to determine when and at which price it is profitable to produce with the CHP units. While method B uses intervals of the probability density function of the price forecast, method D uses sampled scenarios. They analyze the results for the intervals/scenarios and present an offer with the respective bidding price of the interval/scenario, if the CHP units produces according to their optimization method. As these methods also do not make use of the other units in the district heating system, they offer only in hours where the forecast indicates profits. In the HURB method, we explicitly consider the district heating system and make use of the fact that we have to produce the heat either way. Therefore, the electricity price forecast does not determine the amount or price of the offers but only the hours in which to place them. This is also the explanation, why the HURB method bids in more hours than method E [C26]. Although method E also uses the marginal cost as bidding prices and makes uses of the district heating system, the creation of offers regarding bidding amounts and offers is different. Method E places offers at the marginal prices of the units, whenever it is profitable with respect to the price forecast. In contrast, HURB offers as much electricity which is needed to replace the entire heat demand by CHP production, which results in more offers in total. Furthermore, the prices set by HURB ensure no losses regarding the cost minimal production without trading, but only profits if bids are won.

C.7 Summary and outlook

In this work, we propose a new day-ahead market bidding strategy, named Heat Units Replacement Bidding (HURB) method, for CHP units that are operated jointly with other heat or heat-only production units. Our bidding method is based on replacing heat production from heat-only units through CHP production in a iterative manner. The method uses a mathematical program to determine the optimal operation of the portfolio of units. In order to evaluate our bidding method, we implement other bidding methods proposed in literature and compare them in a common case study. We state the results for an entire

year by executing the bidding method on a daily basis with different lengths of receding horizon. Furthermore, we perform an out-of-sample test to get more general results. The results show that compared to the other bidding methods, our method yields the lowest cost and most won bids.

To extend the use of this bidding method, we propose three future research directions. First, the consideration of the balancing market offers further opportunities to reduce the operational cost. Second, the modelling of block bids, start-up cost and minimum operation times for the CHP units is a valuable extension to cover more instruments on the electricity markets. Finally, the increasing presence of solar thermal units at district heating operators introduces an additional source of uncertainty regarding the production amounts. This production has to be taken into account appropriately while determining the offers to the market. Methods based on stochastic programming are able to incorporate this uncertainty by including potential scenarios.

References C

[C1] European Commission. *Efficient district heating and cooling systems in the EU*. https://www.euroheat.org/wp-content/uploads/2017/01/study-on-efficient-dhc-systems-in-the-eu-dec2016_final-public-report6.pdf. (Accessed on 02/02/2018). 2016.

[C2] D. Connolly et al. "Heat Roadmap Europe: Combining district heating with heat savings to decarbonise the EU energy system". In: *Energy Policy* 65 (2014), pp. 475–489. ISSN: 0301-4215.

[C3] Euroheat & Power. *District Energy in Denmark*. https://www.euroheat.org/knowledge-centre/district-energy-denmark/. (Accessed on 03/15/2018). 2017.

[C4] Danish Energy Agency. *Regulation and planning of district heating in Denmark*. https://ens.dk/sites/ens.dk/files/Globalcooperation/regulation/and/planning/of/district/heating/in/denmark.pdf. (Accessed on 12/04/2017). 2017.

[C5] *NordPool*. https://www.nordpoolgroup.com/. (Accessed on 12/05/2017).

[C6] J. M. Morales et al. *Integrating renewables in electricity markets: operational problems*. Vol. 205. Springer Science & Business Media, 2013.

[C7] S. Jaehnert and G. L. Doorman. "The north European power system dispatch in 2010 and 2020". In: *Energy Syst.* 5.1 (2014), pp. 123–143.

[C8] P. A. Østergaard and A. N. Andersen. "Booster heat pumps and central heat pumps in district heating". In: *Applied Energy* 184 (2016), pp. 1374–1388.

[C9] S. Nyborg and I. Røpke. "Heat pumps in Denmark—From ugly duckling to white swan". In: *Energy Research & Social Science* 9 (2015), pp. 166–177.

[C10] I. Dimoulkas and M. Amelin. "Probabilistic day-ahead CHP operation scheduling". In: *2015 IEEE Power Energy Society General Meeting*. 2015, pp. 1–5.

[C11] S. Illerhaus and J. Verstege. "Optimal operation of industrial CHP-based power systems in liberalized energy markets". In: *International Conference on Electric Power Engineering – IEEE PowerTech*. 1999, p. 210.

[C12] C. Schaumburg-Müller. "A partial load model for a local combined heat and power plant". In: *Proceedings of the 1st Nordic optimization symposium, Copenhagen*. 2006.

[C13] T. Fang and R. Lahdelma. "Optimization of combined heat and power production with heat storage based on sliding time window method". In: *Appl. Energy* 162 (2016), pp. 723–732.

[C14] J. Li et al. "Optimal operation of the integrated electrical and heating systems to accommodate the intermittent renewable sources". In: *Appl. Energy* 167 (2016), pp. 244–254.

[C15] M. G. Nielsen et al. "Economic valuation of heat pumps and electric boilers in the Danish energy system". In: *Applied Energy* 167 (2016), pp. 189–200.

[C16] M. Ito et al. "Electricity adjustment for capacity market auction by a district heating and cooling system". In: *Appl. Energy* 206 (2017), pp. 623–633.

[C17] *EMD International A/S energyPRO - Simulate, analyze and optimize operations of energy plants*. https://www.emd.dk/energypro/. (Accessed on 12/05/2017).

[C18] R. Scharff, J. Egerer, and L. Söder. "A description of the operative decision-making process of a power generating company on the Nordic electricity market". In: *Energy Syst.* 5.2 (2014), pp. 349–369. ISSN: 18683975. DOI: 10.1007/s12667-013-0104-2.

[C19] International Energy Agency. *Energy Market Experience - Lessons from Liberalised Electricity Markets*. http://www.iea.org/publications/freepublications/publication/lessonsnet.pdf. (Accessed on 12/06/2017). 2005.

[C20] F. P. Sioshansi. *Competitive electricity markets: design, implementation, performance*. Elsevier, 2011.

[C21] T. Jónsson et al. "Forecasting electricity spot prices accounting for wind power predictions". In: *IEEE Transactions on Sustainable Energy* 4.1 (2013), pp. 210–218.

[C22] A. J. Conejo, F. J. Nogales, and J. M. Arroyo. "Price-taker bidding strategy under price uncertainty". In: *IEEE Trans. Power Syst.* 17.4 (2002), pp. 1081–1088.

[C23] C. P. Rodriguez and G. J. Anders. "Bidding strategy design for different types of electric power market participants". In: *IEEE Trans. Power Syst.* 19.2 (2004), pp. 964–971.

[C24] K. Schulz, B. Hechenrieder, and B. Werners. "Optimal Operation of a CHP Plant for the Energy Balancing Market". In: *Operat. Res. Proceed. 2014*. Springer, 2016, pp. 531–537.

[C25] I. Dimoulkas and M. Amelin. "Constructing bidding curves for a CHP producer in day-ahead electricity markets". In: *2014 IEEE International Energy Conference (ENERGYCON)*. 2014, pp. 487–494.

[C26] H. V. Ravn et al. "Modelling Danish local CHP on market conditions". In: *Proc. 6th IAEE European Conference: Modelling in Energy Economics and Policy*. 2004.

[C27] Energinet & Danish Energy Agency. *Technology Data Catalogue for Energy Plants*. https://ens.dk/sites/ens.dk/files/Analyser/technology_data_catalogue_for_energy_plants_-_aug_2016_update_oct_nov_2017.pdf. (Accessed on 12/21/2017).

[C28] Energinet. *Data about the energy system*. https://en.energinet.dk/Electricity/Energy-data. (Accessed on 12/21/2017).

[C29] F. J. Nogales et al. "Forecasting next-day electricity prices by time series models". In: *IEEE Trans. Power Syst.* 17.2 (2002), pp. 342–348.

[C30] R. Weron. *Modeling and forecasting electricity loads and prices: A statistical approach*. Vol. 403. John Wiley & Sons, 2007.

[C31] T. Jónsson et al. "Predictive densities for day-ahead electricity prices using time-adaptive quantile regression". In: *Energies* 7.9 (2014), pp. 5523–5547.

Paper D

Operational Planning and Bidding for District Heating Systems with Uncertain Renewable Energy Production

Authors:
Ignacio Blanco, Daniela Guericke, Anders N. Andersen and Henrik Madsen

Published in:
Energies, 11(12), 3310.

Operational Planning and Bidding for District Heating Systems with Uncertain Renewable Energy Production

Ignacio Blanco[1], Daniela Guericke[1], Anders N. Andersen[2] and Henrik Madsen[1]

Abstract

In countries with an extended use of district heating (DH), the integrated operation of DH and power systems can increase the flexibility of the power system achieving a higher integration of renewable energy sources (RES). DH operators can not only provide flexibility to the power system by acting on the electricity market, but also profit from the situation to lower the overall system cost. However, the operational planning and bidding includes several uncertain components at the time of planning: electricity prices as well as heat and power production from RES. In this publication, we propose a planning method that supports DH operators by scheduling the production and creating bids for the day-ahead and balancing electricity markets. The method is based on stochastic programming and extends bidding strategies for virtual power plants to the DH application. The uncertain factors are considered explicitly through scenario generation. We apply our solution approach to a real case study in Denmark and perform an extensive analysis of the production and trading behaviour of the DH system. The analysis provides insights on how DH system can provide regulating power as well as the impact of uncertainties and renewable sources on the planning. Furthermore, the case study shows the benefit in terms of cost reductions from considering a portfolio of units and both markets to adapt to RES production and market states.

[1]Department of Applied Mathematics and Computer Science, Technical University of Denmark, DK-2800 Kgs. Lyngby, Denmark
[2]EMD International A/S, Niels Jernesvej 10, 9220 Aalborg Ø, Denmark

D.1 Introduction

To achieve the decarbonization of the energy sector, several countries especially in the European Union started to consider district heating (DH) and cooling systems for CO2-emissions reduction strategies [D1]. Since it is assumed that fossil fuels will be mostly replaced by intermittent renewable energy sources (RES), DH and cooling systems can facilitate a larger share of intermittent energy sources in the energy mix following the concept of integrated energy systems [D2]. DH systems are able to contribute to the grid balancing by the use of flexible heat and power production, power-to-heat technologies and thermal storages.

The efficiency of DH systems has been demonstrated already in countries in northern Europe. In Denmark, more than 60% of the heat consumption is delivered by DH [D3] and there exist a total of approximately 400 DH systems. The major part of those are small/medium DH systems that are usually operated based on a portfolio of different units such as CHP units (e.g. gas engines), fuel boilers, and power-to-heat technologies such as electric boilers and heat pumps. Also the installation of large solar thermal facilities ($\geq$1000 m^2) in Denmark has increased significantly during the last years and it is expected that 20% of the total heat consumption will be covered by solar heating in 2025 [D4]. Furthermore, the wider spread of power-to-heat technologies and decentralization of power production enables DH providers to include renewable power production, e.g., in the form of wind farms, to their portfolio. Although the primary goal of the DH operator is to fulfill the heat demand in the DH network at lowest cost, selling the power production from the CHP units or other RES as well as buying the power for heat-to-power technologies on electricity markets offers the potential for additional income resulting in lower total operating costs. However, as the RES production in the power and heat systems depends on weather conditions, the operation and planning has to deal with an increased complexity and uncertainty, which requires advanced modeling techniques [D5].

In this publication, we pursue two main objectives. First, we propose an operational planning method for DH operators coping with the complexity of a system with several traditional and RES production units. This includes the bidding in two electricity markets, namely day-ahead and balancing market. The method uses stochastic programming to capture the uncertainties and is based on models proposed for virtual power plants (VPPs) [D6]. Second, we use the proposed method to analyze the real case of a district heating system in Hvide Sande, Denmark. The analysis investigates among others the behaviour of the DH system in different situations, the influence of uncertainty in the RES production and benefits from including RES power production. The results offer several insights on how DH systems should operate and can benefit in future

systems with high shares of RES .

D.1.1 Description of electricity markets

Nowadays, the integration of the power and DH system is achieved through the participation of the latter in the electricity markets. Before describing the related work, we want to recall the concepts of the day-ahead and balancing electricity markets that are considered by the proposed planning method.

In most of the EU countries, the short-term trading of electricity is organized in a similar way. Most of the power volume is traded one day before the energy is delivered in the so-called *day-ahead market*. To ensure enough backup generation, producers can also bid offers in the *reserve capacity market* which takes place usually also one day before the delivery of energy. Getting closer to the time of delivery, *intra-day markets* are organized throughout the day to help RES producers submit more accurate power production offers. The purpose of these markets is to correct the imbalances produced by RES allowing producers to reformulate their bids. Finally, *balancing markets* are organized each hour of the day with gate closure one hour before the energy delivery.

Balancing markets are slightly different from intra-day markets and take place shortly before hour of energy delivery. The balancing markets are cleared by the TSO and their goal is to provide flexibility for the operation of the system and not to the producers as it is the case for the intra-day market. Balancing prices are highly volatile and quite unpredictable even for the following hour. In addition, balancing offers are just activated in case the TSO has need for regulation. In the case that there is a lack of power production due to a failure of a unit or an unpredictable demand, the TSO will activate offers for upward regulation paying producers to increase the production of their power plants. On the contrary, if there is more power production than expected due to an excess of RES production, the TSO will activate downward regulation offers for producers to deactivate the production they had previously scheduled in the day-ahead market or incentive more power consumption.

To efficiently operate in these markets, producers and consumers are allowed to submit price dependent bids. These type of bids consist of pair-wise points of power volume and power prices that must follow a merit ascending or descending order. In this way, producers and consumers are able to provide a wider range of offers to hedge against the uncertain electricity prices. In this work, we focus on day-ahead and balancing markets.

D.1.2 Related work

As mentioned before, the integration of heat and power production units complicates the operation of the system requiring suitable tools. Among other techniques, mixed integer linear programming (MILP) has been shown as one well-suited approach to optimize the operation of DH systems. To provide some examples, the authors in [D7] propose a unit commitment model that optimizes the integration of a solar collector in a DH system that includes one fuel boiler and one CHP unit connected to a thermal storage tank. Furthermore, the authors in [D8] work with a DH system that includes several CHP units, fuel boilers, thermal storage as well as a solar thermal plant. The authors propose an optimization model that accounts for the synchronization of the operation of the units providing an extensive analysis of flexibility between units. Finally, the authors in [D9] go a step further by introducing a wind farm in a DH system that can feed both a heat pump and the power grid. To provide flexibility to the system, they also integrate a CHP unit and a thermal storage that increases the complexity of operating the system. All these presented publications have in common that they operate a portfolio of distributed generators and flexible loads.

Apart from the operational planning, planning methods have to consider the bidding in electricity markets. Nowadays, producers often base their offers on the given electricity price forecast, which is very volatile due to the variability of RES production and uncertain one day before the energy is delivered [D10]. Additionally, the production from RES in the DH system itself is uncertain. Consequently, tools that optimize the operation of DH systems and propose bidding strategies need to consider the uncertainty given by price and production. Despite several bidding strategies for price-taker power producers in the day-ahead market have been proposed, (see references in [D11]), the authors in [D6] demonstrate that under high uncertainty of electricity prices the use of stochastic programming [D12] for creating bidding curves for the day-ahead market renders good solutions that consider the uncertainty involved in the bidding process. Based on the representation of the uncertain electricity prices as scenarios, the authors use non-anticipativity constraints that order the bids presented to the market in a step-wise manner to create price dependent bids.

The above mentioned methods consider power production only. Hence, they are not directly applicable for DH operators as the heat production is neglected. The heat production is an important part and a planning method needs to ensure heat demand fulfillment as well as consider the limitations of the production units and storages. Therefore, bidding methods for systems with a connected DH system need to model the heat production as well. For example, the method proposed in [D13] determines the optimal production of a CHP unit. The bid-

ding price is the price forecast, which is the same price used to determined the power production. In [D14] the authors propose a bidding strategy for CHP units that takes into account other heat units to define the heat production costs to determine the bidding price. Finally, the authors in [D15] apply the bidding strategy of [D6] for the day-ahead market using stochastic programming for a DH system that includes one CHP unit, a peak boiler and one heat storage tank.

The so far presented methods focus on the day-ahead market trading only. The consideration of bidding in sequential markets is considered, e.g., in [D16], who created bids using stochastic programming in both day-ahead and intra-day markets for an aggregator combining decentralised RES production and consumption without any connection to DH systems. The presented approach first creates bids for the day-ahead market. After this market is cleared, the already committed power production or consumption in the day-ahead market is used to formulate optimal bids for each intra-day market auction throughout the day. Additionally, the standalone participation of different units in sequential electricity markets (especially day-ahead and balancing markets) has been widely discussed in literature (see for instance these sequence bidding strategies for thermal generators [D17], microgrids [D18], wind farms [D19], hydropower [D20] or CHP units [D21]).

To the best of out knowledge, we see a gap regarding the optimal participation of DH systems in a sequential electricity market structure using a realistic framework that includes bidding strategies. There is a need for a planning method that allows DH operators with a portfolio of units to schedule their production under uncertainty and participate in both day-ahead and balancing markets. In particular, for the case when the DH system contains CHP units, power-to-heat technologies and potentially RES power production, which offer the opportunity to lower the heat production costs by trading on the markets. The consideration of all units as a portfolio hedges against the uncertain RES production and resembles the concept of a VPP power producer. However, the operational planning and bidding method needs to account for the limitations of the heat production with respect to demand and thermal storages. Such a method offers the opportunity to analyze the optimal production behaviour of DH systems in a context with RES production. The contributions of this paper can be summarized as follows:

1. We bridge the above mentioned gap by extending the VPP bidding method of [D6] to a DH setting and including balancing market trading explicitly as second step. The underlying stochastic programs are formulated in a general manner to be applicable to arbitrary sets of production units in DH systems.

2. The method explicitly accounts for the uncertainty coming from RES production in both heat and power and enables us to perform an analysis of the impact of the different uncertainty sources.

3. We use the method to analyze a real case study based on the Hvide Sande district heating system in Denmark allowing us to draw conclusions on a) the behaviour of the system under uncertain RES production; b) the impact of including balancing market trading to the planning method; c) the benefits of including renewable power production to the portfolio; and d) the annual system costs compared to traditional bidding methods based on forecasts.

4. An additional contribution is a new approach to generate scenarios for balancing market price scenarios needed for the stochastic programming addressing the balancing market related operation.

Our study is based on the following assumptions. First, we assume the DH operator is a price-taker, i.e., we do not influence the market price, which is reasonable for small- and medium-size DH systems. Second, we assume that the markets allow the submission of price-dependent bids as it is the case in Nordpool. Third, we do not consider minimum and maximum power volume restrictions in both markets. Fourth, we assume electricity prices and RES production are uncertain when planning the day-ahead bidding. For the balancing bids we consider the RES production known for the next hour. The heat demand is assumed to be known and adjusted to cover the heat losses. The reason we consider heat demand as a known parameter is due to its strong correlation to the ambient temperature and season of the year. Thus, having previous observations, we can obtain very accurate predictability 24 hours ahead [D22]. In addition, if a particular deviation from the predicted heat demand occurs, the DH operator have mechanisms to correct these imbalances such as increasing or decreasing the pressure in the DH network. Finally, we do not consider wind spillage as a recourse variable and therefore, we are responsible for our own imbalances.

The remainder of this paper is organized as follows. In Section D.2 we provide the mathematical formulation that describe the two operational problems for day-ahead and balancing market, respectively. Section D.3 describes the modelling of uncertainty, i.e., the scenario generation for the RES production and electricity prices. Section D.4 describes the bidding strategy. The Hvide Sande case study is described in detail in Section D.5. Section D.6 provides an analysis and discussion of the results obtained for the case study. Finally, Section D.7 summarizes our work and gives an outlook on future work.

D.2 Operational planning model

We start by introducing the two-stage stochastic programs that are the basis for creating bids for the day-ahead and balancing market. The major part of the constraints are valid for both markets and relates to the operation of a portfolio of production units in a district heating system. We start by introducing those constraints. The specific constraints and objectives regarding the two different markets are given in Section D.2.1 and D.2.2 for day-ahead and balancing market, respectively. For an overview of the nomenclature, we refer to Table D.1.

The overall goal is to fulfill the heat demand Q_t^{D} in the district heating network in each period of time $t \in \mathcal{T}$ at lowest cost while taking expected income from bids won on the electricity markets into account. The district heating operator has a set of heat and power production units that are operated as portfolio. We divide the set of units in heat producing units $\mathcal{U}$ and intermittent renewable power-only production units $\mathcal{G}$ (wind power or photo-voltaic). The heat producing units $\mathcal{U}$ are further categorized in combined heat and power plants $\mathcal{U}^{\mathrm{CHP}}$ (producing heat and power simultaneously at a heat-to-power ratio φ_u), heat-only units using electricity $\mathcal{U}^{\mathrm{EL}}$, heat-only units with controllable production based on other fuels $\mathcal{U}^{\mathrm{H}}$ and stochastic heat production units $\mathcal{U}^{\mathrm{RES}}$ (e.g. solar thermal). The stochastic production of both heat and power units are modelled based on a set of scenarios Ω given by the parameters $Q_{u,t,\omega}^{\mathrm{RES}}$ and $P_{g,t,\omega}^{\mathrm{RES}}$, respectively. Each of the heat producing units has a lower and upper limit on the production amount per period given by $\underline{Q}_u$ and $\overline{Q}_u$.

The DH operator further uses thermal storages $\mathcal{S}$ to store heat over several periods. The minimum and maximum level of each storage are denoted by $\underline{S_s}$ and $\overline{S_s}$ where as the initial level is set by S_s^0. The physical connections of the units to the storages and the district heating network are modelled by the binary parameters $A_{u,s}^{\mathrm{S}}$ and A_u^{DH}, respectively (equals 1, if a connections exists and 0, otherwise).

The operational cost for producing one MWh of heat are represented by the coefficients C_u^{H}. A special case is the production of heat based on electricity, i.e., the units $u \in \mathcal{U}^{\mathrm{EL}}$ have additional costs on top of the operational cost based on the electricity needed. We consider a special tariff $C_{g,u}^{\mathrm{T}}$ for producing heat with heat units $u \in \mathcal{U}^{\mathrm{EL}}$ fueled by power produced by our own power generators $g \in \mathcal{G}$. Electricity bought from the grid for units $u \in \mathcal{U}^{\mathrm{EL}}$ is included in the bids to the market. The income from the market is approximated based on the amount of power offered to the market and electricity price scenarios $\lambda_{t,\omega}$.

Table D.1: Nomenclature

Sets	
$\mathcal{T} = \{1, ..., \lvert\mathcal{T}\rvert\}$	Set of time periods t
$\mathcal{U}$	Set of heat production units u
$\mathcal{U}^{\text{CHP}} \subset \mathcal{U}$	Subset of combined heat and power production units
$\mathcal{U}^{\text{H}} \subset \mathcal{U}$	Subset of heat-only production units
$\mathcal{U}^{\text{EL}} \subset \mathcal{U}$	Subset of power to heat production units
$\mathcal{U}^{\text{RES}} \subset \mathcal{U}$	Subset of stochastic heat production units
$\mathcal{G}$	Set of intermittent renewable power-only producers g
$\mathcal{S}$	Set of heat storage tanks s
Ω	Set of scenarios ω
Parameters	
C_u^{H}	Cost for producing heat with unit $u \in \mathcal{U}$ [DKK/MWh-heat]
$C_{g,u}^{\text{T}}$	Tariff cost for producing power with unit $g \in \mathcal{G}$ and use it to produce heat in unit $u \in \mathcal{U}^{\text{EL}}$ [DKK/MWh-heat]
$\overline{Q}_u/\underline{Q}_u$	Maximum/Minimum heat production for unit $u \in \mathcal{U}$ [MWh-heat]
A_u^{DH}	Binary parameter: 1, if unit $u \in \mathcal{U}$ is connected to the district heating system, 0, otherwise
$A_{u,s}^{\text{S}}$	Binary parameter: 1, if unit $u \in \mathcal{U}$ is connected to the thermal storage s, 0, otherwise
φ_u	Heat-to-power ratio for unit $u \in \mathcal{U}^{\text{CHP}}$ [MWh-heat/MWh-el]
S_s^0	Initial level in storage s [MWh-heat]
$\overline{S_s}/\underline{S_s}$	Maximum/Minimum heat level in storage s [MWh-heat]
λ_t	Electricity price for time period $t \in \mathcal{T}$ [DKK/MWh-el]
λ_t^+/λ_t^-	Penalty for positive/negative imbalance in time period $t \in \mathcal{T}$ [DKK/MWh-el]
$\lambda_t^{\text{UP}}/\lambda_t^{\text{DOWN}}$	Upward/Downward regulating price for time period $t \in \mathcal{T}$ [DKK/MWh-el]
Q_t^{D}	Heat demand for time period $t \in \mathcal{T}$ [MWh-heat]
$P_{g,t,\omega}^{\text{RES}}$	Stochastic power production of power-only unit $g \in \mathcal{G}^{\text{RES}}$
$Q_{u,t,\omega}^{\text{RES}}$	Stochastic heat production from heat production unit $u \in \mathcal{U}^{\text{RES}}$
π_ω	Probability of scenario $\omega \in \Omega$
β	Parameter that determines the deviation of the penalty for the positive and negative imbalance
Variables	
$p_{t,\omega}^{\text{BID}} \in \mathbb{R}_0$	Power bid to the day-ahead market unit in period $t \in \mathcal{T}$ [MWh-el]
$q_{u,t,\omega} \in \mathbb{R}_0^+$	Heat production of heat unit $u \in \mathcal{U}$ in period $t \in \mathcal{T}$ [MWh-heat]
$q_{u,t,\omega}^{\text{DH}} \in \mathbb{R}_0^+$	Heat production of unit $u \in \mathcal{U}$ inserted to the grid in period $t \in \mathcal{T}$ [MWh-heat]
$q_{u,s,t,\omega}^{\text{S}} \in \mathbb{R}_0^+$	Heat production of unit $u \in \mathcal{U}$ inserted to the storage s in period $t \in \mathcal{T}$ [MWh-heat]
$p_{u,t,\omega}^{\text{CHP}} \in \mathbb{R}_0^+$	Power production of unit $u \in \mathcal{U}^{\text{CHP}}$ in period $t \in \mathcal{T}$ [MWh-el]
$p_{u,t,\omega}^{\text{GRID}} \in \mathbb{R}_0$	Power obtained from the grid to produce heat with unit $u \in \mathcal{U}^{\text{EL}}$ in period $t \in \mathcal{T}$ [MWh-el]
$p_{g,u,t,\omega}^{\text{HEAT}} \in \mathbb{R}_0^+$	Power production of unit $g \in \mathcal{G}$ that serves heat production of unit $u \in \mathcal{U}^{\text{EL}}$ in period $t \in \mathcal{T}$ [MWh-el]
$p_{g,t,\omega}^{\text{GEN}} \in \mathbb{R}_0^+$	Power generation from unit $g \in \mathcal{G}$ in period $t \in \mathcal{T}$ [MWh-el]
$p_{t,\omega}^{+/-} \in \mathbb{R}_0^+$	Positive/Negative power imbalance purchased/sold in period $t \in \mathcal{T}$ and scenario ω [MWh-el]
$p_{t,\omega}^{\text{UP/DOWN}} \in \mathbb{R}_0^+$	Upward/Downward regulating power purchased/sold in period $t \in \mathcal{T}$ and scenario ω [MWh-el]
$\sigma_{s,t,\omega} \in \mathbb{R}_0^+$	Level in storage s at time period $t \in \mathcal{T}$ [MWh-heat]
$\sigma_{s,t,\omega}^{\text{OUT}} \in \mathbb{R}_0^+$	Heat flowing from the storage s to the district heating in period $t \in \mathcal{T}$ [MWh-heat]

The decisions determined by the model are the production amounts of heat ($q_{u,t,\omega}$) and power ($p^{\text{CHP}}_{u,t,\omega}$) for the dispatchable units as well as the amount of power offered to the electricity market, the latter being the first-stage decisions in our stochastic program. Further variables relate to the storage and feeding to the DH and are described later. All variables and their domains are given in Table D.1.

The following constraints are valid for the production scheduling on both a day-ahead market and balancing market level. The heat production of each unit is limited to the capacities of the unit by constraints (D.1a). In constraints (D.1b) the production of each unit is split in heat used in the district heating network ($q^{\text{DH}}_{u,t,\omega}$) and heat stored in the thermal storage ($q^{\text{S}}_{u,s,t,\omega}$). The possibility of this split is dependent on the existing connections to storages and the district heating network. Flow in non-existent connections is avoided by constraints (D.1c) and (D.1d).

$$\underline{Q}_{u,t} \leq q_{u,t,\omega} \leq \overline{Q_u} \qquad \forall t \in \mathcal{T}, \forall u \in \mathcal{U}, \forall \omega \in \Omega \qquad \text{(D.1a)}$$

$$q_{u,t,\omega} = q^{\text{DH}}_{u,t,\omega} + \sum_{s \in \mathcal{S}} q^{\text{S}}_{u,s,t,\omega} \qquad \forall t \in \mathcal{T}, \forall u \in \mathcal{U}, \forall \omega \in \Omega \qquad \text{(D.1b)}$$

$$q^{\text{DH}}_{u,t,\omega} \leq \overline{Q_u} A^{\text{DH}}_u \qquad \forall t \in \mathcal{T}, \forall u \in \mathcal{U}, \forall \omega \in \Omega \qquad \text{(D.1c)}$$

$$q^{\text{S}}_{u,s,t,\omega} \leq \overline{Q_u} A^{\text{S}}_{u,s} \qquad \forall t \in \mathcal{T}, \forall u \in \mathcal{U}, \forall \omega \in \Omega \qquad \text{(D.1d)}$$

The coupling of heat and power production in CHP units is modelled in constraints (D.1e). Furthermore, the electric boiler production can be based on electricity bought on the market ($p^{\text{GRID}}_{u,t,\omega}$) or from our own power generators ($p^{\text{HEAT}}_{g,u,t,\omega}$) (see constraints (D.1f)). Stochastic renewable heat production from, e.g, solar thermal units, is dependent on the scenario and given as input in constraints (D.1g).

$$q_{u,t,\omega} = \varphi_u p^{\text{CHP}}_{u,t\omega} \qquad \forall t \in \mathcal{T}, \forall u \in \mathcal{U}^{\text{CHP}}, \forall \omega \in \Omega \qquad \text{(D.1e)}$$

$$q_{u,t,\omega} = \varphi_u \big(p^{\text{GRID}}_{u,t,\omega} + \sum_{g \in \mathcal{G}} p^{\text{HEAT}}_{g,u,t,\omega}\big) \qquad \forall t \in \mathcal{T}, \forall u \in \mathcal{U}^{\text{EL}}, \forall \omega \in \Omega \qquad \text{(D.1f)}$$

$$q_{u,t,\omega} = Q^{\text{RES}}_{u,t,\omega} \qquad \forall t \in \mathcal{T}, \forall u \in \mathcal{U}^{\text{RES}}, \forall \omega \in \Omega \qquad \text{(D.1g)}$$

The thermal storage level ($\sigma_{s,t,\omega}$) limitations as well as in- and outflows ($\sigma^{OUT}_{s,t,\omega}$) are modelled in constraints (D.1h) and (D.1i), respectively. At the end of the planning horizon, we impose that the storage level is at least as high as in the beginning of the planning horizon to avoid emptying the storage in every optimization (constraints (D.1j)).

$$\underline{S}_s \leq \sigma_{s,t,\omega} \leq \overline{S}_s \qquad \forall t \in \mathcal{T}, \forall s \in \mathcal{S}, \forall \omega \in \Omega \qquad \text{(D.1h)}$$

$$\sigma_{s,t,\omega} = \sigma_{s,t-1,\omega} + \sum_{u \in \mathcal{U}} q^{\text{S}}_{u,s,t,\omega} - \sigma^{\text{OUT}}_{s,t,\omega} \qquad \forall t \in \mathcal{T}, \forall s \in \mathcal{S}, \forall \omega \in \Omega \qquad \text{(D.1i)}$$

$$\sigma_{s,|\mathcal{T}|,\omega} \geq S_s^0 \qquad \forall s \in \mathcal{S}, \forall \omega \in \Omega \tag{D.1j}$$

The heat demand in the network in each period is ensured by constraints (D.1k) by using either heat directly from the units or from the storage.

$$Q_t^{\mathrm{D}} = \sum_{u \in \mathcal{U}} q_{u,t,\omega}^{\mathrm{DH}} + \sum_{s \in \mathcal{S}} s_{s,t,\omega}^{\mathrm{OUT}} \qquad \forall t \in \mathcal{T}, \forall \omega \in \Omega \tag{D.1k}$$

The renewable power production from the stochastic power generators is modelled in constraints (D.1l) depending on the scenario. The power can be used either to produce heat with the electric boiler ($p_{g,u,t,\omega}^{\mathrm{HEAT}}$) or sold on the market ($p_{g,t,\omega}^{\mathrm{GEN}}$).

$$p_{g,t,\omega}^{\mathrm{GEN}} + \sum_{u \in \mathcal{U}^{\mathrm{EL}}} p_{g,u,t,\omega}^{\mathrm{HEAT}} = P_{g,t,\omega}^{\mathrm{RES}} \qquad \forall t \in \mathcal{T}, \forall g \in \mathcal{G}, \forall \omega \in \Omega \tag{D.1l}$$

Based on this initial set of constraints, the model is extended for day-ahead or balancing market optimization in the succeeding sections.

D.2.1 Optimization for the day-ahead market

The first-stage variables (here-and-now decisions) for the day-ahead market production scheduling are the power bids $p_{t,\omega}^{\mathrm{BID}}$ for each hour of the next day $t \in \{1, \ldots, 24\}$. As these are dependent on the production of all other dispatchable units, we determine the heat ($q_{u,t,\omega}$) and power production ($p_{u,t,\omega}$) of all units as well as the power bid amounts for the remaining planning horizon ($p_{u,t,\omega}^{\mathrm{BID}} \forall t \in \{25, \ldots, |\mathcal{T}|\}$) as second stage variables.

The objective function (D.2a) minimizes the expected cost of producing heat by all units minus the expected income for the day-ahead electricity market. Deviations from the day-ahead market bid are penalized by paying the imbalances ($p_{t,\omega}^{+}, p_{t,\omega}^{-}$) at the balancing stage.

$$\begin{aligned} \min \sum_{t \in \mathcal{T}} \sum_{\omega \in \Omega} \pi_\omega \Bigg[& \sum_{u \in \mathcal{U}^{\mathrm{CHP}}} C_u^{\mathrm{H}} q_{u,t,\omega} + \sum_{u \in \mathcal{U}^{\mathrm{H}}} C_u^{\mathrm{H}} q_{u,t,\omega} + \sum_{u \in \mathcal{U}^{\mathrm{EL}}} C_u^{\mathrm{H}} p_{u,t,\omega}^{\mathrm{GRID}} \\ & + \sum_{g \in \mathcal{G}} \sum_{u \in \mathcal{U}^{\mathrm{EL}}} C_{g,u}^{T} p_{g,u,t,\omega}^{\mathrm{HEAT}} - \left(\lambda_{t,\omega} p_{t,\omega}^{\mathrm{BID}} - \lambda_t^{+} p_{t,\omega}^{+} + \lambda_t^{-} p_{t,\omega}^{-} \right) \Bigg] \end{aligned} \tag{D.2a}$$

The bidding amount $p_{t,\omega}^{\mathrm{BID}}$ is dependent on the power production from CHP units and the generator as well as the power used for the electric boiler (see

constraints (D.2b)). Any deviations from the bidding amount are captured in the variables $p^{+}_{t,\omega}$ and $p^{-}_{t,\omega}$ to be penalized in the objective function.

$$p^{\mathrm{BID}}_{t,\omega} = \sum_{u \in \mathcal{U}^{\mathrm{CHP}}} p^{\mathrm{CHP}}_{u,t,\omega} + \sum_{g \in \mathcal{G}} p^{\mathrm{GEN}}_{g,t,\omega} - \sum_{u \in \mathcal{U}^{\mathrm{EL}}} p^{\mathrm{GRID}}_{u,t,\omega} + p^{+}_{t,\omega} - p^{-}_{t,\omega} \qquad \forall t \in \mathcal{T}, \forall \omega \in \Omega \tag{D.2b}$$

The equations (D.2c) are based on the method in [D6] and ensure that only one bidding curve, i.e., one set of power amount and price pairs, is created per time period t while constraints (D.2d) ensure that the bidding curves are non-decreasing for all time steps $t \in \mathcal{T}$.

$$p^{\mathrm{BID}}_{t,\omega} = p^{\mathrm{BID}}_{t,\omega'} \qquad \forall t \in \mathcal{T}, \forall (\omega, \omega') \in \Omega \qquad : \lambda_{t,\omega} = \lambda_{t,\omega'} \tag{D.2c}$$

$$p^{\mathrm{BID}}_{t,\omega} \leq p^{\mathrm{BID}}_{t,\omega'} \qquad \forall t \in \mathcal{T}, \forall (\omega, \omega') \in \Omega \qquad : \lambda_{t,\omega} \leq \lambda_{t,\omega'} \tag{D.2d}$$

The operational model to optimize the production for the day-ahead market bidding can be summarized as follows in (D.3a) to (D.3c).

$$\min \quad \text{(D.2a)} \tag{D.3a}$$

$$\text{s.t} \quad \text{(D.1a)} - \text{(D.1l)} \tag{D.3b}$$

$$\text{(D.2b)} - \text{(D.2d)} \tag{D.3c}$$

To avoid speculation in the operation of the system, we define the penalty costs for deviation as follows.

$$\lambda^{+}_{t,\omega} = \begin{cases} \lambda_{t,\omega} + \beta \cdot \lambda_{t,\omega} & \text{if } \lambda_{t,\omega} \geq 0 \\ \lambda_{t,\omega} - \beta \cdot \lambda_{t,\omega} & \text{if } \lambda_{t,\omega} < 0 \end{cases}; \quad \lambda^{-}_{t,\omega} = \begin{cases} \lambda_{t,\omega} - \beta \cdot \lambda_{t,\omega} & \text{if } \lambda_{t,\omega} \geq 0 \\ \lambda_{t,\omega} + \beta \cdot \lambda_{t,\omega} & \text{if } \lambda_{t,\omega} < 0 \end{cases}$$

where β is a parameter with value greater than 0. Thus, we ensure that the penalty to pay would be higher than the day-ahead prices in case of positive deviation. On the contrary, in case of producing more power than sold in the day-ahead market, the profits for selling that excess power on the balancing market are always lower than selling that energy in the day-ahead market. Therefore, the model tries to sell the right amount of power on the day-ahead market and avoid imbalances.

D.2.2 Optimization for the balancing market

The balancing market problem is solved once per hour and like in the day-ahead problem (D.3a)-(D.3c), we generate non-decreasing bidding curves using the stochastic formulation of the problem. In this case, the first-stage decisions are the upward ($p^{\mathrm{UP}}_{t,\omega}$) and downward ($p^{\mathrm{DOWN}}_{t,\omega}$) regulation offered to formulate

the bidding curves for the balancing market. The remaining variables can be adapted to the realization of the uncertainty and considered as second-stage decisions. In this formulation of the balancing problem, the committed power production or consumption for the day-ahead is given as a parameter ($\widehat{p}^{\mathrm{BID}}_{t,\omega}$). Due to the high unpredictability of the balancing prices we use $\mathcal{T}^{\mathrm{B}}$ periods as the planning horizon for the balancing problem, which can be shorter than the horizon used in the day-ahead problem. Upward regulation ($p^{\mathrm{UP}}_{t,\omega}$) is provided in case there is a need for more power in the system, therefore the producer has the opportunity to sell additional power at the upward regulating price ($\lambda^{\mathrm{UP}}_{t,\omega}$). On the contrary, if the systems has excess of production, the TSO activates offers for downward regulation, where producers can consume power ($p^{\mathrm{DOWN}}_{t,\omega}$) at the downward regulating price ($\lambda^{\mathrm{DOWN}}_{t,\omega}$).

The objective function (D.4a) for the balancing problem again minimizes the cost considering income from the market and penalties for imbalances.

$$\min \sum_{t\in\mathcal{T}^{\mathrm{B}}}\sum_{\omega\in\Omega}\pi_{\omega}\Bigg[\sum_{u\in\mathcal{U}^{\mathrm{CHP}}} C^{\mathrm{H}}_{u} q_{u,t,\omega} + \sum_{u\in\mathcal{U}^{\mathrm{H}}} C^{\mathrm{H}}_{u} q_{u,t,\omega} + \sum_{u\in\mathcal{U}^{\mathrm{EL}}} C^{\mathrm{H}}_{u} p^{\mathrm{GRID}}_{u,t,\omega} \tag{D.4a}$$
$$+\sum_{g\in\mathcal{G}}\sum_{u\in\mathcal{U}^{\mathrm{EL}}} C^{T}_{g,u} p^{\mathrm{HEAT}}_{g,u,t,\omega} - \left(\lambda^{-}_{t} p^{-}_{t,\omega} - \lambda^{+}_{t} p^{+}_{t,\omega} + \lambda^{\mathrm{UP}}_{t,\omega} p^{\mathrm{UP}}_{t,\omega} - \lambda^{\mathrm{DOWN}}_{t,\omega} p^{\mathrm{DOWN}}_{t,\omega}\right)\Bigg]$$

The balance in the power production is ensured in equations (D.4b). Here the power committed on the day-ahead market is given as a parameter ($\widehat{p}^{\mathrm{BID}}_{t,\omega}$). To balance the production with the bidding amount, constraint (D.4b) can either use the variables determining the upward ($p^{\mathrm{UP}}_{t,\omega}$) or downward regulation ($p^{\mathrm{DOWN}}_{t,\omega}$) amounts or pay imbalances. The imbalances are captured in $p^{+}_{t,\omega}$ and $p^{-}_{t,\omega}$.

$$\widehat{p}^{\mathrm{BID}}_{t,\omega} = \sum_{u\in\mathcal{U}^{\mathrm{CHP}}} p^{\mathrm{CHP}}_{u,t,\omega} + \sum_{g\in\mathcal{G}} p^{\mathrm{GEN}}_{g,t,\omega} - \sum_{u\in\mathcal{U}^{\mathrm{EL}}} p^{\mathrm{GRID}}_{u,t,\omega} + p^{+}_{t,\omega} - p^{-}_{t,\omega} - p^{\mathrm{UP}}_{t,\omega} + p^{\mathrm{DOWN}}_{t,\omega}$$
$$\forall t \in \mathcal{T}^{\mathrm{B}}, \forall \omega \in \Omega \tag{D.4b}$$

To ensure ordered bidding curves in the balancing market, we define constraints (D.4c) and (D.4d) analogously to the day-ahead market problem. Here the offers for upward regulation and downward regulation, present a non-decreasing and non-increasing order, respectively.

$$p^{\mathrm{UP}}_{t,\omega} \le p^{\mathrm{UP}}_{t,\omega'} \qquad \forall t \in \mathcal{T}^{\mathrm{B}}, \forall(\omega,\omega') \in \Omega \qquad : \lambda^{\mathrm{UP}}_{t,\omega} \le \lambda^{\mathrm{UP}}_{t,\omega'} \tag{D.4c}$$
$$p^{\mathrm{DOWN}}_{t,\omega} \ge p^{\mathrm{DOWN}}_{t,\omega'} \qquad \forall t \in \mathcal{T}^{\mathrm{B}}, \forall(\omega,\omega') \in \Omega \qquad : \lambda^{\mathrm{DOWN}}_{t,\omega} \le \lambda^{\mathrm{DOWN}}_{t,\omega'} \tag{D.4d}$$

The formulation for the balancing market problem is given by (D.5a)-(D.5c).

$$\min \quad \text{(D.4b)} \tag{D.5a}$$
$$\text{s.t} \quad \text{(D.1a)} - \text{(D.1l)} \tag{D.5b}$$
$$\text{(D.4b)} - \text{(D.4d)} \tag{D.5c}$$

Furthermore, as in the day-ahead problem, we need to prohibit speculation of the system by defining the penalty prices $\lambda^{+}_{t,\omega}$ and $\lambda^{-}_{t,\omega}$ as follows.

$$\lambda^{+}_{t,\omega} = \begin{cases} \lambda_{t,\omega} + \beta \cdot \lambda_{t,\omega} & \text{if } \lambda_{t,\omega} \geq 0, p^{\text{UP}}_{t,\omega} = 0 \\ \lambda_{t,\omega} - \beta \cdot \lambda_{t,\omega} & \text{if } \lambda_{t,\omega} < 0, p^{\text{UP}}_{t,\omega} = 0 \\ \lambda^{\text{UP}}_{t,\omega} + \beta \cdot \lambda^{\text{UP}}_{t,\omega} & \text{if } \lambda_{t,\omega} \geq 0, p^{\text{UP}}_{t,\omega} \geq 0 \\ \lambda^{\text{UP}}_{t,\omega} - \beta \cdot \lambda^{\text{UP}}_{t,\omega} & \text{if } \lambda_{t,\omega} < 0, p^{\text{UP}}_{t,\omega} \geq 0 \end{cases};$$

$$\lambda^{-}_{t,\omega} = \begin{cases} \lambda_{t,\omega} - \beta \cdot \lambda_{t,\omega} & \text{if } \lambda_{t,\omega} \geq 0, p^{\text{DOWN}}_{t,\omega} = 0 \\ \lambda_{t,\omega} + \beta \cdot \lambda_{t,\omega} & \text{if } \lambda_{t,\omega} < 0, p^{\text{DOWN}}_{t,\omega} = 0 \\ \lambda^{\text{DOWN}}_{t,\omega} - \beta \cdot \lambda^{\text{DOWN}}_{t,\omega} & \text{if } \lambda_{t,\omega} \geq 0, p^{\text{DOWN}}_{t,\omega} \geq 0 \\ \lambda^{\text{DOWN}}_{t,\omega} + \beta \cdot \lambda^{\text{DOWN}}_{t,\omega} & \text{if } \lambda_{t,\omega} < 0, p^{\text{DOWN}}_{t,\omega} \geq 0 \end{cases}$$

D.3 Modeling Uncertainty

In particular the day-ahead market optimization includes uncertainty with respect to the production of the stochastic production units (wind power and solar thermal). But both planning problems also have to consider that the electricity prices are still unknown at the time of planning. To account for these uncertainties, we include them as scenarios to our two-stage stochastic programs. The remainder of this section describes the forecasting and scenario generation process.

D.3.1 Wind power production forecast

For an easy replicability of our experiments, we use a wind forecast based on local linear regressions of the wind power curve [D23]. As Figure D.1a shows, the power curve is divided into intervals with equal distribution based on the normalized wind speed. For each interval, a linear regression is fitted to the data using a least squares estimate. The linear regressions are later integrated into one single function. From this aggregated function, we can predict the wind power production using the wind speed forecast as depicted in Figure D.1b.

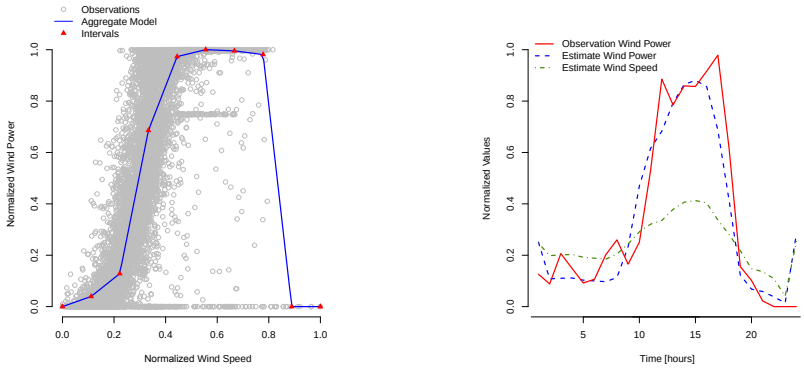

(a) Wind power curve using real data for one year power production and wind speed in NordPool DK1

(b) Wind power predictions for one day receding horizon and the normalized wind speed

Figure D.1: Wind power prediction process

D.3.2 Solar Thermal Forecast

The appropriate function to predict solar thermal forecast depends on the technology used in the solar collectors. In this work, we consider flat thermal solar collectors with a fixed inclination angle and orientated towards maximizing the solar radiation during the summer season. The forecasting technique used here is presented in [D24] and given in (D.6).

$$Q_t = A^{\mathrm{S}}\left[I_t^{\mathrm{D}}\gamma - \eta_1\left(T_t^{\mathrm{AVG}} - T_t^{\mathrm{AMB}}\right) - \eta_2\left(T_t^{\mathrm{AVG}} - T_t^{\mathrm{AMB}}\right)^2\right] \ \forall t \in \mathcal{T} \qquad \text{(D.6)}$$

where Q_t is the heat production at time t, A^{S} is the area of the entire solar thermal field and I_t^{D} is the solar radiation (including direct and diffusive) that heats the solar collectors for time period t. T_t^{AVG} and T_t^{AMB} are the average temperature inside the solar collector and the outside temperature, respectively. The remaining parameters (γ,η_1,η_2) are the coefficients of the equations. The average temperature (T_t^{AVG}) is defined as the average between the cold water entering and the hot water leaving the solar collector. For the sake of simplicity, we consider this temperature as constant $\forall t \in \mathcal{T}$.

D.3.3 Day-ahead electricity price forecast

Electricity prices in day-ahead markets present an autocorrelation and seasonal variation that usually can be detect using time series models. For this work,

the electricity price forecast is obtained using a SARMAX model with a daily seasonality pattern that has been successfully applied to predict electricity prices [D25]. In addition, an exogenous variable based on Fourier series is used to describe the weekly seasonality [D26]. This results in the following model (D.7a).

$$\lambda_t = \mu + \phi_1\lambda_{t-1} + \phi_2\lambda_{t-2} + \phi_{24}\lambda_{t-24} + \theta_1\varepsilon_{t-1} + \theta_2\varepsilon_{t-2} + \theta_{24}\varepsilon_{t-24} + X \tag{D.7a}$$

The estimated electricity price (λ_t) for time period t is calculated by the linear combination of the intercept μ, the autoregressive (AR) terms λ_{t-1}, λ_{t-2} and λ_{t-24} and the moving average (MA) terms ε_{t-1}, ε_{t-2} and ε_{t-24} for 1, 2 and 24 hours prior to time period t. The forecast parameters ϕ_1, ϕ_2, ϕ_{24}, θ_1, θ_2 and θ_{24} are updated on a daily basis. The exogenous variable X allows to integrate external variables into the model, in our case the Fourier series describing the weekly seasonality of the data (D.7b).

$$X = \sum_{k=1}^{K} \alpha_k \sin\left(\frac{2\pi kt}{T}\right) + \sum_{k=1}^{K} \beta_k \cos\left(\frac{2\pi kt}{T}\right) \tag{D.7b}$$

where K determines the number of Fourier terms considered (chosen by minimizing the AICc value). The parameter T represents the seasonality period in the series, in our case we consider a weekly seasonality of $T = 168$. Finally, α_t and β_t represent the forecast parameters for the weekly seasonality, and like the forecast parameters for the AR and MA terms, both are updated on a daily basis.

D.3.4 Scenario generation for RES production and day-ahead market prices

The forecasts for the three previously mentioned data sets are based on probabilistic forecasts. Therefore, we generate scenarios using a Monte-Carlo simulation applying a multivariate Gaussian distribution with zero mean that describes the stochastic process, which we consider as stationary, in our predictions. We use the algorithm presented in [D27] to initialize the scenario generation process and randomly generate the error terms. The algorithm is repeated for each time period in the receding horizon and for all scenarios. In our case, we generate a random walk for the time horizon using normalized white noise that we iteratively add to the predicted value resulting in one scenario.

To get a representative set of scenarios, we generate a large amount of equiprobable scenarios. Those are reduced to the desired number by applying the clustering technique *partition around medoids* (PAM) [D28]. Each medoid scenario

is a scenario in our model, while the probability is obtained by the sum of the scenarios attached to the medoid.

D.3.5 Scenario generation for balancing prices

The generation of scenarios for balancing prices is less intuitive compared to the day-ahead market prices described before. In particular, because there is not always a need for upward or downward regulation, and if there is, the regulating prices are defined as a function of the imbalanced power volume which makes these prices very hard to predict. The method proposed in [D29] is widely used in literature to create balancing price forecasts. The authors develop a model that combines a SARIMA to predict the amount of upward and downward regulating prices in combination with a discrete Markov model representing the discontinuous variability in the activation of upward and downward regulation. This variability is represented through a matrix that indicates the transition probability between states. Using this techniques, scenarios can be generated by sampling the error term in the time series models and creating different sequences for the Markov model.

In this section, we propose a novel approach to generate balancing prices scenarios. Our motivation to use a different new scenario generation technique for real-time balancing prices is due to the fact that the authors in [D29] apply their method in a specific bidding area where prices follow a regular shape and pattern that can be accurately predicted, i.e., regions with low integration of RES. In systems with a high penetration of RES (especially wind power), large imbalances can occur in a very short time and thereby affect the balancing prices, which respond to the volume of the imbalance. Due to this variability, balancing prices do not necessarily follow a trend that can be easily predicted using time series models. Furthermore, the method proposed by [D29] models the probability of imbalance states and does not consider the specific duration of these states. We think that this duration must be taken into account since the upward and downward regulation prices are affected by this duration.

Our approach is based on the algorithm to create unit availability scenarios presented in [D27]. Initially, the following methodology is applied for upward and downward regulation separately. The results are combined in a final step. The generation of the final predicted prices is carried out based on sampling the deviation compared to the day-ahead price (in %).

The first step is to gather previous observations from the balancing market to determine the experimental distribution of the duration (time elapsed) in between two upward regulation periods or downward regulation periods, respectively,

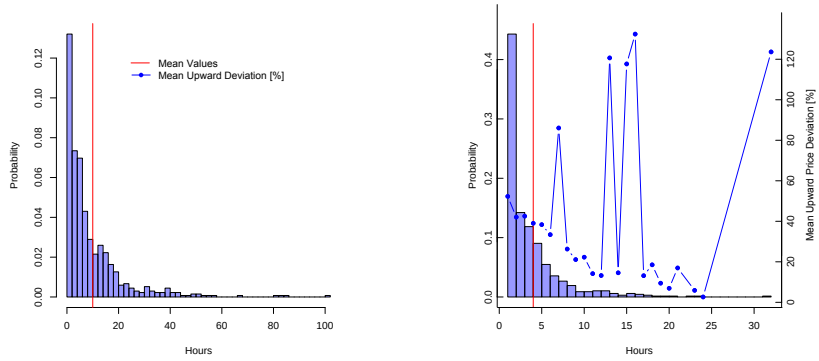

(a) Time elapsed between upward regulation periods

(b) Duration of upward regulation and price deviation

Figure D.2: Distributions of elapsed time between and duration of upward regulation as well as average regulating prices for year 2017 in the NordPool bidding area DK1

and the corresponding mean values $\tau^{\mathrm{T}+}$ and $\tau^{\mathrm{T}-}$. An example for upward regulation is given in Figure D.2a, where the red line represents the mean value. In addition, the distribution of the actual duration for each upward and downward regulation period is also obtained (see Figure D.2b for upward regulation) along with the mean duration $\tau^{\mathrm{D}+}$ and $\tau^{\mathrm{D}-}$. At the same time, the observed deviations between day-ahead and balancing market prices are averaged for each duration of regulation (see function in Figure D.2b). By connecting those mean duration values, we get the functions $f^{+}(x)$ and $f^{-}(x)$ telling us for each duration of regulation the deviation from the day-ahead market price for upward and downward regulation prices, respectively.

Once the experimental distribution and values for $\tau^{\mathrm{T}+}$, $\tau^{\mathrm{T}-}$, $\tau^{\mathrm{D}+}$, $\tau^{\mathrm{D}-}$, $f^{+}(\tau^{\mathrm{D}+})$ and $f^{-}(\tau^{\mathrm{D}-})$ are obtained, the scenario generation is started. As in [D27], we assume that $\tau^{\mathrm{T}+}$, $\tau^{\mathrm{T}-}$, $\tau^{\mathrm{D}+}$ and $\tau^{\mathrm{D}-}$ can be characterized as random variables that follow an exponential distribution, which is a reasonable assumption confirmed by the observations shown in Figure D.2. Therefore, random samples of these values can be obtained by applying equations (D.8), where u_1 and u_2 are uniformly distributed variables between 0 and 1.

$$\tau_{\omega}^{\mathrm{T}(+/-)} = -\tau^{\mathrm{T}(+/-)} \cdot \ln(u_1); \qquad \tau_{\omega}^{\mathrm{D}(+/-)} = -\tau^{\mathrm{D}(+/-)} \cdot \ln(u_2) \tag{D.8}$$

The algorithm to generate $|\Omega|$ with a time horizon of $|\mathcal{T}|$ periods is summarized in Algorithm 5 and works as follows. For each scenario we move through the forecasting horizon starting at period 1. The time to the next regulation period

Algorithm 5 Generate balancing price scenarios

1: **for** each $\omega \in \Omega$ **do**
2: $t \leftarrow 1$
3: **while** $t \leq |\mathcal{T}|$ **do**
4: $\tau_{\omega}^{\mathrm{T}(+/-)}$=-$\tau^{\mathrm{T}(+/-)} \cdot \ln(u_1)$ where $u_1 \sim \mathcal{U}(0,1)$ is random
5: $\tau_{\omega}^{\mathrm{D}(+/-)}$=-$\tau^{\mathrm{D}(+/-)} \cdot \ln(u_2)$ where $u_2 \sim \mathcal{U}(0,1)$ is random
6: $t^{\mathrm{Start}} \leftarrow \min\{|\mathcal{T}|, round(t + \tau_{\omega}^{\mathrm{T}(+/-)})\}$
7: $t^{\mathrm{End}} \leftarrow \min\{|\mathcal{T}|, round(t + \tau_{\omega}^{\mathrm{T}(+/-)} + \tau_{\omega}^{\mathrm{D}(+/-)})\}$
8: **for** $t' = t$ to t^{Start} **do**
9: $\Delta\lambda_{t',\omega}^{(\mathrm{UP/DOWN})} = 0$
10: **end for**
11: **for** $t' = t^{\mathrm{Start}} + 1$ to t^{End} **do**
12: $\Delta\lambda_{t',\omega}^{(\mathrm{UP/DOWN})} = f^{(+/-)}(\tau^{\mathrm{D}(+/-)}) + \varepsilon_{t'}^{(+/-)}$ where $\varepsilon_{t'}^{(+/-)} \sim \mathcal{N}(\mu, \sigma^2)$ is random
13: **end for**
14: $t \leftarrow t^{\mathrm{End}} + 1$
15: **end while**
16: **end for**
17: Return $\Delta\lambda_{t,\omega}^{(+/-)}$

$\tau_{\omega}^{\mathrm{T}(+/-)}$ and the duration of this period $\tau_{\omega}^{\mathrm{D}(+/-)}$ are sampled based on equations (D.8), respectively (lines 4-5). Based on our current time t and the time to the next period, we can calculate the beginning of the next regulation period t^{Start} (line 6). The deviations up until t^{Start} are set to zero (lines 8-10). Starting from period t^{Start} for $\tau_{\omega}^{\mathrm{D}(+/-)}$ periods up to t^{End}, the deviations are set based on the average function $f^{(+/-)}$ and a random error term ϵ (lines 11-13). Next the current time is updated to the t^{End} (line 14). In this way, we move through the time horizon until we reach the end $|\mathcal{T}|$. The process is repeated for each scenario and once for upward and once for downward regulation scenarios.

Since upward and downward regulation can not be activate at the same time, we calculate the final deviation scenario matrix as $\Delta\lambda_{t,\omega} = \Delta\lambda_{t,\omega}^{\mathrm{UP}} - \Delta\lambda_{t,\omega}^{\mathrm{DOWN}}$, where positive values of $\Delta\lambda_{t,\omega}$ represent upward regulation and the negative values downward regulation, respectively. Figure D.3a shows a set of balancing prices scenarios generated by Algorithm 5 compared to the real observations. In comparison to scenarios generated by the method in D.3b, we can see the increased variability of regulating prices in the scenarios generated by Algorithm 5. This is due to the fact that the prices are not based on time-series forecasts like in D.3b but on the observed duration for upward and downward regulation periods. To obtain the final prices the deviation value $\Delta\lambda_{t,\omega}$ is multiplied with respective day-ahead market price.

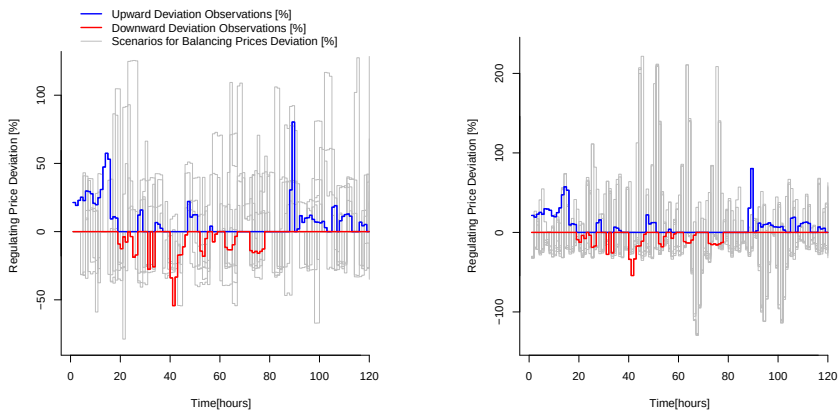

(a) 10 scenarios generated by Algorithm 5.

(b) 10 scenarios generated by the method proposed in [D29].

Figure D.3: Scenarios for balancing prices

D.4 Operational scheduling and bidding method

The overall method, which allows the DH operator to schedule the production and determine the bidding curves for the day-ahead and balancing market, uses the two models presented in Section D.2 with the scenarios generated by the methods in Section D.3. The optimization for one day in practice includes the following steps.

The day before the day in question, the *day-ahead market optimization* (D.3a)-(D.3c) is solved as two-stage stochastic programming. The model includes scenarios representing the uncertainty regarding day-ahead market electricity prices (Section D.3.3), wind power production (Section D.3.1) and solar heat production (Section D.3.2) for at least 24 hours. The scenarios are generated using the Monte Carlo simulation and clustering technique described in Section D.3.4. The planning horizon can be considered as longer than 24 hours in a rolling horizon manner to include future days into the optimization to get better approximation of the thermal storage behaviour, which can store heat longer than just 24 hours. The optimal values of the variables $p^{\mathrm{BID}}_{t,\omega}$ in (D.3a)-(D.3c) return the bidding amounts for each hour $t \in \{1, \ldots, 24\}$, while each scenario ω sets one step in the bidding curve. As constraints (D.2c) and (D.2d) ensure the same production amounts for the same electricity prices and increasing production amounts for increasing prices, the optimal values $p^{\mathrm{BID}}_{t,\omega}$ result automatically in a non-decreasing step-wise bidding curve. The bidding prices for each step in the

bidding curve are the respective electricity price forecast values $\lambda_{t,\omega}$.

After the day-ahead market is cleared, the real electricity prices for each hour become available and the won bids can be determined (i.e. the hours where the bidding price was equal or below the market price). In hours with won bids, the DH operator is committed to provide the offered amount of power, otherwise the caused imbalance is penalized with a payment. However, imbalances from other operators on the market offer an opportunity for profit. The balancing market is used by the TSO to reduce the imbalances in the system by accepting new bids for additional power or reducing production. Thus, we can use the flexibility in our portfolio of production units to also offer upward and downward regulations bids in the balancing market. As the *balancing market* has a time horizon of only one hour and is closed shortly before this hour, an optimization needs to take place every hour before the balancing market closes. Model (D.5a) to (D.5c) optimizes the production for the next hour taking the committed production from the day-ahead market into account. Furthermore, the model can take several hours into the future into account to anticipate impact on the remaining hours of the day. The model is again a two-stage stochastic program considering the balancing market price scenarios (see Section D.3.5) for all hours and wind power scenarios for later on the day (we assume that the wind power for the next hour can be predicted accurately). Again, the optimal values of $p^{\mathrm{UP}}_{t,\omega}$ and $p^{\mathrm{DOWN}}_{t,\omega}$ result automatically in a non-decreasing or non-increasing step-wise bidding curves representing upward and downward regulation bids, respectively. The bidding prices for each step in the bidding curve are the respective electricity price forecast values $\lambda^{\mathrm{UP}}_{t,\omega}$ and $\lambda^{\mathrm{DOWN}}_{t,\omega}$. This step is repeated by the operator for each hour.

D.5 Case study

We use the Hvide Sande district heating system[3] in Western Jutland, Denmark, as a case study to evaluate our method. However, the method presented in this paper is applicable to all district heating systems with a portfolio of units, because the models in Section D.2 are formulated in a general manner and the scenario generation methods D.3 can be replaced by other available forecasting techniques without changing the overall methodology.

An overview of the Hvide Sande system is given in Figure D.4. It has two small gas-fired CHP units (CHP1 and CHP2) acting on the electricity market and feeding heat to the district heating system as well as two gas boilers (GB1 and

[3]see Hvide Sande Fjernvarme A.m.b.A., https://www.hsfv.dk/

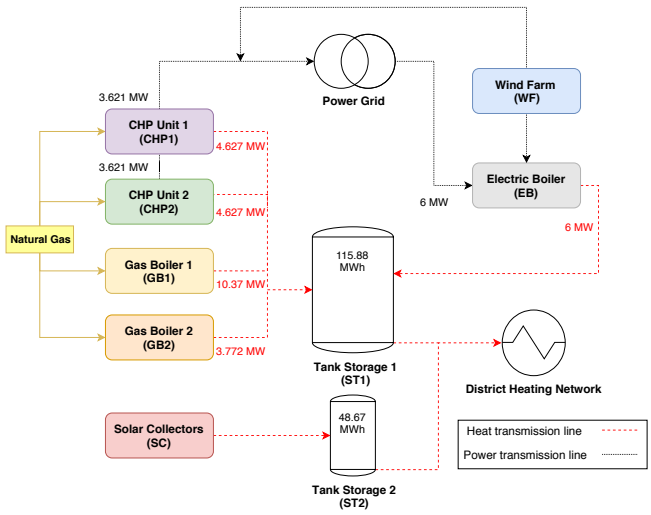

Figure D.4: Flowchart of the Hvide Sande district heating system

GB2) units with dispatchable heat production. Stochastic renewable heat production comes from a solar collector field (SC), which is considered as one unit. Finally, it is also possible to produce heat from electricity using an electric boiler (EB). The electricity can be bought from the power grid as a regular consumer or using a special tariff. This tariff consists of a tax benefit for operating the electric boiler, in which the amount of power injected by the own wind farm (WF) into the grid is at the same time consumed by the electric boiler. This synchronous operation of both units help the power system to reduce imbalances and provides cheap heat production. The DH system has two thermal storages, where one (ST1) is connected only to the solar collector field and the second storage (ST2) is used by all other units. The parameters for costs and capacities as well as the connections between units are given in Table D.2. Furthermore, the table shows to which set the units belong.

D.6 Analysis of experimental results

To evaluate our approach, we have to determine the real costs and behaviour of the system. The actual wind power production, solar thermal production and heat demand values are obtained from the Hvide Sande district heating system for the year 2017. The day-ahead, upward and downward electricity prices are taken from the NordPool market for the bidding area DK1 (where Hvide Sande is located). This data is public and can be downloaded from [D30].

Table D.2: Characteristics of the production units and thermal storages

Unit	Set	C_u^H	C_u^T	$\overline{Q}_u$	$\overline{P}_u$	φ_u	A_u^{DH}	$A_{u,s}^{\mathrm{S}}$	
								ST1	ST2
CHP1	$\mathcal{U}^{\mathrm{CHP}}$	689.01	-	4.63	3.62	1.28	0	1	0
CHP2	$\mathcal{U}^{\mathrm{CHP}}$	689.01	-	4.63	3.62	1.28	0	1	0
GB1	$\mathcal{U}^{\mathrm{H}}$	401.30	-	10.37	0.00	-	0	1	0
GB2	$\mathcal{U}^{\mathrm{H}}$	416.29	-	3.77	0.00	-	0	1	0
EB	$\mathcal{U}^{EL}$	359.98	49.52	6.00	0.00	1.00	0	1	0
SC	$\mathcal{U}^{\mathrm{RES}}$	0.00	-	100.00	0.00	-	0	0	1
WF	$\mathcal{G}$	0.00	-	0.00	0.00	-	-	-	-
		$\overline{S}$	$\underline{S}$	σ_0					
ST1	$\mathcal{S}$	115.88	0.00	57.94					
ST2	$\mathcal{S}$	48.67	0.00	24.34					

The data basis for forecasting and scenario generation is historical data from 15 days before the day in question. The input data for wind speed, solar radiation and ambient temperature are randomly perturbed values of the real data. The overall evaluation process includes the following steps:

1. Before day-ahead market closure for day d (Day $d-1$): Create scenarios for the day-ahead market optimization and solve optimization model (D.3a)-(D.3c) using thermal storage level from the day before. Submit bids to the day-ahead market.
2. After day-ahead market closure for day d (Day $d-1$): Evaluate the day-market bids with the now known electricity prices and save production amounts of won bids.
3. Each hour on day d:
   (a) Before the closure of the balancing market at hour t on day d: Create scenarios for the balancing market optimization, include the committed power production amounts from the day-ahead market and solve optimization model (D.5a)-(D.5c).
   (b) Evaluate the balancing-market bids with the now known balancing electricity prices, fix the committed production amounts and resolve the model to get actual costs and thermal storage levels.
4. Move to the next day

The forecasting and scenario generation are implemented in R 3.2.2, while the optimization models are built in GAMS 24.9.2 using CPLEX 12.1.1 to solve

them. All experiments were executed on the DTU HPC Cluster using 2xIntel Xeon Processor X5550 and 24 GB memory RAM. For the results presented in the remainder of this section, we use a rolling horizon of three days in the day-ahead optimization problem and 12 hours for the balancing market problem. To correlate different scenarios of RES with electricity prices, we generate n different scenarios for wind power and solar heat production and m scenarios for electricity prices. The combination of all scenarios results in a total number of $m \times n$ scenarios. For the sake of simplicity we generate $n = 10$ scenarios of RES production for the experiments that consider bidding curves.

D.6.1 Influence of uncertainty and number of bidding curve steps on the day-ahead market results

In the first experiment, we concentrate on the bidding results from the day-ahead market optimization problem (D.3a)-(D.3c) only. We compare the total annual costs of different setups regarding uncertainty consideration, i.e., which values are known or unknown, and the number of electricity price scenarios resulting in the steps for the bidding curves. The results are given in Figure D.5, where the x-axis represents the number of steps in the bidding curve (i.e. the number of electricity price scenarios) and the y-axis represents the total annual system costs. The depicted lines show the results of different setups regarding uncertainty consideration. The theoretically best result is given by considering that we have perfect knowledge about the future electricity prices and RES production (*Perfect Information*). However, this value can never be reached in practice due to the uncertainty and, therefore, serves only as benchmark. Another value to compare to is a bidding method that submits bids according to the expected electricity price (*Singe Bid Forecast*), i.e., the model considers no electricity price scenarios but the expected value resulting in one bidding amount and price for each hour. This approach is often used in practice. The other four approaches consider the model from Section D.2.1 to create bidding curves based on uncertain electricity prices. We compare four cases regarding the information about RES production: scenarios for wind power and solar thermal production (*RES Uncertain*), scenarios for wind power and perfect information about solar thermal production (*Wind Power Uncertain*), scenarios for solar thermal and perfect information about wind power production (*Solar Heat Uncertain*) as well as perfect information regarding both (*Perfect Information RES*).

The results from Figure D.5 indicate that considering the solar thermal production as uncertain and modelling it as scenarios does not deteriorate the costs significantly compared to the case where the RES production is known. On the other hand, considering the wind power production as uncertainty captured in scenarios, has an impact on the costs and leads to an increase in the cost of

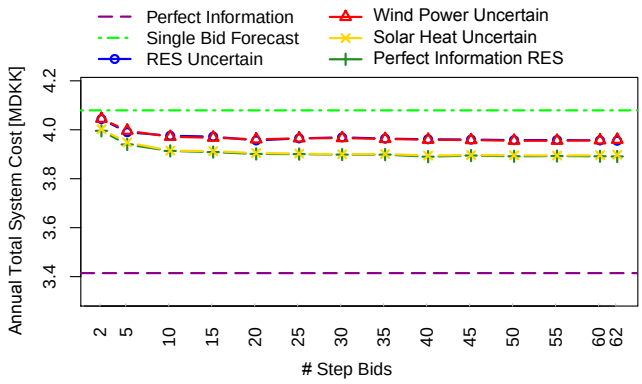

Figure D.5: Comparison of different uncertainty setups and number of steps in the bidding curves in the day-ahead market optimization. The values shown are total annual system cost.

approx. 62000 DKK. Similar results are achieved when considering both RES production sources as uncertain. Based on this results, we can conclude that especially the uncertainty of the wind power production has an influence on the systems costs. This behaviour can be explained based on the fact that the wind power production has a direct effect on the power amount that is traded on the electricity market and therefore on the profits obtained. In contrast, the uncertainty of solar thermal production has no large effect due to the thermal storage in the system, which smooths the effect on the heat production and therefore also the costs. The factor that has the greatest impact on the operational cost is not having information about the day-ahead prices (Perfect Information). In this case having perfect information of RES and uncertain day-ahead electricity prices increased the annual system cost by approx. 500,000 DKK (around 12.5% of the total system cost). However, under the real-world condition that RES and electricity prices are uncertain, using stochastic programming to generate bidding curves decreases the cost by ca. 120,000 DKK per year (3% of the total system cost) compared to the *Single Bid Forecast*.

Figure D.5 also shows the influence of the number of steps in the bidding curves. For this experiment the number of clusters in the PAM algorithm was varied (see Section D.3.4) to obtain different numbers of scenarios representing the number of steps in the bidding curve. We compare in total 14 scenario set sizes ranging from 2 to 62 scenarios, which are the minimum and the maximum number of steps allowed to submit to the NordPool market [D31], respectively. The results show a reduction of costs when the number of steps is increased from two to 20 steps. In this case, including more steps does not lead to further significant

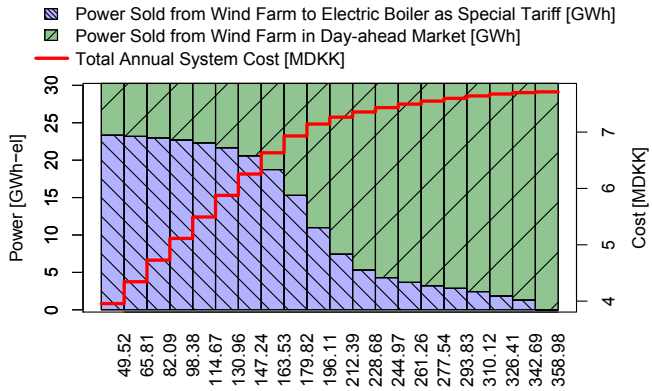

Figure D.6: Power from the wind turbines used for the electric boiler as special tariff or traded on the day-ahead market as well as total annual system cost. The values are given for varying special tariff operation cost of the electric boiler.

reductions in costs.

Based on the analysis in this section, we can conclude that using bidding curves, in particular with at least 20 steps, created from our stochastic program can reduce the annual system cost in particular compared to single bids based on price forecasts. Furthermore, the uncertainty of wind power production influences the results more than the uncertainty regarding solar thermal production.

D.6.2 Impact of special tariff for the electric boiler

As mentioned in the problem description in Section D.2, we assume a special tariff (in terms of tax reduction) if the electric boiler is "using" power that we provide with our wind farm. In this section, we want to analyze the influence of this tariff on the trading on the day-ahead market. The operational cost under the special tariff were given with 49.52 DKK/MWh-heat. Figure D.6 shows the impact on the annual system cost and share of wind power used for the electric boiler and traded on the day-ahead market, respectively, when the tariff is increased in equal step sizes up to the normal operational cost (when fed with power from the grid without special tariff).

Figure D.6 shows clearly the benefits from having a special agreement when feeding in wind power and therefore receiving a special tariff on the electricity

consumption. First, the total annual system cost drastically increase when the special tariff gets more expensive. This is obvious as the production of heat from electricity is getting more expensive. Furthermore, it can be seen that the amount of wind power traded on the day-ahead market increases with a higher tariff, because the income from the market is more promising in most of the hours in the year. This means, using the special tariff for the electric boiler is only beneficial, if the income from the market is expected to be less than the benefit from using the wind power for the electric boiler. This margin is getting smaller with increasing special tariff, resulting in higher trade volumes on the day-ahead market.

This results indicate that DH operators can greatly benefit from receiving a special agreement with respect to using own RES power generation for heat production.

D.6.3 Analysis of yearly production

In this section we provide the results of the annual system behaviour when using the solution approach for day-ahead market and balancing market optimization presented in Section D.4. The results and values for power production and trading, heat production and electricity prices are consolidated on a monthly basis in Figure D.7. The legend can be found in Figure D.7a.

Figure D.7b (top) shows the monthly system cost and the amounts of power traded on the day-ahead market as well as down regulation bought and upward regulation sold on the balancing market. One observation from this figure is that the monthly costs are significantly lower during the summer period due to two reasons. First, the amount of power traded on the different electricity markets is higher during the summer resulting in higher profits. Also the electricity prices are slightly higher during the summer (see Figure D.7c (bottom)). Second, the heat demand is lower during the summer resulting in lower total costs (see Figure D.7c (top)). Furthermore, from Figure D.7c (top) it can be seen that the solar thermal production is higher during summer resulting in less heat needed from the more expensive other units.

A second observation is that the trades on the balancing markets have a higher volume during summer and fall. This behaviour can be explained by taking the power production on a unit-basis into account as provided in Figure D.7b (bottom). During the summer month less of the power is used for heat production, because there is a lower heat demand, and therefore available for trading on the electricity markets.

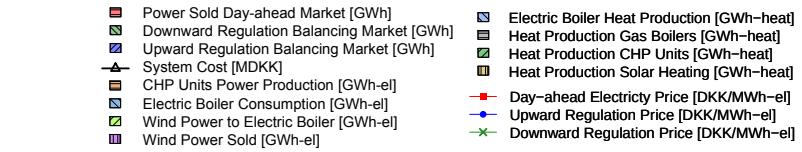

(a) Legend

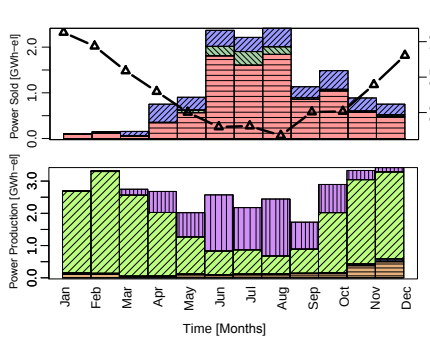

(b) Power sold on the markets and system cost (top) as well as power production by the different units (bottom)

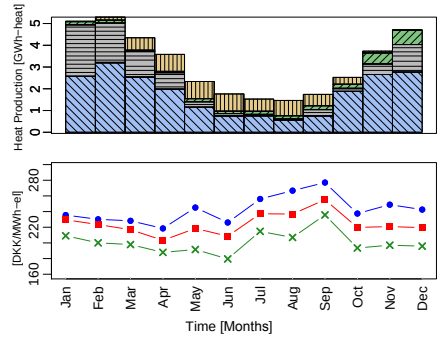

(c) Heat production by the different units (top) and average electricity prices (bottom)

Figure D.7: Annual system behaviour on a monthly time-scale

The results show that the optimization method makes use of the fact that the units are considered as one portfolio and thereby having a flexibility with respect to the production. The trading and production behaviour adjusts itself to the best combination in the different seasons to get lowest heat production costs and highest incomes from the markets. The specific daily system behaviour in case of regulation activities is further analyzed in Section D.6.5.

D.6.4 Value of including balancing market trading

The next analysis investigates the value of including the balancing market trading into the solution approach. Therefore, we compare two settings: Using the solution approach from Section D.4 with and without the balancing market optimization. Furthermore, we run both settings once with perfect information about electricity prices, wind and solar production and once in a stochastic programming setting with scenarios (as presented in the model formulation in Section D.2).

Setting	Total System Cost [DKK]	Δ
Perfect information incl. balancing market	2,499,205	-
Perfect information excl. balancing market	3,414,310	+37%
Stochastic incl. balancing market	3,655,798	+7%
Stochastic excl. balancing market	3,956,530	+8%

Table D.3: Comparison of annual system cost in different setups of the solution approach

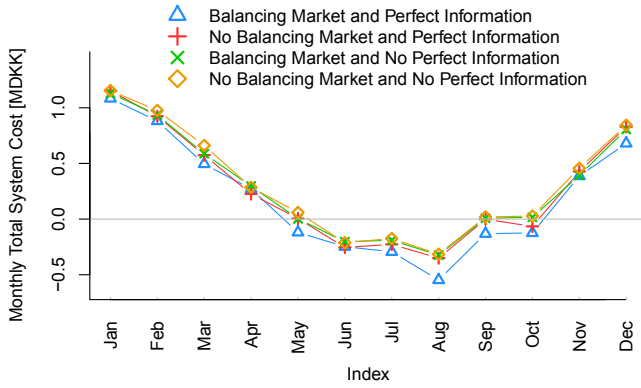

Figure D.8: Comparison of monthly system cost in different setups of the solution approach

The total annual system cost for those four cases in Table D.3 show that even if we have perfect information about the future ignoring trading on the balancing market will increase the total system cost immensely, in this case by 37%. This indicates that a high degree of income can be obtained from the balancing market. The results with perfect information are theoretical values as those can not be reached in a real world application due to the uncertainty at the time of planning. This means that when modelling the uncertainty regarding prices and production in a stochastic setting, the system cost naturally increase, here by 7%. However, lower cost are still achieved by including the balancing market as a second step to avoid imbalances and another opportunity for trading. Not considering the balancing market leads here to 8% higher system cost for the entire year.

These conclusions are mostly independent from the actual months or seasons as it can be seen from Figure D.8. Here the monthly cost for the four settings follow a similar ranking in each month.

D.6.5 Behaviour of system in case of upward and downward regulation

To further investigate the benefits of trading in the balancing market, we analyze the obtained production schedules for four representative days of the year where upward and downward regulation was offered. Section D.6.5.1 and D.6.5.2 each analyze two specific days in which upward and downward regulation was provided, respectively. The legend used for the production schedule figures in this section is the same as in Figure D.7a.

D.6.5.1 Upward regulation

The first case for upward regulation is presented in Figure D.9. Figure D.9a shows the bidding curves for the hours in which upward regulation was won by the DH operator. The vertical lines delimited with "×" represent the real upward prices for those hours and the corresponding power production offered at such prices. Figure D.9b shows the system behaviour and is divided into three parts: upward regulation volume per hour including prices (top), hourly power production per unit (middle) and hourly heat production per unit (bottom). As we can see from D.9b (middle), the upward regulation in this case is entirely provided by the wind farm. Since no wind power was sold on the day-ahead market, the producer decides to bid the entire production of the wind farm into the balancing market for hours 10 and 11. In hour 12, the needed power volume for upward regulation is lower than the actual production from wind. Therefore, the remaining power is used to feed the electric boiler. This behaviour is confirmed by the heat production (Figure D.9b (bottom)). In hours 10 and 11 there is no production with the electric boiler but in hour 12.

The second case for upward regulation is displayed in Figure D.10 that follows the same structure as Figure D.9. Figure D.10a shows that two bids for upward regulation are won. As we can see in Figure D.10b (middle), the upward balancing regulation is provided by the wind farm and the two CHP units in our system during these two hours. For this two hours the upward prices are significantly high and consequently, it is profitable to turn on the two CHP units.

Based on the system behaviour on those two representative days, we can summarize the two cases in which the DH operator can provide upward regulation. First, if we have an higher production of wind power than anticipated and offered in the day-ahead market. Second, if the upward regulation price is high enough that it is beneficial to start up the rather expensive CHP units.

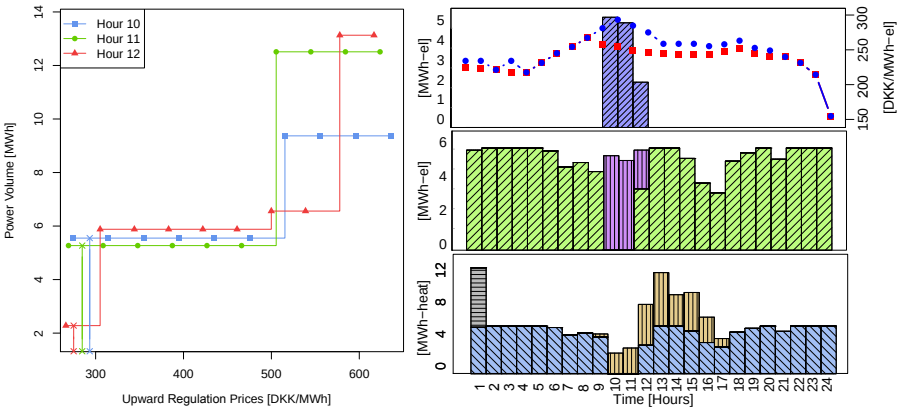

(a) Bidding curves and won bids (marked with ×)

(b) System operation: upward regulation amount including day-ahead and balancing prices (top), power production (middle), heat production (bottom)

Figure D.9: Upward regulation provided on 9th March 2017

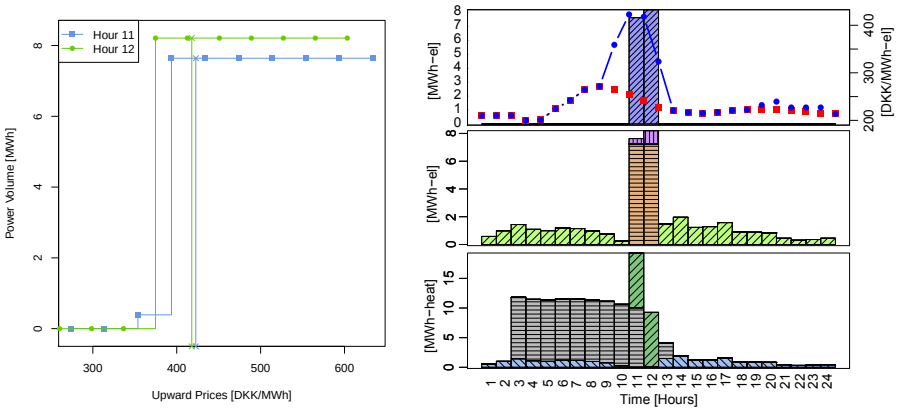

(a) Bidding curves and won bids (marked with ×)

(b) System operation: upward regulation amount including day-ahead and balancing prices (top), power production (middle), heat production (bottom)

Figure D.10: Upward regulation provided on 27th March 2017

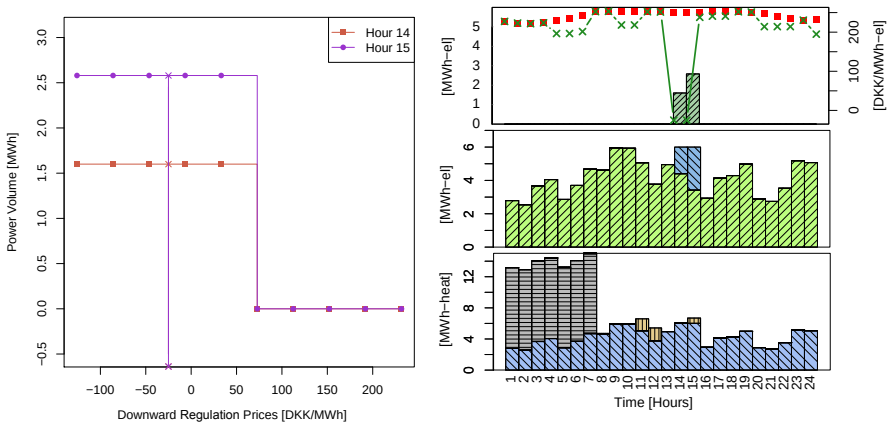

(a) Bidding curves and won bids (marked with ×)

(b) System operation: day-ahead committed amount, downward regulation amount as well as day-ahead and balancing prices (top), power production (middle), heat production (bottom)

Figure D.11: Downward regulation provided on 6th February 2017

D.6.5.2 Downward regulation

In the following we analyze how a DH operator can provide downward regulation. The first option is presented in Figure D.11, which shows downward regulation provided in hour 14 and 15. In this case, the model decides to buy electricity from the grid at the downward price and turn on the electric boiler (see Figure D.11b (middle). In general, electric boilers are good candidates to provide downward regulation because they can absorb large volumes of power in a very short time. Thus, producing heat using the electric boiler constitutes a very economical option when downward regulation is needed.

The second option in which our DH system can benefit from downward regulation is shown in Figure D.12. In this case the system takes advantage of the power sold previously on the day-ahead market to provide downward regulation. As it can be seen from Figure D.12a the system wins 11 bids for downward regulation on that specific day. Here the system stops providing the day-ahead power previously dispatched and buys this lack of production at the downward price. The profit of the system is the difference between the electricity sold at the day-ahead price and the electricity bought at the balancing price. This behaviour is shown in Figure D.12b (top), where the difference between the power sold in the day-ahead market and the one sold in the balancing market is the actual

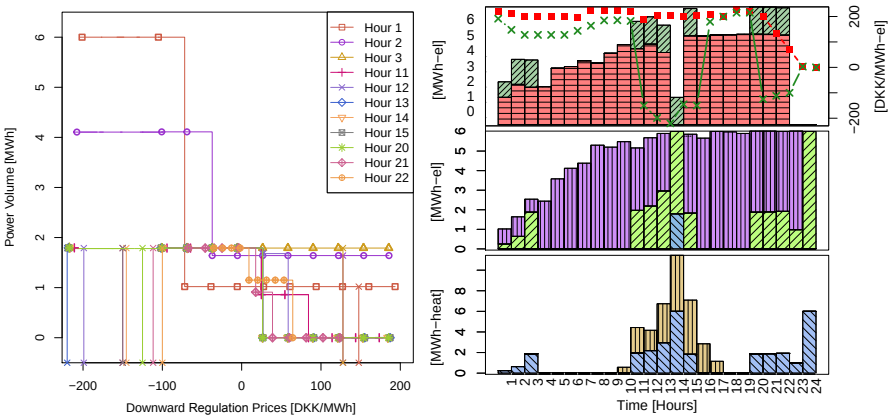

(a) Bidding curves and won bids (marked with ×)

(b) System operation: day-ahead committed amount, downward regulation amount as well as day-ahead and balancing prices (top), power production (middle), heat production (bottom)

Figure D.12: Downward regulation provided on 10th September 2017

production of our wind generators sold to the market (Figure D.12b (middle)). This behaviour is the same for all time periods where downward regulation is provided with the exception of the hour 14 in which no day-ahead auction is won for that hour and therefore, the system decides to buy downward regulation and turn on the electric boiler (Figure D.12b (middle)). Based on the results in this section, we can summarize two ways of providing downward regulation for a DH operator. Either the electric boiler is used to provide downward regulation and produce at a low price or previously won power bids on the day-ahead market are corrected due to lower wind power production than excepted.

D.7 Summary and outlook

In this work, we present a planning method based on two-stage stochastic programming that allows DH providers, which operate a portfolio of units and have uncertain RES production, to create price dependent bids for both day-ahead and balancing markets and optimize the daily production. First, a stochastic program is solved to obtain and present the bids to the day-ahead market. Once the market is cleared, and the producer knows the power production plan, a second stochastic program is used on an hourly basis to generate bids for the

balancing market considering the day-ahead power previously dispatched. After the bids for the balancing market are created and submitted, the market is cleared and the model optimizes the heat production for the new power commitment plan. In addition, we propose a new methodology to define balancing prices scenarios that account for the volatility of these latter based on their observed mean duration and values.

We perform an extensive analysis of the production and trading behaviour of a real DH system in the two markets. The results confirm that uncertain electricity prices have a large impact on the system cost followed by uncertainty in the wind power production. In contrast, solar thermal production uncertainty has a minor influence due to the flexibility given by the heat tank storage. We also show the benefits of using a special tariff that utilizes the power production of wind farms with an electric boiler. This special tariff reduces the yearly total system cost enormously. Regarding the inclusion of balancing market trading into the solution approach, we show that the participation in this market translates in larger profits resulting in lower operational costs. Finally, we investigate the behaviour of the system in case of upward and downward regulation in more detail. The results emphasize the important role of an electric boiler as flexible unit connected to the markets. To summarize, we propose a new planning method to reduce the impact of uncertainties on the production planning for DH systems. In order to achieve this, we hedge against uncertain electricity market prices and production using stochastic programming to create price dependent bids. The integration of RES production is facilitated by re-dispatching the imbalances in the balancing market. Furthermore, we show that considering the DH system as portfolio of units enables the necessary flexibility to react to seasonal changes and uncertainties.

We envision three different lines of future work. First, to use the presented approach to aggregate offers from a portfolio of different DH producers and calculate the optimally combined offer that can maximize the profit of all producers considering that we are now price-makers instead of price-takers. Therefore, a bi-level optimization program should be formulated. Second, to improve the bidding strategies to hedge even more against uncertain electricity prices. Finally, as our results indicate a significant margin of improvement by using the balancing market. Therefore, it becomes essential to develop more accurate forecasting techniques to predict balancing prices and their high volatility for one or two hours in advance.

References D

[D1] European Commission. *Efficient district heating and cooling systems in the EU*. https://www.euroheat.org/wp-content/uploads/2017/01/study-on-efficient-dhc-systems-in-the-eu-dec2016_final-public-report6.pdf. (Accessed on 02/02/2018). 2016.

[D2] D. Connolly et al. "Heat Roadmap Europe: Combining district heating with heat savings to decarbonise the EU energy system". In: *Energy Policy* 65 (2014), pp. 475–489. ISSN: 0301-4215.

[D3] Euroheat & Power. *District Energy in Denmark*. https://www.euroheat.org/knowledge-centre/district-energy-denmark/. (Accessed on 03/15/2018). 2017.

[D4] Danish Energy Agency. *Regulation and planning of district heating in Denmark*. https://ens.dk/sites/ens.dk/files/Globalcooperation/regulation_and_planning_of_district_heating_in_denmark.pdf. (Accessed on 09/10/2018).

[D5] H. Madsen et al. "Integrated energy systems; aggregation, forecasting, and control". In: *DTU International Energy Report 2015*. Technical University of Denmark (DTU), 2015, pp. 34–40.

[D6] H. Pandžić et al. "Offering model for a virtual power plant based on stochastic programming". In: *Appl. Energy* 105 (2013), pp. 282–292.

[D7] E. Carpaneto, P. Lazzeroni, and M. Repetto. "Optimal integration of solar energy in a district heating network". In: *Renewable Energy* 75 (2015), pp. 714–721.

[D8] H. Wang et al. "Modelling and optimization of CHP based district heating system with renewable energy production and energy storage". In: *Appl. Energy* 159 (2015), pp. 401–421.

[D9] J. Li et al. "Optimal operation of the integrated electrical and heating systems to accommodate the intermittent renewable sources". In: *Appl. Energy* 167 (2016), pp. 244–254.

[D10] F. Paraschiv, D. Erni, and R. Pietsch. "The impact of renewable energies on EEX day-ahead electricity prices". In: *Energy Policy* 73 (2014), pp. 196–210.

[D11] R. H. Kwon and D. Frances. "Optimization-Based Bidding in Day-Ahead Electricity Auction Markets: A Review of Models for Power Producers". In: *Handbook of Networks in Power Systems I*. Ed. by A. Sorokin et al. Berlin, Heidelberg: Springer Berlin Heidelberg, 2012, pp. 41–59. ISBN: 978-3-642-23193-3. DOI: 10.1007/978-3-642-23193-3_2. URL: https://doi.org/10.1007/978-3-642-23193-3_2.

[D12] J. R. Birge and F. Louveaux. *Introduction to stochastic programming*. Springer Science & Business Media, 2011.

[D13] K. Schulz, B. Hechenrieder, and B. Werners. "Optimal Operation of a CHP Plant for the Energy Balancing Market". In: *Operat. Res. Proceed. 2014*. Springer, 2016, pp. 531–537.

[D14] H. V. Ravn et al. "Modelling Danish local CHP on market conditions". In: *Proc. 6th IAEE European Conference: Modelling in Energy Economics and Policy*. 2004.

[D15] I. Dimoulkas and M. Amelin. "Constructing bidding curves for a CHP producer in day-ahead electricity markets". In: *2014 IEEE International Energy Conference (ENERGYCON)*. 2014, pp. 487–494.

[D16] X. Ayón, M. Á. Moreno, and J. Usaola. "Aggregators' Optimal Bidding Strategy in Sequential Day-Ahead and Intraday Electricity Spot Markets". In: *Energies* 10.4 (2017), p. 450.

[D17] M. A. Plazas, A. J. Conejo, and F. J. Prieto. "Multimarket optimal bidding for a power producer". In: *IEEE Trans. Power Syst.* 20.4 (2005), pp. 2041–2050.

[D18] W. Pei et al. "Optimal bidding strategy and intramarket mechanism of microgrid aggregator in real-time balancing market". In: *IEEE Trans. Ind. Inf.* 12.2 (2016), pp. 587–596.

[D19] M. Hosseini-Firouz. "Optimal offering strategy considering the risk management for wind power producers in electricity market". In: *Int. J. Electr. Power Energy Syst.* 49 (2013), pp. 359–368.

[D20] Y. Vardanyan and M. R. Hesamzadeh. "The coordinated bidding of a hydropower producer in three-settlement markets with time-dependent risk measure". In: *Electr. Power Syst. Res.* 151 (2017), pp. 40–58.

[D21] N. Kumbartzky et al. "Optimal operation of a CHP plant participating in the German electricity balancing and day-ahead spot market". In: *Eur. J. Oper. Res.* 261.1 (2017), pp. 390–404.

[D22] R. Petrichenko et al. "District heating demand short-term forecasting". In: *2017 IEEE International Conference on Environment and Electrical Engineering and 2017 IEEE Industrial and Commercial Power Systems Europe (EEEIC / I&CPS Europe)*. 2017, pp. 1–5.

[D23] P. Pinson et al. "Local linear regression with adaptive orthogonal fitting for the wind power application". In: *Statistics and Computing* 18.1 (2008), pp. 59–71.

[D24] EMD International A/S. *Solar collectors and photovoltaics in energyPRO*. https://www.emd.dk/files/energypro/HowToGuides/Solar%20collectors%20and%20photovoltaics%20in%20energyPRO.pdf. (Accessed on 09/05/2018).

[D25] V. Gonzalez, J. Contreras, and D. W. Bunn. "Forecasting power prices using a hybrid fundamental-econometric model". In: *IEEE Trans. Power Syst.* 27.1 (2012), pp. 363–372.

[D26] J. Ringwood, P. C. Austin, and W. Monteith. "Forecasting weekly electricity consumption: A case study". In: *Energy Econ.* 15.4 (1993), pp. 285–296.

[D27] A. J. Conejo, M. Carrión, J. M. Morales, et al. *Decision making under uncertainty in electricity markets*. Vol. 1. Springer, 2010.

[D28] A. P. Reynolds et al. "Clustering rules: a comparison of partitioning and hierarchical clustering algorithms". In: *Journal of Mathematical Modelling and Algorithms* 5.4 (2006), pp. 475–504.

[D29] M. Olsson and L. Soder. "Modeling real-time balancing power market prices using combined SARIMA and Markov processes". In: *IEEE Trans. Power Syst.* 23.2 (2008), pp. 443–450.

[D30] *Energinet - energy data service*. https://www.energidataservice.dk/en/. (Accessed on 10/03/2018).

[D31] *NordPool Spot Glossary*. https://www.energiforetagen.se/globalassets/energiforetagen/det-erbjuder-vi/kurser-och-konferenser/krisutbildningar/nord-pool-spot-glossary.pdf. (Accessed on 10/03/2018).

Paper E

A Two-phase Stochastic Programming Approach to Biomass Supply Planning for Combined Heat and Power Plants

---

Authors:
Ignacio Blanco, Daniela Guericke, Juan M. Morales and Henrik Madsen

Under review in:
OR Spectrum (Springer).

A Two-phase Stochastic Programming Approach to Biomass Supply Planning for Combined Heat and Power Plants

Ignacio Blanco[1], Daniela Guericke[1], Juan M. Morales[2] and Henrik Madsen[1]

Abstract

Due to the new carbon neutral policies, many district heating operators start operating their combined heat and power (CHP) plants using different types of biomass instead of fossil fuel. The contracts with the biomass suppliers are negotiated months in advance and involve many uncertainties from the energy producer's side. The demand for biomass is uncertain at that time, and heat demand and electricity prices vary drastically during the planning period. Furthermore, the optimal operation of combined heat and power plants has to consider the existing synergies between the power and heating systems. We propose a solution method using stochastic optimization to support the biomass supply planning for combined heat and power plants. Our two-phase approach determines mid-term decisions about biomass supply contracts as well as short-term decisions regarding the optimal production of the producer to ensure profitability and feasibility. We present results based on two realistic test cases.

E.1 Introduction

The integration of different energy systems is one step towards a fossil-free energy system, which many developed countries target today. By integrating different energy systems, such us heat and power, a higher share of volatile renewable energies, e.g., wind energy, can be used efficiently [E1]. In areas with large district heating networks, one way to achieve this integration is using

[1]Department of Applied Mathematics and Computer Science, Technical University of Denmark, DK-2800 Kgs. Lyngby, Denmark

[2]Department of Applied Mathematics, University of Malaga, SP-29071, Málaga, Spain

combined heat and power (CHP) plants that produce heat and power simultaneously. By co-optimizing the production of both, the efficiency of the system is increased while providing flexibility to the power grid and satisfying the heat demand in the district heating network. Due to the neutral carbon policies imposed by the authorities, a shift from traditional fuels to renewable resources is taking place. Denmark has a widespread use of district heating and CHP plants and the government supports the use of biomass to produce heat and power. With subsidies and tax benefits, it has become profitable for large-scale CHP plants to change from, e.g., coal or natural gas to biomass [E2].

The use of biomass as fuel for CHP plants raises some challenges in the planning of the supply and in the operation of the plant. Many different types of biomass are used to produce heat and power [E3] but the most common type of biomass used for large-scale CHP producers is wood pellets. Due to their high energy content, wood pellets facilitate a more efficient transport because smaller volumes are required. In addition, the low moisture content of wood pellets allows a better conservation of the product resulting in a larger storage capacity [E4]. In combination with neutral carbon policy incentives for biomass, the wood pellet is becoming a candidate to substitute coal in CHP plants. However, comparing the supply of wood pellets, or biomass in general, with supply of natural gas, the former has some disadvantages. First, natural gas prices have been dropping since 2008 and, second, it exists a well-developed infrastructure for natural gas, which allows the producer to be directly connected to the gas network. On the contrary, biomass is transported long ways and contracts with the supplier must be agreed beforehand for a long horizon (one to three years) involving a high degree of uncertainty at negotiation because the final amount is unknown. It is crucial for CHP operators to optimize their biomass contracts to be competitive with gas-fired plants.

In this work, we propose a solution approach based on stochastic programming [E5] to optimize the yearly biomass contracting decisions for a CHP operator taking into account the uncertainty at the point of negotiation. Furthermore, the approach also determines the optimal operation of the plant to maximize profits and satisfy the heat demand on weekly basis throughout the year.

E.2 Literature review

Several models for the optimal operation of CHP systems, where different aspects of the problem are highlighted, have been proposed. We refer for example to [E6, E7, E8, E9, E10, E11]. These solution approaches determine the optimal production of both commodities (heat and power) at different levels of detail,

but do not consider uncertainties and supply contracts for fuel explicitly.

Since then several approaches that apply stochastic programming for the operational planning were developed. [E12] solve the operational scheduling for an industrial customer that owns an integrated system formed by CHP units, conventional power production and heat only units. The method uses electricity market sales and demand response programs to integrate the uncertainty caused by electricity prices and load. An optimal operation of a portfolio of different CHP systems in a district heating network is studied in [E13]. The authors consider uncertain heat demand and electricity prices and show that the system profits from leveraging a thermal storage to handle this uncertainty. [E14] present a multi-stage stochastic program for optimizing the operation of a gas-fired CHP plant and deriving bids for the German spot and balancing markets. The considered uncertainty are electricity prices. [E15] propose a stochastic program including technical aspects of a extraction-condensing CHP plant for optimizing the hourly operation under price and demand uncertainty. The authors use this model to determine bidding curves for the day-ahead market. In [E16] this model is revisited with more focus on the joint production scheduling of two CHP plants. The operational planning problem in our work is similar to these two formulations, but extended with further characteristics regarding the biomass contracts deliveries and technical constraints.

The above mentioned publications assume instantaneous fuel supply and, therefore, do not consider fuel supply decisions. Another stream of publications explicitly concentrates on the biomass supply chain planning for power generation considering processing of biomass, transport and logistics aspects. The OPTIMASS model for strategic and tactical biomass supply chain planning is presented in [E17]. The formulation is based on a facility location planning problem that includes the processing of the biomass to determine locations and capacities of facilities in the supply chain and allocation of biomass sites to conversion facilities. The final usage of biomass in electricity production is not part of this study. [E18] present a decision support system for a forest biomass supply chain deciding on the locations and capacities as well as assignment of biomass sources to power plants. [E19] present a two-stage stochastic program with chance constraints for biomass supply chain planning under biomass availability uncertainty. The demand is based on markets and not single plants. [E20] model the biomass-based energy production process, which includes deciding the location of plants as well as flow and conversion of commodities where one commodity is electricity. The model focuses on long-term decisions.

In this work the perspective of a power plant that receives biomass from third party suppliers is considered. Furthermore, we investigate the integration of long-term biomass supply decisions with the operational planning of the production. Similar settings have been studied in the following publications. [E21]

consider the fuel supply of gas for a consumer having a micro CHP and a heat boiler. Their multi-stage stochastic program decides on how much gas to buy on the spot or the monthly and weekly futures market, while electricity can be sold with similar market instruments. The model has a monthly planning horizon and abstracts from more detailed considerations regarding the operation of the system. In [E22], a general overview of the benefits of using stochastic programming to incorporate the uncertainty involved in the biomass supply chain for a power producer on a tactical planning level is given. The authors formulate a one year planning problem considering the amount of biomass supply from different suppliers, storage and the expected power production on a monthly basis. [E23] consider the supply chain connected to a biogas CHP plant and use a network flow model formulation. The model includes conversion to biogas and production with a CHP or heat boiler as well as transportation costs. [E24] address biomass supplier selection combining an analytic hierarchy process (AHP) with a chance constraint program to address stakeholders and uncertainties in this setting. Their focus is ensuring the quality of the biomass by blending biomass from different kinds and suppliers to fulfill the overall demand. The solution approach disregards the production level and delivery times. Finally, [E25] use stochastic programming for optimal biomass contracting decisions in a long-term planning horizon. The model decides which biomass contracts should be settled with the suppliers. They model the contracts as well as the deliveries and production to provide a basis for this decision. Due to the planning horizon and short time periods, the model results in a computationally hard two-stage stochastic program.

Our work differs from [E25] regarding the modeling of contracting decisions and the overall solution approach. Delivery times and amounts for contracts in [E25] are fixed and the decision-maker can just decide which contracts are selected. On the contrary, our approach allows more flexibility to decide on the amount to be supplied and the delivery time. As a consequence, the exact delivery time and precise quantity are determined once we are getting closer to the energy delivery. Furthermore, we reduce the computational complexity of the planning problem by presenting a two-phase approach.

The main contributions of our work are the following:

1. We propose a two-phase solution approach that combines biomass contracting decisions with the optimal operation of the CHP plant. Therefore, it provides two models that can be used by an operator for long-term and operational planning, respectively. The first phase concentrates on the biomass contract selection at the beginning of the year considering production on a weekly less detailed basis and, therefore, reducing the complexity of the problem. The second phase optimizes the weekly operation of the

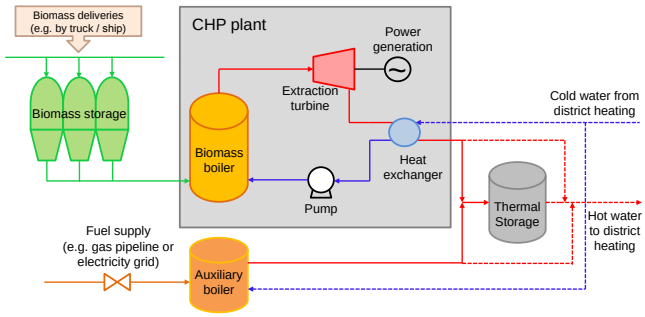

Figure E.1: Overview of components in the planning problem

system on a detailed hourly basis and takes the biomass contract decisions into account. The overall solution approach considers relevant technical requirements and resembles the planning process in practice.

2. Our modeling of biomass contracts offers a high degree of flexibility. Completely fixed contracts can be investigated as well as more flexible contracts regarding amounts of deliveries. We include the possibility to buy options on the biomass amount to be able to adjust the delivery quantity during the course of the year. This is a new feature whose benefits are worth of investigation, at least from the standpoint of a CHP producer.

3. Furthermore, we use a receding horizon approach to improve the results of our weekly operational planning, because it is important to take initial information from previous weeks into account and have a feasible transition. This also allows us to update the scenarios with new information.

The remainder of this papers is organized as follows. A detailed description of the planning problem is given in Section E.3. Our solution approach and the respective model formulations are presented in Section E.4. In Section E.5, we analyze two realistic case studies. The section includes a description of the data, experimental setup and scenario generation. The numerical results are stated in Section E.6. Finally, Section E.7 summarizes our work and gives an outlook.

E.3 Problem description

In this section, we describe the biomass supply planning problem including used sets and parameters. For quick reference, we also provide an overview of parameters and sets in Table E.1.

An overview of the components in the planning problem is given in Fig. E.1. We consider a power and heat producer directly connected to a district heating network. The producer operates a CHP plant fueled by biomass and an auxiliary heat producing unit (e.g. gas boiler, electric boiler or heat pump). Both units can supply the district heating network directly but are also connected to a thermal storage, which can store hot water for later heat supply.

The biomass delivered by suppliers according to the contracts is unloaded into the biomass storage and withdrawn from the storage for later use (i.e. no direct supply to the boiler). We assume that fuel for the additional heat-only unit is provided directly and instantaneously without storage and deliveries. This assumption stems from the setting of a gas boiler connected to the gas network or an electric boiler connected to the electricity grid.

In practice, biomass contracts are often agreed for a period of one year or more, defining the amount of biomass and a preliminary delivery schedule. The actual delivery time is revised in the course of the year. We model two different types of contracts, namely fixed and flexible. *Fixed* contracts are cheaper but offer no possibility to alter the delivery amount afterward. *Flexible* contracts are more expensive than fixed contracts, but the operator has the opportunity to buy an option of changing the amount. In the beginning of the year, in addition to the delivery amount, the options for up- and/or down-scaling the amount are settled, while the producer has to pay extra for those options. The possibility of buying options to change the biomass delivery amount is a new concept that is studied in this paper. It provides the power producer with additional flexibility that can be beneficial especially in the long term when the actual demand is still uncertain. Also from the supplier's side this could be an interesting instrument, because it offers additional incomes from selling options while the amounts can be shifted between different customers. However, the supplier side is not the focus of this paper.

The input to our solution approach is a set of possible contracts $\mathcal{J}$, a set of scenarios Ω and a set of periods $\mathcal{T} = \{1, \ldots, |\mathcal{T}|\}$. The first planning period is always denoted with 1, so that initial values are given values for period 0 (e.g. for storage levels $\delta_{0,\omega}$ and $s_{0,\omega}$). Each contract j has a minimum and maximum amount per delivery $(\underline{B}_j, \overline{B}_j)$, a minimum and maximum number of deliveries per planning horizon $(\underline{N}_j, \overline{N}_j)$ and a minimum time between deliveries (F_j). If contract j offers up-scaling and down-scaling options, the maximum limitations are given by O_j^+ and O_j^- (in percent deviation from the nominal amount), respectively. For fixed contracts these parameters are set to zero $(O_j^+ = O_j^- = 0)$. The cost for the fixed, up-scaling and down-scaling amount are given by C_j^B, C_j^{B+} and C_j^{B-}, respectively. The cost are given per MWh, because the payment in practice is determined based on the energy content

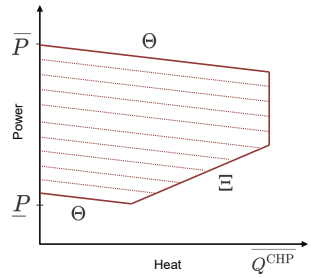

Figure E.2: Feasible production region of extraction-condensing unit in CHP plant

of the biomass in Gigajoule, which can be directly transformed to MWh. This means that the payment does not depend only on the amount in tonnes but also on the quality of the biomass, the so-called calorific value. Transportation costs are considered only indirectly, because the supplier has to cover these and can include them in the biomass cost per MWh. Furthermore, we assume that the supplier has the responsibility to deliver the contracted amount. As mentioned above, the biomass is delivered to the biomass storage, which is limited by a minimum safety and maximum storage level $(\underline{\Delta}_t, \overline{\Delta})$. The initial storage level is given for period 0 and the outflow per period is restricted to a maximum of Δ^{F}. To avoid congestion at the storage due to several deliveries at the same time, the time distance between deliveries must be at least Δ^{W} periods.

Biomass from the storage is used by the CHP plant to produce power and heat. The production of both is limited to the feasible production region of an extraction condensing unit depicted with the relevant parameters Θ and Ξ [E26] in Figure E.2. The efficiency of a conversion from biomass to power and heat is denoted by E_P^{CHP} and E_Q^{CHP}, respectively. From one hour to the next, the power production of the CHP can be ramped up or down but only in the limits of the parameters R^U and R^D. If the unit is started up or shut down it has to be in that state for at least M^U or M^D time periods. Starting up and shutting down is priced with C^{SU} and C^{SD}, respectively. The operation of the CHP itself has a cost of C^{CHP}. The power produced is sold on the electricity market and the profit depends on the market price $L^E_{t,\omega}$ in scenario ω. In Denmark, the production of electricity by biomass is supported with an incentive of I, while the production of electricity with any fuel is taxed with T^{EP}. Thus, the overall cost $L_{t,\omega}$ is given by $L_{t,\omega} = T^{\mathrm{EP}} - I - L^E_{t,\omega}$, where negative values of $L_{t,\omega}$ are profits.

The auxiliary boiler has a maximum capacity of $\overline{Q^{\mathrm{AUX}}}$ with an efficiency of E^{AUX}. The operational costs $C^{\mathrm{AUX}}_{t,\omega}$ of the boiler consists of several components

Table E.1: Sets and parameters

$\mathcal{J}$	Set of biomass contracts j
$\mathcal{W}$	Set of weeks w $\left(\mathcal{W} = \{1, \ldots, \lvert\mathcal{W}\rvert\}\right)$
$\mathcal{T}$	Set of time periods t
$\mathcal{T}_{\mathrm{w}}$	Set of time periods t in week w
Ω	Set of scenarios ω
π_ω	Probability of scenario ω
$D_{t,\omega}$	Heat demand in period t in scenario ω [MWt/period]
$L_{t,\omega}$	Negative costs, i.e. profit, for selling electricity in period t in scenario ω [€/MWe]
$C^{\mathrm{AUX}}_{t,\omega}$	Operational cost of auxiliary boiler in period t in scenario ω [€/MWt]
C^{CHP}	Operational cost of CHP plant [€/MWt]
C^{SU}	Start up cost for CHP [€/MWt]
C^{SD}	Shut down cost for CHP [€/MWt]
C^{I}	Inventory cost for biomass storage [€/MWt]
$C^{\mathrm{F}}_{t,\omega}$	Cost of fuel for auxiliary boiler in period t and scenario ω [€/MWt]
$C^{\mathrm{O\&M}}_{AUX}$	Operational cost for auxiliary boiler [€/MWt]
T^{EP}	Tax for electricity production [€/MWe]
T^{AUX}	Tax for production with auxiliary boiler [€/MWt]
$T^{\mathrm{CO_2}}$	CO_2 emission tax [€/MWt]
C^{B}_j	Cost for biomass in contract j [€/MWt]
$C^{\mathrm{B}+}_j$	Cost for up-scaling biomass amount in contract j [€/MWt]
$C^{\mathrm{B}-}_j$	Cost for down-scaling biomass amount in contract j [€/MWt]
$\underline{B_j}, \overline{B_j}$	Minimum/maximum amount biomass offered per delivery by contract j [MWt]
$\underline{N_j}, \overline{N_j}$	Minimum/maximum number of deliveries offered by contract j
$\overline{F_j}$	Frequency of deliveries in contract j [hours]
O^+_j, O^-_j	Maximum up-scaling/down-scaling option offered in contract j [pu]
$\overline{\Delta}$	Maximum biomass storage level [MWt]
$\underline{\Delta}_t$	Safety storage level of biomass in period t [MWt]
Δ^{F}	Maximum outflow from biomass storage per period [MWt/period]
Δ^{W}	Time distance between deliveries to biomass storage [periods]
$\underline{S}, \overline{S}$	Minimum/maximum thermal storage level [MWt]
S^{F}	Maximum in/outflow to/from thermal storage per period [MWt/period]
$\underline{P}, \overline{P}$	Minimum/maximum production of CHP plant per period [MWe/period]
$\overline{Q^{\mathrm{CHP}}}$	Maximum heat production of CHP plant per period [MWt/period]
E^{CHP}_P	Electric efficiency of the CHP plant [pu]
E^{CHP}_Q	Heat efficiency of the CHP plant [pu]
E^{B}	Calorific value of the biomass [MWt/tonnes]
Θ	Fraction of power reduction
Ξ	Maximum heat to power ratio
M^U, M^D	Minimum up time / down time of CHP plant [periods]
R^U, R^D	Ramp-up and ramp-down limits of CHP plant [MWe/period]
$\overline{Q^{\mathrm{AUX}}}$	Maximum heat production of auxiliary boiler per period [MWt/period]
E^{AUX}	Auxiliary boiler efficiency [pu]
P^{B}	Target percentage of heat produced by biomass [pu]
ϕ^{Sto}	Penalty for excess of storage at the end of time horizon [€]
ϕ^{Miss}	Penalty for missed heat demand [€]
ϕ^{BM}	Penalty to fail the minimum required heat demand by biomass [€]
ψ_t	Small incentive for concentrating biomass options in period t [€]

and is dependent on the scenario ω due to the uncertain fuel (e.g. gas or electricity) spot price $C^{\mathrm{F}}_{t,\omega}$. Further components are the operation and maintenance costs $C^{\mathrm{O\&M}}_{AUX}$, taxes T^{AUX} and CO_2 taxes $T^{\mathrm{CO_2}}$. Thus, the overall operational costs are given by $C^{\mathrm{AUX}}_{t,\omega} = C^{\mathrm{F}}_{t,\omega} + C^{\mathrm{O\&M}}_{AUX} + T^{\mathrm{AUX}} + T^{\mathrm{CO_2}}$.

Both units can feed the thermal storage. In the beginning of the planning horizon (period 0), the heat tank has a given level and the level has to be always between $\underline{S}$ and $\overline{S}$. The in-/outflow per period is limited to S^F.

The producer is obliged to fulfill the heat demand in the district heating network $D_{t,\omega}$, which is modeled in scenarios ω. Due to regulations, the heat production based on biomass is aimed at covering at least P^B percent of the total demand. The probability of scenario ω is given by π_ω. To sum the uncertain parameters up, a scenario ω resembles the heat demand $D_{t,\omega}$, the electricity price $L^E_{t,\omega}$ and the fuel spot price for the auxiliary boiler $C^{\mathrm{AUX}}_{t,\omega}$.

The overall objective of the solution approach is to select the portfolio of biomass contracts and their configurations that minimizes the cost while fulfilling the heat demand taking the technical characteristics of the plant into account. In this paper, we consider a planning horizon of one year ranging from summer to summer as it is done in practice. Thus, the heating seasons lies in the middle of the planning horizon. However, in general the method can be used with any length of the planning horizon starting and ending at an arbitrary point in time during the year.

E.4 Two-phase solution approach

The time scales in the above mentioned planning problem have a broad range. As the contracts are often agreed for up to one year, this results in a medium-term planning problem. However, many technical characteristics of the CHP unit and the electricity market relate to an hourly level. Additionally, the production does not need to be scheduled more than one week in advance, because then information especially regarding the heat demand gets more accurate. Therefore, we divide the overall planning problem into two-phases:

Biomass contract selection: This model decides which suppliers should be contracted for the next year and which amount of biomass they should deliver (including options). The model is based on heat demand scenarios and includes the production by the CHP plant and auxiliary boiler on a weekly time scale excluding ramping and unit commitment decisions. For this long planning horizon the electricity and fuel prices are approximated by an expected value, because

the prices are very volatile and hard to predict for a long time horizon. The thermal heat storage is excluded from this model, because it is not reasonable to model the flows on a weekly scale due the small size of those storages. Set $\mathcal{T}$ represents weekly periods in this model. The mathematical formulation is presented in Section E.4.1.

Operational planning problem: Here the input of biomass is fixed based on the contracts selected in phase 1, but the amounts of contracts with agreed options can still be altered. The model is solved week-by-week taking the input from the previous week into account (storage levels, status of the unit) and decides on the actual production of the CHP plant and auxiliary boiler on an hourly basis incorporating technical requirements and scenario-based price and demand information. Set $\mathcal{T}$ represents hourly periods in this model. The model formulation is described in Section E.4.2.

Based on the scenario-based representation of the uncertain parameters, both models are two-stage stochastic programming model formulations. The division of the planning problem into two phases not only reduces the complexity of the problem, but also resembles the planning process in practice in a more accurate way. Furthermore, solving the operational planning problem week-by-week enables us to make use of more recent information to update the scenarios for the next week. We do not consider an integrated problem for the entire year in an hourly resolution because the addition of such precise information can negatively affect the solution of the problem towards the real realization of the uncertainty due to forecasting inaccuracies. Furthermore, preliminary experiments showed that the large number of integer variables makes the problem computationally hard and not solvable in a reasonable amount of time.

E.4.1 Biomass contract selection

The following model represents the biomass contract selection in phase 1. The model has a weekly time-scale, therefore, the set $\mathcal{T}$ consists of weeks. The relevant parameters like capacities and flow restrictions of the units and storage are scaled up to weekly values accordingly.

The first-stage decision variables in this model decide on the contracts to be selected (u_j) as well as the number of deliveries in each week ($d_{j,t}$) and amounts ($b_{j,t}$) including up- ($b^+_{j,t}$) and down-scaling ($b^-_{j,t}$) options for each contract $j \in \mathcal{J}$ and period $t \in \mathcal{T}$. Based on the second-stage variables, these amounts can be altered with the variables $\overline{b^+}_{j,t,\omega}$ and $\overline{b^-}_{j,t,\omega}$ within the limits of the selected options in the first-stage. Further second-stage variables relate to the biomass storage level ($\delta_{t,\omega}$) as well as heat ($q^{\text{CHP}}_{t,\omega}, q^{\text{AUX}}_{t,\omega}$) and power production ($p_{t,\omega}$).

Table E.2: Variables

$u_j \in \{0,1\}$	Equals 1, if contract j is used, 0 otherwise
$d_{j,t} \in \mathbb{N}_0$	Number of deliveries by contract j in period t
$\hat{d}_{j,t} \in \{0,1\}$	Equals 1, if contract j delivers in period t, 0 otherwise
$b_{j,t} \in \mathbb{R}_0^+$	Amount of biomass contracted in contract j for period t [tonnes]
$b_{j,t}^+ \in \mathbb{R}_0^+$	Up-scaling option contracted in contract j for period t [tonnes]
$b_{j,t}^- \in \mathbb{R}_0^+$	Down-scaling option contracted in contract j for period t [tonnes]
$\overline{b^+}_{j,t,\omega} \in \mathbb{R}_0^+$	Actual amount used of up-scaling option in contract j [tonnes]
$\overline{b^-}_{j,t,\omega} \in \mathbb{R}_0^+$	Actual amount used of down-scaling option in contract j [tonnes]
$\delta_{t,\omega} \in \mathbb{R}_0^+$	Biomass storage level [MWt]
$\delta_{t,\omega}^+ \in \mathbb{R}_0^+$	Inflow to biomass storage [MWt/period]
$\delta_{t,\omega}^- \in \mathbb{R}_0^+$	Outflow from biomass storage [MWt/period]
$s_{t,\omega} \in \mathbb{R}_0^+$	Thermal storage level [MWt]
$s_{t,\omega}^+ \in \mathbb{R}_0^+$	Inflow to thermal storage [MWt/period]
$s_{t,\omega}^- \in \mathbb{R}_0^+$	Outflow from thermal storage [MWt/period]
$x_{t,\omega} \in \{0,1\}$	Equals 1, if CHP plant is on in period t, 0 otherwise
$y_{t,\omega} \in \{0,1\}$	Equals 1, if CHP plant is started up in period t, 0 otherwise
$z_{t,\omega} \in \{0,1\}$	Equals 1, if CHP plant is shut down in period t, 0 otherwise
$p_{t,\omega} \in \mathbb{R}_0^+$	Power production by CHP [MWe/period]
$q_{t,\omega}^{\mathrm{CHP}} \in \mathbb{R}_0^+$	Total heat production by CHP [MWt/period]
$q_{t,\omega}^{\mathrm{CHP,N}} \in \mathbb{R}_0^+$	Heat from CHP flowing to DH [MWt/period]
$q_{t,\omega}^{\mathrm{CHP,S}} \in \mathbb{R}_0^+$	Heat from CHP to thermal storage [MWt/period]
$q_{t,\omega}^{\mathrm{AUX}} \in \mathbb{R}_0^+$	Total heat production by auxiliary boiler [MWt/period]
$q_{t,\omega}^{\mathrm{AUX,N}} \in \mathbb{R}_0^+$	Heat from auxiliary boiler to DH [MWt/period]
$q_{t,\omega}^{\mathrm{AUX,S}} \in \mathbb{R}_0^+$	Heat from auxiliary boiler to thermal storage [MWt/period]
$q_{t,\omega}^{\mathrm{Miss}} \in \mathbb{R}_0^+$	Missed heat demand [MWt/period]
$q_{t,\omega}^{\mathrm{BM}} \in \mathbb{R}_0^+$	Required amount of heat not supplied with biomass [MWt/period]
$\delta_{t,\omega}^{\mathrm{EX}} \in \mathbb{R}_0^+$	Amount of biomass above storage capacity [MWt]
$\delta_{\omega}^{\mathrm{T}} \in \mathbb{R}_0^+$	Amount of biomass in excess at the end of the time horizon [MWt]

An overview of the variables and their domains is given in Table E.2.

$$\min \sum_{t\ \in\mathcal{T}} \Bigg[\sum_{j\in\mathcal{J}} \Bigg(C_j^{\mathrm{B}} b_{j,t} + C_j^{\mathrm{B}+} b_{j,t}^+ + C_j^{\mathrm{B}-} b_{j,t}^- + \sum_{\omega\in\Omega} \pi_\omega C_j^{\mathrm{B}} (\overline{b^+}_{j,t,\omega} - \overline{b^-}_{j,t,\omega}) \Bigg) \tag{E.1a}$$

$$+ \sum_{\omega\in\Omega} \pi_\omega \Bigg(C^{\mathrm{CHP}} \left[p_{t,\omega} - \Theta q_{t,\omega}^{\mathrm{CHP}} \right] + \widehat{L_t} p_{t,\omega} + \widehat{C_t^{\mathrm{AUX}}} \frac{q_{t,\omega}^{\mathrm{AUX}}}{E^{\mathrm{AUX}}} + C^{\mathrm{I}} \delta_{t,\omega} \Bigg) \Bigg] \tag{E.1b}$$

$$+ \sum_{\omega\in\Omega} \pi_\omega \Bigg(\phi^{\mathrm{Sto}} \delta_\omega^{\mathrm{T}} + \sum_{t\in\mathcal{T}} \left(\phi^{\mathrm{Miss}} q_{t,\omega}^{\mathrm{Miss}} + \phi^{\mathrm{BM}} q_{t,\omega}^{\mathrm{BM}} \right) \Bigg) - \sum_{t\ \in\mathcal{T}} \sum_{j\in\mathcal{J}} \psi_t (b_{j,t}^+ + b_{j,t}^-) \tag{E.1c}$$

The objective function (E.1) minimizes the expected cost of the biomass contract selection. The first part (E.1a) contains the costs related to the biomass supply and the contract selection. In (E.1b), operational costs of the system, profits from electricity sales and inventory costs for biomass are modeled. Note, that the parameters $\widehat{L_t}$ and $\widehat{C_t^{\mathrm{AUX}}}$ are expected values for this tactical problem. The third part (E.1c) represents penalty and virtual costs. First, we penalize leftover biomass at the end of the planning period ($\phi^{\mathrm{Sto}}\delta_{\omega}^{\mathrm{T}}$), since we try to empty the storage at the end of the year. Second, missed heat-demand ($\phi^{\mathrm{Miss}}q_{t,\omega}^{\mathrm{Miss}}$) is penalized. Finally, we add a penalty for failing to meet the minimum share of heat production by biomass ($\phi^{\mathrm{BM}}q_{t,\omega}^{\mathrm{BM}}$). The second sum incentivizes the use options in certain periods with a very small profit (ψ_t). This allows to concentrate options in periods with a high variance in scenarios. In preliminary experiments it turned out, that there are equally good solutions as the price for options is the same over the year. When the inventory costs are low, the options and amounts can be shifted without deteriorating the objective. Therefore, we introduce this incentive to prioritize weeks with a high variance in demand.

$$\underline{N_j}u_j \leq \sum_{t\in\mathcal{T}} d_{j,t} \leq \overline{N_j}u_j \qquad \forall j \in \mathcal{J} \tag{E.2}$$

$$\sum_{\tau=t-\max\{\lfloor\frac{F_j}{168}\rfloor,0\}}^{t} d_{j,\tau} \leq \max\left\{\frac{168}{F_j},1\right\} \qquad \forall j \in \mathcal{J}, \forall t \in \mathcal{T} \tag{E.3}$$

$$b_{j,t} + b_{j,t}^{+} \leq \overline{B_j}d_{j,t} \qquad \forall j \in \mathcal{J}, \forall t \in \mathcal{T} \tag{E.4}$$

$$b_{j,t} - b_{j,t}^{-} \geq \underline{B_j}d_{j,t} \qquad \forall j \in \mathcal{J}, \forall t \in \mathcal{T} \tag{E.5}$$

$$b_{j,t}^{+} \leq O_j^{+}b_{j,t} \qquad \forall j \in \mathcal{J}, \forall t \in \mathcal{T} \tag{E.6}$$

$$b_{j,t}^{-} \leq O_j^{-}b_{j,t} \qquad \forall j \in \mathcal{J}, \forall t \in \mathcal{T} \tag{E.7}$$

$$\overline{b^{+}}_{j,t,\omega} \leq b_{j,t}^{+} \qquad \forall j \in \mathcal{J}, \forall t \in \mathcal{T}, \forall \omega \in \Omega \tag{E.8}$$

$$\overline{b^{-}}_{j,t,\omega} \leq b_{j,t}^{-} \qquad \forall j \in \mathcal{J}, \forall t \in \mathcal{T}, \forall \omega \in \Omega \tag{E.9}$$

Constraints (E.2) to (E.9) model the selection of biomass contracts. In constraints (E.2) the number of deliveries is restricted by the contract limits. Constraint (E.3) restricts the number of deliveries per week to a maximum according to the frequency of the contract. The left-hand side sums over several weeks, if the minimum time between visits F_j is longer than one week (168 hours). The right-hand side determines the maximum number of deliveries in that period with at least one delivery or more if the time difference is less than 168 hours. The total amount including up- and down-scaling options is limited by constraints (E.4) and (E.5) and the use of options in constraints (E.6) and (E.7). In constraints (E.8) and (E.9), it is ensured that the second-stage alterations

respect the first-stage decisions.

$$\underline{\Delta}_t \leq \delta_{t,\omega} \leq \overline{\Delta} \qquad \forall t \in \mathcal{T}, \forall \omega \in \Omega \qquad \text{(E.10)}$$

$$\delta_{t,\omega} = \delta_{t-1,\omega} + \delta^{+}_{t,\omega} - \delta^{-}_{t,\omega} \qquad \forall t \in \mathcal{T}, \forall \omega \in \Omega \qquad \text{(E.11)}$$

$$\delta^{+}_{t,\omega} = \sum_{j \in \mathcal{J}} \left(b_{j,t} + \overline{b^{+}}_{j,t,\omega} - \overline{b^{-}}_{j,t,\omega} \right) \cdot E^{\mathrm{B}} \qquad \forall t \in \mathcal{T}, \forall \omega \in \Omega \qquad \text{(E.12)}$$

$$\delta^{+}_{t,\omega} \leq \Delta^{\mathrm{F}} \qquad \forall t \in \mathcal{T}, \forall \omega \in \Omega \qquad \text{(E.13)}$$

$$\delta_{|\mathcal{T}|,\omega} \leq \delta_{0,\omega} + \delta^{\mathrm{T}}_{\omega} \qquad \forall \omega \in \Omega \qquad \text{(E.14)}$$

The biomass storage is modeled by constraints (E.10) to (E.14). The model ensures that the storage level is kept within the limits (E.10) and calculated correctly based on the previous level and in- and outflows (E.11). The initial storage level is given by $\delta_{0,\omega}$, which is the same for all scenarios. The inflow from supplier deliveries is calculated in constraints (E.12), where the incoming biomass is converted from tonnes to MWht using the calorific value of the biomass E^{B} and the outflow is restricted by constraints (E.13). Finally, the storage level at the end of the planning horizon is determined in (E.14) for penalty cost calculations.

$$\delta^{-}_{t,\omega} = \frac{p_{t,\omega}}{E^{\mathrm{CHP}}_{P}} - \Theta \cdot \frac{q^{\mathrm{CHP}}_{t,\omega}}{E^{\mathrm{CHP}}_{Q}} \qquad \forall t \in \mathcal{T}, \forall \omega \in \Omega \qquad \text{(E.15)}$$

$$\underline{P} \leq p_{t,\omega} - \Theta \cdot q^{\mathrm{CHP}}_{t,\omega} \leq \overline{P} \qquad \forall t \in \mathcal{T}, \forall \omega \in \Omega \qquad \text{(E.16)}$$

$$\Xi \cdot q^{\mathrm{CHP}}_{t,\omega} \leq p_{t,\omega} \qquad \forall t \in \mathcal{T}, \forall \omega \in \Omega \qquad \text{(E.17)}$$

$$q^{\mathrm{CHP}}_{t,\omega} \leq \overline{Q^{\mathrm{CHP}}} \qquad \forall t \in \mathcal{T}, \forall \omega \in \Omega \qquad \text{(E.18)}$$

$$q^{\mathrm{AUX}}_{t,\omega} \leq \overline{Q^{\mathrm{AUX}}} \qquad \forall t \in \mathcal{T}, \forall \omega \in \Omega \qquad \text{(E.19)}$$

The production capacities of the CHP plant and auxiliary boiler are enforced by constraints (E.15) to (E.19). In (E.15) the consumption of biomass from the storage for CHP production is determined based on the corresponding efficiency. The feasible region of the CHP, which was previously presented in Figure E.2, is modeled by constraints (E.16) to (E.18) and limits of the auxiliary boiler in (E.19).

$$D_{t,\omega} = q^{\mathrm{CHP}}_{t,\omega} + q^{\mathrm{AUX}}_{t,\omega} + q^{\mathrm{Miss}}_{t,\omega} \qquad \forall t \in \mathcal{T}, \omega \in \Omega \qquad \text{(E.20)}$$

$$q^{\mathrm{CHP}}_{t,\omega} \geq P^{\mathrm{B}} \cdot D_{t,\omega} - q^{\mathrm{BM}}_{t,\omega} \qquad \forall t \in \mathcal{T}, \omega \in \Omega \qquad \text{(E.21)}$$

Finally, the heat demand is ensured in constraint (E.20) while at least P^{B} percent per week have to be produced by biomass otherwise causing penalty costs (E.21).

Table E.3: Input parameters from biomass contract selection

$\mathbf{U_{j,w}} \in \mathbb{N}_0$	Number of deliveries of contract j in week w
$\mathbf{B_{j,w}} \in \mathbb{R}_0^+$	Contracted delivery amount of contract j in week w
$\mathbf{B^+_{j,w}} \in \mathbb{R}_0^+$	Contracted up-scaling of delivery amount of contract j in week w
$\mathbf{B^-_{j,w}} \in \mathbb{R}_0^+$	Contracted down-scaling of delivery amount of contract j in week w

E.4.2 Operational planning

The operational planning model relates to the second phase of the solution approach. For the overall solution approach, the model is solved consecutively week-by-week with a receding horizon to determine the production schedule and to adjust the biomass deliveries, if possible. Therefore, the planning horizon is $|\mathcal{W}|$ weeks with an hourly resolution. The week in focus is $\mathcal{W}_1$ and the remaining weeks $\mathcal{W}_2$ to $\mathcal{W}_\text{w}$ are used in the receding horizon to already include predictions for future periods. Thus, the decisions for weeks $\mathcal{W}_2$ to $\mathcal{W}_\text{w}$ can be altered again later, when the respective week comes in focus. Set $\mathcal{T}$ consists of all hours in the planning horizon, whereas $\mathcal{T}_\text{w}$ relates to the hours in specific week $\text{w} \in \mathcal{W}$.

The decision variables for this model decide the amount ($b_{j,t,\omega}$) and up- and down- scaling biomass ($\overline{b^+}_{j,t,\omega}$ and $\overline{b^-}_{j,t\omega}$) and the actual delivery times ($\hat{d}_{j,t,\omega}$) for the deliveries of contract j. Further variables are related to the biomass storage level ($\delta_{t,\omega}$), the thermal storage level ($s_{t,\omega}$), the heat and power production ($q^{\text{CHP}}_{t,\omega}$, $q^{\text{AUX}}_{t,\omega}$ and $p_{t,\omega}$) and the commitment status of the CHP plant ($x_{t,\omega}$, $y_{t,\omega}$ and $z_{t,\omega}$). The variables are also included in Table E.2.

Because the first week of the receding horizon is the week in focus, the first-stage decisions of the stochastic program are the delivery times and amounts $\hat{d}_{j,t,\omega}$, $b_{j,t,\omega}$, $\overline{b^+}_{j,t,\omega}$ and $\overline{b^-}_{j,t\omega}$ for periods t in the first week $\mathcal{T}_1$. For all other weeks, the decisions can be revised later and therefore are second-stage decisions. To ensure non-anticipativity, we include specific constraints.

The selection of biomass contracts and amounts are input parameters to this model (given in Table E.3) and determined by the biomass contract selection model in phase 1. Set $\mathcal{J}$ is reduced to only selected contracts for the corresponding week to limit the number of variables.

Furthermore, the storage levels and unit status of the preceding week are set as initial values. For example, the initial biomass storage level $\delta_{0,\omega}$ in the current week equals the storage level in the last period of previous week.

$$\min \sum_{\mathrm{w}\in\mathcal{W}} \sum_{j\in\mathcal{J}} \left(C_j^{\mathrm{B}} \mathbf{B}_{\mathbf{j},\mathrm{w}} + C_j^{\mathrm{B}+} \mathbf{B}_{\mathbf{j},\mathrm{w}}^{+} + C_j^{\mathrm{B}-} \mathbf{B}_{\mathbf{j},\mathrm{w}}^{-} \sum_{t\in\mathcal{T}_{\mathrm{w}}} C_j^{\mathrm{B}} (\overline{b^{+}}_{j,t} - \overline{b^{-}}_{j,t}) \right) \tag{E.22a}$$

$$+ \sum_{t\in\mathcal{T}} \sum_{\omega\in\Omega} \pi_\omega \left(C^{\mathrm{CHP}} (p_{t,\omega} - \Theta q_{t,\omega}^{\mathrm{CHP}}) - L_{t,\omega} p_{t,\omega} + C^{\mathrm{SU}} y_{t,\omega} + C^{\mathrm{SD}} z_{t,\omega} \right) \tag{E.22b}$$

$$+ \sum_{t\in\mathcal{T}} \sum_{\omega\in\Omega} \pi_\omega \left(C_{t,\omega}^{\mathrm{AUX}} \frac{q_{t,\omega}^{\mathrm{AUX}}}{E^{\mathrm{AUX}}} + C^{\mathrm{I}} \delta_{t,\omega} \right) + \sum_{t\in\mathcal{T}} \sum_{\omega\in\Omega} \pi_\omega \left(\phi^{\mathrm{Sto}} \delta_{t,\omega}^{\mathrm{EX}} + \phi^{\mathrm{Miss}} q_{t,\omega}^{\mathrm{Miss}} \right) \tag{E.22c}$$

As in the biomass contract selection model, the objective function (E.22) minimizes the expected costs composed of biomass contract costs (E.22a), operational for the CHP (E.22b), operational costs for the auxiliary and the biomass storage (E.22c), and penalty costs (E.22c). However, the following changes have to be made. First, the profit for electricity sales ($L_{t,\omega}$) and operational costs for the auxiliary boiler ($C_{t,\omega}^{\mathrm{AUX}}$) depend on scenarios (E.22b). Second, the operational cost (E.22b) now includes costs for starting up and shutting down the CHP plant. Third, the term (E.22c) penalizes unfulfilled heat demands and exceeding the biomass storage capacity. Note that to resemble the total weekly cost of the system, we keep the constant term $C_j^{\mathrm{B}} \mathbf{B}_{\mathbf{j},\mathrm{w}} + C_j^{\mathrm{B}+} \mathbf{B}_{\mathbf{j},\mathrm{w}}^{+} + C_j^{\mathrm{B}-} \mathbf{B}_{\mathbf{j},\mathrm{w}}^{-}$ in (E.22a).

$$\sum_{t\in\mathcal{T}_{\mathrm{w}}} \hat{d}_{j,t,\omega} = \mathbf{U}_{\mathbf{j},\mathrm{w}} \qquad \forall j \in \mathcal{J}, \forall \mathrm{w} \in \mathcal{W}, \forall \omega \in \Omega \tag{E.23}$$

$$\sum_{t\in\mathcal{T}_{\mathrm{w}}} b_{j,t,\omega} = \mathbf{B}_{\mathbf{j},\mathrm{w}} \qquad \forall j \in \mathcal{J}, \forall \mathrm{w} \in \mathcal{W}, \forall \omega \in \Omega \tag{E.24}$$

$$\sum_{t\in\mathcal{T}_{\mathrm{w}}} \overline{b^{+}}_{j,t,\omega} \leq \mathbf{B}_{\mathbf{j},\mathrm{w}}^{+} \qquad \forall j \in \mathcal{J}, \forall \mathrm{w} \in \mathcal{W}, \forall \omega \in \Omega \tag{E.25}$$

$$\sum_{t\in\mathcal{T}_{\mathrm{w}}} \overline{b^{-}}_{j,t,\omega} \leq \mathbf{B}_{\mathbf{j},\mathrm{w}}^{-} \qquad \forall j \in \mathcal{J}, \forall \mathrm{w} \in \mathcal{W}, \forall \omega \in \Omega \tag{E.26}$$

$$b_{j,t,\omega} + \overline{b^{+}}_{j,t,\omega} \leq \overline{B}_j \hat{d}_{j,t,\omega} \qquad \forall j \in \mathcal{J}, \forall t \in \mathcal{T}, \forall \omega \in \Omega \tag{E.27}$$

$$b_{j,t,\omega} - \overline{b^{-}}_{j,t,\omega} \geq \underline{B}_j \hat{d}_{j,t,\omega} \qquad \forall j \in \mathcal{J}, \forall t \in \mathcal{T}, \forall \omega \in \Omega \tag{E.28}$$

$$\sum_{\tau=t-F_j}^{t} \hat{d}_{j,\tau,\omega} \leq 1 \qquad \forall j \in \mathcal{J}, \forall t \in \mathcal{T}, \forall \omega \in \Omega \tag{E.29}$$

$$\sum_{j\in\mathcal{J}} \sum_{\tau=t}^{t+\Delta^{\mathrm{W}}} \hat{d}_{j,\tau,\omega} \leq 1 \qquad \forall t \in \mathcal{T}, \forall \omega \in \Omega \tag{E.30}$$

The biomass deliveries are handled in constraints (E.23) to (E.30). If deliveries were scheduled for the weeks in the planning horizon by phase 1, the operation model decides on the actual delivery times during the week (E.23). The weekly contracted amount is split on the deliveries in constraints (E.24). The delivery amount can be altered in the given limits of the options (constraints (E.25) and (E.26)), but the total amount must be within the limits of the contract (constraints (E.27) and (E.28)). Constraints (E.29) imposes a maximum frequency on the deliveries associated with each contract, while constraints (E.30) ensures an elapsed time of at least Δ^{W} periods between two deliveries irrespective of the supplier.

$$\hat{d}_{j,t,\omega} = \hat{d}_{j,t,\omega'}, \quad b_{j,t,\omega} = b_{j,t,\omega'} \qquad \forall j \in \mathcal{J}, \forall t \in \mathcal{T}_1, \forall \omega, \omega' \in \Omega, \omega \neq \omega' \tag{E.31}$$

$$\overline{b^+}_{j,t,\omega} = \overline{b^+}_{j,t,\omega'}, \quad \overline{b^-}_{j,t,\omega} = \overline{b^-}_{j,t,\omega'} \quad \forall j \in \mathcal{J}, \forall t \in \mathcal{T}_1, \forall \omega, \omega' \in \Omega, \omega \neq \omega' \tag{E.32}$$

As the decisions for the biomass delivery in the first week are first-stage decisions of the stochastic program, we have to ensure that they have the same values for each scenario. This is forced by the non-anticipativity constraints (E.31) to (E.32).

$$\delta^+_{t,\omega} = \sum_{j \in \mathcal{J}} \left(b_{j,t,\omega} + \overline{b^+}_{j,t,\omega} - \overline{b^-}_{j,t,\omega} \right) \cdot E^{\mathrm{B}} \qquad \forall t \in \mathcal{T}, \forall \omega \in \Omega \tag{E.33}$$

$$\delta_{t,\omega} = \delta_{t-1,\omega} + \delta^+_{t,\omega} - \delta^-_{t,\omega} \qquad \forall t \in \mathcal{T}, \forall \omega \in \Omega \tag{E.34}$$

$$\delta^-_{t,\omega} \leq \Delta^{\mathrm{F}} \qquad \forall t \in \mathcal{T}, \forall \omega \in \Omega \tag{E.35}$$

$$\delta_{t,\omega} \leq \overline{\Delta} + \delta^{\mathrm{EX}}_{t,\omega} \qquad \forall t \in \mathcal{T}, \forall \omega \in \Omega \tag{E.36}$$

$$\underline{\Delta}_t \leq \delta_{t,\omega} \qquad \forall \mathrm{w} \in \{2, \ldots, |\mathcal{W}|\}, \forall t \in \mathcal{T}_{\mathrm{w}}, \forall \omega \in \Omega \tag{E.37}$$

$$0 \leq \delta_{t,\omega} \qquad \forall t \in \mathcal{T}_1, \forall \omega \in \Omega \tag{E.38}$$

The inflow to the biomass storage in each period (E.33) is dependent on the scheduled delivery and adjustments based on the options. The storage level is given by equation (E.34). The outflow and capacity of the storage is limited in constraints (E.35) and (E.36), respectively. The safety storage for biomass is incorporated in constraints (E.37), but only for future weeks in the receding horizon. In the current week, the storage can be used for production (E.38).

$$\delta^-_{t,\omega} = \frac{p_{t,\omega}}{E^{\mathrm{CHP}}_P} - \Theta \cdot \frac{q^{\mathrm{CHP}}_{t,\omega}}{E^{\mathrm{CHP}}_Q} \qquad \forall t \in \mathcal{T}, \forall \omega \in \Omega \tag{E.39}$$

$$\underline{P} \cdot x_{t,\omega} \leq p_{t,\omega} - \Theta \cdot q_{t,\omega}^{\mathrm{CHP}} \leq \overline{P} \cdot x_{t,\omega} \qquad \forall t \in \mathcal{T}, \forall \omega \in \Omega \qquad \text{(E.40)}$$

$$\Xi \cdot q_{t,\omega}^{\mathrm{CHP}} \leq p_{t,\omega} \qquad \forall t \in \mathcal{T}, \forall \omega \in \Omega \qquad \text{(E.41)}$$

$$q_{t,\omega}^{\mathrm{CHP}} \leq \overline{Q^{\mathrm{CHP}}} \cdot x_{t,\omega} \qquad \forall t \in \mathcal{T}, \forall \omega \in \Omega \qquad \text{(E.42)}$$

$$y_{t,\omega} - z_{t,\omega} = x_{t,\omega} - x_{t-1,\omega} \qquad \forall t \in \mathcal{T}, \forall \omega \in \Omega \qquad \text{(E.43)}$$

$$y_{t,\omega} + z_{t,\omega} \leq 1 \qquad \forall t \in \mathcal{T}, \forall \omega \in \Omega \qquad \text{(E.44)}$$

$$\sum_{\tau=t-M^U+1}^{t} y_{\tau,\omega} \leq x_{t,\omega} \qquad \forall t \in \mathcal{T}, \forall \omega \in \Omega \qquad \text{(E.45)}$$

$$\sum_{\tau=t-M^D+1}^{t} z_{\tau,\omega} \leq 1 - x_{t,\omega} \qquad \forall t \in \mathcal{T}, \forall \omega \in \Omega \qquad \text{(E.46)}$$

$$p_{t,\omega} - p_{t-1,\omega} \leq R^U \cdot x_{t-1,\omega} + \underline{P} \cdot y_{t-1,\omega} \qquad \forall t \in \mathcal{T}, \forall \omega \in \Omega \qquad \text{(E.47)}$$

$$p_{t,\omega} - p_{t-1,\omega} \geq -R^D \cdot x_{t,\omega} - \underline{P} \cdot z_{t,\omega} \qquad \forall t \in \mathcal{T}, \forall \omega \in \Omega \qquad \text{(E.48)}$$

Constraints (E.39) to (E.42) regarding biomass consumption and feasible production region of the CHP unit constraints are similar to constraints (E.15) to (E.18) for the biomass selection problem. However, here the production depends also on the status of the unit ($x_{t,\omega} = 1$ means the unit is on). The status of the unit is determined by constraints (E.43) to (E.44) while constraints (E.45) and (E.46) ensure minimum up- and down times, respectively. The change of production volume is restricted to the ramping requirements in constraints (E.47) and (E.48). The initial status of the CHP plant depends on the previous week and is given by $x_{0,\omega}$ and $p_{0,\omega}$ as input parameters.

$$q_{t,\omega}^{\mathrm{AUX}} \leq \overline{Q^{\mathrm{AUX}}} \qquad \forall t \in \mathcal{T}, \forall \omega \in \Omega \qquad \text{(E.49)}$$

$$s_{t,\omega}^{+} = q_{t,\omega}^{\mathrm{CHP,S}} + q_{t,\omega}^{\mathrm{GB,S}} \qquad \forall t \in \mathcal{T}, \forall \omega \in \Omega \qquad \text{(E.50)}$$

$$s_{t,\omega} = s_{t-1,\omega} + s_{t,\omega}^{+} - s_{t,\omega}^{-} \qquad \forall t \in \mathcal{T}, \forall \omega \in \Omega \qquad \text{(E.51)}$$

$$\underline{S} \leq s_{t,\omega} \leq \overline{S} \qquad \forall t \in \mathcal{T}, \forall \omega \in \Omega \qquad \text{(E.52)}$$

$$s_{t,\omega}^{-} \leq S^{\mathrm{F}} \qquad \forall t \in \mathcal{T}, \forall \omega \in \Omega \qquad \text{(E.53)}$$

$$s_{t,\omega}^{+} \leq S^{\mathrm{F}} \qquad \forall t \in \mathcal{T}, \forall \omega \in \Omega \qquad \text{(E.54)}$$

$$s_{t,\omega}^{-} \leq s_{t-1,\omega} \qquad \forall t \in \mathcal{T}, \forall \omega \in \Omega \qquad \text{(E.55)}$$

$$s_{|\mathcal{T}_{\mathrm{w}}|,\omega} = s_{0,\omega} \qquad \forall \omega \in \Omega \qquad \text{(E.56)}$$

Constraints (E.49) sets the heat production capacity of the auxiliary boiler. The heat storage is modeled by constraints (E.50) to (E.56). The inflow is determined by the heat from the CHP unit and auxiliary boiler inserted into the storage (E.50). The current storage level depends on the inflow, outflow and previous level (E.51) ($s_{0,\omega}$ for the initial value) and has to satisfy the capacity restrictions (E.52). Outflow (E.53) and inflow (E.54) are limited and the inflow

Algorithm 6 Two-phase solution approach

1: Solve the biomass contract selection model (E.1)-(E.21)
2: **for** each week in the overall planning horizon **do**
3: Select the corresponding contract decisions from line 1 and set limits
4: Generate scenarios for the current receding horizon
5: Solve the operational planning model (E.22)-(E.59)
6: **end for**

cannot directly flow out again (E.55). To avoid emptying the storage at the end, the initial level $s_{0,\omega}$ must be reached again at the end of the receding horizon (E.56).

$$q_{t,\omega}^{\text{CHP}} = q_{t,\omega}^{\text{CHP,N}} + q_{t,\omega}^{\text{CHP,S}} \qquad \forall t \in \mathcal{T}, \forall \omega \in \Omega \qquad \text{(E.57)}$$

$$q_{t,\omega}^{\text{AUX}} = q_{t,\omega}^{\text{AUX,N}} + q_{t,\omega}^{\text{AUX,S}} \qquad \forall t \in \mathcal{T}, \forall \omega \in \Omega \qquad \text{(E.58)}$$

$$D_{t,\omega} = q_{t,\omega}^{\text{CHP,N}} + q_{t,\omega}^{\text{AUX,N}} + s_{t,\omega}^{-} + q_{t,\omega}^{\text{Miss}} \qquad \forall t \in \mathcal{T}, \forall \omega \in \Omega \qquad \text{(E.59)}$$

The heat production by both units is used for filling the heat storage and covering the demand. Therefore, the production is split up into those two components in constraints (E.57) and (E.58). For fulfilling the heat demand, heat directly fed to the district heating network and heat from the thermal storage is used (E.59). Any shortfall of heat is penalized in the objective function.

E.4.3 Overall solution approach

For the overall solution approach, the above mentioned stochastic programming models are combined. To solve the planning problem for one year, we need to perform the steps shown in Algorithm 6. First, the contract selection takes place (line 1). Afterward, this decision is transfered to the weekly planning (line 3). The scenario generation and solution of the operational problem is carried once every week for the next week (line 2 to 6).

E.5 Case studies

In the following we analyze two case studies for different municipalities in Denmark, named A and B, that are connected to the Aarhus district heating network. The planning horizon we consider in the numerical results in Section E.6 is 1st of June 2016 to 31st of May 2017.

E.5.1 Technical data

The heat demand data in the district heating networks is obtained from [E27], NordPools' hourly electricity prices for DK1 zone from [E28] and daily natural gas prices from [E29]. Extreme outlier values in electricity prices are limited to a maximum or minimum of four standard deviations from the mean.

The technical parameters for the CHP and auxiliary units as well as the operation costs are based on [E13, E30, E31] and [E2] and shown in Tables E.4, E.5 and E.6. Both systems comprise a CHP unit and one auxiliary boiler. Municipality A uses a gas boiler in addition to the CHP, while municipality B uses an electric boiler. The biomass storage minimum level $\underline{\Delta}_t$ is divided in two values. In weeks 20 - 45 (i.e. in the heating season), we have a higher minimum level as in the remaining weeks of the year. The penalty costs for both case are the same and set to $\Phi^{\text{Sto}} = 1000, \Phi^{\text{Miss}} = 10000$ and $\Phi^{\text{BM}} = 5000$.

The parameters of the biomass contracts data are given in Table E.7, where they are organized from *fixed* contracts at the top of the table and gradually going down to more *flexible* contracts. Both cases use the same set of contracts.

The very small incentive ψ_t for using options preferably in periods with a high variance in heat demand scenarios is calculated as follows. As this is a weekly value for the biomass contract selection phase only, we consider the weekly heat demand scenarios in phase 1. This data is known before solving the model and therefore we can use the scenario information to calculate the incentive. We order the weeks t in descending order of difference in heat demands in the scenarios, i.e, $max_{\omega\in\Omega}\{D_{t,\omega}\} - min_{\omega\in\Omega}\{D_{t,\omega}\}$. The week with the largest difference gets the highest incentive of 5.2. We reduce the incentive every week by 0.1 resulting in an incentive of 0.1 for the week with the smallest difference. These values are far less than the cost of the biomass options themselves and, therefore, have barely influence on the amounts contracted in options but only on the weeks where they are placed. Note that this incentive is not part of the evaluation in Section E.6 as it is only in the biomass contract selection and the cost are based on the operational planning.

Table E.4: Technical parameters of the CHP unit

	$\overline{P}$	$\underline{P}$	$\overline{Q^{\mathrm{CHP}}}$	Θ	Ξ	R^U	R^D	E_P^{CHP}	E_Q^{CHP}	M^U	M^D
A	13.24	3.8	20.8	-0.18	0.55	3.7	3.7	0.62	0.31	6	4
B	35.18	5.72	47.28	-0.12	0.64	4.6	4.6	0.64	0.29	8	5

Table E.5: Technical parameters of the auxiliary unit and storages

	Aux. boiler		Thermal storage				Biomass storage					
	E^{AUX}	$\overline{Q^{\mathrm{AUX}}}$	S^0	S^F	$\overline{S}$	$\underline{S}$	Δ^{F}	Δ^0	Δ^{W}	$\overline{\Delta}$	$\underline{\Delta}_t$	E^{B}
A	0.97	15	5	3	7	0	35	500	24	20000	4000 (20-45) 2000	4.9971
B	0.99	30	6.5	4.5	9.5	0	70	850	24	35000	7000 (20-45) 3500	4.9971

Table E.6: Cost parameters

	CHP					Aux. boiler			Storage
	C^{CHP}	C^{SU}	C^{SD}	T^{EP}	I	$C_{Aux}^{\mathrm{O\&M}}$	T^{AUX}	$T^{\mathrm{CO_2}}$	C^{I}
A	19.85	14250	0	55.62	20.25	0.07	28.22	6.34	0.0002
B	20.32	16870	0	55.62	20.25	0.5	52.07	0	0.0002

Table E.7: Biomass contract data

Contract	C_j^{B}	$C_j^{\mathrm{B}+}$	$C_j^{\mathrm{B}-}$	O_j^+	O_j^-	$\overline{B_j}$	$\underline{B_j}$	F_j	$\overline{N_j}$	$\underline{N_j}$
1	150.8	0	0	0	0	19000	18000	2016	4	4
2	156.4	0	0	0	0	17000	12000	1344	5	2
3	170.83	0	0	0	0	15000	11000	1008	8	4
4	181.31	30.56	30.56	0.1	0.1	12000	8000	504	17	15
5	181.43	24.45	24.45	0.15	0.15	12000	8000	504	15	15
6	183.59	30.56	30.56	0.25	0.25	5100	2380	336	25	24
7	183.43	36.67	36.67	0.25	0.25	5100	2380	336	25	15
8	201.89	18.34	18.34	0.5	0.5	1200	1200	168	50	50
9	202.17	18.34	18.34	0.5	0.5	1200	1000	168	50	25
10	204.29	28.12	28.12	0.5	0.5	850	850	120	60	50
11	202.24	28.12	28.12	0.65	0.65	850	500	120	60	30
12	202.05	12.22	12.22	0.75	0.75	350	100	48	100	80
13	202.64	12.22	12.22	0.75	0.75	350	100	48	100	50

E.5.2 Scenario generation

Apart from the deterministic parameters mentioned in the previous section, we have to handle uncertainty regarding heat demands, gas prices and electricity prices to be used in the optimization. Since both municipalities are within the same bidding region in Nordpool (DK1) and the same gas trading region, the electricity and natural gas prices are identical. However, differences exist regarding the heat demand. We use historical data from 1st June 2011 to 31st May 2016 for electricity prices, natural gas prices and heat demands. Based on this data, different techniques for scenario generation are implemented. The resulting scenarios and expected values depend on the municipality due to the different auxiliary boilers and heat consumption in previous years. Furthermore, the input time series varies with the phase of the solution approach regarding time scales and need for scenarios. The scenario generation for both phases is described in Appendix E.8.

E.5.3 Evaluation of solution approach

To evaluate our solution approach, we have to obtain the costs under different realizations of the uncertainty. We use 11 samples, i.e, 11 different realizations of uncertainty, for each municipality. Sample 0 is the actual realization of the heat demand, electricity prices and gas prices from 1st June 2016 to 31st May 2017. The remaining 10 samples (from 1 to 11) are a composite of different real data sets obtained from the same sources as the previous data. The electricity and gas prices are obtained from real data of 2015, 2016 and 2017 from other regions in Nordpool and other European hubs, respectively. The heat consumption is obtained from other municipalities in the Aarhus district heating system and scaled to the size of the system capacity accordingly.

The scenarios used in the evaluations are based on a combination of past data and time series forecasts (see description in Appendix E.8). To decide the biomass supply contracts, we use expected values for electricity and gas prices based on the last five years, while the heat demand is modeled using five scenarios resembling the heat demand from the last five years. In the operational planning problem, the scenarios for electricity prices and heat demand consist of a time series forecast for the next week while the corresponding historical values of electricity prices and heat demand in previous years are taken for the remaining weeks of the receding horizon (denoted as method *F1*). See Appendix E.9 for a comparison of different scenario generation methods.

Evaluating one sample with a configuration of our method requires to extend

Table E.8: Objective value and penalty costs [x100,000€] for different lengths of receding horizon

Sample		Objective				Penalty q^{miss}			
		1	2	3	4	1	2	3	4
Municipality A	0	91.635	**84.505**	84.548	84.687	7.576	1.376	1.376	1.376
	1	96.483	84.571	84.540	**84.505**	10.993	0.000	0.000	0.000
	2	87.707	81.793	81.810	**81.710**	4.653	0.000	0.000	0.000
	3	96.915	**84.364**	84.407	84.389	11.521	0.000	0.000	0.000
	4	90.140	**82.205**	82.455	82.394	6.582	0.000	0.000	0.000
	5	86.659	83.756	83.735	**83.707**	2.130	1.010	1.010	1.010
	6	104.655	82.764	82.660	**82.511**	21.334	0.000	0.000	0.000
	7	89.979	**87.009**	87.027	87.031	5.832	2.904	2.904	2.904
	8	89.700	82.035	**81.846**	81.847	7.187	0.000	0.000	0.000
	9	84.836	**82.469**	82.588	82.609	1.192	0.000	0.000	0.000
	10	84.900	**83.515**	83.635	83.580	0.439	0.131	0.131	0.131
Municipality B	0	400.734	**169.017**	169.186	169.682	231.804	1.297	1.297	1.297
	1	246.238	**174.582**	175.025	175.056	71.916	0.000	0.000	0.000
	2	267.247	167.181	**167.022**	167.371	95.517	0.000	0.0 00	0.000
	3	286.542	175.332	175.059	**175.059**	111.651	0.000	0.000	0.000
	4	318.557	169.592	169.334	**168.766**	147.841	0.000	0.000	0.000
	5	386.050	170.939	170.776	**170.597**	216.553	1.335	1.335	1.335
	6	171.352	170.397	**170.390**	171.026	0.000	0.000	0.000	0.000
	7	275.865	172.744	172.742	**172.672**	104.186	0.000	0.000	0.000
	8	169.469	168.003	167.982	**167.525**	0.000	0.000	0.000	0.000
	9	323.960	**171.312**	171.693	171.845	152.953	0.000	0.000	0.000
	10	397.496	169.546	169.399	**168.974**	225.878	0.000	0.000	0.000

Algorithm 6 by one step. Each week after the operational problem is solved (line 5 in Algorithm 6), we fix the first-stage decisions and solve the model using the realizations of the uncertainty of the first week. Thus, we obtain the real costs for the first week and the initial status for the next week.

E.6 Experimental results

For the experimental evaluation, we implemented Algorithm 6 using Python 3.5.1 and Gurobi 7.0.1 (default parameters). All experiments are run on Intel Xeon Processor X5550 with 24 GB RAM. The objective values in this section comprise the real costs summed over all weeks in the year.

E.6.1 Analysis of receding horizon length

Table E.8 shows the objective value and penalty costs using scenarios generated by method *F1* for different lengths of the receding horizon, namely one, two, three and four weeks. Note that in no case, penalty costs for exceeding the biomass storage capacity occurred and therefore those are omitted from the table. The most important result is that the objective values drastically improves by including at least a second week into the optimization. For the most part, this is due to the reduction in penalty costs for not fulfilling the heat demand (see Table E.8). This can be explained by the opportunity of using of options. Indeed, if the receding horizon already considers scenarios for weeks apart from the current week, we make use of this information now. If the biomass contract selection (phase 1) scheduled a delivery only in the current week, but not in the next week, having a longer planning horizon can be beneficial. If we only consider the current week, we may not make use of an upward option, because it is not needed now. However, if the scenarios for the next week(s) show a trend with a higher heat demand than expected, we can get more biomass than scheduled now instead of running out of storage and missing the demand.

For a receding horizon of more than one week, the results are quite similar. The maximum deviation between costs for the different lengths is 82548 for municipality B in sample 4, which is in total approximately 0.48% higher costs. For all other cases, the relative and absolute difference is less. In some cases, a longer horizon can lead to slightly poorer results due to the fact, that the heat demand is still uncertain and we may make use of an upward or downward option that corrects the delivery amount according to the uncertain scenarios. If the scenarios show a wrong trend in later weeks, it can be more beneficial to just include a second week (e.g. sample 0, mun. A). The penalty cost for missing the heat demand is $\phi^{\text{Miss}} = 10000$ [€/MWh], which means we miss at most 29.0356 MWh of heat in sample 7 for municipality A in a whole year. In all cases with penalty cost, the missing demand occurs in periods with an exceptionally high demand close to the capacity of the system. Those very high demands are often not covered by the scenarios and therefore wrong planning decisions may cause a shortage of biomass and a penalization for not satisfying the heat demand. Note that in practice a lack of supply in the district heating network would never occur, because the heat producer can gradually decrease the supply temperature or reduce the water flow to increase the demand covered. However, these cases must be avoid and therefore we penalize them in the objective.

Table E.9: Comparison stochastic programming (Sto.) vs. expected value solution (Exp.) [x100,000€]. The maximum, minimum and average values are based on 2 to 4 weeks horizon

	Sample	Max. Sto.	Min. Exp.	Delta	Avg. Sto.	Avg. Exp.	Delta
Municipality A	0	**84.687**	84.975	0.34%	**84.580**	85.117	0.63%
	1	**84.571**	85.331	0.89%	**84.539**	85.343	0.94%
	2	**81.810**	82.010	0.24%	**81.771**	82.208	0.53%
	3	**84.407**	85.205	0.94%	**84.387**	85.315	1.09%
	4	**82.455**	82.853	0.48%	**82.352**	83.008	0.79%
	5	**83.756**	84.354	0.71%	**83.733**	84.462	0.86%
	6	**82.764**	83.210	0.54%	**82.645**	83.253	0.73%
	7	**87.031**	87.744	0.81%	**87.022**	87.769	0.85%
	8	**82.035**	82.445	0.50%	**81.909**	82.501	0.72%
	9	**82.609**	83.381	0.93%	**82.556**	83.475	1.10%
	10	**83.635**	84.006	0.44%	**83.577**	84.072	0.59%
	Avg.	**83.615**	84.138	0.62%	**83.552**	84.229	0.80%
Municipality B	0	**169.682**	172.264	1.50%	**169.295**	172.264	1.72%
	1	**175.056**	177.669	1.47%	**174.888**	177.694	1.58%
	2	**167.371**	170.974	2.11%	**167.191**	170.986	2.22%
	3	**175.332**	176.147	0.46%	**175.150**	176.183	0.59%
	4	**169.592**	171.702	1.23%	**169.231**	171.720	1.45%
	5	**170.939**	172.536	0.93%	**170.770**	172.546	1.03%
	6	**171.026**	171.303	0.16%	**170.604**	171.328	0.42%
	7	**172.744**	174.844	1.20%	**172.719**	174.844	1.22%
	8	**168.003**	168.231	0.14%	**167.837**	168.234	0.24%
	9	**171.845**	172.635	0.46%	**171.617**	172.641	0.59%
	10	169.546	**169.456**	-0.05%	**169.306**	169.703	0.23%
	Avg.	**171.012**	172.524	0.87%	**170.783**	172.558	1.03%

E.6.2 Stochastic programming vs. expected value solution

To show the benefit of using stochastic programming instead of using an expected value approach, we compare the results in Table E.9. We limit our results to *F1* scenarios and 2 to 4 weeks of receding horizon. The first three columns in Table E.9 compare the worst case among the three lengths of receding horizon in the stochastic approach with the best case of the expected value solution. The worst case stochastic solution gives on average a 0.75% better solution and it dominates in all cases except one (municipality B, sample 10). When comparing the average objective values, the stochastic approach improved the results on average by 0.80% for municipality A and 1.03% for municipality B. Although the improvement is not relatively large, in absolute terms it results in saving on average €67743 and €177583, respectively.

The improvement can be explained by the fact that the stochastic solution makes use of options while the expected value solution does not contract any options (see Section E.6.3 for more details).

E.6.3 Interpretation of results for real data from 2016-2017

In this section, we describe the results of the contract selection and operational planning in more detail. As an example, we analyze sample 0 for both municipalities, which contains the real data from 1st June 2016 to 31 May 2017. We would like to point out that the conclusions drawn in this section coincides with the observations from the other samples.

Figure E.3 shows the selected biomass contracts for municipalities A and B in the stochastic (*Sto*) and expected value solution (*Exp*), respectively. The contracts are valid for all samples. The points show the contracted biomass amount and the vertical lines that extent from some of the crosses are the amount of upward and downward options bought. We see that only the solutions obtained by the stochastic approach make use of options. As the deterministic solution has no scenarios and assumes the expected values of uncertain parameters as deterministic, the contracts are selected in such a way that the solution fits these expected values. Thus, no use of options is reasonable in this case. However, when other biomass amounts are needed in the course of the year, the options contracted in the stochastic solution bring an advantage and reduce the overall cost (see Table E.9). From Figure E.3 also the difference in the delivery patterns for the two municipalities can be seen. The selected contract for municipality A (contract 12) has smaller amounts but more frequent deliveries. Whereas

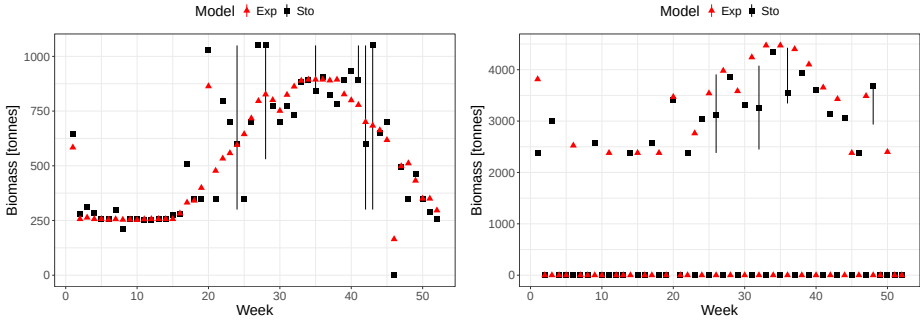

(a) Municipality A (selected contract: 12) **(b)** Municipality B (selected contract: 7)

Figure E.3: Biomass contracts from 1 June 2016 to 31 May 2017

the selected contract for municipality B has larger amounts and less deliveries, which relates also to the higher heat demand in municipality B.

The actual delivery amounts, i.e., after making use of options, and the biomass storage level are depicted in Figure E.4 for the real data of the year 2016 to 2017. The amounts are cumulated per week. Furthermore, the contracted delivery amount is depicted to show if the options are actually used in the course of the year. For both municipalities the operational problem uses both upward and downward options, for example, week 24 (downward) and 42 (upward) in municipality A or week 26 (downward) and 48 (upward) in municipality B.

The heat production from June 2016 to May 2017 for municipality A and B is shown in Figure E.5. In both cases the heat demand was always fulfilled and the production follows similar behavior. At start of the season, the demand can be covered by the biomass-fired CHP. During the winter periods with a high demand, the gas boiler is used in addition to the CHP to cover the heat demand. Furthermore, at the end of the season the boiler is used more often as in the beginning of the season due to a slightly higher demand and the biomass contract decisions contracting less biomass in the end of the season.

E.6.4 Runtime analysis

Figure E.6 shows the runtimes for different lengths of the receding horizon averaged over the 11 samples. The corresponding MIP model sizes for the biomass selection and the operational planning problem with different lengths of the receding horizon are given in E.10. Note that the model size for each week in the operational planning phase is the same throughout the planning horizon.

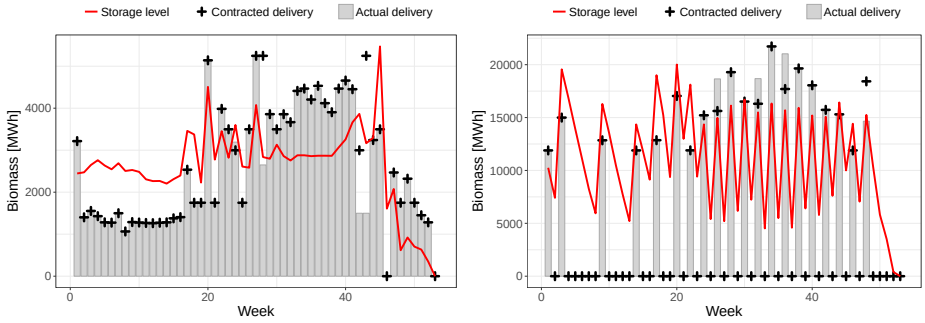

(a) Municipality A **(b)** Municipality B

Figure E.4: Biomass storage level and deliveries for the real realization of uncertainties from 1st June 2016 to 31 May 2017 (based on *F1* scenarios and two weeks of receding horizon)

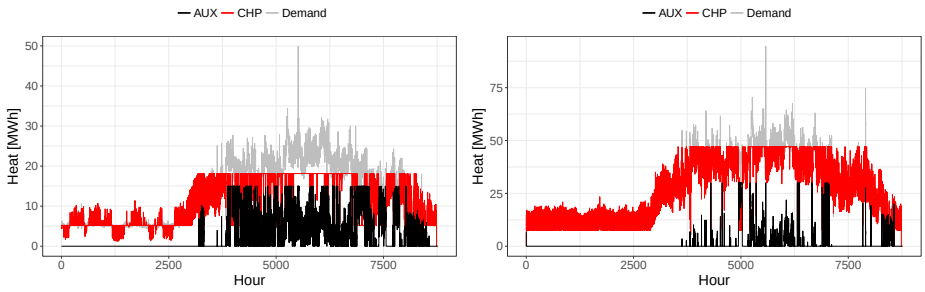

(a) Municipality A **(b)** Municipality B

Figure E.5: Heat production for real realization of uncertainties from 1st June 2016 to 31 May 2017 (based on *F1* scenarios and two weeks of receding horizon)

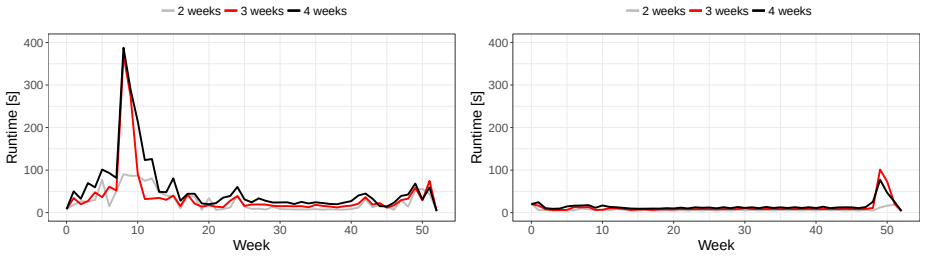

(a) Municipality A **(b)** Municipality B

Figure E.6: Average runtimes per week (week 0 corresponds to biomass contract selection)

Table E.10: Model sizes

	Cont. var.	Int. var.	(thereof bin. var.)	Constraints	NZs
Biomass selection	10,878	689	(13)	1,3812	40,479
Operational - 1 week	15,125	3,360	(3,360)	39,495	152,180
Operational - 2 weeks	30,250	6,720	(6,720)	65,530	284,900
Operational - 3 weeks	45,375	10,080	(10,080)	91,615	417,620
Operational - 4 weeks	60,500	13,440	(13,440)	117,675	550,340

Therefore, the model sizes depend only on the length of the receding horizon. For most of the cases, the runtime to solve the operational model for one week is less than 60 seconds. Also, the biomass contract selection model is solved in less than 20 seconds for both municipalities (see week 0 in Fig. E.6). The runtime slightly increases with a longer receding horizon, but not significantly.

For the few cases with a high runtime the average lies below 400 seconds (see E.6a), which is short enough for a weekly planning problem to be used in practice. The weeks with higher runtime relate to samples where the heat demand is higher than expected in the biomass contract selection phase, which leads to a shortage of biomass in the subsequent weeks (in the beginning of the year in municipality A and in the end of the year in municipality B). Due to this shortage the model tries to avoid penalties for getting below the safety storage level while producing as much as possible with the CHP to get income from the electricity market. As the production is not possible in all hours, the model has to select the hours with highest expected electricity prices making it harder for the solver to find the best solution as the electricity prices are close to each other.

E.7 Summary and outlook

In this work, we propose a solution approach that optimizes the biomass supply planning for a large-scale CHP producer using biomass. The decision-making process is divided into two phases both using two-stage stochastic programs. The first model, named *biomass contract selection*, is solved for a long-term horizon with weekly periods and configures the contracts from a set of biomass suppliers. Those decisions are used in the second model, named *operational planning*, to optimize the heat production. This solutions approach corresponds to the planning process in practice. We evaluate our method on two case studies with realistic requirements and historical data to create scenarios. We analyze several scenario generation possibilities to create the scenarios based on past data and different forecasting tools. Our analysis investigates the results obtained for 11 samples of realizations of uncertainty.

The results reflect that the use of a receding horizon improves the solution obtained due to a better operation of both heat and biomass storages. However, as a result of the forecast uncertainty, very long receding horizons may not improve the results. Furthermore, we show that applying stochastic programming is required to make use of the options, yielding better results than in the expected value case where no options are purchased.

We envision four future research directions. First, further uncertainties regarding the delivery of biomass such as amount and quality variations could be included in a supply chain planning model. Second, the configuration of our algorithm can be investigated further to determine the length of the receding horizon in a better way and improve the results. Third, an economic analysis of the options can be made to assess their benefit for the entire supply chain. That is from both supplier's and producer's points of view. Finally, the comparison of different long-term forecasting tools with the use of data from previous years to create long-term scenarios is another future research direction.

Table E.11: Minimum objective value [x100,000€] for each mode of scenario generation. The minimum refers to the lowest objective value of 1, 2, 3 or 4 weeks of receding horizon

S.	Municipality A					Municipality B				
	P	F1	F1+P	F2	F2+P	P	F1	F1+P	F2	F2+P
0	84.61	**84.51**	84.63	84.88	85.08	169.25	**169.02**	169.20	169.28	169.27
1	84.62	**84.50**	84.61	84.78	84.59	174.94	**174.58**	174.66	174.99	174.63
2	81.69	81.71	**81.67**	81.72	81.79	167.19	**167.02**	167.30	167.69	167.33
3	84.55	**84.36**	84.46	84.53	84.48	175.23	**175.06**	175.20	175.23	175.18
4	82.52	**82.21**	82.46	82.32	82.48	169.13	**168.77**	169.05	169.36	169.26
5	83.85	**83.71**	83.82	83.82	83.83	170.66	170.60	170.61	170.71	**170.53**
6	82.61	**82.51**	82.58	83.36	83.14	170.56	**170.39**	170.45	170.82	170.82
7	87.04	**87.01**	87.02	87.34	87.21	172.94	**172.67**	172.76	173.09	173.02
8	82.09	**81.85**	81.87	81.85	81.95	167.82	167.52	167.71	**167.03**	167.48
9	82.59	**82.47**	82.52	82.54	82.57	171.42	**171.31**	171.36	171.32	171.52
10	83.55	83.52	**83.51**	83.71	83.65	169.45	168.97	169.31	169.04	**168.82**

Appendices

E.8 Scenario generation

In this section, we describe the different approaches used for scenario generation in biomass contract selection and operational planning problem, respectively.

E.8.1 Biomass contract selection

In phase one of the solution approach, scenarios for the heat demand and the expected value for auxiliary boiler costs and electricity prices are part of the model. In this tactical planning problem, we use the heat consumption of the five previous years (i.e. 1st June 2011 - 31st May 2016) from summer to summer of the respective community as heat demand scenarios ($D_{t,\omega}$) resulting in five scenarios. The probability for each scenario is determined based on the year while giving a higher probability to more recent years (first three years: 0.15, last two years: 0.275).

The expected values for electricity and natural gas prices are obtained by calculating a linear combination of the observations of the last five years weighted by the probability ($\widehat{x_t} = \sum_{i=1}^{5} \pi_{\omega_i} x_{t,i}$ where x_t is the price for time period $t \in \mathcal{T}$ in year i). Due to the weekly time periods, the values are averaged per week.

E.8.2 Operational planning problem

In the operational planning more recent information is available for the scenario generation, because we obtain new observations after each week. Furthermore, we are closer to actual delivery time than in the biomass contract selection problem. Consequently, we can use time series analysis to better predict the uncertainties by updating the models in every week.

There a different possibilities to obtain scenarios for the operational model. We implement and analyze five different types of scenario generation:

Using past data as predictions (P) Data from previous years is used to built scenarios analog to the biomass contract selection scenarios. The scenarios consist of the data from the respective week(s) in previous years.

Combining time series models and past data as predictions (F1) In this method, we use time series models to predict the first week of the receding horizon and use data from previous years for the remaining weeks of the receding horizon. The time series model uses the most recent observations to update the forecast for the following week. We use an ARMAX model [E32] with weekly seasonality of prices and consumption using Fourier series in the form of exogenous parameters [E33]. We use past data for the remaining weeks because they are further into the future and the risk of inaccurate predictions is higher. To create scenarios from the time series model, we follow the scenario generation process described in [E34]. More specifically, we generate 2500 equiprobable scenarios using Monte Carlo simulation and cluster them using the k-medoid algorithm to obtain five representative scenarios [E35]. The forecasted scenarios for the first week have to be combined with data from previous years to get a scenario for the entire receding horizon. Therefore, we add the data from the most recent year to the scenario with the highest probability.

Using time series models as predictions (F2) This method is similar to *F1*, because it also uses time series models for predictions and uses Monte Carlo simulation and clustering for generating scenarios. However, in this case we make predictions for the entire receding horizon and do not combine with past data. The time series models, forecasts and scenarios are obtained following the same method as for *F1*.

All three above mentioned methods result in five scenarios for the operational

planning problem. As two further possibilities for scenario generation, we use combinations of these methods. Namely, we combine the scenarios obtained from historical data (P) with the two time-series-based methods ($F1$ and $F2$) resulting in ten scenarios. Note that the probabilities are normalized to result in a sum of one again. These methods are denoted by $P{+}F1$ and $P{+}F2$.

Note that the above mentioned scenario generation is used for electricity prices and heat demands. For the gas prices in case study A with the gas boiler, we also use an expected value in the operational model. This is due to the fact, that gas prices are daily prices and are not as volatile as, e.g., the electricity price, and we deem the expected value as accurate enough for this model.

E.9 Analysis of scenario generation methods

In this section, we compare the different methods for scenario generation. The results show the performance of the scenario method configuration for the operational planning problem presented in Section E.8 of this Appendix.

Table E.11 shows the results for each sample of both municipalities. The value shown is the minimum overall costs per scenario generation method, where the minimum is taken over the minimum objective value obtained for four different lengths of the receding horizon (one, two, three or four weeks). The analysis of different receding horizon lengths is described in Section 6.1 of the main article. Based on Table E.11, the best of the implemented scenario generation methods is *F1*, i.e., updating the scenarios every week by forecasting the next week of heat demand and using previous years for the remaining weeks of the receding horizon. Method *F1* achieves the best result in 9 out of 11 samples for municipality A and in 8 out of 11 cases for municipality B. For the remaining 2 and 3 cases, respectively, no common favorable can be determined, as it differs per case. However, in all cases using the scenarios of method *F1* is better than using expected values, as we show in Section 6.2 of the main article.

Based on these results, we conclude for our test cases that it is beneficial to update the scenarios every week instead of using previous years' data. However, using time series models for more than the first week often leads to worse results, which means that the scenarios are misleading the optimization. Therefore, using updated information just for the first week is a compromise and improves the results. For application in practice, this should be evaluated individually. Furthermore, our scenario generation methods can be easily replaced with already existing proved and tested forecasting methods of the operator.

References E

[E1] H. Lund. "Renewable energy strategies for sustainable development". In: *Energy* 32.6 (2007), pp. 912–919.

[E2] Danish Energy Agency. *Regulation and planning of district heating in Denmark*. https://ens.dk/sites/ens.dk/files/Globalcooperation/regulation_and_planning_of_district_heating_in_denmark.pdf. [accessed 07/05/2017]. 2017.

[E3] C. Yin, L. A. Rosendahl, and S. K. Kær. "Grate-firing of biomass for heat and power production". In: *Prog Energ Combust* 34.6 (2008), pp. 725–754.

[E4] S. Sénéchal et al. *Logistic management of wood pellets: Data collection on transportation, storage and delivery management*. EUBIA-European Biomass Industry Association, Brussels, Belgium, 2009.

[E5] J. R. Birge and F. Louveaux. *Introduction to stochastic programming*. Springer Science & Business Media, 2011.

[E6] R. Aringhieri and F. Malucelli. "Optimal operations management and network planning of a district heating system with a combined heat and power plant". In: *Ann Oper Res* 120.1-4 (2003), pp. 173–199.

[E7] B. Rolfsman. "Combined heat-and-power plants and district heating in a deregulated electricity market". In: *Appl Energ* 78.1 (2004), pp. 37–52.

[E8] M. Dvořák and P. Havel. "Combined heat and power production planning under liberalized market conditions". In: *Appl Therm Eng* 43 (2012), pp. 163–173.

[E9] A. Christidis et al. "The contribution of heat storage to the profitable operation of combined heat and power plants in liberalized electricity markets". In: *Energy* 41.1 (2012), pp. 75–82.

[E10] A. Rong and R. Lahdelma. "Efficient algorithms for combined heat and power production planning under the deregulated electricity market". In: *Eur J Oper Res* 176.2 (2007), pp. 1219–1245. ISSN: 03772217. DOI: 10.1016/j.ejor.2005.09.009.

[E11] M. Pirouti et al. "Optimal operation of biomass combined heat and power in a spot market". In: *PowerTech, 2011 IEEE Trondheim*. IEEE. 2011, pp. 1–7.

[E12] M. Alipour, B. Mohammadi-Ivatloo, and K. Zare. "Stochastic risk-constrained short-term scheduling of industrial cogeneration systems in the presence of demand response programs". In: *Appl Energ* 136 (2014), pp. 393–404.

[E13] M. G. Nielsen et al. "Economic valuation of heat pumps and electric boilers in the Danish energy system". In: *Applied Energy* 167 (2016), pp. 189–200.

[E14] N. Kumbartzky et al. “Optimal operation of a CHP plant participating in the German electricity balancing and day-ahead spot market”. In: *Eur J Oper Res* 261.1 (2017), pp. 390–404.

[E15] I. Dimoulkas and M. Amelin. “Constructing bidding curves for a CHP producer in day-ahead electricity markets”. In: *2014 IEEE International Energy Conference (ENERGYCON)*. 2014, pp. 487–494.

[E16] I. Dimoulkas and M. Amelin. “Probabilistic day-ahead CHP operation scheduling”. In: *2015 IEEE Power Energy Society General Meeting*. 2015, pp. 1–5.

[E17] A. De Meyer, D. Cattrysse, and J. Van Orshoven. “A generic mathematical model to optimise strategic and tactical decisions in biomass-based supply chains (OPTIMASS)”. In: *Eur J Oper Res* 245.1 (2015), pp. 247–264.

[E18] F. Frombo et al. “A decision support system for planning biomass-based energy production”. In: *Energy* 34.3 (2009), pp. 362–369.

[E19] M. A. Quddus et al. “A two-stage chance-constrained stochastic programming model for a bio-fuel supply chain network”. In: *Int J Prod Econ* 195 (2018), pp. 27–44. ISSN: 0925-5273.

[E20] M. Bruglieri and L. Liberti. “Optimal running and planning of a biomass-based energy production process”. In: *Energ Policy* 36.7 (2008), pp. 2430–2438.

[E21] L. Maurovich-Horvat, P. Rocha, and A. S. Siddiqui. “Optimal operation of combined heat and power under uncertainty and risk aversion”. In: *Energ Buildings* 110 (2016), pp. 415–425.

[E22] N. Shabani et al. “Tactical supply chain planning for a forest biomass power plant under supply uncertainty”. In: *Energy* 78 (2014), pp. 346–355.

[E23] I. G. Jensen, M. Münster, and D. Pisinger. “Optimizing the supply chain of biomass and biogas for a single plant considering mass and energy losses”. In: *Eur J Oper Res* 262.2 (2017), pp. 744–758.

[E24] J. Scott et al. “A decision support system for supplier selection and order allocation in stochastic, multi-stakeholder and multi-criteria environments”. In: *Int J Prod Econ* 166.Supplement C (2015), pp. 226–237.

[E25] M. Chiarandini, N. H. Kjeldsen, and N. Nepomuceno. “Integrated planning of biomass inventory and energy production”. In: *IEEE T Comput* 63.1 (2013), pp. 102–114.

[E26] M. Zugno, J. M. Morales, and H. Madsen. “Robust management of Combined Heat and Power systems via linear decision rules”. In: *2014 IEEE International Energy Conference (ENERGYCON)*. 2014, pp. 479–486.

[E27] Aarhus Kommune. *Dataadgang*. http://varmeplanaarhus.dk/dataadgang/. [accessed 08/03/2017]. 2017.

[E28] Energinet. *Energy Data*. https://en.energinet.dk/Electricity/Energy-data. [accessed 08/03/2017]. 2017.

[E29] Powernext. *Pegas markets - Spot market data*. https://www.powernext.com/spot-market-data. [accessed 08/03/2017]. 2017.

[E30] E. R. Soysal et al. "Electric Boilers in District Heating Systems: A Comparative Study of the Scandinavian market conditions". In: *Swedish Association for Energy Economics Conference 2016*. 2016.

[E31] C. J. Levitt and A. Sørensen. *The Cost of Producing Electricity in Denmark*. The Rockwool Foundation, Denmark, 2014.

[E32] H. Madsen. *Time series analysis*. CRC Press, 2007.

[E33] R. Weron. *Modeling and forecasting electricity loads and prices: A statistical approach*. Vol. 403. John Wiley & Sons, 2007.

[E34] A. J. Conejo, M. Carrión, J. M. Morales, et al. *Decision making under uncertainty in electricity markets*. Vol. 1. Springer, 2010.

[E35] T. Hastie, R. Tibshirani, and J. Friedman. "Unsupervised learning". In: *The elements of statistical learning*. Springer, 2009, pp. 485–585.